AD_____

AWARD NUMBER: W81XWH-10-1-0125

TITLE: Activation of Hh Signaling: A Critical Biological Consequence of ETS Gene Anomalies in Prostate Cancer

PRINCIPAL INVESTIGATOR: Mengqian Chen, Ph.D.

CONTRACTING ORGANIZATION: University of South Carolina
Columbia, SC, 29208

REPORT DATE: January 2013

TYPE OF REPORT: Annual Summary

PREPARED FOR: U.S. Army Medical Research and Materiel Command
Fort Detrick, Maryland 21702-5012

REPORT DOCUMENTATION PAGE

Form Approved
OMB No. 0704-0188

1. REPORT DATE	2. REPORT TYPE	3. DATES COVERED
January 2013	Annual Summary	1 March 2011 – 31 December 2012

4. TITLE AND SUBTITLE
Activation of Hh signaling: A Critical Biological Consequence of ETS Gene Anomalies in Prostate Cancer

5a. CONTRACT NUMBER

5b. GRANT NUMBER
W81XWH-10-1-0125

5c. PROGRAM ELEMENT NUMBER

6. AUTHOR(S)
Mengqian Chen, Ph.D.

Email: chenm@sccp.sc.edu

5d. PROJECT NUMBER

5e. TASK NUMBER

5f. WORK UNIT NUMBER

7. PERFORMING ORGANIZATION NAME(S) AND ADDRESS(ES)
University of South Carolina
715 Sumter Street, Columbia, South Carolina, 29208

8. PERFORMING ORGANIZATION REPORT NUMBER

9. SPONSORING / MONITORING AGENCY NAME(S) AND ADDRESS(ES)
U.S. Army Medical Research and Materiel Command
Fort Detrick, Maryland 21702-5012

10. SPONSOR/MONITOR'S ACRONYM(S)

11. SPONSOR/MONITOR'S REPORT NUMBER(S)

12. DISTRIBUTION / AVAILABILITY STATEMENT
Approved for Public Release; Distribution Unlimited

13. SUPPLEMENTARY NOTES

14. ABSTRACT
One of the most notable early molecular changes in prostate cells associated with neoplastic development involves the acquisition of genetic anomalies (chromosomal rearrangements or deletions) that increase expression of gene products of the ETS family (exemplified by ERG, ETV-1, ETV-4 or ELK-4). We propose that one important consequence of ETS gene overexpression in prostate cells is increased expression and activity of Gli transcription factors that are normally induced by classical Hedgehog signaling. In this study, we have identified that GLI1 is regulated by androgens in both LNCaP and VCaP prostate cancer cells. We also identified Gli overexpression induces androgen-independent growth of prostate cancer cells and this action is mediated by a direct interaction between GLIs and androgen receptor (AR) which leads to enhanced AR signaling under both androgen-supplemented and androgen-deprived conditions. Additionally we discovered CDK8/19 as novel regulators of AR-mediated transcription in prostate cancer cells, which may provide helpful information in developing effective treatment of advanced prostate cancer in near future.

15. SUBJECT TERMS
None provided.

16. SECURITY CLASSIFICATION OF:			17. LIMITATION OF ABSTRACT	18. NUMBER OF PAGES	19a. NAME OF RESPONSIBLE PERSON
a. REPORT	b. ABSTRACT	c. THIS PAGE			USAMRMC
U	U	U	UU	117	19b. TELEPHONE NUMBER *(include area code)*

Table of Contents

Final Report

DOD Project: W81XWH-10-1-0125
Title: *Activation of Hh Signaling: A Critical Biological Consequence of ETS Gene Anomalies in Prostate Cancer*
Principal Investigator: Mengqian Chen, Ph.D.
Progress Period: 03/01/2010~04/26/2011 and 05/01/2012~01/31/2013

INTRODUCTION:

Prostate cancer (PCa) still remains the most frequent malignancy found in US men and the most common cause of cancer-related death in men over 75 years old. The cause of this disease remains enigmatic and the two overarching challenges in prostate cancer treatment today are how to discriminate the aggressive disease form from the indolent disease form and how to treat the PCa patients with advanced disease. One of the most notable early molecular changes in prostate cells associated with neoplastic development involves the acquisition of genetic anomalies (chromosomal rearrangements or deletions) that affect genes of the ETS family[1]. These anomalies result in increased expression of ETS gene products (exemplified by ERG, ETV1, ETV4 or ELK4) because the genomic rearrangement brings the ETS gene coding sequences under the control of gene promoters that are transcriptionally active in prostate cells (such as androgen-responsive gene promoters or housekeeping gene promoters) compared to the normal ETS gene promoters that are usually silenced in differentiated prostate epithelial cells[2-4]. On one hand, the discovery and characterization of ETS gene fusions in early prostate cancer cells has the potential to benefit prostate cancer patients by creating an opportunity for early detection and there is ongoing effort to correlate ETS gene fusions in tumor cells with patient outcomes to prognosticate disease recurrence or the need for early aggressive treatment[5-7]. Yet we still do not fully understand the functional consequence of increased ETS expression in prostate cells. Overexpression of ERG, the most common ETS fusion gene product, in benign prostate epithelial cells renders a more motile and invasive phenotype but is not overtly transforming[8, 9]. Likewise, transgenic mice with elevated ERG expression in prostate developed prostatic intraepithelial neoplasia (PIN) instead of prostatic carcinoma[8]. These evidences suggest that the ETS gene fusions contribute to prostate cancer development but require additional oncogenic alterations for full-scale malignant transformation. We propose that one important consequence of ETS gene overexpression in prostate cells is increased expression and activity of Gli transcription factors that are normally induced by classical Hedgehog signaling[10-12]. This hypothesis has several important implications since overactive Gli shares properties in common with ETS overexpression including an increased motile phenotype and ability to synergize with other genetic changes to induce overt malignancy. The work in this project is going to test whether ETS genes activate Hedgehog signaling by turning on Gli expression and activities in prostate cells. We will also explore the downstream signaling profile regulated by ETS or GLI

overexpression in prostate cells to determine whether molecular events induced by ETS gene anomalies are mediated by GLI activation. Furthermore we will study whether Gli reactivation, induced by ETS family, affects androgen signaling in prostate cells and induce androgen-independent growth of prostate cancer cells. Additionally, we will also expand our research interest into understanding the molecular mechanism(s) of prostate cancer progression to the aggressive therapy-resistant stage and identifying the potential targets for developing effective treatment for prostate cancer patients with the advanced disease.

BODY:

This project has 3 Specific Aims and progress will be discussed for each Aim.

Specific Aim 1. Determine the relationship between the expression of ETS genes (ERG, ETV1 or ETV4) and expression and activity of Gli (1 and/or 2) transcription factors in benign and malignant prostate cells.

In our previously published work, GLI1 gene expression in androgen-dependent prostate cancer cell line LNCaP cells was shown to be upregulated by androgen treatment in a dosage-dependent manner and this up-regulation requires newly protein synthesis[13]. We first confirmed that GLI1 gene expression is induced by androgen treatment in two prostate cancer cell lines known with ETS gene fusion, LNCaP and VCaP cells (Figure 1). In both cell lines, GLI1 gene expression is upregulated by R1881 treatment in a dose-dependent manner. In VCaP cells, we confirmed the reported ETS-gene fusion, ERG fused with TMPRSS2 gene promoter, and that ERG is upregulated by androgen in a similar dosage-dependent manner. However, the previously reported ETS fusion gene in LNCaP cells[14], the ETV1 gene is highly

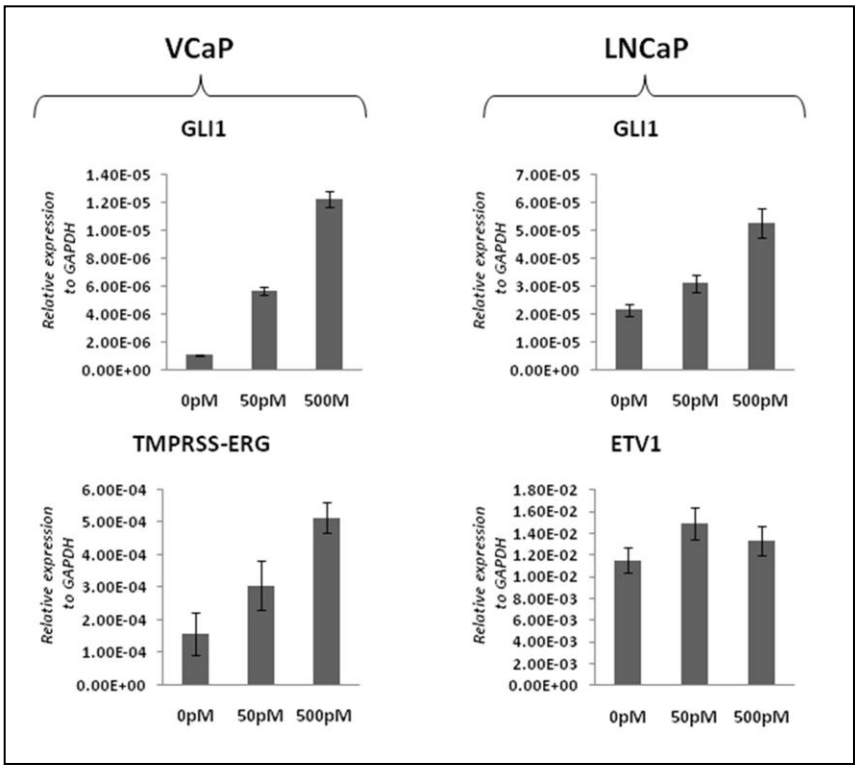

Figure 1 Gene expression of GLI1 and ETS genes in VCaP and LNCaP cells treated with androgen. VCaP and LNCaP cells were seeded into 60mm dishes at density of $5x10^5$ cells per dish and cultured in Charcoal-stripped FBS (CS-FBS) media for 3 days. After androgen deprivation, cells were treated with R1881 at indicated concentration for 24 hours before lysed for RNA extraction and quantitative PCR for relative mRNA expression level of indicated genes. Data are representative of duplicate experiments.

expressed but is not regulated by androgen treatment.

We further tested whether androgen-regulated GLI1 expression in LNCaP cells is dependent on ETV1 overexpression by siRNA knockdown experiment (Figure 2). Surprisingly,

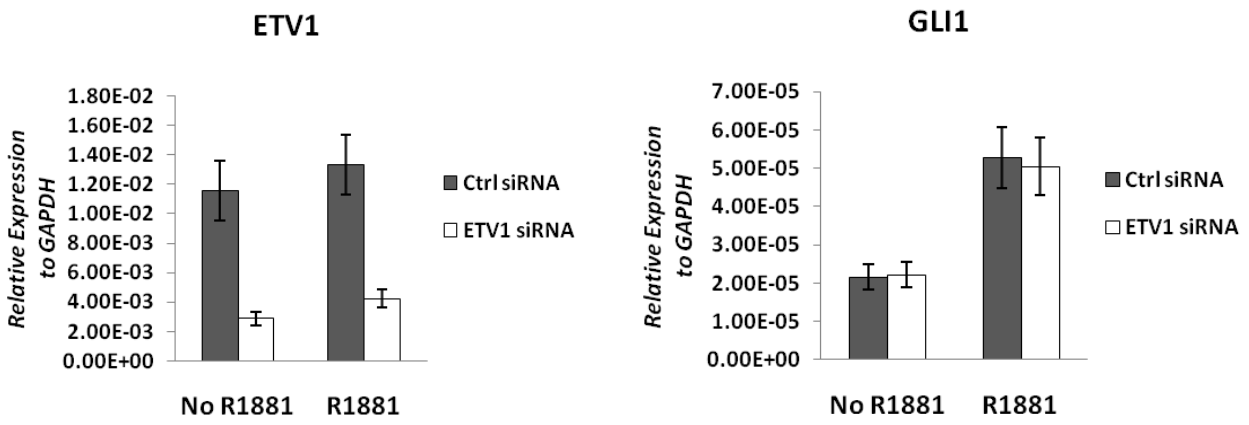

Figure 2 Knock-down ETV1 in LNCaP cells does not affect GLI1 expression in LNCaP cells. LNCaP cells were transfected with 20nM ETV1 siRNA or non-specific Ctrl siRNA for 48 hours and further cultured in CSFBS media for 48 hours. Cells were treated with or without 500pM R1881 for 24 hours before RNA extraction and qPCR analysis for ETV1 and GLI1 mRNA expression. Data are representative of duplicate experiments.

downregulation of ETV1 expression does not reduce GLI1 expression to any extent at either no-androgen or androgen-treated conditions. Combined with the data that ETV1 is not androgen-regulated gene in LNCaP, It is very possible that there are some other members of ETS family, regulated by androgen through gene fusion, to mediate androgen-dependent activation of GLI1 in LNCaP cells. To test whether there are any other known ETS gene family members which may contribute to the androgenic up-regulation of GLI1 gene in LNCaP cells, we performed the microarray analysis for gene expression profiles between androgen-treated and untreated LNCaP cells to identify potential ETS candidates that are regulated by androgen in LNCaP cells. The result of microarray analysis revealed that ERG/ETV2/ETV3L/ETV4/ETV5/ETV7 gene expressions are not activated in LNCaP cell, while ETV1, ETV3, ETV6, ELK3 and ELK4 are abundantly expressed in LNCaP cells but none of them is positively regulated by androgen treatment. These findings suggest that androgenic regulation of GLI1 expression in LNCaP cells may not be dependent on any known ETS family members and other androgen-induced transcription factors might be involved in this regulation. Considering the high frequent observation of ERG gene fusion in clinical prostate tumor samples, LNCaP cells may not be the best cell line model to study the functions of ETS gene fusion in prostate cancer progression since the cell line has no genomic rearrangement that alters the transcription of ETS gene family members under an androgen-responsive promoter (such as TMPRSS2 or SLC45A3 gene promoters). We have shown in our preliminary data that ERG overexpression dramatically induced both GLI1 and GLI2 expression in prostate

cancer cells and also that androgen treatment has more inductive effects on GLI1 expression in VCaP cells, which harbor the TMPRSS2-ERG fusion (Figure 1), when compared with LNCaP cells. Cumulatively, VCaP cells might be a better cell line model to test our hypothesis that activation of GLI1 gene expression in prostate cancer cells can be mediated by androgen-stimulated ETSs genes (such as ERG in VCaP cells). Currently we are finishing up the experiment of evaluating GLI1 expression in ERG-knockdown VCaP cells to confirm this androgen→ERG→GLI1 signaling cascade.

On the other hand, we were trying to overexpress the EST genes (ERG, ETV1 and ETV4) in benign prostate cells (RWPE1 and BPH1) to establish the functional relationship between EST genes and GLI1 expression. We successfully sub-cloned the cDNAs of ERG, ETV1 and ETV4 genes into the lentiviral-based expression vector pLenti6 and transduced the RWPE1 and BPH1 cells with the lentiviruses, followed by blasticidin selection to generate stable-expression cell lines. Unfortunately, after moving from Ordway Research Institute to University of South Carolina, we had hard time to rescue the selected ESTs-overexpressing prostate cells. This may due to the harsh environment during the transfer (Ordway Research Institute filed a bankruptcy in April, 2012 and terminated our lab without any pre-notice) or the possible fragility of the non-malignant prostate cells. We are working on regenerate the EST-overexpressing prostate cells and will test the hypothesis whether GLIs induction is a consequence event of EST gene overexpression in benign prostate cells.

Specific Aim 2. Determine whether ERG overexpression, through Gli, induces expression and activity of Polycomb Group proteins

During the period that we were waiting for the stable ERG overexpression benign and malignant prostate cells, we also generated Doxycycline (Dox) -inducible GLI expression LNCaP cells to profile the gene expression pattern regulated by GLI overexpression (Figure 3).

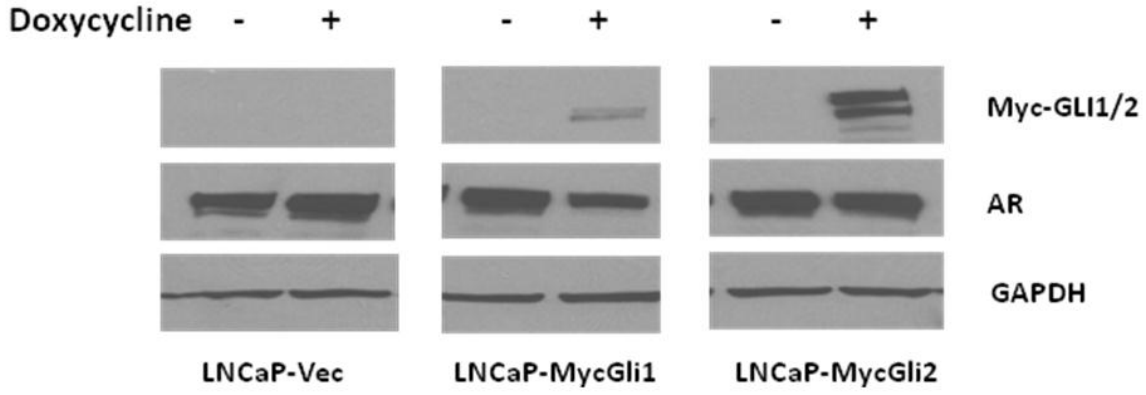

Figure 3 Western blot for Myc-tagged GLI1/2 and AR expression in Dox-inducible GLI expression LNCaP cells. Cells were seeded in regular culture media and treated with or without 100ng/ml Doxycycline for 48 hours. Cells were lysed in RIPA buffer and analyzed for protein expression of Myc-tagged GLIs, AR and GAPDH with specific antibodies.

We discovered that overexpression of GLI1 or GLI2 is able to enhance the AR transcriptional activity, which is consistent with our recently published findings that treatment of LNCaP cells with Hedgehog signaling inhibitor cyclopamine is able to down-regulate the expression of androgen-responsive genes including PSA, KLK2, PGC and TMPRESS2[15]. Moreover, we also found that GLI-overexpressing LNCaP cells are able to grow in the androgen-depleted media, suggesting that GLI-enhanced AR activity might be one of the consequences of ETS-GLI cascade activation that contributes androgen-independence progression. We further set out to determine whether GLI proteins interact with androgen receptor and directly regulate androgen receptor transcriptional activity since we felt that this work is very relevant to the outcome of this project: identifying the roles of GLI proteins in prostate cancer progression. We identified that all GLI transcription factors (GLI1/GLI2/GLI3) are able to interact with androgen receptor (AR), evaluated by the co-immunoprecipitation (co-IP) experiments when they are co-expressed with AR in FT293 cells (Figure 4). This GLI-AR interaction is not dependent on

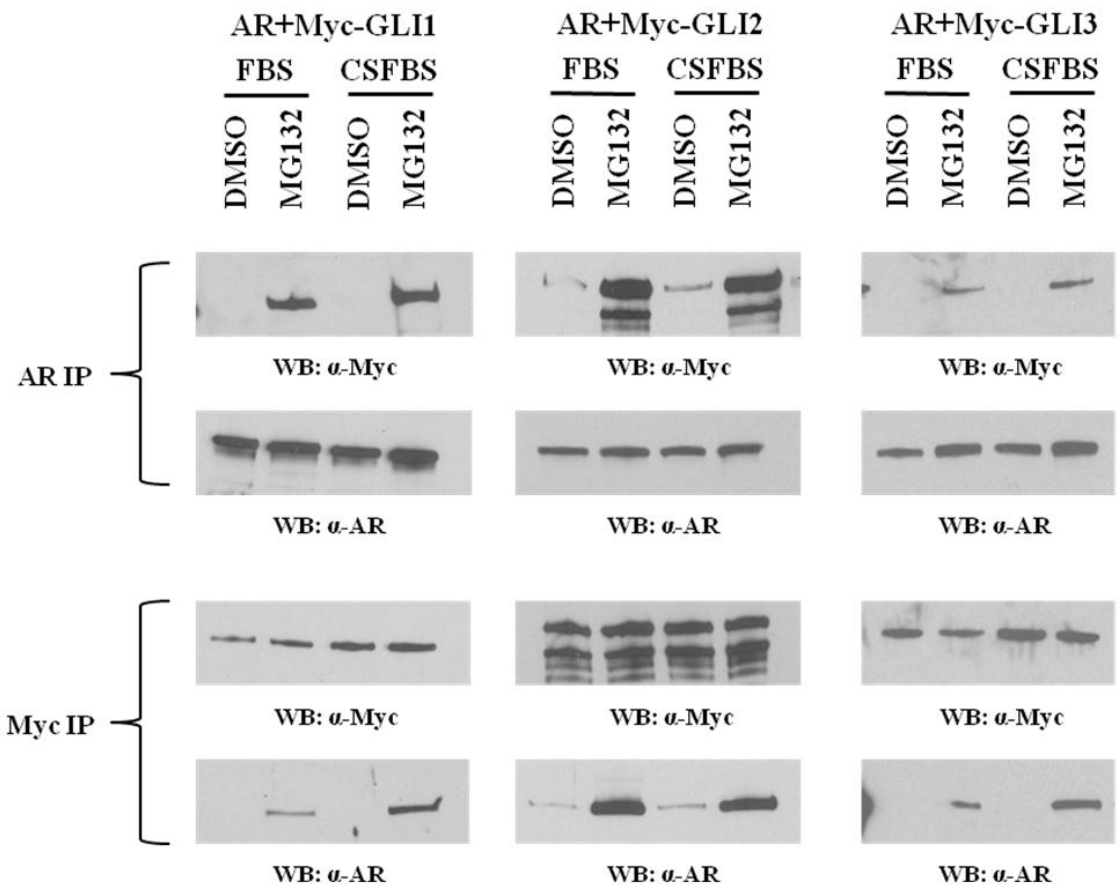

Figure 4 Androgen receptor (AR) interacts with GLIs in FT293 cells. A human AR cDNA expression plasmid was co-transfected with Myc-tagged GLIs (GLI1/2/3) expression plasmid into FT 293 cells under FBS or CSFBS culture condition. 48 hours after transfection, cells were lysed and protein-protein interaction was analyzed by immunoprecipitation (IP) with Anti-AR or Anti-Myc Antibodies. AR-GLI interaction was greatly enhanced by MG132 treatment (20μM) for 4 hours before protein extraction.

ligand-AR association, as indicated by that similar co-IP results were obtained from the experiments performed under either androgen-supplemented or androgen-depleted conditions. We also discovered that all three GLI proteins possess the abilities to enhance the AR transcriptional activity, measured by the luciferase activities of the reporter constructs with androgen-responsive gene promoters (Figure 5). Interestingly, there is no direct correlation between GLI transcriptional activity (represented by the GLI reporter activity) and AR transcriptional activity. GLI2 and GLI3, which are much weaker transcription activators of canonical GLI-responsive genes, enhance the AR transcription at a similar or even stronger level when compared to GLI1, suggesting that the GLI family proteins may function as co-activators through the conserved protein domain to facilitate AR mediated transcription in prostate cancer cells.

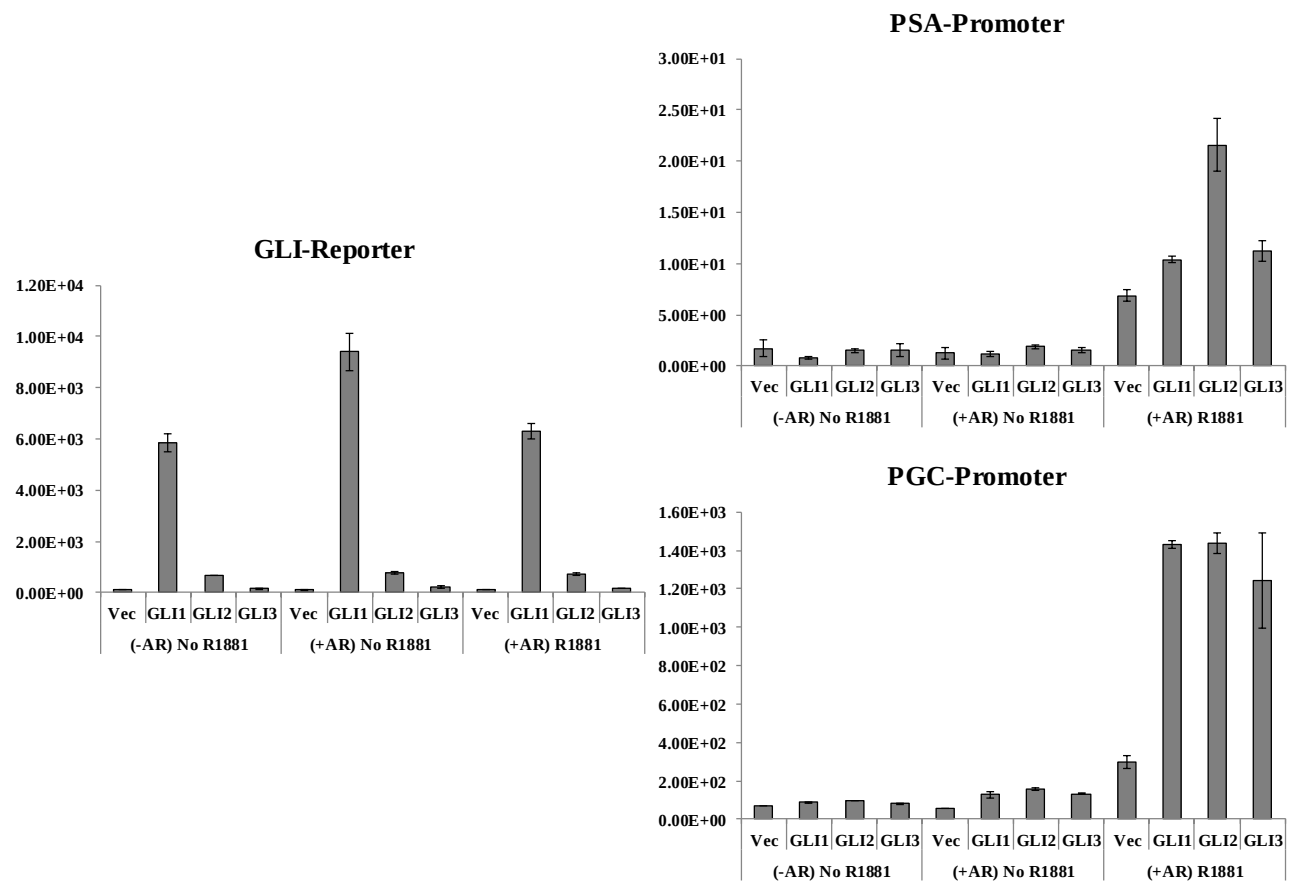

Figure 5 Co-expression of GLIs enhances AR transcriptional activity in FT293 cells. Luciferase-based promoter constructs (pGL4-GLI, pGL4-PGC, pGL3-PSA) with CMV-GFP plasmid was co-transfected with AR and GLI expressing plasmids into FT293 cells as indicated. Twenty-four hours after transfection, cells were switched to CSFBS media with or without 1nM R1881 and cultured for 24 hours. Cell extracts were quantified for luciferase activity that was normalized by GFP intensity. *: $p<0.01$ between GLI group and vector (Vec) control group.

To further understand the molecular mechanism by which Gli proteins function as positive regulators of AR transcriptional activities, we sub-cloned the N-terminal and C-terminal domain of GLI2 protein and co-expressed these sub-fragments with AR in FT293 cells to determine whether they are able to interact with AR and enhance AR transcriptional activity. Data from these experiments indicated that it is the C-terminal domain of GLI2 protein that is required for GLI-AR interaction and AR activation while N-terminal domain and DNA-binding domain of GLI2 are not involved (Figure 6). On the other hand, we also narrowed down the subdomain

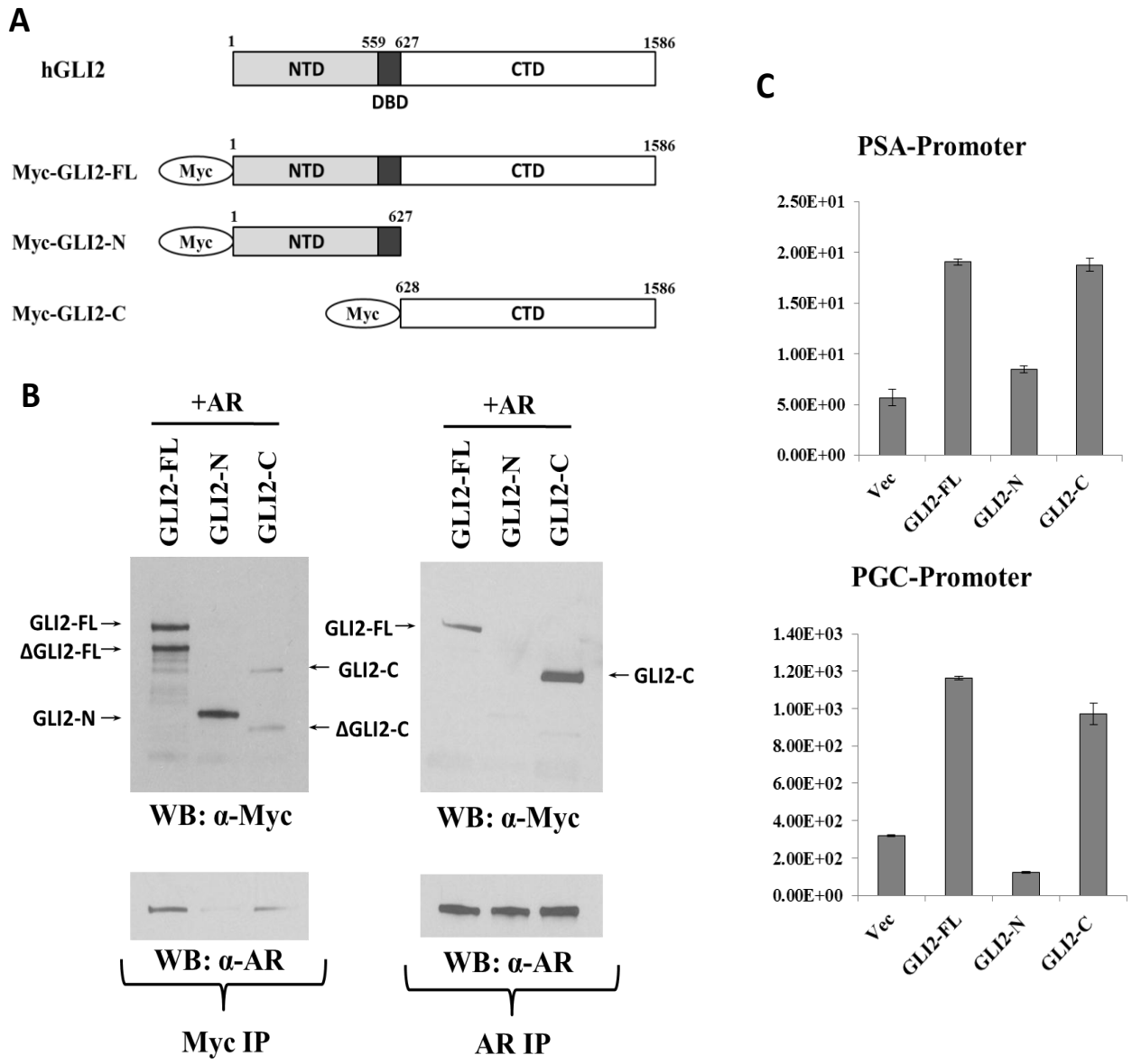

Figure 6 GLI2 protein interacts with AR and enhances its transcriptional activity through the C-terminal domain. Schematic presentation **(A)** of the GLI2 sub-fragments used in the co-IP experiments **(B)** or androgen-responsive promoter activity assays **(C)** in FT293 cells co-overexpressing AR.

of AR participating in GLI2 interaction to the region of aa.391~aa.558 through GST-pull down assay (Figure 7). This result not only presents a proof of direct interaction between AR and GLI2 proteins but also indicates that GLI2 interact with AR through the Tau5 domain which has been shown playing a key role in both ligand-dependent and ligand-independent transcriptional activities of AR[16, 17]. Finally we performed chromatin precipitation (ChIP) analysis using the LNCaP-MycGLI2 cells (Figure 3) and confirmed that GLI2 and AR proteins do co-localize at the genomic loci with androgen-responsive elements (AREs). In summary of all the data we presented in this section, we identified AR signaling as one of the major signaling pathways downstream of GLI activation. One critical biological consequence of ETS gene anomaly might be the enhanced AR transcriptional activity endowed by ETS-induced GLI overexpression in prostate cancer cells.

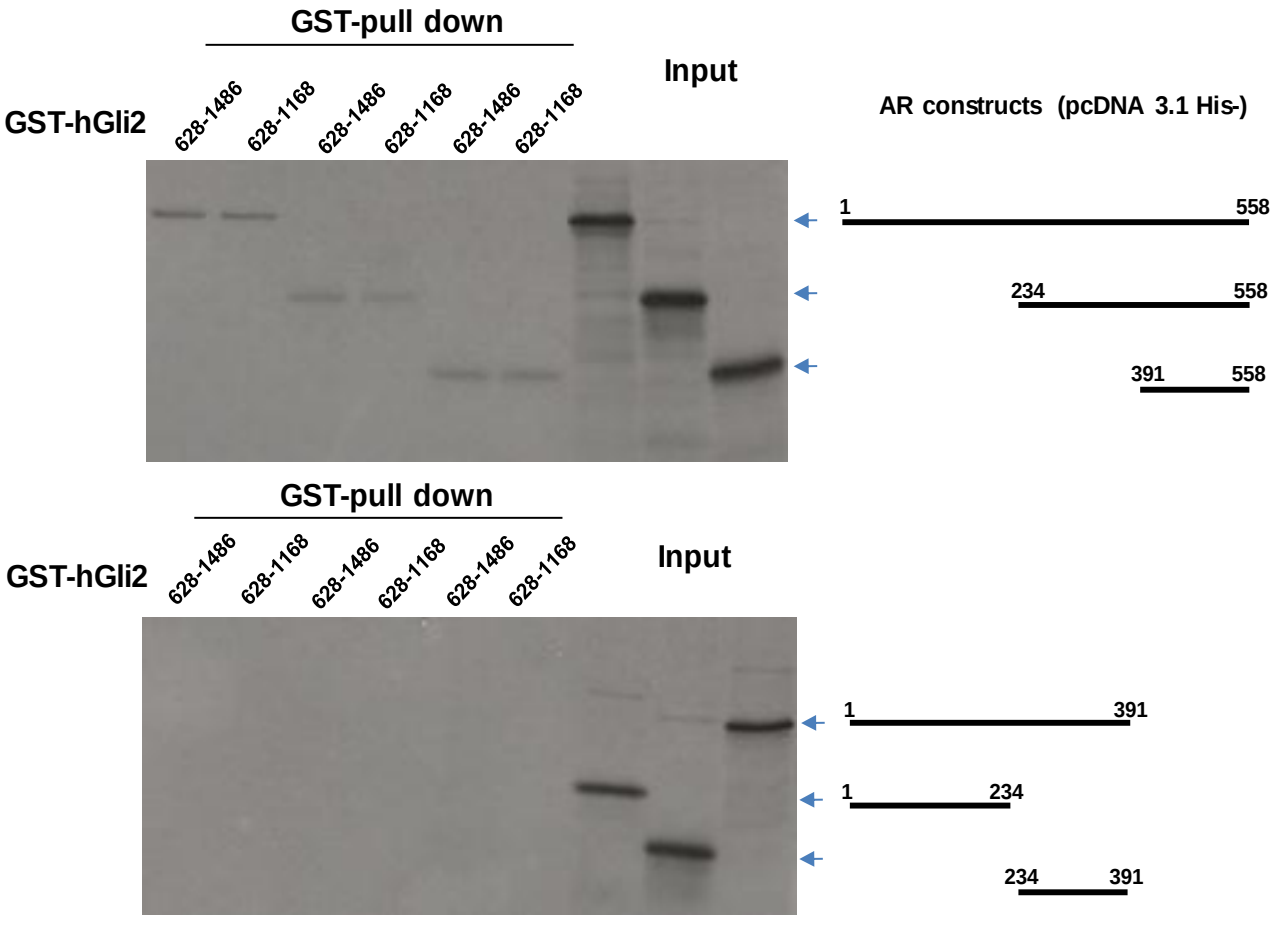

Figure 7 GST pull-down assay to map the subdomain in AR that contributes the GLI-AR interaction. Recombinant GST-tagged GLI2 sub-fragment (628-1486 or 628-1168) proteins were purified and used for the GST pull-down assay with the in vitro translated S^{35} methionine labeled truncated AR proteins (as indicated by the arrows and the illustration on the right.

Specific Aim 3. Determine whether ERG overexpression in benign prostate cells induces gene methylation and gene silencing.

No work has been done on this specific aim so far since we are still waiting for the stable ERG overexpression benign prostate cells. However, additional work was also undertaken during the funding period to explore molecular targets which play critical roles in prostate cancer progression. After recruited to the Translational Cancer Therapeutics (TCT) Program in South Carolina College of Pharmacy (SCCP) as a Research Assistant Professor, I expanded my research interests onto two very promising novel molecular targets for treatment of advanced prostate cancer: CDK8 and CDK19. The project was initiated from a collaborative project with Dr. Igor Roninson, the head of TCT program, who developed the highly selective CDK8/19 kinase inhibitor and identified CDK8 as a critical player in the damage-induced tumor-promoting paracrine activities[18].

CDK8 and CDK19 are two closely related transcription-regulating serine/threonine kinases that do not regulate cell cycle progression, unlike better-known members of the cyclin-dependent kinase (CDK) family[19]. CDK8/19 depletion does not inhibit the growth of normal cells[20] or some tumor cells[18, 21], but dramatically affects gene transcription. Most of our current knowledge about CDK8 is that it forms a unique transcription-regulating module with three other proteins (the kinase regulatory subunit Cyclin C, MED12 and MED13) and this CDK8-subcomplex is associated with the large core Mediator complex[22], but CDK8 can also function outside of the Mediator[23, 24]. A series of recent reports demonstrated that CDK8 serves as a positive transcription regulator in multiple signaling pathways with biomedical relevance, including the p53 pathway[25], Wnt/β-catenin pathway[26], the serum response network[21], the TGFβ signaling pathway[25], as well as thyroid receptor (TR)[27] and SREBP[28]-dependent transcription. In regard to cancer, CDK8 has been recognized as an oncogene in melanoma and colorectal cancers[26, 29], and was recently implicated in the cancer stem cell phenotype[30]. In contrast to many studies on CDK8, its vertebrate paralog CDK19 has been poorly studied because it is not expressed as highly as CDK8 in most tissues. However, prostate is one of the few normal tissues where CDK19 is also abundantly expressed[31]. The functions of CDK8 and CDK19 in normal and malignant prostate cells have never been investigated but there are several published observations support the hypothesis of CDK8/19 involvement in androgen signaling and prostate cancer: (1) AR can be phosphorylated by some other members of CDK family and impairment of phosphorylation at these sites significantly reduces the AR transcriptional activity[32-34]. It is possible that CDK8/19 may participate in AR activation by phosphorylating AR at these or other sites. (2) MED1, a core subunit of the Mediator complex, plays a key co-regulatory role in AR transcription through direct interaction with AR[35]. It is very likely that CDK8/19 is enriched in AR-associated transcriptional protein complexes regulating AR activities since CDK8/19 is a part of the Mediator[36]. (3) MED12, a subunit of the CDK8-subcomplex of the Mediator, has been recently identified as one of the frequently mutated genes in PCa through sequencing the exomes of over one hundred prostate tumor and normal

tissue pairs[37]. This mutation could lead to loss of CDK8/19 regulation and subsequent AR hyper-activation. Given the evidence that CDK8 is a key positive transcription regulator implicated in some human cancers and all the indications that CDK8/19 may participate in AR-mediated transcription, we set out to study the roles of CDK8/19 in androgen signaling in prostate cancer cells.

We started to evaluate CDK8 and CDK19 expression in different PCa cell lines, in comparison to certain cancer cell lines derived from other tissues. As shown in Figure 8A, CDK8 is expressed in all of the PCa cell lines to a similar extent as in tumor cell lines derived from other tissues, and CDK19 is also expressed in all of the PCa cell lines. Importantly, CDK19 appears to be overexpressed in AR-positive (LNCaP, LN3, C42, CWR22rv1) PCa cells compared to AR-negative (DU145 and PC3) PCa cells (Figure 8A). I also found that androgen treatment downregulates CDK8 whereas androgen-deprivation up-regulates CDK8 and CDK19 proteins in LNCaP cells (Figure 8B). These data suggest that overexpression of CDK8/19 may be associated with hyperactive androgen signaling in PCa cells and that androgen may also regulate CDK8/19 expression in PCa cells.

Figure 8 Expression of CDK8/CDK19/AR/GAPDH/α-Tubulin in HT1080 (fibrosarcoma), HEK-293 (kidney), MDA-231 (breast), HCT116 (colon) and PCa cell lines **(A)** and in LNCaP cells cultured in FBS or CSS media (Androgen-deprived, AD) or CSS media supplemented with 100pM R1881 (R1881) for indicated days **(B)**.

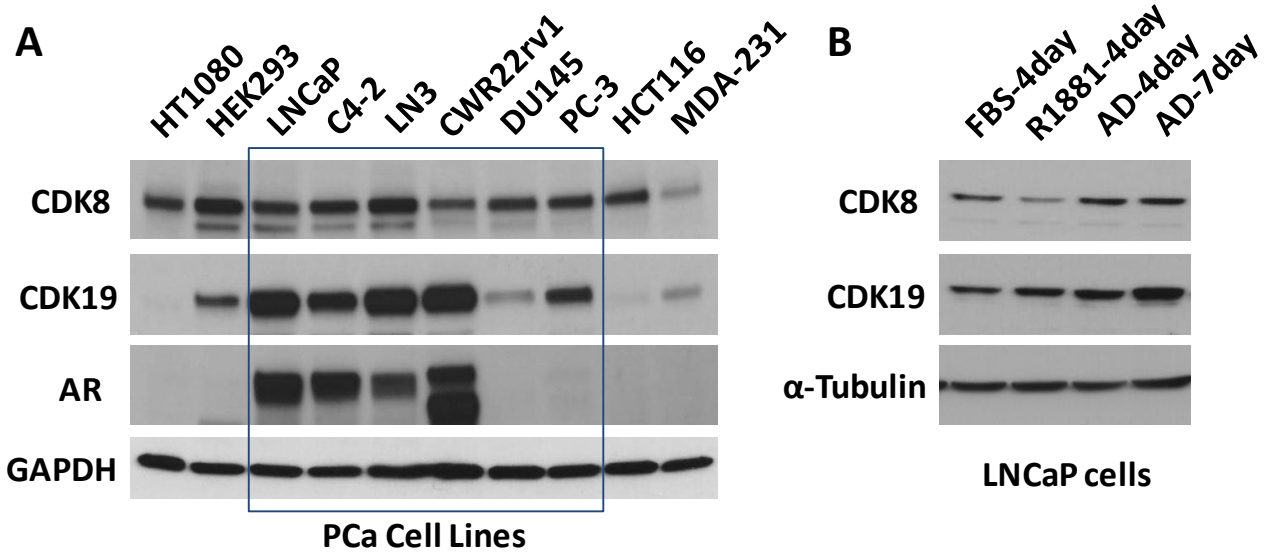

Then we began analyzing the roles of CDK8/19 in AR regulation by utilizing novel selective CDK8/19 kinase inhibitors recently developed by my collaborator, Dr. Roninson. These small molecules selectively bind to the ATP pockets of CDK8/19 to inhibit their kinase activity. The first-generation selective CDK8/19 inhibitor (Senexin A) was shown to block known CDK8 cellular functions and to inhibit various tumor promoting paracrine activities of chemotherapy-damaged cells *in vitro* and *in vivo*[18]. Senexin B is a new unpublished derivative of Senexin A, with much greater solubility and potency. It inhibits CDK8 and CDK19 with Kd of

140 nM and 80 nM respectively and possesses water solubility as high as 50 mM. Unlike any other known protein kinase inhibitors, Senexin B is very selective for CDK8/19 since it has minimal inhibitory effects on any other kinases that we tested (including all the other CDKs), as indicated by the data from screening the human kinome with Senexin B at the concentration of 2 μM (Figure 9A). Pretreatment of androgen-deprived LNCaP cells, a commonly used PCa cell line whose growth is dependent on androgen, by Senexin B significantly inhibited androgen-stimulated transcriptional activation of several androgen-responsive genes (ARGs) such as PSA, KLK2, PGC and TMPRSS2 (Figure 9B). To further confirm the role of CDK8/19 in AR activation, I analyzed the inhibitory effects of Senexin B by a promoter activity assay in

Figure 9 (A) Effects of Senexin B (2μM) on 450 kinases, measured by ATP binding competition assay (inhibited kinases are marked with red circles on the evolutional dendrogram). **(B)** Effects of Senexin B (1 and 4μM) on androgen responsive gene expression in LNCaP cells cultured in CSS media for 3d [R1881(-)] or in androgen-supplemented media (500pM R1881) for 24hr after 2-day androgen-deprivation [R1881(+)]. Senexin B was added 1hr before R1881 treatment and maintained in culture till RNA sample collection. Gene expression was measured by qPCR, with housekeeping gene RPL13A as normalization standard (*: p<0.05 between Senexin B and DMSO).

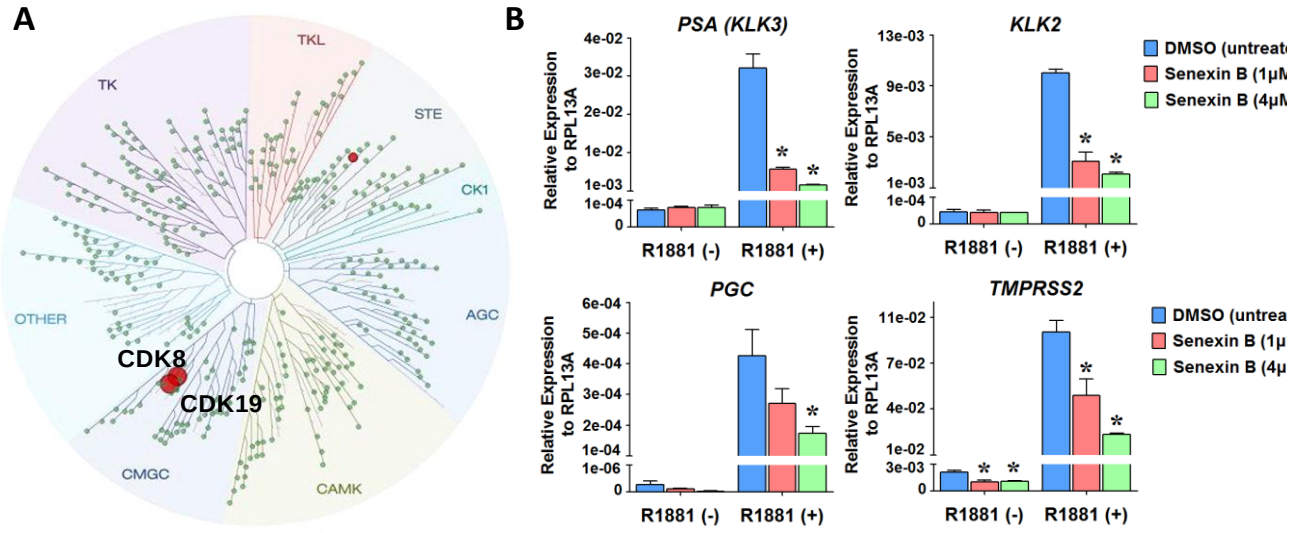

HEK293 cells that express both CDK8 and CDK19 (Figure 8A). When AR was overexpressed in HEK-293 cells, Senexin B significantly inhibited the activation of androgen-responsive constructs (luciferase reporters under PSA or PGC gene promoter) by R1881 (data not shown). All the above results indicate that CDK8/19 positively regulates AR function. We are currently verifying this conclusion through shRNA-mediated knockdown of CDK8 and CDK19, as we have previously done to test the role of CDK8/19 in p21-stimulated transcription[18].

We also tested whether the CDK8/19 inhibitor is able to block hyperactive AR signaling in several androgen-independent PCa cell lines (LN3, C42 and CWR22rv1). These CRPC cells

were derived from castration-relapse or metastatic xenografts of parental androgen-dependent PCa cell lines (LNCaP and CWR22) and grow well under androgen-depleted conditions (in Charcoal-Stripped Serum [CSS] media). Endogenous AR activities were estimated by qPCR analysis of PSA and KLK2 mRNA expression, and all three CRPC cell lines showed much higher expression of these ARGs compared to the androgen-dependent parental LNCaP cells after 3-day androgen deprivation (AD3, Figure 10A). Senexin B down-regulated the expression of PSA and KLK2 in all three CRPC cell lines grown in the absence of androgen (Figure 10B) as effectively as it inhibits androgen-stimulated PSA/KLK2 expression in LNCaP

Figure 10 Effects of Senexin B on ARG expression in AI-PCa cells. **(A)** Basal ARG expression in LNCaP and AI-PCa cells under 3-day androgen-deprivation (AD3) conditions. **(B)** ARG expression in cells cultured in CSS media (2d) and treated with Senexin B or vehicle control for 24 hours. *: p<0.05 between Senexin B and DMSO.

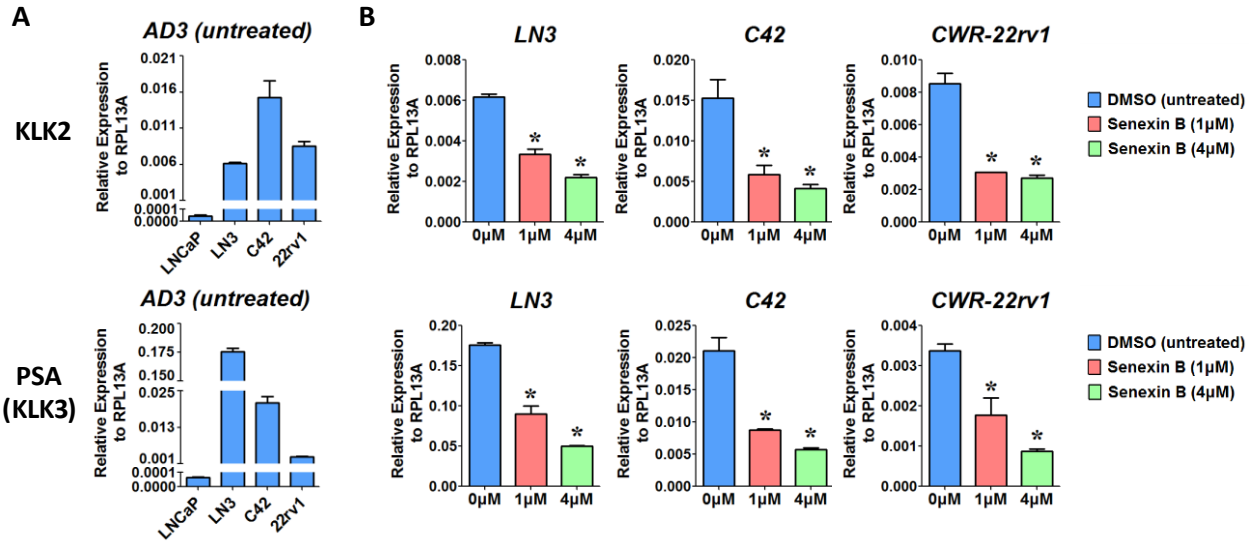

cells (Figure 9B). This result suggests that Senexin B suppresses ligand-independent AR signaling in CRPC cells, which is required for CRPC cells to proliferate in a low-androgen environment. The observation that Senexin B is able to downregulate expression of ARGs in CWR22rv1 cells is of special interest since constitutive androgen signaling in this cell line is rendered by an AR splice variant[38, 39]. This truncated AR form is resistant to current anti-androgen drugs designed for targeting the AR ligand binding domain because the C-terminal truncation deletes the domain and makes it ligand-independent. Hence CDK8/19 may also play an important role in active transcription mediated by activated ARs (full-length, mutated or truncated) in CRPC cells, and it may inhibit the growth of CRPC cells resistant to conventional AR inhibitors. To determine if blocking AR signaling in CRPC cells by targeting CDK8/19 leads to inhibition of tumor cell growth, I tested the effects of Senexin B on the androgen-independent growth of LN3, C42 and CWR22rv1 cells in androgen-deprived media. As shown

in Figure 11A, Senexin B inhibits the growth of all three cell lines that I tested, consistent with the model that active CDK8/19 potentiates the hyperactive AR signaling that is necessary for tumor cell proliferation. Moreover, I performed a small-scale preliminary in vivo experiment to evaluate effects of Senexin B on the growth of subcutaneous (s.c.) xenografts of LN3 cells in nude mice. Strikingly, treatment with Senexin B dramatically reduced the tumor growth rate without apparent toxicity, as indicated by unaltered body weight of the hosts (Figure 11B).

Figure 11 (A) Effects of Senexin B on AI-PCa cell growth in androgen-free media. $2x10^5$ PCa cells were seeded in CSS media with different concentrations of Senexin B and cultured for indicated time before total cell number was counted (n=4). **(B)** Effects of Senexin B on the growth of s.c. xenografts of LN3 in nude mice. Left: effects on growth of tumor volume; Middle: effects on change of mice body weight; Right: effects on final tumor weights.

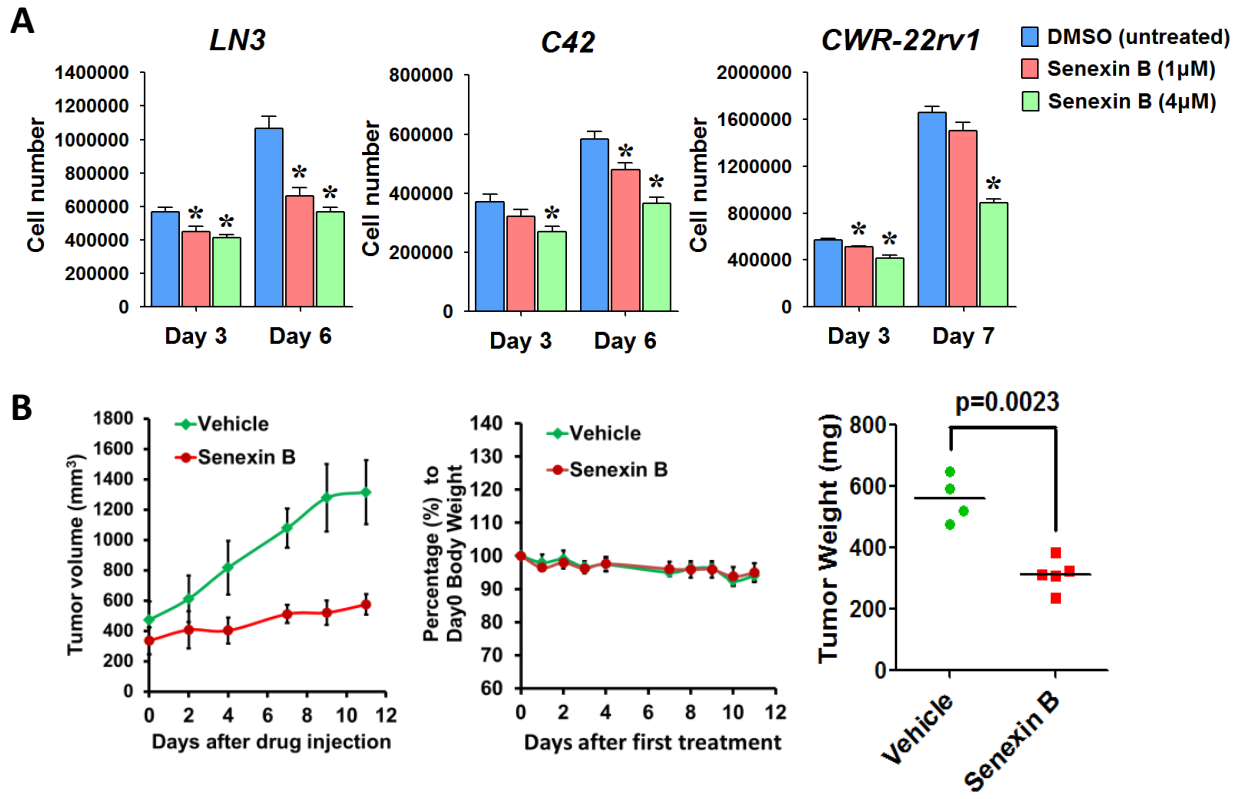

In summary, our new findings implicate CDK8/19, transcription-regulating kinases that are not involved in cell cycle progression, as novel effectors of AR activity in CRPC. Since selective and non-toxic inhibitors of CDK8/19 have become available, it is now possible to investigate CDK8/19 as a potential candidate for targeting AR signaling in PCa cells. The preliminary data generated during this DOD training award period will lead to a multiyear grant application to investigate in detail the molecular function of CDK8/19 in prostate cancer and to conduct preclinical studies to develop CDK8/19 inhibition as a novel therapy for CRPC.

KEY RESEARCH ACCOMPLISHMENTS:

- Demonstrated that GLI1 expression is upregulated by androgen in prostate cancer cells with ETS gene fusion.
- Determined that GLI1 expression is not regulated by ETV1 in LNCaP cells.
- Generated lentiviral expression vectors to overexpress ERG, ETV1, and ETV4 in prostate cells.
- Generated Tetracycline-inducible GLI1- and GLI2- overexpressing LNCaP cells for gene expression profiling.
- Identified that GLI family proteins interact with AR and enhance AR transcriptional activity in prostate cells.
- Mapped the sub-domains of GLI2 and AR that contribute to the interaction.
- Confirmed that GLI2 directly interacts with AR at the Tau-5 region.
- Demonstrated the high CDK8 and CDK19 expression in AR-positive prostate cancer cells and the regulation of their expression by androgen signaling in prostate cancer cells.
- Discovered that CDK8/19 kinase activity is essential for the active transcription mediated by various forms of AR in both androgen-dependent and androgen-independent prostate cancer cells.
- Generated abundant preliminary data suggesting blocking CDK8/19 kinase activity as a novel anti-androgen method that blocks AR transcription activity independent of ligand-receptor association.

REPORTABLE OUTCOMES:

Published Manuscripts:

1. **Chen M**, Feuerstein MA, Levina E, Baghel PS, Carkner RD, Tanner MJ, Shtutman M, Vacherot F, Terry S, de la Taille A, Buttyan R. Hedgehog/Gli supports androgen signaling in androgen deprived and androgen independent prostate cancer cells. *Mol Cancer,* 2010, 9: 89. PMID: 20420697
2. Mechlin CW, Tanner MJ, **Chen M**, Buttyan R, Levin RM, Mian BM. Hedgehog Signaling Pathway Activation in Bladder Transitional Cell Carcinoma (TCC). *J Urol*., 2010, 184(1):344-351. PMID: 20488474
3. Tanner MJ, Welliver RC Jr, **Chen M**, Shtutman M, Godoy A, Smith G, Mian BM, Buttyan R. Effects of Androgen Receptor and Androgen on Gene Expression in Prostate Stromal Fibroblasts and Paracrine Signaling to Prostate Cancer Cells. *Plos One,* 2010, 6(1):e16027. PMID: 21267466
4. **Chen M**, Carkner R, Buttyan R. The hedgehog/Gli Signaling Paradigm in Prostate Cancer. *Expert Rev. Endocrinol. Metab.* 2011, 6(3):453-467. (Review). PMID: 21776292
5. Levina E, **Chen M**, Carkner R, Shtutman M, Buttyan R. Paracrine hedgehog increases the steroidogenic potential of prostate stromal cells in a Gli-dependent manner. *Prostate*, 2011, 72(8):817-824. PMID: 22025366
6. Wang H, Jiang M, Cui H**, Chen M**, Buttyan R, Hayward SW, Hai T, Wang Z, Yan C. The Stress Response Mediator ATF3 Represses Androgen Signaling by Binding the Androgen Receptor. *Mol Cell Biol.* 2012, 32(16):3190-202. PMID: 22665497
7. Porter DC, Farmaki E, Altilia S, Schools GP, West DK, **Chen M**, Chang BD, Puzyrev AT, Lim CU, Kittella RR, Friedhoff LT, Papavassiliou AG, Kalurupalle S, Hurteau G, Shi J, Baran PS, Gyorffy B, Wentland MP, Broude EV, Kiaris H, Roninson IB. CDK8 mediates chemotherapy-induced tumor-promoting paracrine activities. *Proc. Natl. Acad. Sci. USA,* 2012, 109(34):13799-804. PMID: 22869755

Manuscripts in Preparation

1. **Chen M*** (co-first author), Li N*, Carkner R, and Buttyan R. The GLI2 enhances androgen receptor action via interaction with the Tau-5 domain of the receptor.
2. **Chen M,** Yang Z, Broude EV, Porter DC, Lim C, and Roninson IB. CDK8/19 potentiate NFkB-mediated induction of tumor-promoting and proinflammatory cytokines.
3. **Chen M,** Kaza V, Yang Z, Porter DC, Broude EV, Kiaris H, and Roninson IB. CDK8/19 are positive mediators of androgen receptor signalizing and androgen-independent prostate cancer growth.

Attended Conference:

March 9-12, 2011
Innovative Minds in Prostate Cancer Today (IMPaCT) Conference, Orlando, FL, USA
Poster: Activation of Hh Signaling: A Critical Biological Consequence of ETS Gene Anomalies in Prostate Cancer

Academic Position:

PI got a Research Assistant Professor position at South Carolina College of Pharmacy, University of South Carolina, Columbia, SC

CONCLUSION:

Work in this project has suggested that ETS gene overexpression in prostate cancer can mimic the activity of the classical hedgehog signaling pathway through the ability of ETS transcription factors to directly upregulate expression of Gli genes in prostate cells. Activated GLIs are able to enhance androgen signaling in prostate cancer cells through interacting with androgen receptor Tau-5 subdomain. Therefore the ETS-GLI-AR signaling cascade may play a central role in inducing or maintaining the hyperactive androgen signaling during prostate cancer progression. In addition, our studies revealed novel potential targets for blocking AR signaling in advanced prostate cancer: the transcription regulating kinases CDK8/19. With the availability of the selective CDK8/19 kinase inhibitor, it is becoming possible to develop novel anti-androgen therapeutic treatment for CRPC patients in near future.

REFERENCES:

1. Kumar-Sinha, C., Tomlins, S.A. & Chinnaiyan, A.M. Recurrent gene fusions in prostate cancer. *Nat Rev Cancer* **8**, 497-511 (2008).
2. Hu, Y. et al. Delineation of TMPRSS2-ERG splice variants in prostate cancer. *Clin Cancer Res* **14**, 4719-25 (2008).
3. Rickman, D.S. et al. SLC45A3-ELK4 is a novel and frequent erythroblast transformation-specific fusion transcript in prostate cancer. *Cancer Res* **69**, 2734-8 (2009).
4. Tomlins, S.A. et al. Distinct classes of chromosomal rearrangements create oncogenic ETS gene fusions in prostate cancer. *Nature* **448**, 595-9 (2007).
5. Tomlins, S.A. et al. ETS Gene Fusions in Prostate Cancer: From Discovery to Daily Clinical Practice. *Eur Urol* (2009).
6. St John, J., Powell, K., Conley-Lacomb, M.K. & Chinni, S.R. TMPRSS2-ERG Fusion Gene Expression in Prostate Tumor Cells and Its Clinical and Biological Significance in Prostate Cancer Progression. *J Cancer Sci Ther* **4**, 94-101 (2012).
7. Morris, D.S., Tomlins, S.A., Montie, J.E. & Chinnaiyan, A.M. The discovery and application of gene fusions in prostate cancer. *BJU Int* **102**, 276-82 (2008).
8. Klezovitch, O. et al. A causal role for ERG in neoplastic transformation of prostate epithelium. *Proc Natl Acad Sci U S A* **105**, 2105-10 (2008).
9. Tomlins, S.A. et al. Role of the TMPRSS2-ERG gene fusion in prostate cancer. *Neoplasia* **10**, 177-88 (2008).
10. Jenkins, D. Hedgehog signalling: emerging evidence for non-canonical pathways. *Cell Signal* **21**, 1023-34 (2009).
11. Jiang, J. & Hui, C.C. Hedgehog signaling in development and cancer. *Dev Cell* **15**, 801-12 (2008).
12. Varjosalo, M. & Taipale, J. Hedgehog: functions and mechanisms. *Genes Dev* **22**, 2454-72 (2008).
13. Chen, M. et al. Androgenic regulation of hedgehog signaling pathway components in prostate cancer cells. *Cell Cycle* **8**, 149-57 (2009).
14. Cai, C. et al. ETV1 is a novel androgen receptor-regulated gene that mediates prostate cancer cell invasion. *Mol Endocrinol* **21**, 1835-46 (2007).
15. Chen, M. et al. Hedgehog/Gli supports androgen signaling in androgen deprived and androgen independent prostate cancer cells. *Mol Cancer* **9**, 89 (2010).

16. Callewaert, L., Van Tilborgh, N. & Claessens, F. Interplay between two hormone-independent activation domains in the androgen receptor. *Cancer Res* **66**, 543-53 (2006).

17. Buchanan, G. et al. Corepressor effect on androgen receptor activity varies with the length of the CAG encoded polyglutamine repeat and is dependent on receptor/corepressor ratio in prostate cancer cells. *Mol Cell Endocrinol* **342**, 20-31 (2011).

18. Porter, D.C. et al. CDK8 mediates chemotherapy-induced tumor-promoting paracrine activities *Proc Natl Acad Sci USA* (2012).

19. Malumbres, M. et al. Cyclin-dependent kinases: a family portrait. *Nat Cell Biol* **11**, 1275-6 (2009).

20. Westerling, T., Kuuluvainen, E. & Makela, T.P. Cdk8 is essential for preimplantation mouse development. *Mol Cell Biol* **27**, 6177-82 (2007).

21. Donner, A.J., Ebmeier, C.C., Taatjes, D.J. & Espinosa, J.M. CDK8 is a positive regulator of transcriptional elongation within the serum response network. *Nat Struct Mol Biol* **17**, 194-201 (2010).

22. Galbraith, M.D., Donner, A.J. & Espinosa, J.M. CDK8: A positive regulator of transcription. *Transcription* **1**, 4-12 (2010).

23. Knuesel, M.T., Meyer, K.D., Donner, A.J., Espinosa, J.M. & Taatjes, D.J. The human CDK8 subcomplex is a histone kinase that requires Med12 for activity and can function independently of mediator. *Mol Cell Biol* **29**, 650-61 (2009).

24. Knuesel, M.T., Meyer, K.D., Bernecky, C. & Taatjes, D.J. The human CDK8 subcomplex is a molecular switch that controls Mediator coactivator function. *Genes Dev* **23**, 439-51 (2009).

25. Donner, A.J., Szostek, S., Hoover, J.M. & Espinosa, J.M. CDK8 is a stimulus-specific positive coregulator of p53 target genes. *Mol Cell* **27**, 121-33 (2007).

26. Firestein, R. et al. CDK8 is a colorectal cancer oncogene that regulates beta-catenin activity. *Nature* **455**, 547-51 (2008).

27. Belakavadi, M. & Fondell, J.D. Cyclin-dependent kinase 8 positively cooperates with Mediator to promote thyroid hormone receptor-dependent transcriptional activation. *Mol Cell Biol* **30**, 2437-48 (2010).

28. Zhao, X. et al. Regulation of lipogenesis by cyclin-dependent kinase 8-mediated control of SREBP-1. *J Clin Invest* **122**, 2417-27 (2012).

29. Kapoor, A. et al. The histone variant macroH2A suppresses melanoma progression through regulation of CDK8. *Nature* **468**, 1105-9 (2010).

30. Adler, A.S. et al. CDK8 Maintains Tumor Dedifferentiation and Embryonic Stem Cell Pluripotency. *Cancer Res* **72**, 2129-39 (2012).

31. Tsutsui, T., Fukasawa, R., Tanaka, A., Hirose, Y. & Ohkuma, Y. Identification of target genes for the CDK subunits of the Mediator complex. *Genes Cells* (2011).

32. Chen, S., Xu, Y., Yuan, X., Bubley, G.J. & Balk, S.P. Androgen receptor phosphorylation and stabilization in prostate cancer by cyclin-dependent kinase 1. *Proc Natl Acad Sci U S A* **103**, 15969-74 (2006).

33. Chymkowitch, P., Le May, N., Charneau, P., Compe, E. & Egly, J.M. The phosphorylation of the androgen receptor by TFIIH directs the ubiquitin/proteasome process. *EMBO J* **30**, 468-79 (2011).

34. Gordon, V. et al. CDK9 regulates AR promoter selectivity and cell growth through serine 81 phosphorylation. *Mol Endocrinol* **24**, 2267-80 (2010).

35. Jin, F., Claessens, F. & Fondell, J.D. Regulation of androgen receptor-dependent transcription by coactivator MED1 is mediated through a newly discovered noncanonical binding motif. *J Biol Chem* **287**, 858-70 (2012).

36. Liao, S.M. et al. A kinase-cyclin pair in the RNA polymerase II holoenzyme. *Nature* **374**, 193-6 (1995).

37. Barbieri, C.E. et al. Exome sequencing identifies recurrent SPOP, FOXA1 and MED12 mutations in prostate cancer. *Nat Genet* **44**, 685-9 (2012).

38. Tepper, C.G. et al. Characterization of a novel androgen receptor mutation in a relapsed CWR22 prostate cancer xenograft and cell line. *Cancer Res* **62**, 6606-14 (2002).

39. Dehm, S.M. & Tindall, D.J. Alternatively spliced androgen receptor variants. *Endocr Relat Cancer* **18**, R183-96 (2011).

MOLECULAR CANCER

RESEARCH Open Access

Hedgehog/Gli supports androgen signaling in androgen deprived and androgen independent prostate cancer cells

Mengqian Chen[1], Michael A Feuerstein[2], Elina Levina[1], Prateek S Baghel[1], Richard D Carkner[1], Matthew J Tanner[1], Michael Shtutman[1], Francis Vacherot[3], Stéphane Terry[3,4], Alexandre de la Taille[3] and Ralph Buttyan*[1,2]

Abstract

Background: Castration resistant prostate cancer (CRPC) develops as a consequence of hormone therapies used to deplete androgens in advanced prostate cancer patients. CRPC cells are able to grow in a low androgen environment and this is associated with anomalous activity of their endogenous androgen receptor (AR) despite the low systemic androgen levels in the patients. Therefore, the reactivated tumor cell androgen signaling pathway is thought to provide a target for control of CRPC. Previously, we reported that Hedgehog (Hh) signaling was conditionally activated by androgen deprivation in androgen sensitive prostate cancer cells and here we studied the potential for cross-talk between Hh and androgen signaling activities in androgen deprived and androgen independent (AI) prostate cancer cells.

Results: Treatment of a variety of androgen-deprived or AI prostate cancer cells with the Hh inhibitor, cyclopamine, resulted in dose-dependent modulation of the expression of genes that are regulated by androgen. The effect of cyclopamine on endogenous androgen-regulated gene expression in androgen deprived and AI prostate cancer cells was consistent with the suppressive effects of cyclopamine on the expression of a reporter gene (luciferase) from two different androgen-dependent promoters. Similarly, reduction of smoothened (Smo) expression with siRNA co-suppressed expression of androgen-inducible KLK2 and KLK3 in androgen deprived cells without affecting the expression of androgen receptor (AR) mRNA or protein. Cyclopamine also prevented the outgrowth of AI cells from androgen growth-dependent parental LNCaP cells and suppressed the growth of an overt AI-LNCaP variant whereas supplemental androgen (R1881) restored growth to the AI cells in the presence of cyclopamine. Conversely, overexpression of Gli1 or Gli2 in LNCaP cells enhanced AR-specific gene expression in the absence of androgen. Overexpressed Gli1/Gli2 also enabled parental LNCaP cells to grow in androgen depleted medium. AR protein co-immunoprecipitates with Gli2 protein from transfected 293T cell lysates.

Conclusions: Collectively, our results indicate that Hh/Gli signaling supports androgen signaling and AI growth in prostate cancer cells in a low androgen environment. The finding that Gli2 co-immunoprecipitates with AR protein suggests that an interaction between these proteins might be the basis for Hedgehog/Gli support of androgen signaling under this condition.

Background

When detected in the advanced stage, prostate cancer patients are treated with hormone therapies that reduce systemic androgen levels [1-3]. This action palliates the symptoms of metastases, induces regression of metastatic lesions and slows prostate tumor growth [4]. Over time, however, the cancer can recur in a castration resistant form (CRPC) that continues to grow despite the ability of hormone therapy to maintain systemic androgens at castrate levels and deaths from prostate cancer are inevitably associated with complications from this form of disease [5]. Progression of prostate cancer to CRPC appears to involve a reactivation of androgen signaling in the cancer

* Correspondence: rbuttyan@ordwayresearch.org
[1] The Ordway Research Institute, Albany, New York, USA
Full list of author information is available at the end of the article

cells [6-8] and a variety of mechanisms may account for residual androgen signaling in a low androgen environment. These include expression of variant forms of androgen receptor (AR) that are transcriptionally active without ligand [9,10], acquisition of an ability to endogenously synthesize androgens by the tumor cells themselves [11,12] or activation of aberrant AR transcriptional activity through cross-talk with alternate signaling pathways [6,13]. While all of these mechanisms are of interest from a scientific viewpoint, the ones that are readily targetable by drugs are the most clinically imperative as they offer an opportunity to test novel therapies to treat a disease that will kill almost 28,000 men in the United States this year. Recent reports that Abiraterone, an inhibitor of androgen biosynthesis, has clinical effects against castration resistant prostate cancer, reflects a potential treatment advance that might target tumor cell androgen biosynthesis [14]. Here we describe findings that suggest that inhibitors of the Hedgehog/Gli signaling pathway, currently in clinical testing for a variety of cancers, might also have a role for the treatment of castration resistant prostate cancer due to an ability to suppress reactivated androgen signaling in tumor cells.

Hedgehog (Hh) is best known for its role in tissue patterning and morphogenesis during embryonic development [15-18]. In the developmental situation, Hh is a ligand-driven process in which a ligand (referred to as a Hedgehog) engages the Patched 1 (Ptch) receptor on the cell surface and this relieves repression of Smoothened (Smo), a member of the extended G protein coupled receptor family [18]. Smo, when activated, then acts downstream to alter the processing and intracellular localization of Gli transcription factors and to increase Gli-mediated transcriptional activity. The plant-derived alkaloid, cyclopamine, is a prototype for a drug that antagonizes the Hh signaling process [19]. Cyclopamine antagonizes Smo activation and this action explains the teratogenic effects of this drug when it is ingested during pregnancy [20,21].

Aside from its role in development, Hh signaling also supports stem cells in adult tissues [22-24]. However, chronically hyperactive Hh/Gli signaling in adult tissues can be oncogenic, especially for the skin or brain [25,26]. Basal cell carcinoma of the skin and medulloblastoma are models for human Hh-mediated oncogenesis [27]. The aberrant Hh activity in these tumors can result from a loss of the Ptch gene or its function [28,29], mutations in Smo [30] or SuFu [31] that activate endogenous Hh signaling or cryptic overexpression of Gli proteins in tumor cells. For prostate cancer, the question as to whether Hh/Gli signaling plays any role is controversial. Although cyclopamine treatment or Gli knockdown suppresses the *in vitro* growth of prostate cancer cell lines or xenograft tumor growth in mice [32-34], the commonly used prostate cancer cell lines show little, if any, evidence for active canonical Hh signaling activity when they are grown in standard culture conditions [35,36]. For the androgen-growth dependent LNCaP prostate cancer cells and its variants, C4-2 and C4-2B, however, the situation was found to be changed by chronic exposure of these cells to androgen depleted medium. Androgen deprivation highly upregulated the expression and secretion of Hh ligands and increased endogenous expression of Hh/Gli target genes in these cells [37]. The clinical relevance of this observation is supported by the observation that Hh ligand production was found to be increased in prostate tumors by neoadjuvant hormone treatment [38]. Since cyclopamine suppresses the expression of Hh target genes in androgen-deprived LNCaP cells (37), this also suggests that active Hh/Gli signaling activity is awakened by growth under androgen deprived conditions. Others have observed that the high basal expression of Hh/Gli target genes in androgen independent (AI) variants of LNCaP was reduced by cyclopamine [39] and, collectively, the outcomes of these studies imply that Hh signaling in LNCaP cells is restricted to the androgen deprived or AI state. The question remains as to whether active Hh signaling has any biological consequences for the androgen deprived or AI prostate cancer cell. Here we show that, by manipulating the activity of canonical Hh signaling in androgen deprived or AI prostate cancer cells, we also affected the expression of androgen regulated genes and the ability of these cells to grow in the absence of androgen. Our results indicate that Hh/Gli signaling activity supports androgen signaling and AI growth in prostate cancer under low/no androgen conditions. Furthermore, we report that Gli2 protein can bind to AR and this interaction might define the point of cross-talk between the two signaling pathways.

Results and Discussion

Previously we reported evidence for conditional activation of canonical Hh signaling in androgen sensitive human prostate cancer cells by culture in an androgen depleted conditions [37]. Here, we used androgen sensitive parental LNCaP cells, other derivatives of LNCaP that are less dependent on androgens for growth (C4-2, LN3, LNCaP-AI) or androgen responsive VCaP cells that are unrelated to LNCaP, to study the effects of Hh signaling manipulation on the expression of androgen regulated genes in these cells. The LNCaP-AI variant cells that we used were independently isolated in our lab following long-term (> 1 year) culture of parental LNCaP cells in androgen depleted medium. These cells downregulate basal expression of Ptch1 when treated with cyclopamine (Additional file 1, Figure S1) so they appear to have basal-active Hh signaling activity similar to other AI derivatives of LNCaP that were previously described (39).

Initially, we tested the effects of the classic Hh inhibitor drug, cyclopamine on androgen regulated gene expression. All experiments were done using a medium that was depleted for androgens (phenol red-free RPMI with charcoal-stripped FBS) that could be re-supplemented with androgen (R1881) to mimic androgen-stimulated conditions. For parental LNCaP cells grown in androgen supplemented medium (+R1881), the presence of cyclopamine had no significant effects on the expression of four model androgen-regulated genes; KLK2, KLK3 [PSA] and PGC (androgen-inducible), or SHH that is repressed by androgen (Figure 1A). However, when these cells were switched to androgen depleted medium (-R1881) for 3 days, cyclopamine treatment had a distinct dose-dependent effect that further suppressed expression of KLK2, KLK3 and PGC and further increased expression of SHH (Figure 1A). Likewise, cyclopamine significantly downregulated expression of KLK2, KLK3 and PGC in the LNCaP-AI cells that are normally propagated in androgen-free medium, and it upregulated the expression of SHH in these cells (Figure 1A). Cyclopamine also suppressed the expression of KLK2 and KLK3 in VCaP, LN3 or C4-2B cells grown in androgen depleted medium for 3 days (Additional file 1, Figure S2), so the effects of cyclopamine on androgen regulated genes were not limited to LNCaP or its derivatives. We also tested whether a more water-soluble cyclopamine derivative, KAAD-cyclopamine, had a similar effect and found that this drug (at 0.5 or 1 μM) was as effective in reducing KLK2/3 and PGC expression in androgen-deprived LNCaP or LNCaP-AI cells as the 5 or 10 μM dose of cyclopamine (Additional file 1, Figure S3). Finally, we found that cyclopamine also significantly diminished the expression of a reporter gene (luciferase) from either of two androgen dependent promoters (Probasin [PRB] or PGC) in LNCaP or LNCaP AI cells in androgen depleted medium (Figure 1B) in a dose dependent manner. As for endogenous androgen-regulated genes, cyclopamine did not affect the expression of the reporter when cells were cultured in medium supplemented with 10 pM R1881 (data not shown).

Cyclopamine represses Hh signaling through its ability to antagonize Smo activation so we also tested whether Smo expression knockdown (using siRNA) could mimic the effects of cyclopamine with regards to suppression of androgen-inducible gene expression. LNCaP cells were transfected either with control (non-targeting) siRNA or with siRNA targeting AR or Smo and were thereafter maintained in androgen-depleted medium. AR siRNA selectively reduced expression of AR mRNA and protein (Figures 2A, C) but did not reduce the expression of Smo. Likewise, Smo siRNA reduced Smo mRNA levels but did not affect expression of AR mRNA or protein (Figure 2C). However, both AR and Smo siRNAs similarly reduced expression of KLK2 and KLK3 (Figure 2A). Further assessment of the effects of AR or Smo siRNA on expression of a luciferase reporter from either a Gli- or androgen-responsive promoter showed that AR knockdown selectively reduced expression of the androgen reporter but did not affect expression of the Gli reporter (Figure 2B). In contrast, Smo knockdown significantly reduced expression of both the Gli and androgen reporters (Figure 2B) in androgen deprived LNCaP cells. In summary, the above data shows that suppression of Hh signaling with a Smo antagonist, cyclopamine, or by reduction of Smo expression itself, suppresses expression of androgen inducible genes and induces expression of androgen repressed genes, but only when these human prostate cancer cells were cultured in a medium lacking androgen. The fact that Smo knockdown reduced expression of androgen regulated genes but did not affect expression of AR mRNA or protein suggests that some aspect of Hh signaling regulates the activity of the AR rather than its expression.

Since cyclopamine suppressed residual/reactivated androgen gene expression in androgen deprived and AI prostate cancer cells, we also sought evidence that this effect had biological consequences relevant to AI growth. First, we tested whether the presence of cyclopamine might prevent the development of AI cells from parental LNCaP cells chronically maintained in androgen depleted medium. LNCaP cells were seeded onto 10 plates at low density and then 5 plates each were switched to androgen depleted medium supplemented with vehicle (EtOH) or with 5 μM cyclopamine. The media were changed every 3 days. Within 2 months, cell numbers in the cyclopamine-treated cultures were significantly reduced compared to vehicle-treated cultures and most surviving cells in the cyclopamine-treated cultures were shrunken with optically dense nuclei that contrasted with the neuroendocrine cell-like appearance of cells in vehicle-treated cultures (Figure 3A). By the third month, cyclopamine-treated cultures had less than 1% of the cells of vehicle-treated cultures and all remaining cells showed the presence of the optically dense nuclei. No cells remained on cyclopamine-treated plates by 4 months of culture but the cells in the vehicle-treated cultures were increasing in numbers by this time and these cultures gave rise to growing lawns of cells by 6 months that typify AI growth. For overt LNCaP-AI cells, we found that treatment with 5 μM cyclopamine significantly inhibited their growth over a 10 day period (Figure 3B) but when cyclopamine treatment was accompanied by supplemental androgen (10 pM R1881), the growth rate of these cells was no different than vehicle treated cells. This indicates that the presence of androgen can overcome the growth-inhibiting effects of cyclopamine on overt AI cells.

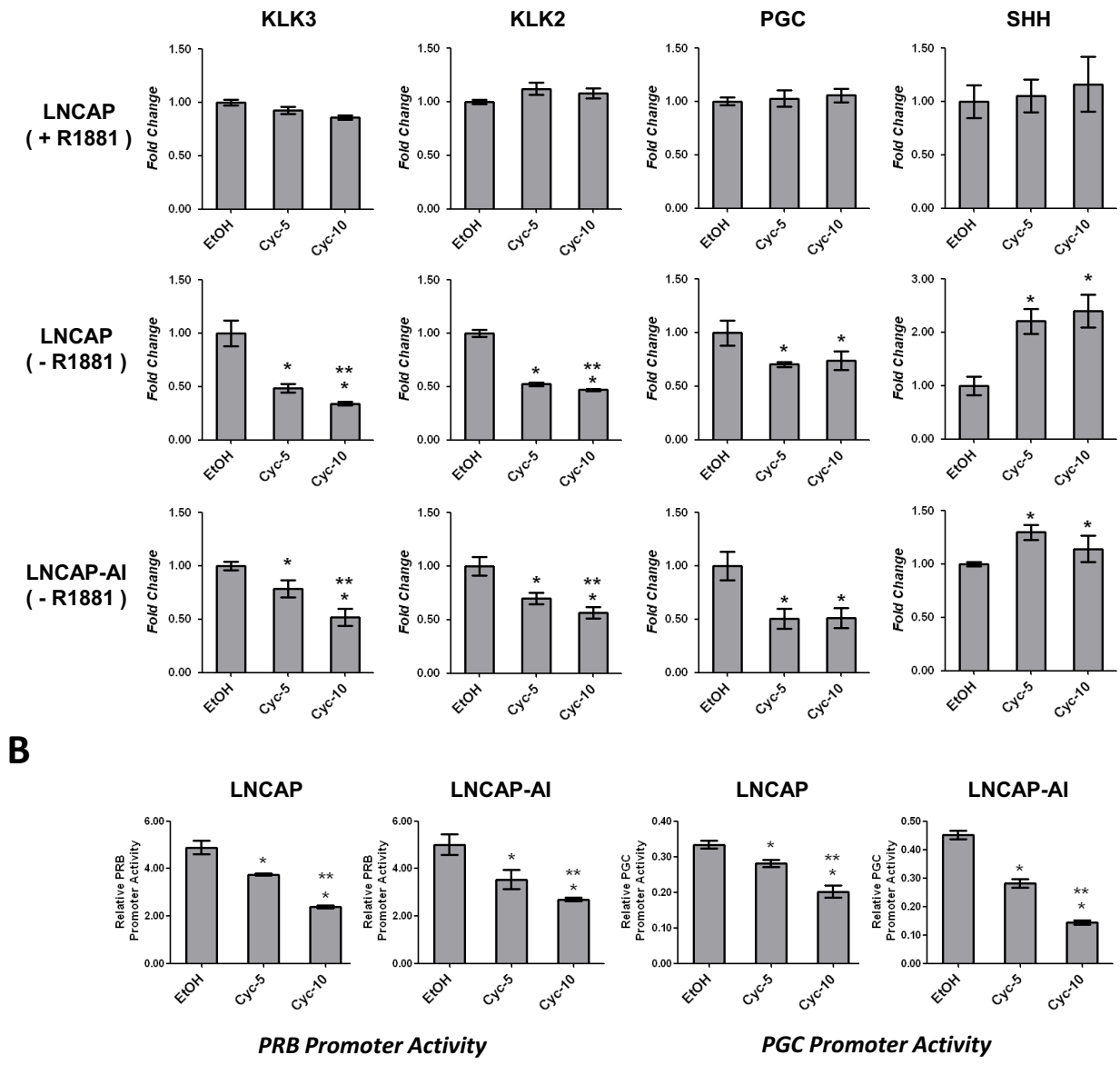

Figure 1 Effect of cyclopamine on androgen signaling in LNCaP cells. (A) Real time qPCR was used to measure relative expression of KLK3, KLK2, PGC or SHH mRNA in androgen-supplemented (+R1881) or androgen deprived (-R1881) LNCaP or in LNCaP-AI cells (-R1881) in the presence of vehicle (EtOH) or with 5 or 10 μM cyclopamine (Cyc-5, Cyc-10) (also see Additional file 2, Table S2). (B) LNCaP or LNCaP-AI cells were infected with probasin (PRB) or PGC promoter reporter vectors along with a CMV-GFP reference reporter and were cultured in androgen depleted medium with vehicle (EtOH) or with 5 or 10 μM cyclopamine (Cyc-5 or Cyc-10) for 72 hrs. Cell extracts were assayed for luciferase that was normalized by GFP intensity. Bars represent the means of triplicate experiments ± S.E. (* = $P < 0.05$ compared to vehicle control; ** = $P < 0.05$ between 5 and 10 μM cyclopamine treatment groups).

Finally, we sought to test whether overexpression of Gli1 or Gli2, transcription factors that lie at the endpoint of the Hh signaling process, might act oppositely to Smo antagonism/inhibition to increase androgen signaling or AI growth when LNCaP cells were grown in androgen free medium. Parental LNCaP cells were transduced with a Gli1- or Gli2- (Gli2ΔN) expressing lentivirus and these cells were compared to control cells transduced with empty virus to determine the effects of Gli overexpression on androgen regulated gene expression and cell growth in androgen depleted medium. The Gli overexpressing variants of LNCaP were also found to express significantly higher levels of KLK2 or KLK3 when compared to control (vector transduced) cells in androgen

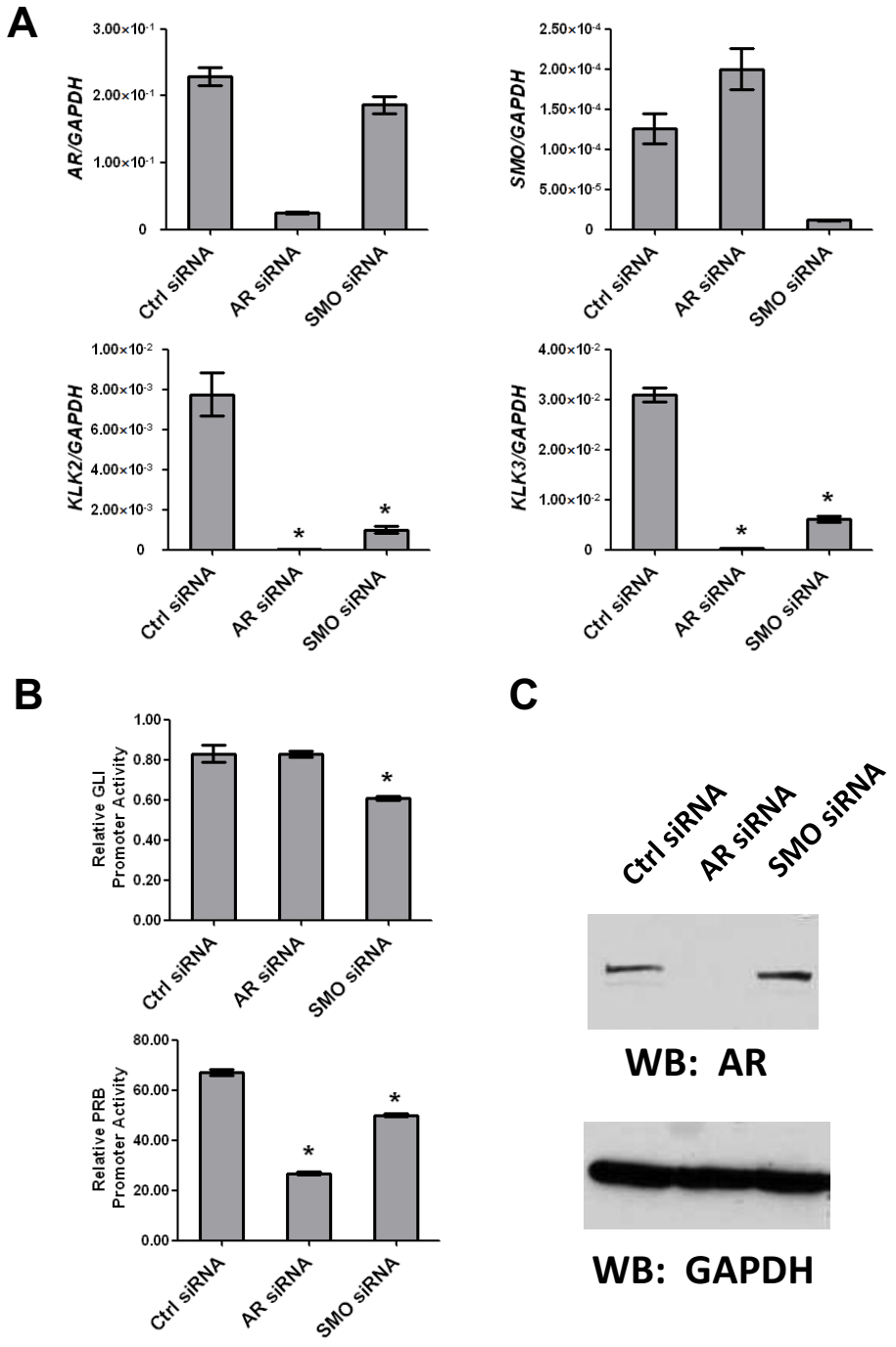

Figure 2 Smo knockdown affects androgen responsive gene expression in androgen-deprived LNCaP cells. (A) LNCaP cells were transfected with control (Ctrl) siRNA, AR or Smo siRNA and grown in androgen-depleted medium for 72 hrs. RNAs were extracted and assayed by real-time qPCR for expression of AR, Smo, KLK2 or KLK3. Bars represent the means of three experiments ± S.E. (* = $P < 0.05$ compared to control siRNA). (B) Cells transfected with siRNA were infected with a Gli or Probasin (PRB) FF luciferase reporter lentivirus along with a CMV-GFP lentivirus control reporter and were switched to androgen-depleted medium for 72 hrs. Cell extracts were quantified for luciferase activity that was normalized by GFP intensity. Bars represent the means of triplicate experiments ± S.E. (* = $P < 0.05$ compared to control siRNA). (C) Western blot shows effects of siRNA on expression of AR protein in cell lysates.

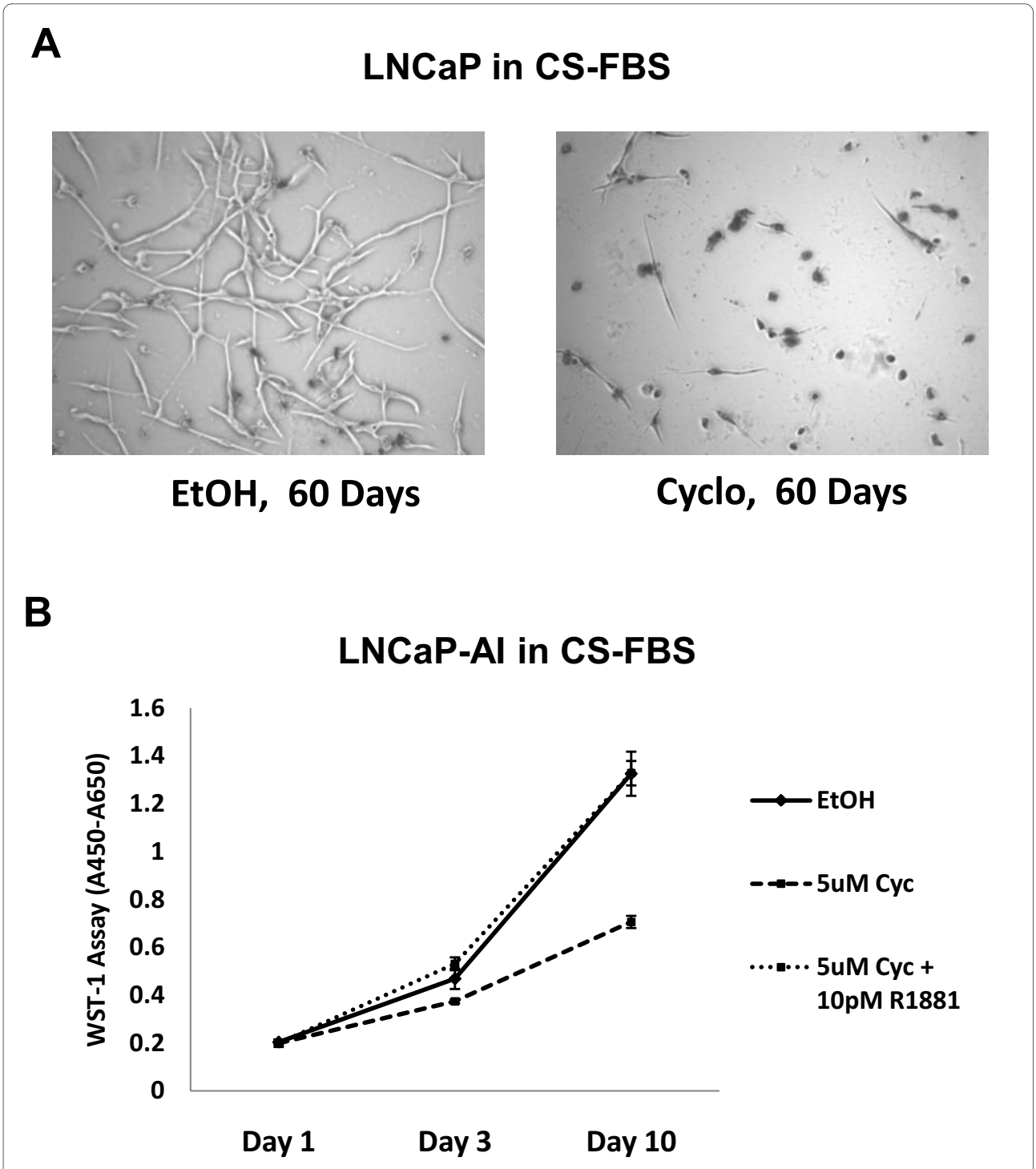

Figure 3 Cyclopamine prevents the development of AI prostate cancer cell growth and suppresses the growth of LNCaP-AI cells. (A) Phase contrast photomicrographs (40×) of LNCaP cells cultured for 60 days in androgen depleted medium (CS-FBS) supplemented with vehicle (EtOH) or 5 μM cyclopamine (Cyclo). Cell numbers in cyclopamine are greatly reduced and cells have optically dense, fragmented nuclei. (B) LNCaP-AI cells grown in androgen-depleted medium (CS-FBS) supplemented with vehicle (EtOH) or 5 μM cyclopamine. Cell numbers were counted at various days as indicated. Points represent the means of triplicate cultures ± S.E.

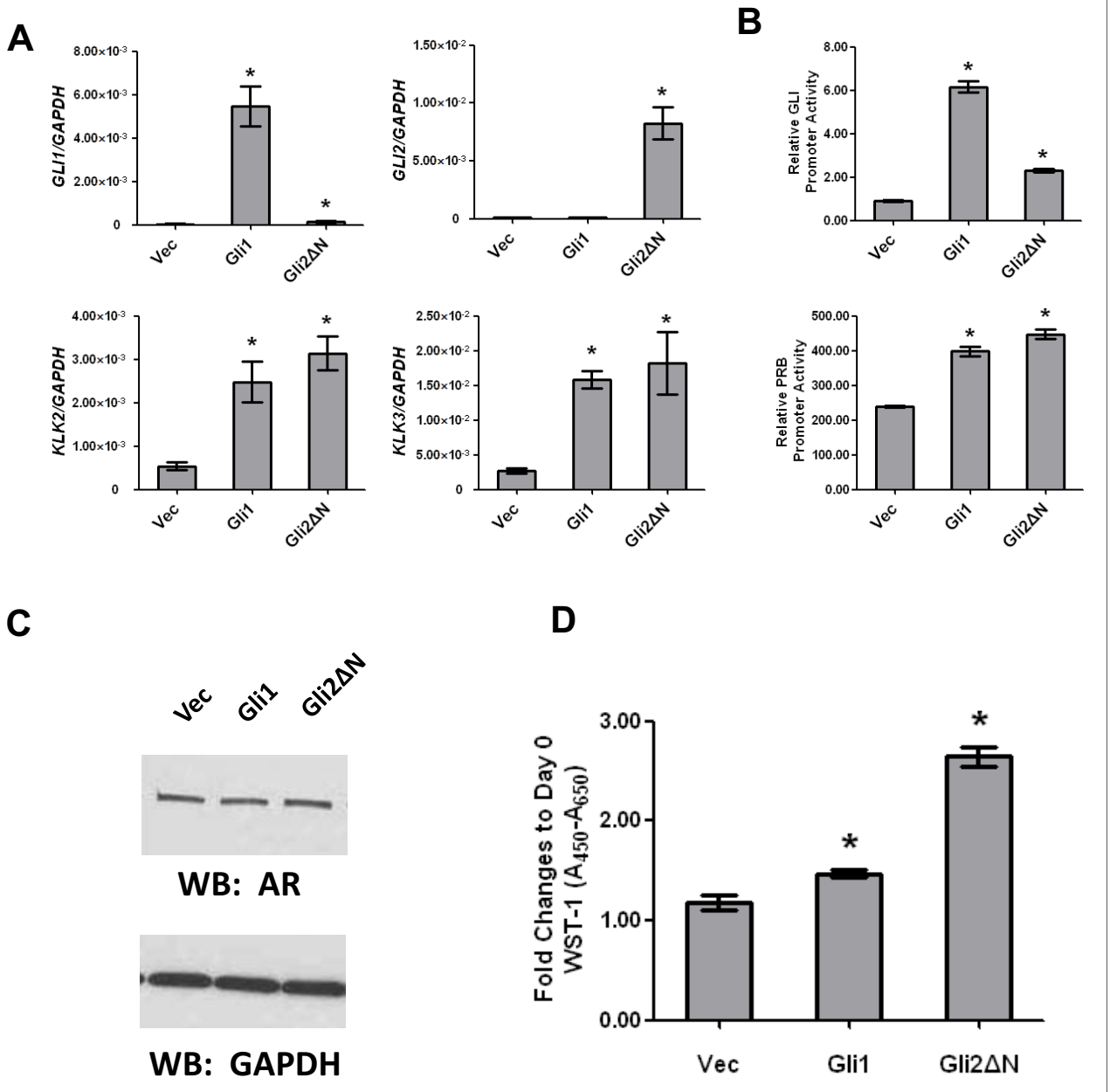

Figure 4 Gli overexpression affects androgen regulated gene expression in androgen-deprived LNCaP cells. (A) RNAs from control (Vec) or Gli1 or Gli2 (Gli2ΔN) overexpressing LNCaP cells cultured in androgen-depleted medium for 72 hrs were assayed by real-time qPCR for expression of Gli1, Gli2, KLK2 and KLK3. Bars represent the means of three experiments ± S.E. (* = P < 0.05 compared to vector control). (B) Cells were infected with a Gli or Probasin (PRB) reporter with CMV-GFP and switched to androgen-depleted medium for 72 hrs. Cell extracts were quantified for luciferase that was normalized by GFP intensity. Bars represent the means of triplicate experiments ± S.E. (* = P < 0.05 compared to vector control). (C) Western blot shows that Gli1 or Gli2 overexpression does not affect expression of AR protein. (D) Gli overexpression enables androgen independent cell growth. Control (Vec) or Gli1 or Gli2 (Gli2ΔN) overexpressing LNCaP cells were cultured in androgen depleted medium for 12 days and growth was measured by WST-1 assay and compared to Day 0. Bars represent the means of three experiments ± S.E. (* = P < 0.05 compared to vector control).

depleted medium (Figure 4A). Gli1 or Gli2 overexpressing LNCaP cells also expressed significantly higher levels of luciferase reporter from both AR and Gli dependent promoters compared to control cells (Figure 4B). Despite higher basal expression of androgen regulated genes, the Gli transduced cells expressed AR protein at equivalent levels to the control cells (Figure 4C) so here again, these effects appear to be independent of changes in AR expression. The Gli transduced LNCaP cells also showed significant increased growth in androgen depleted medium compared to the control cells (Figure 4D), though Gli2 cells appeared to be more robust than Gli1 in

this regard. Regardless of this differential hierarchy, this data shows that Gli function supports androgen regulated gene expression in a low androgen environment as well as AI growth.

The evidence that Gli1 or Gli2 overexpression upregulates androgen inducible gene expression and AI growth of androgen deprived LNCaP cells without affecting AR expression suggests that some function of the Gli proteins may support AR transcriptional activity in a low androgen environment. We tested for some potential direct interaction between these Gli and AR proteins in co-immunoprecipitation experiments. Human 293FT cells were transfected with an expression plasmid for full-length human AR, myc-tagged Gli2 or a combination of these plasmids. Forty-eight hrs later, extracts from the cells were immunoprecipitated with anti-AR or anti-myc antibody and the immunoprecipitates (IPs) were analyzed by Western blot for the presence of AR or myc-tagged Gli2. When the Western blot was probed with anti-AR, we found that AR co-immunoprecipitated with myc-tagged Gli2 only in extracts from cells co-transfected with both plasmids (Figure 5). Similarly, myc-tagged Gli2 was co-immunoprecipitated in the AR IPs from extracts of cells co-transfected with both plasmids (Figure 5). This apparent interaction between Gli2 and AR in the 293FT cells was not diminished by supplementation with 1 nM R1881.

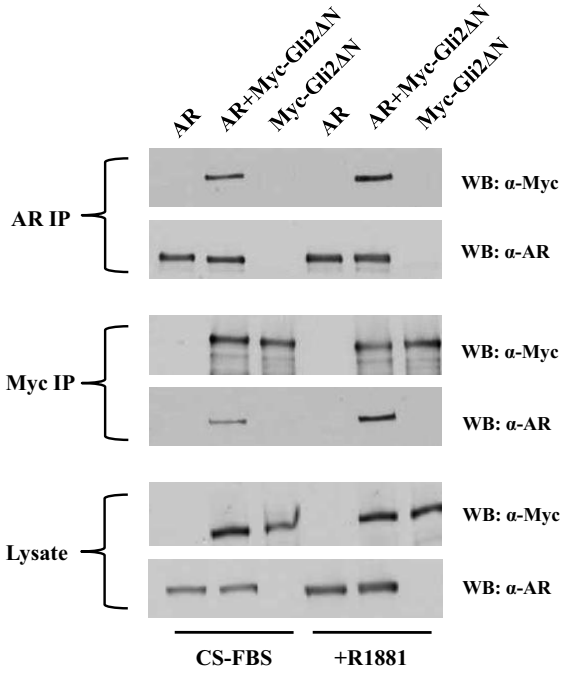

Figure 5 Co-immunoprecipitation of AR with Gli2 protein. Lysates of cells (293FT) transfected with AR, myc-tagged Gli2 (Myc-Gli2ΔN) or both for 48 hrs (under androgen-supplemented [R1881] or depleted [CS-FBS] conditions) were immunoprecipitated with α-AR or α-myc antibody. IPs or lysates were electrophoresed and blotted. The Western blot (WB) was probed with α-AR or α-myc antibody as indicated.

Here we provided evidence that aspects of the canonical Hh signaling pathway can play a role in supporting residual/reactivated androgen signaling in androgen deprived and AI prostate cancer cells and this finding has important implications with regards to both the mechanistic basis for AI growth in the castration resistant prostate cell and for treatment strategies for CRPC in patients. Smo inactivation by cyclopamine, a cyclopamine variant drug (KAAD-cyclopamine) or reduction in Smo expression by siRNA downregulated androgen inducible genes in androgen deprived and AI prostate cancer cells and these findings suggest that some action of Smo might be important for reactivation of androgen signaling under low androgen conditions. The effects of cyclopamine on androgen regulated genes was common to several types of human prostate cancer cell lines grown under androgen deprived conditions so the effect was not limited to LNCaP cells and derivatives. Cyclopamine also suppressed expression of reporter genes from two different androgen responsive promoters in LNCaP cells in androgen depleted medium and these findings support the idea that Smo activity supports AR-mediated transcriptional activity in the androgen deprived state. Finally, the modulatory effects of cyclopamine on AR regulated gene expression were consistent with the effect of this drug on AI growth. Chronic cyclopamine treatment prevented the development of androgen growth independent cells from parental androgen growth-dependent LNCaP cells and significantly inhibited the growth of an overt AI variant of LNCaP. The cyclopamine-mediated growth suppression was reversed by returning a low level of androgen to the cells, providing further evidence that effects of cyclopamine on development and growth of AI cells are based upon cyclopamines' actions on residual androgen signaling.

Smo action ultimately drives transcription by Gli family proteins so we also tested whether exogenous expression of active Gli had opposite effects of cyclopamine or Smo reduction. Here, our findings that Gli1 or Gli2 overexpression enhanced androgen regulated gene expression in androgen depleted medium and enabled AI growth for androgen growth-dependent cells strongly argues that the active Gli proteins resulting from Hh signaling play the most critical role in Hh-support of residual/reactivated androgen signaling regulation. Although the Gli2 overexpressing LNCaP cells exhibited more robust androgen independent growth than the Gli1 overexpressing cells, it is not possible to rank the effectiveness of the Gli proteins on growth control from this study since the cells may be expressing different amounts of transcriptionally active Gli protein. However, the recent report that Gli2 protein was abundantly expressed in tumor cells

from patients with AI (CRPC) prostate cancer [40] does provide further support for the idea that Gli2 protein expression might have a specific role in AI cancer cell growth in CRPC patients and Gli2 may be the preferred target for CRPC treatments.

With regards to the potential mechanism(s) through which Hh/Gli cross-talks to the androgen signaling pathway, it does not appear to involve changes in the expression of AR mRNA or protein as this was not affected by cyclopamine, Smo knockdown or Gli overexpression. However, the finding that Gli2 and AR proteins co-immunoprecipitate when they were co-expressed in 293T cells does suggest that Gli2 might directly interact with AR to influence the expression of AR target genes in the same manner that other co-activator proteins support AR function [41]. Previously Gli2 was shown capable of binding to CREB or to Zic family transcription factor proteins [42,43] so this finding extends the potential repertoire of transcription factors capable of interacting with Gli2. It is of further interest that the interaction between AR and Gli2 proteins was not diminished by androgen supplementation. Therefore, the lack of effects of cyclopamine on androgen regulated gene expression in androgen supplemented LNCaP cells might be due to some additional role of other upstream elements of the Hh signaling pathway that are only manifest in androgen depleted cells. Additionally, we must consider the possibility that Hh/Gli signaling is involved in the endogenous production of androgen (intracrine androgen biosynthesis) that is reportedly associated with AI prostate cancer cells [11], especially since Hh signaling is required for steroidogenesis in the testis and for androgen production by other types of cells [44,45]. This is an aspect that we will test for in future experiments.

Regardless of the mechanism(s) involved, the outcome of this research suggests that Hh/Gli inhibitors offer a specific means to target reactivated androgen signaling in CRPC and to test the idea that inhibition of anomalous androgen signaling in CRPC cells has therapeutic benefit for patients. Although cyclopamine is difficult to use as a therapeutic agent, several pharmaceutical companies are in the process of developing similar drugs that are easier to use in the clinical setting and some of these drugs are through Phase I testing [46]. Therefore, translation of these experimental studies to patients should be able to proceed fairly rapidly. Alternatively, there are non-canonical signaling pathways that increase Gli activity in cancer cells [47] so a clinical focus on Smo antagonists may not be sufficient to deal with all forms of CRPC. Reports of small molecular inhibitors of Hh/Gli signaling that act independently of Smo antagonism [48], suggests that Hh/Gli signaling provides a rich array of targets for the development of more effective treatments for CRPC.

Conclusions

Modulation of Hh signaling in prostate cancer cells by reduction of Smo expression or activity or by overexpression of active Gli proteins affected androgen signaling and the expression of androgen regulated genes in these cells but only when they were cultured in a low androgen medium. The effects of Hh modulation on androgen regulated gene expression in prostate cancer cells were consistent with the coordinate effects on AI cancer cell development and growth in low androgen medium but these effects were reversed by the presence of androgens. Since we have found that Gli2 protein, at least, interacts with the AR protein, the mechanism through which Hh signaling affects AR-dependent gene expression and AI cell growth may involve a direct interaction of AR with Gli proteins.

Methods

Cells and Culture

Human prostate carcinoma cell lines LNCaP and VCaP were obtained from the ATCC (Manassas, VA). LNCaP variants, LN3 or C4-2B were obtained from Curtis Pettaway, M.D. Anderson Cancer Center (Houston, TX) or ViroMed Laboratories (Minnetonka, MN), respectively. The LNCaP-AI variant was derived from parental LNCaP cells after more than one year growth in androgen-depleted medium. Cells were maintained in RPMI-1640 medium with 10% fetal bovine serum (FBS) or switched to phenol red-free RPMI-1640 with 10% charcoal-stripped FBS (CS-FBS) for androgen-depleted conditions as previously described (37). The 293FT cells were obtained from Invitrogen, Inc. (Carlsbad, CA) and were maintained in DMEM with 10% FBS. Synthetic androgen, R1881 (methyltrienolone), was obtained from PerkinElmer Life Sciences (Boston, MA) and was supplemented to androgen-depleted medium at 10 pM where indicated. Cyclopamine was obtained from Enzo Life Sciences, Intl. (Plymouth Meeting, PA) and KAAD-cyclopamine from Toronto Research Chemicals Inc. (North York, ON, Canada). Cultured cells were imaged by a Leica DMIRE2 inverted microscope (Leica Microsystems Inc., Bannockburn, IL).

Generation of LNCaP Lines Stably Expressing Gli Transcription Factors

The ViraPower™ Lentiviral Expression System (Invitrogen) was used for generating replication-incompetent lentiviruses expressing recombinant human Gli1 or Gli2ΔN. All procedures were performed according to the manufacturers' protocols with modifications: 1) cDNAs encoding the full-length human Gli1 and the N-terminal-truncated human Gli2 were cloned from the plasmid GLI K12 [49] and pCS2-MT GLI2(ΔN) [50] (Addgene, Cam-

bridge, MA) into pLenti6 (Invitrogen); 2) For production of lentivirus in 293FT cells, 3 μg of pLenti6-Gli1, pLenti6-Gli2ΔN or pLenti6-Vec (empty vector control) were mixed with 9 μg of ViraPower Packaging Mix, and 36 μl of Lipofectamine-2000 (Invitrogen). The mixture was applied to 2 × 10^6 293FT cells in medium overnight. Transfection medium was removed and fresh medium was added for another 72 hours. Lentivirus containing medium was collected and filtered and used for infections; 3) LNCaP cells were seeded at 50% confluence overnight in preparation for viral transduction. Virus supernatants were added (diluted 1:5 with medium) and 48 hrs later, blasticidin was added at a concentration of 10 μg/ml for selection. Selection was carried out for 2-3 weeks and ~200 colonies were obtained and pooled as stably-expressing sublines, LNCaP-Vec, LNCaP-Gli1, or LNCaP-Gli2ΔN.

RNA Isolation and Reverse Transcription - Real-Time PCR Assays (RT-qPCR)

RNA was isolated from cells using the RNeasy Mini Kit with RNase-Free DNase digestion (QIAGEN, Valencia, CA). Reverse transcription was carried out using SuperScript® III First-Strand Synthesis SuperMix for qRT-PCR (Invitrogen) per the supplier's protocol. Real-time PCR was performed on an ABI 7900HT detection system (Applied Biosystems, Foster City, CA) using RT² SYBR Green/ROX qPCR Master Mix (SABiosciences, Frederick, MD) according to the manufacturer's protocol. The thermal cycling conditions were as previously described (37). The message number of glyceraldehyde-3-phosphate dehydrogenase (GAPDH) was used as the reference for calculating specific gene messages. The sequences of qPCR primers used are listed in Additional file 2, Table S1.

Promoter activity assays

Firefly luciferase reporter vectors under the control of a promoter containing eight repeats of the Gli consensus sequence (pLLRM-GLI-Luc) was generated by sub-cloning the GLI-responsive promoter fragment from pGL3B/8XGliBS-lc-luc (JHU-73, ATCC) into a lentiviral luciferase reporter vector, pLLRM. Reporter vectors with rat probasin (PRB) or human Pepsinogen C (PGC) gene promoters and a reference construct expressing GFP under the CMV promoter (pLLCM-GFP) were prepared (Ohouo *et al*., in preparation) and were used to produce lentiviruses in 293FT cells as described above. Cells were lysed 72 hrs after infection with Passive Lysis Buffer (Promega, Madison, WI) and lysates were analyzed for luciferase activity with the 20/20 n Single Tube Luminometer (Turner Biosystems Inc., Sunnyvale CA) using a Luciferase Assay Kit (Promega). GFP intensity was measured by the BMG FLUOstar Optima plate reader (Imgen Technologies, Alexandria, VA) and used to normalize viral-infection efficiency.

Silencing AR and Smo expression in LNCaP cells by siRNA transfection

The siRNAs specifically targeting human Smo, human AR and control siRNA were purchased from QIAGEN. LNCaP cells were seeded at 70% confluence. siRNAs (40 pM) were mixed with 3 μl of SiLentFect Lipid Reagent for RNAi (Bio-Rad, Hercules, CA) in Opti-MEM I (Invitrogen) for 20 min and this was added to each well in 1.5 ml of medium. Medium was changed 24 hrs after transfection and 72 hrs later, cells were collected for total RNA isolation or lysed in RIPA buffer for Western blot analysis.

Western blot analysis

Cells lysates were assayed for protein and equal amounts of protein were analyzed by Western blot with appropriate antibodies. Each membrane was re-blotted with GAPDH antibody as a control for protein loading. Antibodies were used at the following dilutions: GAPDH at 1:5,000, AR at 1:10,000, and Myc at 1:5,000. Appropriate secondary antibodies conjugated to horseradish peroxidase were used at 1:10,000, and blots were developed by enhanced chemilluminescence reagent (Thermo Fisher Scientific Inc., Rockford, IL). Antibodies to GAPDH or AR receptor (H-280) were from Santa Cruz Biotechnology, Inc. (Santa Cruz, CA). The monoclonal antibody to Myc-tag (4A6) was purchased from Millipore (Billerica, MA).

Cell Proliferation WST-1 Assay

Cells were seeded onto a 96-well plate at a density of 5,000 cells/well in CS-FBS media and were maintained for indicated days (media refreshed every 3 days). At appropriate times, 10 μl WST-1 (Roche, Indianapolis, IN) was added to each well and plates were kept at 37°C for two hrs. Color intensity was read at 450 nm (reference wavelength 650 nm) on the SpectraMax M2 microplate reader (Molecular Devices, Sunnyvale, CA)

Co-immunoprecipitation of AR and Gli2 in 293FT cells

Transfection of 293FT cells (2 × 10^6 cells) with AR or Gli2ΔN plasmids was carried out with Lipofectamine-2000. Cells were lysed in a 1% Triton X-100 lysis buffer with protease inhibitor cocktail (Roche) 48 hrs later. Aliquots of extract containing equal amounts of protein were precipitated at 4°C overnight with 50 μl Dynabeads Protein G (Invitrogen) pre-bound with 5 μg appropriate antibodies. Beads were washed by lysis buffer four times and immunoprecipitated proteins were eluted in 2× SDS sample buffer. The elutant was split into equivalent portions and blotted onto 2 membranes for Western blot analysis.

Statistical Analysis

Expression levels determined using RT-qPCR and promoter activity assay data were compared by comparison of the "means", wherein the data graphed or listed in the table represent the Means ± Standard Error (S.E.). The *Student t-Test* (one-tailed, equal variance) was employed for assessing statistical difference (defined as when $p < 0.05$) between data groups.

List of Abbreviations Used

AI: Androgen Independent (Growth); AR: Androgen Receptor; CRPC: Castration Resistant Prostate Cancer; Cyc: Cyclopamine; EtOH: Ethanol; GAPDH: Glyceraldehyde-3-Phosphate Dehydrogenase; Hh: Hedgehog; KLK2: Kallikreinin 2; KLK3: Kallikreinin 3 (Prostate Specific Antigen); IP: Immunoprecipitate; PRB: Probasin; PGC: Pepsinogen C; PSA: Prostate Specific Antigen; Ptch: Patched 1; SHH: Sonic Hedgehog; Smo: Smoothened; Vec: Vector;

Additional material

Additional file 1 Supplemental Figures S1-S3 and the Legends for the Figures.

Additional file 2 Supplemental Tables S1-S2; List of PCR primer sets used in experiments and real-time data for Figure1.

Competing interests

The authors declare that they have no competing interests.

Authors' contributions

MC conducted the majority of bench experimentation involved in this manuscript and assisted in experimental design and manuscript drafting and editing. MAF conducted some qPCR bench experimentation and reviewed the manuscript for accuracy. EL conducted promoter activity assays and reviewed the manuscript for accuracy. RDC conducted some qPCR bench experimentation and reviewed the manuscript for accuracy. MJT prepared some vectors used in the experimentation and reviewed the manuscript for accuracy. MS prepared some vectors used in the experimentation and reviewed the manuscript for accuracy. FV conducted confirmatory experimentation using the same cells in his laboratory and reviewed the manuscript for accuracy. ST conducted confirmatory experimentation using the same cells in the Vacherot laboratory and reviewed the manuscript for accuracy. AdlT provided funding for the confirmatory experimentation in France and reviewed the manuscript for accuracy. RB provided funding for the experimentation in the US, was responsible for experimental design and data oversight and review and drafted and edited the final manuscript. All authors read and approved the final manuscript.

Acknowledgements

The authors thank the following sources for the funding used to support this work:
NIH/NCI RO1 CA11618 (to RB)
DOD W81XWH-06-01 (to RB)Equinox Foundation of Albany (to RB)
Association pour la Recherche sur le Cancer (to AdlT)
Matthew J. Tanner is an AUA Foundation Research Scholar
Mengqian Chen is the recipient of a DOD Training Award (W81XWH-10-1-0125)

Author Details

[1]The Ordway Research Institute, Albany, New York, USA, [2]Division of Urology, Albany Medical College, Albany, New York, USA, [3]INSERM U955Eq07 and University of Paris XII, Creteil, France and [4]Department of Pathology and Laboratory Medicine, Weil Cornell Medical College, New York, USA

Received: 1 March 2010 Accepted: 26 April 2010
Published: 26 April 2010

References

1. Rini BI, Small EJ: **Hormone-refractory Prostate Cancer.** *Curr Treat Options Oncol* 2002, **3:**437-446.
2. McConnell JD: **Physiologic basis of endocrine therapy for prostatic cancer.** *Urol Clin North Am* 1991, **18:**1-13.
3. Kessler B, Albertsen P: **The natural history of prostate cancer.** *Urol Clin North Am* 2003, **30:**219-226.
4. Miyamoto H, Messing EM, Chang C: **Androgen deprivation therapy for prostate cancer: current status and future prospects.** *Prostate* 2004, **61:**332-353.
5. Attar RM, Takimoto CH, Gottardis MM: **Castration-resistant prostate cancer: locking up the molecular escape routes.** *Clin Cancer Res* 2009, **15:**3251-3255.
6. Grossmann ME, Huang H, Tindall DJ: **Androgen receptor signaling in androgen-refractory prostate cancer.** *J Natl Cancer Inst* 2001, **93:**1687-1697.
7. Agoulnik IU, Weigel NL: **Androgen receptor action in hormone-dependent and recurrent prostate cancer.** *J Cell Biochem* 2006, **99:**362-372.
8. Zhang L, Johnson M, Le KH, Sato M, Ilagan R, Iyer M, Gambhir SS, Wu L, Carey M: **Interrogating androgen receptor function in recurrent prostate cancer.** *Cancer Res* 2003, **63:**4552-4560.
9. Guo Z, Yang X, Sun F, Jiang R, Linn DE, Chen H, Kong X, Melamed J, Tepper CG, Kung HJ, *et al.*: **A novel androgen receptor splice variant is up-regulated during prostate cancer progression and promotes androgen depletion-resistant growth.** *Cancer Res* 2009, **69:**2305-2313.
10. Dehm SM, Schmidt LJ, Heemers HV, Vessella RL, Tindall DJ: **Splicing of a novel androgen receptor exon generates a constitutively active androgen receptor that mediates prostate cancer therapy resistance.** *Cancer Res* 2008, **68:**5469-5477.
11. Locke JA, Guns ES, Lubik AA, Adomat HH, Hendy SC, Wood CA, Ettinger SL, Gleave ME, Nelson CC: **Androgen levels increase by intratumoral de novo steroidogenesis during progression of castration-resistant prostate cancer.** *Cancer Res* 2008, **68:**6407-6415.
12. Dillard PR, Lin MF, Khan SA: **Androgen-independent prostate cancer cells acquire the complete steroidogenic potential of synthesizing testosterone from cholesterol.** *Mol Cell Endocrinol* 2008, **295:**115-120.
13. Zhu ML, Kyprianou N: **Androgen receptor and growth factor signaling cross-talk in prostate cancer cells.** *Endocr Relat Cancer* 2008, **15:**841-849.
14. Attard G, Reid AH, A'Hern R, Parker C, Oommen NB, Folkerd E, Messiou C, Molife LR, Maier G, Thompson E, *et al.*: **Selective inhibition of CYP17 with abiraterone acetate is highly active in the treatment of castration-resistant prostate cancer.** *J Clin Oncol* 2009, **27:**3742-3748.
15. Nusslein-Volhard C, Wieschaus E: **Mutations affecting segment number and polarity in Drosophila.** *Nature* 1980, **287:**795-801.
16. Jacob L, Lum L: **Deconstructing the hedgehog pathway in development and disease.** *Science* 2007, **318:**66-68.
17. Jiang J, Hui CC: **Hedgehog signaling in development and cancer.** *Dev Cell* 2008, **15:**801-812.
18. Varjosalo M, Taipale J: **Hedgehog: functions and mechanisms.** *Genes Dev* 2008, **22:**2454-2472.
19. Cooper MK, Porter JA, Young KE, Beachy PA: **Teratogen-mediated inhibition of target tissue response to Shh signaling.** *Science* 1998, **280:**1603-1607.
20. Chen JK, Taipale J, Cooper MK, Beachy PA: **Inhibition of Hedgehog signaling by direct binding of cyclopamine to Smoothened.** *Genes Dev* 2002, **16:**2743-2748.
21. Wang Y, Zhou Z, Walsh CT, McMahon AP: **Selective translocation of intracellular Smoothened to the primary cilium in response to Hedgehog pathway modulation.** *Proc Natl Acad Sci USA* 2009, **106:**2623-2628.
22. Blank U, Karlsson G, Karlsson S: **Signaling pathways governing stem-cell fate.** *Blood* 2008, **111:**492-503.

23. Lewis MT, Visbal AP: **The hedgehog signaling network, mammary stem cells, and breast cancer: connections and controversies.** *Ernst Schering Found Symp Proc* 2006:181-217.
24. Schugar RC, Robbins PD, Deasy BM: **Small molecules in stem cell self-renewal and differentiation.** *Gene Ther* 2008, **15**:126-135.
25. Oro AE, Higgins KM, Hu Z, Bonifas JM, Epstein EH Jr, Scott MP: **Basal cell carcinomas in mice overexpressing sonic hedgehog.** *Science* 1997, **276**:817-821.
26. Ruiz i Altaba A, Stecca B, Sanchez P: **Hedgehog--Gli signaling in brain tumors: stem cells and paradevelopmental programs in cancer.** *Cancer Lett* 2004, **204**:145-157.
27. Epstein EH: **Basal cell carcinomas: attack of the hedgehog.** *Nat Rev Cancer* 2008, **8**:743-754.
28. Hahn H, Wicking C, Zaphiropoulous PG, Gailani MR, Shanley S, Chidambaram A, Vorechovsky I, Holmberg E, Unden AB, Gillies S, *et al.*: **Mutations of the human homolog of Drosophila patched in the nevoid basal cell carcinoma syndrome.** *Cell* 1996, **85**:841-851.
29. Johnson RL, Rothman AL, Xie J, Goodrich LV, Bare JW, Bonifas JM, Quinn AG, Myers RM, Cox DR, Epstein EH Jr, Scott MP: **Human homolog of patched, a candidate gene for the basal cell nevus syndrome.** *Science* 1996, **272**:1668-1671.
30. Xie J, Murone M, Luoh SM, Ryan A, Gu Q, Zhang C, Bonifas JM, Lam CW, Hynes M, Goddard A, *et al.*: **Activating Smoothened mutations in sporadic basal-cell carcinoma.** *Nature* 1998, **391**:90-92.
31. Cheng SY, Yue S: **Role and regulation of human tumor suppressor SUFU in Hedgehog signaling.** *Adv Cancer Res* 2008, **101**:29-43.
32. Karhadkar SS, Bova GS, Abdallah N, Dhara S, Gardner D, Maitra A, Isaacs JT, Berman DM, Beachy PA: **Hedgehog signalling in prostate regeneration, neoplasia and metastasis.** *Nature* 2004, **431**:707-712.
33. Sanchez P, Clement V, Ruiz i Altaba A: **Therapeutic targeting of the Hedgehog-GLI pathway in prostate cancer.** *Cancer Res* 2005, **65**:2990-2992.
34. Sanchez P, Hernandez AM, Stecca B, Kahler AJ, DeGueme AM, Barrett A, Beyna M, Datta MW, Datta S, Ruiz i Altaba A: **Inhibition of prostate cancer proliferation by interference with SONIC HEDGEHOG-GLI1 signaling.** *Proc Natl Acad Sci USA* 2004, **101**:12561-12566.
35. McCarthy FR, Brown AJ: **Autonomous Hedgehog signalling is undetectable in PC-3 prostate cancer cells.** *Biochem Biophys Res Commun* 2008, **373**:109-112.
36. Zhang J, Lipinski R, Shaw A, Gipp J, Bushman W: **Lack of demonstrable autocrine hedgehog signaling in human prostate cancer cell lines.** *J Urol* 2007, **177**:1179-1185.
37. Chen M, Tanner M, Levine AC, Levina E, Ohouo P, Buttyan R: **Androgenic regulation of hedgehog signaling pathway components in prostate cancer cells.** *Cell Cycle* 2009, **8**:149-157.
38. Azoulay S, Terry S, Chimingqi M, Sirab N, Faucon H, Gil Diez de Medina S, Moutereau S, Maille P, Soyeux P, Abbou C, *et al.*: **Comparative expression of Hedgehog ligands at different stages of prostate carcinoma progression.** *J Pathol* 2008, **216**:460-470.
39. Shaw G, Price AM, Ktori E, Bisson I, Purkis PE, McFaul S, Oliver RT, Prowse DM: **Hedgehog signalling in androgen independent prostate cancer.** *Eur Urol* 2008, **54**:1333-1343.
40. Narita S, So A, Ettinger S, Hayashi N, Muramaki M, Fazli L, Kim Y, Gleave ME: **GLI2 knockdown using an antisense oligonucleotide induces apoptosis and chemosensitizes cells to paclitaxel in androgen-independent prostate cancer.** *Clin Cancer Res* 2008, **14**:5769-5777.
41. Wang G, Wang J, Sadar MD: **Crosstalk between the androgen receptor and beta-catenin in castrate-resistant prostate cancer.** *Cancer Res* 2008, **68**:9918-9927.
42. Dan S, Tanimura A, Yoshida M: **Interaction of Gli2 with CREB protein on DNA elements in the long terminal repeat of human T-cell leukemia virus type 1 is responsible for transcriptional activation by tax protein.** *J Virol* 1999, **73**:3258-3263.
43. Koyabu Y, Nakata K, Mizugishi K, Aruga J, Mikoshiba K: **Physical and functional interactions between Zic and Gli proteins.** *J Biol Chem* 2001, **276**:6889-6892.
44. Yao HH, Whoriskey W, Capel B: **Desert Hedgehog/Patched 1 signaling specifies fetal Leydig cell fate in testis organogenesis.** *Genes Dev* 2002, **16**:1433-1440.
45. Barsoum IB, Bingham NC, Parker KL, Jorgensen JS, Yao HH: **Activation of the Hedgehog pathway in the mouse fetal ovary leads to ectopic appearance of fetal Leydig cells and female pseudohermaphroditism.** *Dev Biol* 2009, **329**:96-103.
46. Von Hoff DD, LoRusso PM, Rudin CM, Reddy JC, Yauch RL, Tibes R, Weiss GJ, Borad MJ, Hann CL, Brahmer JR, *et al.*: **Inhibition of the hedgehog pathway in advanced basal-cell carcinoma.** *N Engl J Med* 2009, **361**:1164-1172.
47. Lauth M, Toftgard R: **Non-canonical activation of GLI transcription factors: implications for targeted anti-cancer therapy.** *Cell Cycle* 2007, **6**:2458-2463.
48. Lauth M, Bergstrom A, Shimokawa T, Toftgard R: **Inhibition of GLI-mediated transcription and tumor cell growth by small-molecule antagonists.** *Proc Natl Acad Sci USA* 2007, **104**:8455-8460.
49. Kinzler KW, Ruppert JM, Bigner SH, Vogelstein B: **The GLI gene is a member of the Kruppel family of zinc finger proteins.** *Nature* 1988, **332**:371-374.
50. Roessler E, Ermilov AN, Grange DK, Wang A, Grachtchouk M, Dlugosz AA, Muenke M: **A previously unidentified amino-terminal domain regulates transcriptional activity of wild-type and disease-associated human GLI2.** *Hum Mol Genet* 2005, **14**:2181-2188.

doi: 10.1186/1476-4598-9-89
Cite this article as: Chen *et al.*, Hedgehog/Gli supports androgen signaling in androgen deprived and androgen independent prostate cancer cells *Molecular Cancer* 2010, **9**:89

Figure S1. ***Effect of cyclopamine on expression of Ptch1 in LNCaP-AI cells.*** LNCaP-AI cells were cultured in the presence of vehicle (EtOH) or in the presence of 5 or 10 μM cyclopamine (Cyc-5 or Cyc-10) for 3 days and extracted for qPCR analysis of Ptch1 mRNA expression. Bars represent the mean of triplicate experiments ± S.E. (*=P<0.05 compared to vehicle control).

Figure S2. ***Effects of cyclopamine on expression of KLK2 or KLK3 in androgen-deprived VCaP, LN3 or C4-2B cells.*** Real time qPCR was used to measure expression of KLK2 or KLK3 (PSA) in androgen-deprived VCaP, LN3 or C42B cells grown in the presence of vehicle (EtOH) or 5 or 10μM cyclopamine (Cyc-5 or Cyc-10) for 72 hrs. Bars represent the mean of triplicate experiments ± S.E. (*=P<0.05 compared to vehicle control; **=P<0.05 between 5 and 10 μM cyclopamine treatment groups).

Figure S3. ***Effect of KAAD-cyclopamine on KLK2, KLK3, PGC in LNCaP or LNCaP-AI cells.*** Real time qPCR was used to measure expression of KLK2, KLK3 (PSA), or PGC in androgen-deprived LNCaP or in LNCaP-AI cells in the presence of vehicle (EtOH) or 0.5μM (For LNCaP) or 1μM (For LNCaP-AI) KAAD-cyclopamine (KAAD-Cyc) for 72 hrs. Bars represent the means of triplicate experiments ± S.E. (*=P<0.05 compared to vehicle control).

Figure S1

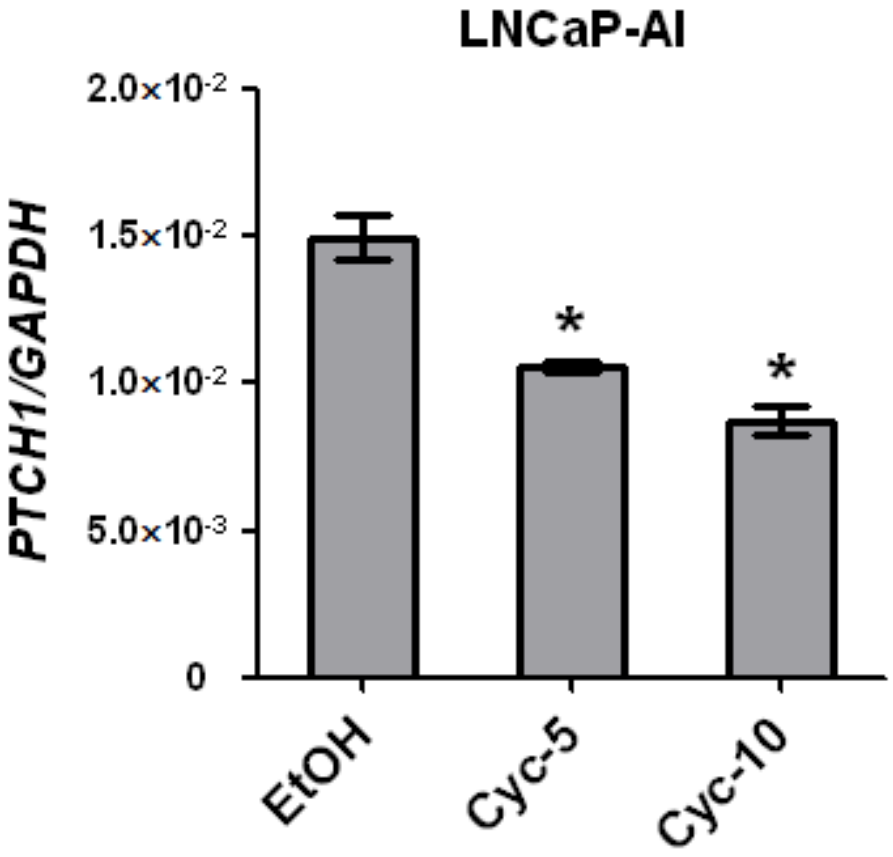
LNCaP-AI
PTCH1/GAPDH
2.0×10-2
1.5×10-2
1.0×10-2
5.0×10-3
0
*
*
EtOH
Cyc-5
Cyc-10

Figure S2

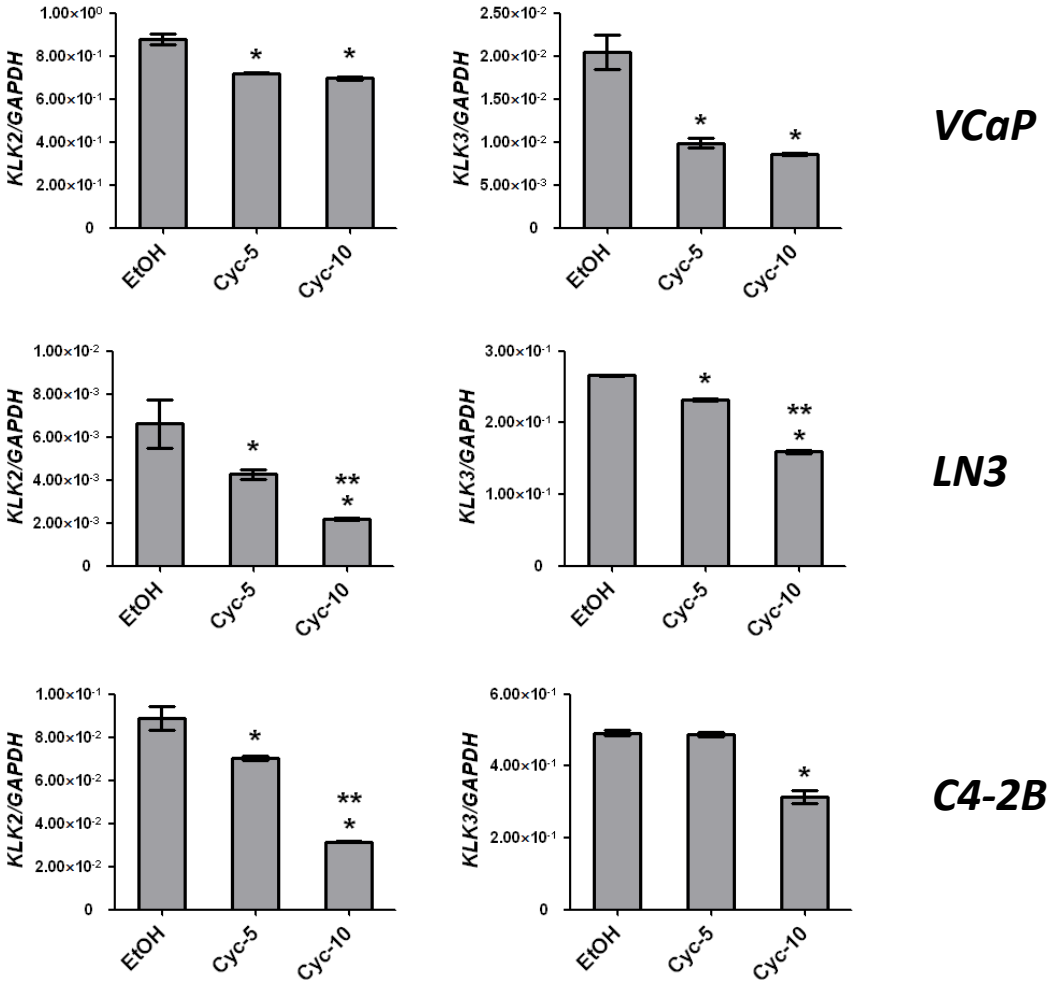

Figure S3

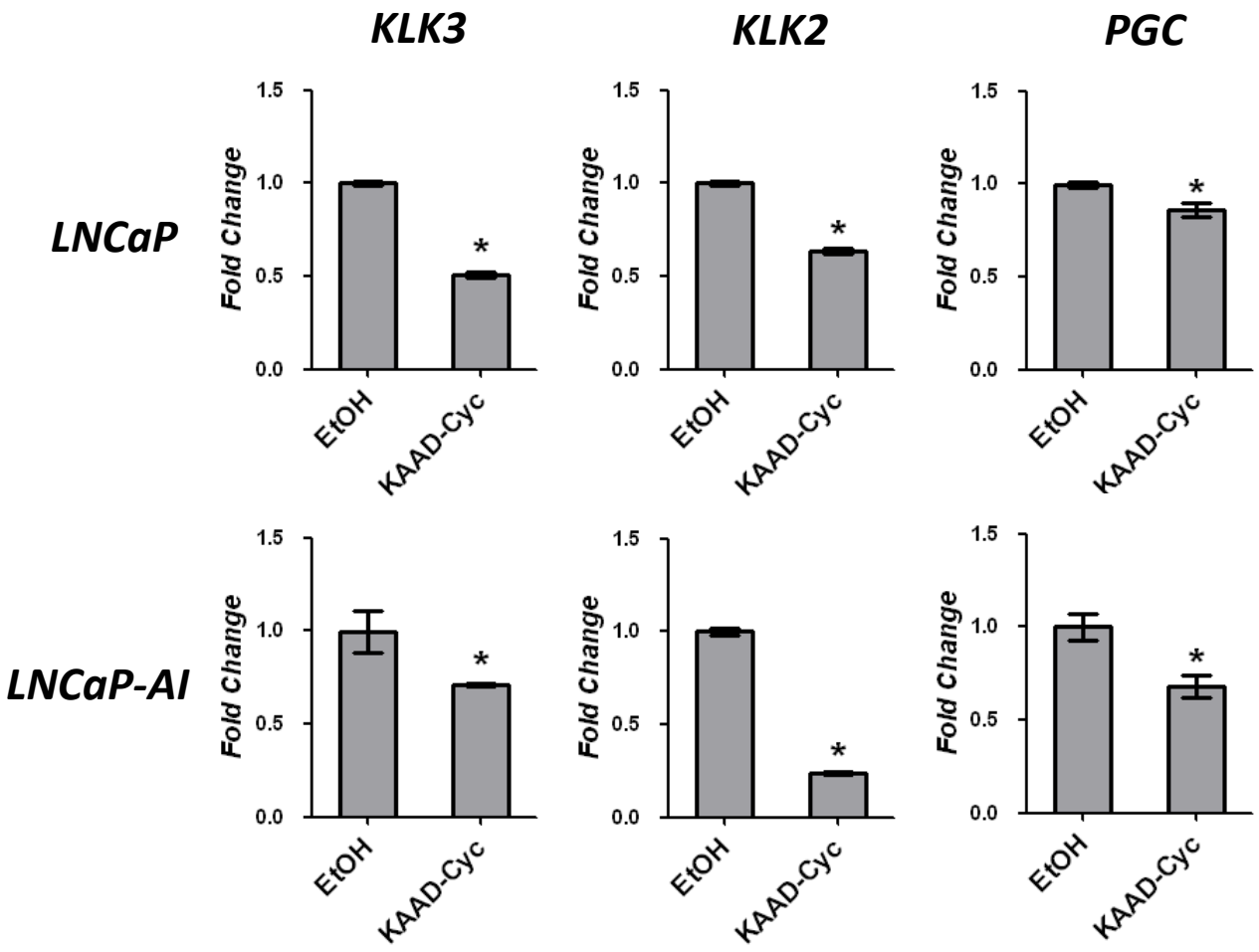
KLK3
KLK2
PGC
LNCaP
LNCaP-AI
Fold Change
1.5
1.0
0.5
0.0
*
EtOH
KAAD-Cyc

Table S1. ***Sequences of gene-specific primers used for quantitative Real-Time PCR.***

GAPDH	5'- CCATCACCATCTTCCAGGAGCG -3'
	5'- AGAGATGATGACCCTTTTGGC -3'
AR	5'-GCAGGAAGCAGTATCCGAAG-3'
	5'-CGTTGTCAGAAATGGTCGAA-3'
KLK2	5'-GCTGCCCATTGCCTAAAGAAG-3'
	5'-TGGGAAGCTGTGGCTGACA-3'
KLK3	5'-AGCTGTGGCTGACCTGAAAT-3'
	5'-GTCCTCACAGCTGCCCAC -3'
PGC	5'- GTCCACCTACTCCACCAATG -3'
	5'- TCACTCAAGCCGAACTCCTG -3'
SHH	5'- CCAAAGCGTTCAACTTGTCC -3'
	5'- TTTAAGGAACTCACCCCCAA -3'
SMO	5'- GTCATTCTCACACTTGGGCA-3'
	5'- AAGCTCGTGCTCTGGTCG -3'
GLI1	5'- GGCTCGCCATAGCTACTGAT -3'
	5'- CCAGCGCCCAGACAGAG -3'
GLI2	5'- AGCAGCAGCAGCAACTGTC -3'
	5'- GAATGGCGACAGGGTTGAC -3'
PTCH1	5'- TCTCCAATCTTCTGGCGAGT -3'
	5'- TGGGATTAAAAGCAGCGAAC -3'

Table S2. ***Expression of androgen-regulated genes evaluated by Real-time PCR.*** Values are means ± SEM. Experimental groups are as indicated: LNCaP and LNCaP-AI cells grown under androgen-supplemented (+R1881) or androgen-depleted (-R1881) conditions were treated with cyclopamine (Cyc) or ethanol vehicle control (EtOH) for 3 days before they were extracted for mRNA expression analysis. a Statistical difference ($p<0.05$) between the cyclopamine-treated group (Cyc) and vehicle (ethanol) control group (EtOH). b Statistical difference ($p<0.05$) between the high-dosage cyclopamine (10μM) and low-dosage cyclopamine (5μM) treated groups.

Experiment Group			**Gene**	**Expression Level Normalized to GAPDH**	**Fold Change**		**Gene**	**Expression Level Normalized to GAPDH**	**Fold Change**
LNCaP (+R1881)	*EtOH*		KLK3	$1.32 \pm 0.03 \times 10^{-1}$	1.00		KLK2	$1.95 \pm 0.04 \times 10^{-2}$	1.00
	Cyc-5 μM		KLK3	$1.22 \pm 0.04 \times 10^{-1}$	0.93		KLK2	$2.19 \pm 0.11 \times 10^{-2}$	1.12
	Cyc-10 μM		KLK3	$1.14 \pm 0.04 \times 10^{-1}$	0.86		KLK2	$2.10 \pm 0.10 \times 10^{-2}$	1.08
LNCaP (-R1881)	*EtOH*		KLK3	$1.87 \pm 0.22 \times 10^{-2}$	1.00		KLK2	$2.25 \pm 0.08 \times 10^{-3}$	1.00
	Cyc-5 μM		KLK3	$9.12 \pm 0.74 \times 10^{-3}$	0.49 [a]		KLK2	$1.18 \pm 0.04 \times 10^{-3}$	0.52 [a]
	Cyc-10 μM		KLK3	$6.39 \pm 0.33 \times 10^{-3}$	0.34 [a,b]		KLK2	$1.06 \pm 0.02 \times 10^{-3}$	0.47 [a,b]
LNCaP-AI (-R1881)	*EtOH*		KLK3	$7.36 \pm 0.28 \times 10^{-6}$	1.00		KLK2	$1.75 \pm 0.15 \times 10^{-5}$	1.00
	Cyc-5 μM		KLK3	$5.76 \pm 0.57 \times 10^{-6}$	0.78 [a]		KLK2	$1.22 \pm 0.09 \times 10^{-5}$	0.70 [a]
	Cyc-10 μM		KLK3	$3.60 \pm 0.55 \times 10^{-6}$	0.52 [a,b]		KLK2	$9.26 \pm 0.80 \times 10^{-6}$	0.57 [a,b]
LNCaP (+R1881)	*EtOH*		PGC	$1.14 \pm 0.04 \times 10^{-4}$	1.00		SHH	$4.05 \pm 0.63 \times 10^{-7}$	1.00
	Cyc-5 μM		PGC	$1.18 \pm 0.09 \times 10^{-4}$	1.03		SHH	$4.26 \pm 0.63 \times 10^{-7}$	1.05
	Cyc-10 μM		PGC	$1.21 \pm 0.07 \times 10^{-4}$	1.06		SHH	$4.71 \pm 1.05 \times 10^{-7}$	1.16
LNCaP (-R1881)	*EtOH*		PGC	$5.38 \pm 0.63 \times 10^{-5}$	1.00		SHH	$6.71 \pm 1.15 \times 10^{-7}$	1.00
	Cyc-5 μM		PGC	$3.80 \pm 0.14 \times 10^{-5}$	0.71 [a]		SHH	$1.48 \pm 0.16 \times 10^{-6}$	2.21 [a]
	Cyc-10 μM		PGC	$4.00 \pm 0.05 \times 10^{-5}$	0.74 [a]		SHH	$1.76 \pm 0.17 \times 10^{-6}$	2.40 [a]
LNCaP-AI (-R1881)	*EtOH*		PGC	$7.07 \pm 0.94 \times 10^{-6}$	1.00		SHH	$1.26 \pm 0.03 \times 10^{-4}$	1.00
	Cyc-5 μM		PGC	$3.59 \pm 0.67 \times 10^{-6}$	0.51 [a]		SHH	$1.63 \pm 0.09 \times 10^{-4}$	1.30 [a]
	Cyc-10 μM		PGC	$3.63 \pm 0.68 \times 10^{-6}$	0.51 [a]		SHH	$1.51 \pm 0.09 \times 10^{-4}$	1.14 [a]

OPEN ACCESS Freely available online

PLoS one

Effects of Androgen Receptor and Androgen on Gene Expression in Prostate Stromal Fibroblasts and Paracrine Signaling to Prostate Cancer Cells

Matthew J. Tanner[1], R. Charles Welliver Jr.[2,3], Mengqian Chen[1], Michael Shtutman[1], Alejandro Godoy[4], Gary Smith[4], Badar M. Mian[2,3], Ralph Buttyan[1,2]*

1 Ordway Research Institute, Albany, New York, United States of America, **2** Division of Urology, Department of Surgery, Albany Medical College, Albany, New York, United States of America, **3** Stratton Veterans Affairs Medical Center, Albany, New York, United States of America, **4** Department of Urology, Roswell Park Cancer Institute, Buffalo, New York, United States of America

Abstract

The androgen receptor (AR) is expressed in a subset of prostate stromal cells and functional stromal cell AR is required for normal prostate developmental and influences the growth of prostate tumors. Although we are broadly aware of the specifics of the genomic actions of AR in prostate cancer cells, relatively little is known regarding the gene targets of functional AR in prostate stromal cells. Here, we describe a novel human prostate stromal cell model that enabled us to study the effects of AR on gene expression in these cells. The model involves a genetically manipulated variant of immortalized human WPMY-1 prostate stromal cells that overexpresses wildtype AR (WPMY-AR) at a level comparable to LNCaP cells and is responsive to dihydrotestosterone (DHT) stimulation. Use of WPMY-AR cells for gene expression profiling showed that the presence of AR, even in the absence of DHT, significantly altered the gene expression pattern of the cells compared to control (WPMY-Vec) cells. Treatment of WPMY-AR cells, but not WPMY-Vec control cells, with DHT resulted in further changes that affected the expression of 141 genes by 2-fold or greater compared to vehicle treated WPMY-AR cells. Remarkably, DHT significantly downregulated more genes than were upregulated but many of these changes reversed the initial effects of AR overexpression alone on individual genes. The genes most highly effected by DHT treatment were categorized based upon their role in cancer pathways or in cell signaling pathways (transforming growth factor-β, Wnt, Hedgehog and MAP Kinase) thought to be involved in stromal-epithelial crosstalk during prostate or prostate cancer development. DHT treatment of WPMY-AR cells was also sufficient to alter their paracrine potential for prostate cancer cells as conditioned medium from DHT-treated WPMY-AR significantly increased growth of LNCaP cells compared to DHT-treated WPMY-Vec cell conditioned medium.

Citation: Tanner MJ, Welliver RC Jr., Chen M, Shtutman M, Godoy A, et al. (2011) Effects of Androgen Receptor and Androgen on Gene Expression in Prostate Stromal Fibroblasts and Paracrine Signaling to Prostate Cancer Cells. PLoS ONE 6(1): e16027. doi:10.1371/journal.pone.0016027

Editor: Paraskevi Giannakakou, Weill Cornell Medical College of Cornell University, United States of America

Received October 12, 2010; **Accepted** December 2, 2010; **Published** January 18, 2011

Funding: This work was funded by the Equinox Foundation and the Medical Research Foundation of Albany, New York. MT was an American Urological Association (URA) Foundation Research Fellow. MC and AG are recipients of Department of Defense (DoD) Prostate Cancer Research Program (PCRP) Postdoctoral Research Fellowships (W81XWH-10-100125 [to MC] and W81XWH-09-1-0330 [to AG]). The funders had no role in study design, data collection and analysis, decision to publish, or preparation of the manuscript.

Competing Interests: The authors have declared that no competing interests exist.

* E-mail: rbuttyan@ordwayresearch.org

Introduction

The prostate gland requires androgenic steroids for development, adult maintenance and function. Males with inactivating mutations in key genes required for androgen metabolism develop only a rudimentary prostate gland [1] and males with inactivating mutations in the androgen receptor (AR) gene, that mediates the effects of androgens, do not develop prostates [2]. Androgens and AR action also play an important role in prostate carcinogenesis. Drugs that inhibit androgen biosynthesis have chemopreventative effects that significantly reduce the risk for developing prostate cancer in men [3] and androgen ablation therapies provide the most clinically useful means for palliative disease control when prostate cancer is detected in the advanced stage [4]. These clinical facts identify the relevance of androgen signaling for prostate biology and carcinogenesis and drive research efforts to characterize the consequences of androgen signaling in prostate cells.

Since the AR protein is an extended member of the nuclear transcription factor that conditionally regulates the expression of genes [5], it is reasonable to expect that the availability of a comprehensive catalogue of androgen regulated genes in prostate cells could significantly contribute to our knowledge of androgen action in the prostate. To this end, the use of contemporary mass gene expression profiling technology, especially involving gene microarrays on Chips, has already greatly expanded the list of known androgen regulated genes in prostate cancer cells [6–9]. Studies using this approach have supported the eventual identification of novel genetic anomalies (ETS gene rearrangements) [10–12] and have helped to identify abnormally active signaling pathways in prostate cancer cells [13,14] that have translational potential for improving prostate cancer diagnostic or treatment strategies. This type of technology, however, has not yet been used to characterize androgen/AR effects on gene expression in prostate stromal cells, despite the extensive evidence that cells

from the prostate stroma actively participate in the processes through which androgens regulate normal or malignant prostate development [15–19]. The principal reason for this deficit is the lack of suitable cultured human prostate stromal cell models that robustly express the AR protein and are demonstrably responsive to the presence of androgens as indicated by changes in gene expression when cultured in an androgen containing medium. Here, we describe our experience in testing some available (benign) human prostate stromal cell models for their responsiveness to androgens *in vitro* and in developing a specific androgen-responsive human prostate stromal cell model (WPMY-AR cells) that was profiled for AR- and androgen-induced changes in gene expression using human gene Chip microarrays. Furthermore, we used this model cell system to test the idea that androgens alter the paracrine signaling environment of a prostate tumor by affecting the output of secreted factors from prostate stromal fibroblasts.

Results

Androgen receptor expression and activity in cultured human prostate stromal cells

Two available immortalized human prostate stromal cell lines, PS-30 and WPMY-1, and non-immortalized primary human prostate stromal cell myofibroblasts were evaluated for AR expression and responsiveness to androgens. None of these cells require androgen for *in vitro* growth, however, WPMY-1 cells were previously reported to grow slightly faster in the presence of synthetic androgen, R1881 [20]. AR expression was assessed in these cells by quantitative RT-PCR (qPCR) and Western blot procedures and was compared to cultured primary human prostate stromal fibroblasts (PrSC) and to LNCaP prostate cancer cells that are models for AR action in prostate cancer (Figure 1A). Of the surveyed cells, LNCaP cells expressed the highest levels of AR mRNA. AR mRNA was expressed at only 3.4% of this level in PS30 cells, 1.1% in PrSC and at slightly over 0.1% of this level in WPMY-1 cells. This pattern was consistent with our Western blot data where we were unable to detect a band corresponding to AR in extracts of either of the immortalized cells or in PrSC though it was readily detected in the extract from LNCaP cells (Fig. 1B). Likewise, when parental WPMY-1 cells were transfected with an androgen responsive reporter vector, they showed no evidence of increased expression of the reporter (luciferase) in response to increasing amounts of DHT (Fig. 1C). However, when WPMY-1 cells were co-transfected with the androgen reporter along with an AR expression vector, the expression of the reporter was significantly increased by the presence of DHT (Fig. 1C). In summary, the low endogenous AR expression in these human prostate stromal cell lines and their unresponsiveness to androgen stimulation suggests that they are poor models for the study of androgen action in stromal cells, but exogenous expression of AR, at least in the WPMY-1 cells, conferred upon these cells an androgen-responsive phenotype that could be more conducive to the study of androgen action.

In order to make WPMY-1 cells more amenable for the study of androgen effects on gene expression, we transduced the cells with human wildtype AR expression lentivirus and then used antibiotic selection to obtain a stable population of AR overexpressing WPMY-1 cells (WPMY-AR). Other WPMY-1 cells were transduced with empty lentivirus and selected under the same conditions to obtain a control cell population (WPMY-Vec). WPMY-AR cells express AR mRNA and protein at a level comparable with androgen-sensitive LNCaP prostate cancer cells (Figs. 1A, B). Immunofluorescence staining using anti-AR antibody showed that AR was mostly in the cytoplasm when these cells were grown in the absence of DHT, although there was light nuclear immunofluorescent staining in most cells (Fig. 1D). In contrast, when WPMY-AR cells were grown in DHT-containing medium, AR immunostaining was exclusively nuclear. The AR expressed in the stable WPMY-AR cells was functional for genomic activation of gene expression. When these cells were transfected with the androgen-reporter, luciferase activity was significantly increased by treatment with DHT whereas DHT did not affect luciferase expression in reporter-transfected WPMY-Vec control cells (Fig. 1E). Otherwise, WPMY-AR cells showed no other overt phenotypic differences when compared to WPMY-Vec control cells; they were indistinguishable by morphology under microscopic observation (not shown) and have similar growth rates in both androgen-free and androgen-containing medium (Fig. 1F).

Comparative Gene Expression Profiling of Prostate Stromal Cell Variants Grown in the Presence or Absence of DHT

WPMY-Vec and WPMY1-AR cells were plated in equal numbers in androgen-free medium for attachment then transferred to fresh medium with or without supplemental 10 nM DHT for 72 hrs. RNAs extracted from biological duplicates of these cultures were labeled then profiled on Affymetrix Human Gene ST 1.0 Array Gene Chips. The microarray expression data was analyzed to identify those genes that were differentially expressed between a given cell under differing conditions (−/+ DHT) or between the two cell types (WPMY-Vec vs WPMY-AR) under equivalent conditions. Using a cutoff of 1.5-fold changes in RNA expression, WPMY-Vec control cells had only 8 genes that were differentially expressed in the presence of DHT and the graph showing the range of these changed genes was generated by the GeneSpring program and is shown in Figure 2A. We attempted to confirm differential expression of these 8 genes in WPMY-Vec DHT-treated/-untreated cells using real-time qPCR to assess expression of each gene on a fresh set of biological duplicate samples but the outcomes of this analysis showed no significant differences in expression for any of them using this method (not shown). Comparison of the gene expression profiles of DHT-treated/-untreated WPMY-AR cells, however, did show much more striking and robust changes in gene expression associated with DHT treatment. DHT affected the expression of 172 individual genes by 1.5-fold or greater (Fig. 2B). However, the majority of these changes (141 or 81.9%) were at the level of 2-fold or greater. In this latter category, more genes were downregulated by DHT (85 genes) than were upregulated (56 genes). The genes that were changed by 2-fold or greater are identified in Table S2 and Table S3. We then chose 10 different genes from these lists, including 6 upregulated and 4 downregulated genes, for further validation by real-time qPCR on a fresh set of RNAs extracted from biological duplicate samples. Each of these selected genes was confirmed to be significantly up- or down-regulated by the presence of DHT in the same manner as the results of the microarray expression analysis (Fig. 3A). Finally, the list of genes (up- and down-regulated) that were changed by 2-fold or greater in the presence of DHT was functionally assessed using the *Pathway Express* software program (http://vortex.cs.wayne.edu/projects.htm) [21] that assigns genes into specific KEGG functional pathways and then the different KEGG pathways associated with these genes were quantitatively prioritized by either of two different parameters: 1) the number of input genes that are assigned to a specific KEGG pathway; or 2) the percent of individual KEGG pathway genes that were present in the input gene set (Table 1). The top 10 KEGG pathway rankings using the two different parameters shared the categories, Pathways in Cancer, Cytokine-Cytokine Receptor Interaction, TGF-β Path-

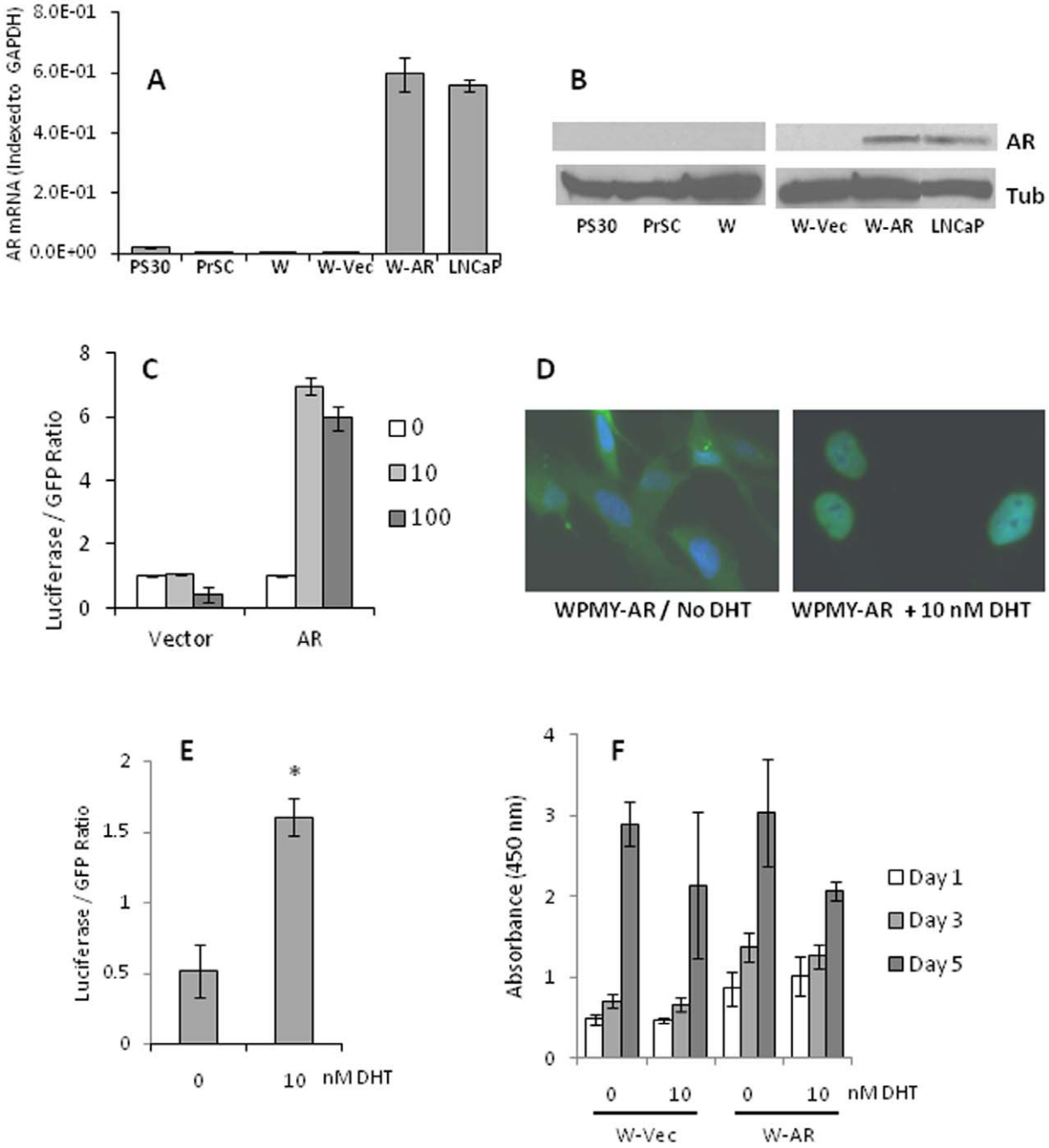

Figure 1. Androgen receptor expression and activity in prostate stromal cell lines. (A) AR mRNA levels in PS30, primary prostate stromal (PrSC), WPMY-1 (W), WPMY-Vec (W-Vec), WPMY-AR (W-AR) or LNCaP cells detected by real-time qPCR of RNAs extracted from the cells. Expression levels are indexed to the expression of GAPDH in each cell line. (B) AR protein (upper lanes) in PS30, PrSC, W, W-Vec, W-AR or LNCaP cells detected by Western blot. The blot was re-probed for GAPDH protein (lower lanes) as a control. (C) Luciferase reporter expression in WPMY-1 cells co-transfected with the ARE-luc reporter vector and a control (empty) vector (Vector) or the pLenti6.2-hAR vector (AR). Luciferase levels are normalized for GFP fluorescence in the same extract as the transfection control marker. (D) Immunofluorescent staining for AR in W-AR cells grown for 72 hrs in the absence (left) or presence (right) of 10 nM DHT. Cells were co-stained with DAPI to identify nuclei. (E) Luciferase activity in W-AR cells transfected with ARE-Luc and GFP in the absence or presence of 10 nM DHT. Luciferase activity was normalized by comparison to GFP levels in the same extract. (F). Growth of W-Vec or W-AR cells in the absence or presence of 10 nM DHT as measured by the WST-1 assay.
doi:10.1371/journal.pone.0016027.g001

way, Wnt Pathway, and Hedgehog Signaling Pathway but other prominent cell signaling pathways were represented in one ranking or the other.

To better determine whether these gene changes associated with DHT treatment were specific for the WPMY-AR cells or whether they might also occur in other human prostate stromal cells with sufficient AR expression, we transiently transfected PS30 cells with the AR expression vector or an empty control vector then treated these cells without or with 10 nM DHT for 72 hrs. RNAs extracted from these cells were tested by real-time qPCR analysis

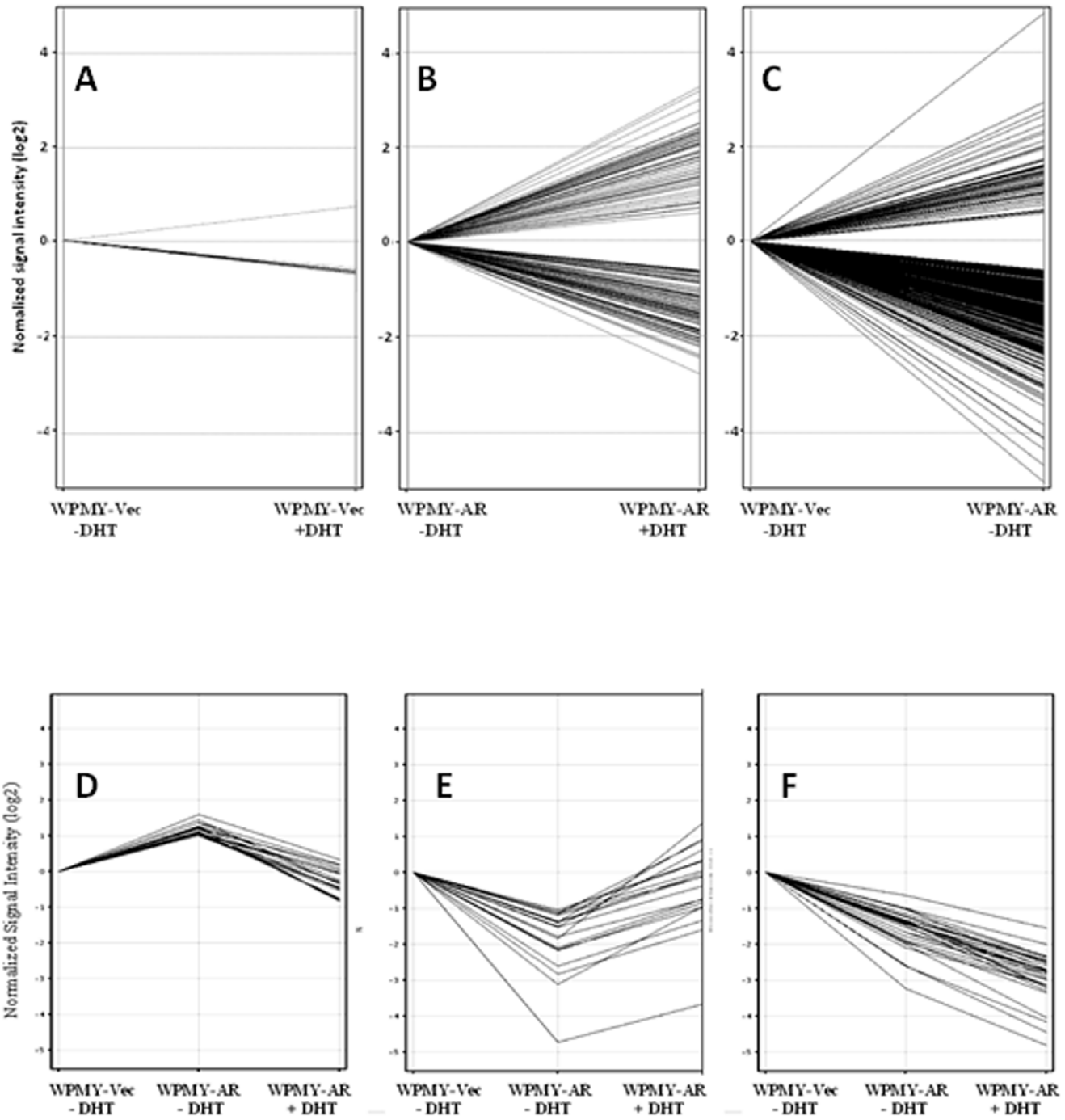

Figure 2. Gene expression changes associated with expression of AR in the absence or presence of DHT in WPMY-1 prostate stromal cells. (A) GeneSpring-generated line plot of significant ($P<0.05$) gene expression differences greater than 1.5-fold in WPMY-Vec cells treated for 72 hrs with 10 nM DHT. (B) GeneSpring-generated line plot of significant ($P<0.05$) gene expression differences greater than 1.5-fold in WPMY-AR cells treated for 72 hrs with 10 nM DHT. (C) GeneSpring-generated line plot of significant ($P<0.05$) gene expression differences greater than 1.5-fold between WPMY-Vec and WPMY-AR cells grown without DHT. (D) GeneSpring-generated line plot showing effect of DHT treatment on genes that were differentially upregulated by 2-fold or greater by AR expression alone (no DHT). (E) GeneSpring generated line plot showing effect of DHT treatment on genes that were differentially down-regulated by 2-fold or greater by AR expression alone (no DHT) and were subsequently up-regulated by 2-fold in the presence of DHT. (F) GeneSpring generated line plot showing effect of DHT treatment on genes that were differentially down-regulated by 2-fold or greater by AR expression alone (no DHT) and were subsequently further down-regulated by 2-fold or greater in the presence of DHT.

doi:10.1371/journal.pone.0016027.g002

for expression of AR and for expression of the same 10 genes that were selectively analyzed in WPMY-AR cells. The outcomes showed that AR was expressed 923-fold more in AR-transfected than in control-transfected PS30 cells. As is shown in Figure 3B, expression of 6 of the other 10 genes were changed in the same manner as for the WPMY-AR cells treated with DHT, whereas 4

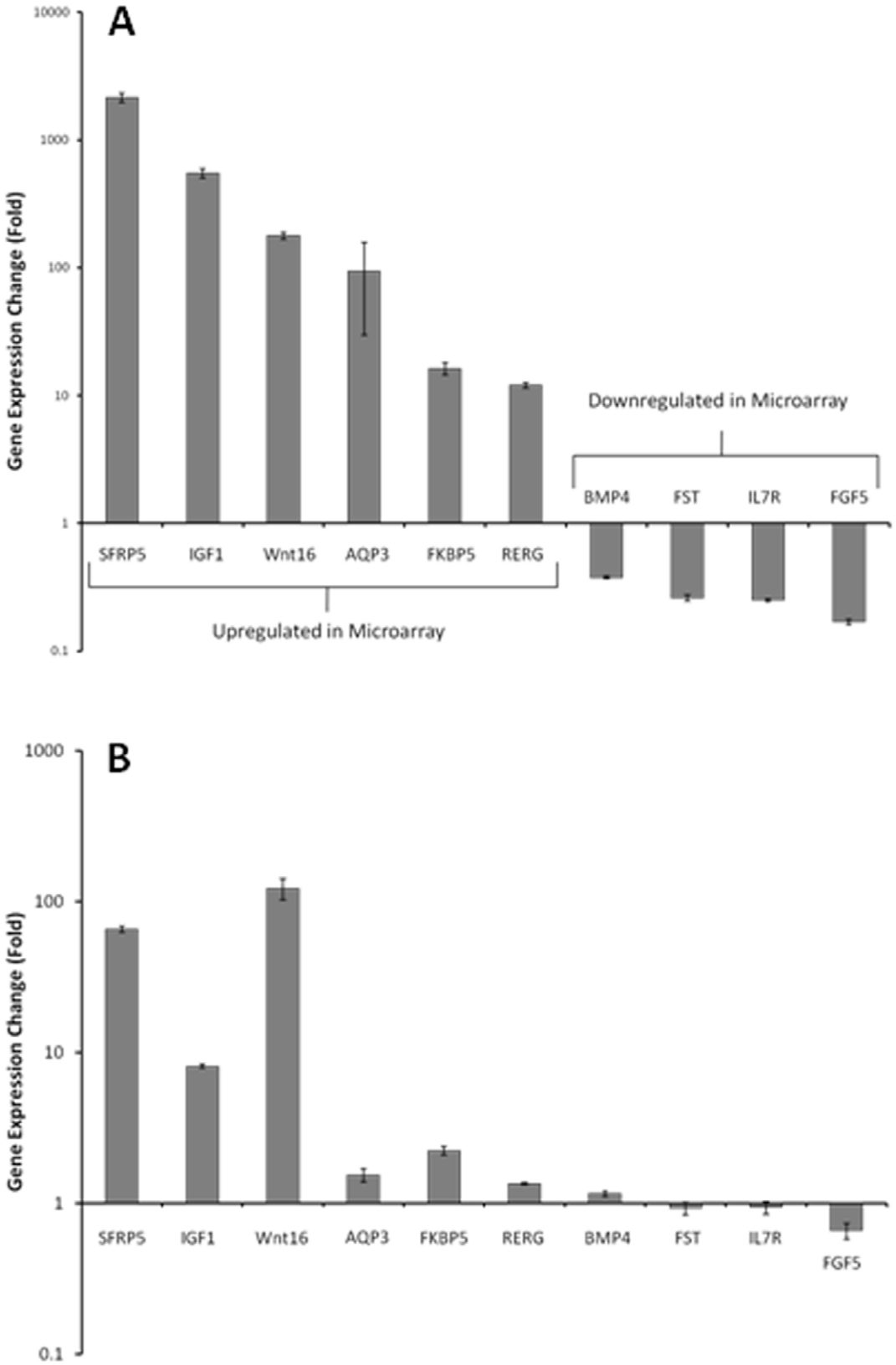

Figure 3. Confirmation of microarray-identified androgen-regulated genes (>2-fold changed) by real-time qPCR measurement. (A). Assessment of individual gene expression changes associated with DHT treatment of WPMY-AR cells by qPCR. Six of the genes in this panel (SFRP-5, IGF-1, Wnt-16, AQP3, FKBP5 and RERG) were identified as DHT-up-regulated genes in the microarray gene expression analysis and four genes (BMP-4, FST, IL7R and FGF5) were identified as DHT-down-regulated genes in the microarray gene expression analysis and these changes were confirmed in the qPCR assay. All changes detected by qPCR were significant changes ($P<0.05$). (B) Assessment of individual gene expression changes associated

with DHT treatment of PS30 cells transiently transfected with pLenti6.2-hAR by qPCR. Measurement of changes in SRBP5, IGF1, Wnt-16, AQP3, FKBP5, RERG and FGF5 were significant ($P<0.05$) whereas changes in BMP-4, FST and IL7R were not significant ($P>0.05$).
doi:10.1371/journal.pone.0016027.g003

of the 10 genes were not significantly changed between untreated- or DHT-treated cells. Finally, the primary human prostate cell fibroblasts were also cultured in medium with or without DHT for 72 hrs and RNAs were extracted for real-time qPCR analysis. The cDNAs from these cells were then assayed for DHT effects on expression of 5 different genes from our panel. The outcomes showed that SFRP5 and IGF1 were upregulated by 1.67- to 1.73-fold by DHT ($p<0.05$) and FGF5 was downregulated by 1.5-fold ($p<0.05$) compared to no-DHT controls whereas expression of FST and Wnt16 was not significantly changed by DHT treatment of these cells.

Gene Expression Changes Associated with Overexpression of AR in WPMY-1 Cells

To determine whether AR expression (in the absence of ligand) affected gene expression in the WPMY cells, we also compared the gene expression profiles between WPMY-Vec and WPMY-AR cells grown without DHT treatment. Remarkably 443 genes were found to be differentially expressed between these cells at a level of 1.5-fold or greater (Fig. 2C) and 374 of these genes are differentially expressed by 2-fold or greater between these cells. In this latter subset, 55 genes were selectively upregulated and 319 genes were selectively downregulated in the AR-expressing cells. It was of further interest to determine how these two categories of genes were subsequently affected by DHT treatment. First, we selected those genes (55) that were upregulated by overexpression of AR (at least 2-fold) in the absence of DHT. Sixty percent of these genes (33 genes) were subsequently downregulated (by 2-fold or greater) again in the presence of DHT (Fig. 2D) whereas the other 40% were either unchanged or changed less than 2-fold by DHT and, therefore, excluded from our analysis. For those 319 genes that were downregulated by 2-fold or greater by AR overexpression alone, 21 genes (6.58%) were subsequently upregulated by 2-fold or greater by the addition of DHT (Figure 2E) whereas 21 genes (6.58%) were further downregulated by 2-fold or greater by the addition of DHT (Figure 2F). The remaining genes in this category (277 or 86.8%) were either unchanged by addition of DHT or were changed less than 2-fold and excluded from our analysis. No genes were upregulated by AR expression then further upregulated by DHT even in those that were affected by DHT<2- to 1.5-fold. In summary, AR overexpression alone in the absence of ligand can induce but mainly repress expression genes in WPMY-1 cells, but these effects were sometimes reversed in the presence of ligand. However, some gene expression changes induced by AR overexpression (gene downregulations) were further augmented by the treatment with the androgen ligand in these cells.

Direct or Indirect Regulation of Genes by DHT

We described here altered patterns of gene expression in prostate stromal cells induced by AR overexpression, with or without ligand, that were based upon measurements of mRNA levels. We sought further to evaluate a small subset of these DHT-regulated genes to determine whether the effects of DHT required intermediary protein synthesis. To this end, trypsinized WPMY-AR cells were allowed to attach overnight and then briefly treated (30 min) with high dose cycloheximide (40 μgs/ml) to block protein synthesis and thereafter switched to medium with or without DHT (10 nM) in the presence of lower dose cycloheximide (10 μgs/ml) for 24 hrs. Control cells were treated similarly except that no cyclohexmide was included at any time. RNAs extracted from these cells were then assessed for expression of select DHT-upregulated (RERG, Wnt16 and SFRP5) or DHT-down-regulated (FST, FGF5 and BMP4) genes. Our results (Figure 4) showed that the DHT effect on expression changes for four of these genes (RERG, WNT16, SFRP5, and FST) were not changed by cycloheximide treatment, whereas the DHT effects on BMP4 and FGF5 expressions were blocked by cycloheximide.

Effects of DHT-Stimulated WPMY1-AR Conditioned Media on LNCaP Cell Growth

Finally, we sought to test whether DHT action in the WPMY-AR model cells might affect the production of secreted factors

Table 1. Hierarchy of KEGG pathway assignments of genes significantly changed by 2-fold or greater in WPMY-AR cells treated with DHT.

Top KEGG Pathway Ranking Based Upon the Number of Input Genes in Pathway	# Input Genes In Pathway	Top KEGG Pathway Ranking Based Upon the Percent Of Pathway Genes in Input	% Pathway Genes in Input
Pathways in Cancer	8	TGF-β Pathway	5.747
Cytokine-Cytokine Receptor Interaction	6	Hedgehog Signaling Pathway	3.509
TGF-β Pathway	5	Hematopoietic Pathway	3.448
MAPK Signaling Pathway	5	Cell Adhesion Molecules	2.985
Regulation of Actin Cytoskeleton	4	Wnt Signaling Pathway	2.632
Wnt Signaling Pathway	4	Focal Adhesion	2.463
Neuroactive-Ligand Receptor Pathway	4	Pathways in Cancer	2.424
Hematopoietic Pathway	3	ECM-Receptor Interaction	2.381
Insulin Signaling Pathway	2	Cytokine-Cytokine Receptor Interaction	2.281
Hedgehog Signaling Pathway	2	Type II Diabetes Mellitus	2.222

Genes listed in Table S1 and Table S2 were input into the gene classification alogorithm found at the Pathway Express site (http://vortex.cs.wayne.edu/projects.htm) to rank the KEGG pathway assignments based upon the numbers of input genes in any given pathway or based upon the percentage of input genes in any given pathway and the rankings were concordant.
doi:10.1371/journal.pone.0016027.t001

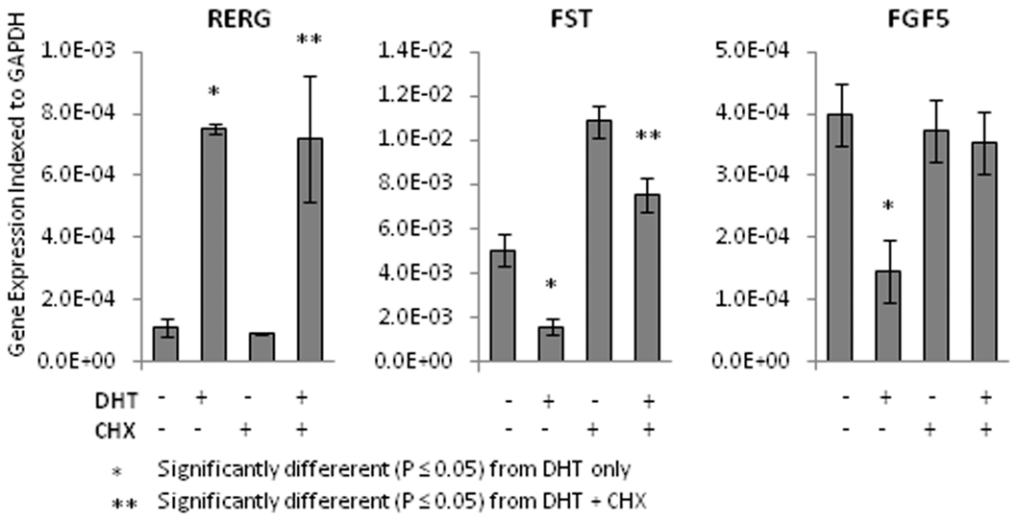

Figure 4. Effects of cycloheximide on gene expression changes in WPMY-AR cells induced by DHT treatment. WPMY-AR cells were pre-treated then treated with cycloheximide in the absence or presence of 10 nM DHT for 24 hrs. RNAs were analyzed by qPCR for the expression of RERG, FST or FGF5, as indicated and expression levels were normalized to GAPDH expression levels.
doi:10.1371/journal.pone.0016027.g004

from these cells that influence prostate cancer cell growth. Three day conditioned medium from 10 nM DHT-treated WPMY-Vec or WPMY-AR cells was diluted 1:1 with fresh medium (with 10 nM DHT) and was then added to fresh LNCaP cells monolayers and the cells were followed for 9 days with medium replacement every 3 days. Growth over this period was measured using the WST-1 assay and results are shown in Figure 5. Treatment with the conditioned medium from the DHT-treated WPMY-AR cells was found to be significantly more growth-stimulatory for LNCaP compared to treatment with conditioned medium from DHT-treated WPMY-Vec cells.

Discussion

Like other tissues, the prostate is made up of an admixture of disparate cell types that are broadly segregated into an epithelial or a stromal compartment based upon their localization with regards to the basement membrane. Prostate cancer cells that are derived from the prostate epithelium have historically provided the models to study how androgen action affects prostate cell gene expression. However, several cell types within the prostate stroma are also known to express AR *in vivo* [22–24] and to contribute to the process(es) through which androgens regulate prostate development and disease yet we know very little regarding the effects of androgen on gene expression in these types of cells. Efforts to this end are hindered by the lack of suitable cultured stromal cell models, especially ones that express AR at sufficient levels to allow the use of contemporary mass gene expression profiling techniques. Here, we attempted to characterize AR expression and androgen signaling activity in two available immortalized prostate stromal cell lines, PS30 and WPMY-1, that were previously reported to express AR [20,25] to assess whether they might provide models to study androgen regulated gene expression. These cells are both classified as myofibroblasts based upon their morphology in culture and their co-expression of vimentin and smooth muscle actin. We found that both types of cells express extremely low levels of AR mRNA and protein and neither cell type responded to DHT treatment after transfection with an androgen-responsive luciferase reporter vector so neither is likely a good model for studying androgen regulated gene expression. However, when the androgen reporter vector was co-transfected with a wildtype AR expression vector, WPMY-1 cells were then able to respond to DHT treatment by upregulating androgen-responsive reporter expression. This result showed that WPMY-1 cells might be made amenable for study of androgen regulated gene expression when provided with exogenous AR. Transduction by an antibiotic-selectable AR-expression lentivirus allowed us then to derive a stable cell line, WPMY-AR, that expressed AR mRNA and protein at a level comparable to LNCaP cells that are often used to model a prostate cancer cells' response to androgens. The WPMY-AR cells relocated AR protein to the nucleus in the presence of DHT and appropriately upregulate luciferase expression from an androgen-regulated reporter vector after

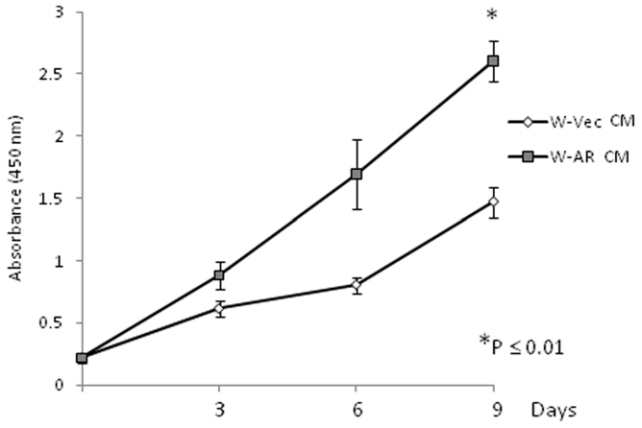

Figure 5. Growth curves of LNCaP cells in the presence of DHT-treated WPMY-AR conditioned medium (W-AR) or DHT-treated WPMY-Vec conditioned medium (W-Vec). Relative cell numbers at different days were estimated by WST-1 assay. Use of conditioned medium from DHT-treated WPMY-AR cells significantly stimulated growth ($P<0.01$, two way ANOVA) of LNCaP cells compared to conditioned medium from DHT-treated WPMY-Vec cells. Slopes of the two growth curves were also significantly different ($P = 0.0181$, Linear Regression Analysis).
doi:10.1371/journal.pone.0016027.g005

DHT treatment identifying that they have a functional androgen signaling system that is consistent with their use in gene expression profiling experiments. It was notable that the WPMY-AR cells were morphologically indistinguishable from parental or control transduced (WPMY-Vec) cells and that their relative growth rate (in the presence or absence of androgen) was not significantly affected by AR overexpression, especially since AR is known to affect prostate cancer cell growth, either when it is expressed endogenously or exogenously [26,27].

The WPMY-Vec and WPMY-AR cells were then profiled for overall gene expression patterns and for changes in these patterns associated with DHT treatment using a gene Chip microarray approach. Our preliminary effort involved a more prolonged treatment with DHT (72 hrs) than is commonly used in studies of prostate cancer cells, but we hoped that this longer treatment period would also allow detection of potential secondary gene expression changes that might be relevant to aspects of cross-talk between prostate stromal and epithelial cells that affect prostate development or prostate cancer cell growth. For the WPMY-Vec control cells, DHT treatment significantly altered the expression of only 8 genes (out of 28,712 gene probe sets on the Chip) and these changes were relatively low, ranging from a 1.62- to 1.74-fold change compared to untreated WPMY-Vec cells. None of these gene changes were subsequently confirmed using a real-time qPCR approach. We feel then, that these minor changes in our control cells (+/− DHT) detected using the gene Chip microarray approach represent the "noise" of the system and that this noise is extremely low and easily filtered using the secondary qPCR approach. In striking contrast, treatment of WPMY-AR cells with DHT altered the expression of 141 different genes by 2-fold or greater. The vast majority of these changes (60.2%) involved gene expression down-regulations associated with DHT treatment. Considering that transcriptionally active (liganded) AR is most often thought of as an inducer of gene expression, this is a remarkably high number of potentially androgen-repressed genes. However, AR/androgen repressed genes have been previously described in prostate cancer cells [8] and one report describing the effects of androgen on gene expression in LNCaP cells did show that androgen treatment suppressed almost as many genes as were induced in these cells [9] so our observation is supported by observations in other prostate cell systems. It was also interesting that a comparison of our DHT-changed stromal cell gene lists with already known androgen-regulated genes assembled at a website resource (http://argdb.fudan.edu.cn/index_info.php, [28] showed that approximately 21% of the genes present on our lists (Tables S1 and S2) were previously described to be "androgen regulated" based on surveyed literature sources mainly involving studies of prostate cancer cells. The presence of this significant percentage of previously described "androgen regulated" genes on our lists supports the idea that we are identifying many genes that may be commonly regulated by liganded AR in many types of prostate cells as well as genes that may be selectively affected by AR/androgens in prostate stromal cells.

With regards to the nature of these DHT-regulated stromal cell genes, there were few, if any genes that are functionally classified as regulators of cell proliferative processes or apoptosis and this is consistent with our observations that androgen treatment did not significantly affect WPMY-AR growth. The assessment of gene function for the up-regulated/down-regulated genes on our lists based upon KEGG pathway designation was remarkable since it identified a predominance of genes that are involved in generic "cancer pathways" that might be relevant to our findings that conditioned medium from DHT-stimulated WPMY-AR cells affected LNCaP cell growth. Likewise, the presence of multiple genes on our list classified as effectors of the cytokine-cytokine receptor signaling, TGF-β, WNT, Hedgehog or MAP Kinase signaling pathways would support previous published studies suggesting that these particular signaling pathways are involved in the cross-talk that occurs between prostate stromal and prostate epithelial/cancer cells in development or disease [29–31]. Categorization of genes on the list based upon Gene Ontology (GO) assignments were also done using the DAVID program and the outcome showed similar categories to those assigned under the KEGG Pathway (not shown). Finally, our limited survey for an effect of cycloheximide on DHT-induced gene changes does support the idea that many of the gene changes we observed are primarily associated with AR functional activity. Yet our ability to identify some DHT-affected genes in WPMY-AR cells that were not changed when cycloheximide was included with DHT treatment also shows that there are genes on our lists that are secondarily regulated by some other protein affected by DHT as we suspected. Use of WPMY-AR cells with a shorter period of DHT treatment may help us sort out the primary affected vs the secondary affected genes and we will attempt this in the future.

For validation purposes, we had selected a panel of 10 genes from our lists of DHT-changed genes and all 10 of them were confirmed to be appropriately changed by DHT using an alternate assay (real-time qPCR). We believe that this limited effort helps validate the outcome of the overall gene expression profiling for androgen regulated prostate stromal cell genes, especially when we focus on those genes that were changed by 2-fold or greater. Moreover, 7 of these 10 select genes were similarly changed by DHT when we assessed a different prostate stromal cell line, PS30, that was only transiently transfected with the AR expression vector. Considering that the WPMY-AR cells were more enriched for AR expressing cells by stable antibiotic selection, it is possible that all 10 genes in this panel would be similarly regulated if we had also selected the AR-expressing PS30 population with antibiotic. However, this outcome still indicates that there is effective similarity in gene changes induced by liganded AR in WPMY-1 cells as in the PS30 cells. Finally, 4 of 7 genes from this panel were also shown to be regulated by DHT in a similar manner in cultured primary prostate stromal cells that were not manipulated to overexpress AR. Although these primary prostate fibroblasts express AR mRNA in a similar range to the PS30 and WPMY-1 cells, we were, at least, able to show that these cells had increased nuclear AR immunostaining (Figure S1) when they were cultured in DHT so this supports the idea that endogenous AR in primary prostate stromal cells operates in a similar fashion to exogenous AR in the WPMY-AR cells.

Finally, our results were noteworthy in that they showed a significant effect of AR expression alone (in the absence of ligand) on the gene expression patterns of WPMY-1 cells. In fact, there were more gene changes between control (WPMY-Vec) cells and WPMY-AR cells than were found after DHT treatment of WPMY-AR cells. The gene changes associated with AR overexpression alone were even more highly repressive than after DHT treatment in that 85% of genes changed by AR overexpression alone involved gene down-regulation. This raises some concern since our immunostaining work showed that most of the AR expressed in WPMY-AR was cytoplasmically localized in the absence of DHT. It may be that the unliganded AR has an effect on gene expression in WPMY-AR cells through a non-genomic pathway similar to that described in some types of prostate cancer cells where the receptor interacts with cell membrane complex to effect gene changes [32]. However, since there was, at least, minimal nuclear AR immunostaining in non-treated WPMY-AR cells that was not observed in cells similarly stained with IgG non-immune antibody, it is more likely that some exogenous AR expressed in WPMY-AR was afforded access to the nucleus where it

affected gene expression patterns through genomic interactions that were significantly more repressive of gene expression in the absence of ligand. Genomic action of unliganded AR in our model is also supported by the fact that addition of DHT reversed or amplified (by at least 2-fold) the expression of 23.5% of the genes that were changed by AR expression alone.

Finally, we attempted to test whether DHT treatment affects the WPMY-AR cells by altering their output of soluble factors that influence prostate cancer cell growth. We chose LNCaP as the cancer test cell model despite the complication introduced by its own endogenous androgen sensitivity because it best represents the phenotype of the prostate cancer cell found in the natural situation. To address the complication of LNCaP's endogenous androgen sensitivity, our approach involved the use of conditioned medium from WPMY-AR or WPMY-Vec cells, both treated with DHT, that was then supplemented into fresh medium that also contained DHT. Here, the WPMY-AR conditioned medium significantly increased the growth of the LNCaP cells over 9 days, compared to the WPMY-Vec conditioned medium. Consistent with this result, we found that LNCaP cells grown for 7 days in WPMY-AR conditioned medium expressed 2.7-fold less p21 mRNA than cells grown in WPMY-Vec conditioned medium. The outcome of this experiment implies either that androgen action selectively increased the production and release of some factor from WPMY-AR cells that increased LNCaP growth or that it reduced the production of some inhibitory factor (made more abundantly by WPMY-Vec cells) that suppresses LNCaP growth. Regardless of the mechanism, this experimental outcome further supports the idea that androgen action in AR-positive fibroblasts has consequences for prostate cancer growth.

In summary, we believe that our efforts represent a step towards identifying the role of AR/androgens in prostate stromal cell gene expression and prostate biology. We have created a cell model to study androgen action on prostate stromal cell genes and we have shown that this model cell responds to androgen stimulation in some ways that are sometimes similar to prostate cancer cells but mostly differs significantly from prostate cancer cells that are usually used to model androgen effects on prostate cell gene expression. In our stromal cell model, AR alone is remarkably suppressive of gene expression, yet this effect does not alter their superficial cell morphology nor growth behavior. We believe this effect involves interaction of AR with the prostate stromal cell genome since it can often be reversed or augmented when ligand is provided. Through the use of gene profiling technology, we have provided a preliminary list of genes that are affected by liganded AR function and several of these same genes are also affected by DHT treatment of other types of prostate stromal cells that overexpress exogenous AR or primary prostate stromal cells that simply express low levels of endogenous AR. Many of the androgen affected genes are associated with signaling pathways involved in stromal-epithelial cell cross-talk in the prostate or with cancer pathways. This latter category of genes affected by androgens was consistent with our findings that conditioned medium from androgen-stimulated WPMY-AR cells more support prostate cancer cell growth than from androgen-stimulated control cells that lack AR. Collectively, the work represents a preliminary characterization that can be extended in the future to significantly enhance our understanding of androgen function in human prostate stromal cells.

Materials and Methods

Cells and Reagents

Benign immortalized human prostate stromal cells, WPMY-1 [20] were obtained from ATCC (Manassas, VA); PS30 cells [25] were kindly provided by Debra Schwinn (Duke University, NC); and primary human prostate stromal fibroblasts were grown from a non-cancerous region of a human prostate [33] as previously described. Human prostate cancer, LNCaP cells, were purchased from ATCC. PS30 and LNCaP cells were cultured in RPMI-1640 (Hyclone, Waltham, MA) supplemented with 10% heat-inactivated fetal bovine serum (FBS) (Hyclone), 1% penicillin/streptomycin, 1% glutamine and 1% sodium pyruvate (Invitrogen, Inc., Carlsbad, NC). WPMY cells were cultured in Dulbecco's Modified Eagle's Medium (Hyclone) supplemented 10% FBS, 1% penicillin/streptomycin, 1% glutamine and 1% sodium pyruvate. Charcoal/dextran-Stripped FBS (CS-FBS) was obtained from Hyclone. Dihydrotestosterone (DHT) was obtained from Sigma-Aldrich Chemical Co. (St. Louis, MO). Mouse monoclonal anti-human AR antibody (clone 441) and mouse monoclonal anti-human GAPDH (clone 6C5) was purchased from Santa Cruz Biosciences (Santa Cruz, CA). Secondary sheep anti-mouse HRP was purchased from GE Healthcare (Pittsburgh, PA). Blastocidin S HCl was purchased from Invitrogen (Carlsbad, CA).

DNA Vectors and Cell Manipulation Procedures

An androgen reporter vector with a synthetic androgen-responsive promoter (ARE-Luc, Panomics, Inc., Fremont, CA) and pEGFP (Clontech, Mountain View, CA) were transfected into cells using Lipofectamine 2000 (Invitrogen). Replication-deficient lentivirus pLenti6-hAR was derived from inserting the human AR full length wildtype cDNA into the pLenti6.2 plasmid (Invitrogen). Conditioned medium containing infectious virus was obtained by transfection of 293FT HEK cells with pLenti6-hAR or pLenti6.2 (empty vector control) along with accessory lentiviral packaging plasmids VSV-G and delta 8.91. Medium from these transfected cells was collected 48 hrs after transfection and was filtered. Stable cells were derived after incubation with viral conditioned medium for 48 hrs followed by selection in fresh medium containing in Blasticidin S (1 μg/ml, Invitrogen) and were pooled and designated WPMY-Vec (pLenti6.2 empty vector) or WPMY-AR (pLenti6-hAR).

Gene Expression Profiling Using Gene Chip Microarrays

WPMY-Vec or WPMY-AR cells were trypsinized then plated at 1×10^6 cells per 60 mm dish in DMEM with 10% FBS. After overnight attachment, medium was removed, plates were rinsed with PBS and fresh medium with 10% CS-FBS, with or without 10 nM DHT was added and cells were maintained for 72 hrs. Cells were washed with PBS then lysed and RNA was purified with the RNEasy Plus micro kit (Qiagen Inc., Valencia, CA) as directed by the manufacturer. Individual RNAs were analyzed for RNA quality by Bioanalyzer Chips (Agilent Technologies, Santa Clara, CA) and only RNAs with a RIN of 9.0 or higher we used for subsequent gene expression profiling. RNA labeling and hybridization were performed by the Ordway Research Institute microarray core facility according to the Affymetrix microarray analysis protocols. Briefly, single-standed cDNA was generated from amplified cRNA with the WT cDNA Synthesis Kit (Affymetrix, Santa Clara, CA) and then fragmented a labeled with the WT Terminal Labeling Kit (Affymetrix) s. Samples were hybridized with Affymetrix Human ST 1.0 Gene Chips (Affymetrix) and scanned on the Affymetrix Gene Chip Scanner 3000 in the core facility and were collected into CEL files for further analysis. Resulting signal analysis was performed with GeneSpring GX 11.0.2 (Agilent Technologies) software. Expressions of genes under different conditions was filtered by statistical significance (students T-test, $p>0.05$) by GeneSpring program and comparisons between treatment groups fold induction cut-offs of 1.5 or 2.0 fold or higher between sample groups.

Quantitative Real-Time RT-PCR

Cells (biological duplicate specimens) were lysed and total RNAs were extracted using the RNeasy mini-kit (Qiagen, Inc.). RNA concentrations were estimated by absorbance at 260 nm. First strand cDNA synthesis was performed using the SuperScript^{TM} III First-Strand Synthesis System for qRT-PCR (Invitrogen). Gene-specific primer sets used for real-time analysis are described in Table S1. Primer sets (0.5 μM) were mixed with cDNA template and RT^{2} SYBR Green Master Mix (SABiosciences, Inc., Frederick, MD), and qRT-PCR was performed using an ABI Prism 7900 HT sequence detector as previously described [34]. Relative mRNA expression levels were determined by comparison to the GAPDH internal control and plotted as ratio to GAPDH expression values.

Luciferase Assay

Cells were seeded into 6 well plates at 2×10^5 cells per well. After overnight attachment, cells were transfected with 2 μg pLenti6.2 or pLenti6-hAR with 1.5 μg ARE-Luc reporter vector and 0.5 μg pEGFP. Medium was changed after 4 hrs to DMEM with 10% CS-FBS with or without DHT as indicated. After 72 hrs, medium was removed, cells were lysed in 1% Triton X-100 buffer, and the lysates analyzed by on a Fluostar Optima fluorometer (for GFP fluorescence) (BMG Labtechnologies, Durham, NC) and on a 20/20n Luminometer (Turner Biosystems, Sunnyvale, CA) after incubation with firefly luciferase reagent (Promega, Inc., Madison, WI). GFP values were used to normalize luciferase values and data is presented as a ratio of luciferase to GFP levels.

Western Blot Analysis

Sub-confluent monolayers of cells were lysed and their protein contents measured as was previously described [35]. SDS-PAGE loading dye was added to aliquots containing equal protein amounts from each cell line, boiled, and loaded onto an SDS-PAGE gel for electrophoresis. The gel was electro-transferred to a nitrocellulose membrane, blocked in 5% milk, and probed with anti-AR or anti-GAPDH antibodies overnight. The membrane was then washed, and probed with sheep anti-mouse conjugated HRP (GE Healthcare, UK). After incubation, the membrane was washed, treated with ECL reagent (SuperSignal West Pico Chemiluminescent Substrate, Thermo Scientific, Rockford, IL) and exposed to x-ray film.

Conditioned Medium Preparation and LNCaP Proliferation Assay

WPMY1-Vector or WPMY1-AR cells were plated at 3×10^6 cells in a 100 mm culture dish in RPMI with 10% CS-FBS supplemented with 10 nM DHT and grown for 72 hrs. Medium was then filtered through a 0.22 μm filter and used immediately or frozen. LNCaP cells were plated in 96 well plates (5000 cells/well) in replicates of 6 wells per assay condition or incubation day. After attachment, medium was removed and wells were treated with a 1:1 mixture of RPMI, 10% CS-FBS, 10 nM DHT with 72 hr conditioned medium from WPMY1-Vector or WPMY1-AR cells. Medium was changed every three days. WST-1 reagent (Dojindo Laboratories, Kamimashiki, Japan) was added to individual wells at 3-day intervals for 9 days and the plate was then read after 90 min at 450 nm (SpectraMax M2 plate reader, Molecular Diagnostics, Sunnyvale, CA). Values for six samples at each point were averaged and data was graphed as absorbance vs time.

Statistical Analysis

Comparative quantitative RT-PCR outcomes from DHT-untreated/-treated cells were based on 2 measurements each from 2 biological replicate samples and they were statistically analyzed using a two-tailed students T test. Differences in the growth curves of LNCaP cells grown with different conditioned stromal cell medium were analyzed by two-way Anova and curve slopes were compared using multiple linear regression analysis. P Values of ≤0.05 were considered significant.

Supporting Information

Table S1. Primers used in qPCR reactions.
(DOC)

Table S2. Genes up-regulated by 2-fold or greater in WPMY-AR cells by DHT. * Indicates genes that were previously described to be androgen regulated.
(DOC)

Table S3. Genes down-regulated by 2-fold or greater in WPMY-AR cells by DHT. * Indicates genes that were previously described to be androgen regulated.
(DOC)

Figure S1. AR expression in primary human prostate stromal cells (PrSC). Primary cell cultures were incubated for 24 h with vehicle (ethanol, a) or 10 nM DHT (b) before immunostaining. Cells were fixed in 4% p-formaldehyde and stained with a polyclonal antibody against AR (Santa Cruz Biotechnology). Immunoreaction was visualized using a secondary antibody HRP-conjugated. AR nuclear translocation was evident in presence of DHT (b-c, high magnification picture). Images a and b: x300. Image c: x600.
(TIF)

Author Contributions

Conceived and designed the experiments: RB MJT MC AG. Performed the experiments: MJT RCW MC MS AG. Analyzed the data: MC MJT MS RB. Contributed reagents/materials/analysis tools: MS AG GS BM. Wrote the paper: RB MJT MC AG GS. Obtained permission for use of cell line: RB AG.

References

1. Imperato-McGinley J, Zhu YS (2002) Androgens and male physiology the syndrome of 5alpha reductase-2 deficiency. Mol Cell Endocrinol 198: 51–59.
2. Sultan C, Lumbroso S, Poujol N, Belon C, Boudon C, et al. (1993) Mutations of androgen receptor gene in androgen insensitivity syndromes. J Steroid Biochem Mol Biol 46: 519–530.
3. Thompson IM, Tangen CM, Goodman PJ, Lucia MS, Klein EA (2009) Chemoprevention of prostate cancer. J Urol 182: 499–507.
4. Miyamoto H, Messing EM, Chang C (2004) Androgen deprivation therapy for prostate cancer: current status and future prospects. Prostate 61: 332–353.
5. Dehm SM, Tindall DJ (2006) Molecular regulation of androgen action in prostate cancer. J Cell Biochem 99: 333–344.
6. Xu LL, Su YP, Labiche R, Segawa T, Shanmugam N, et al. (2001) Quantitative expression profile of androgen-regulated genes in prostate cancer cells and identification of prostate-specific genes. Int J Cancer 92: 322–328.
7. Velasco AM, Gillis KA, Li Y, Brown EL, Sadler TM, et al. (2004) Identification and validation of novel androgen-regulated genes in prostate cancer. Endocrinol 145: 3913–3924.
8. Jariwala U, Prescott J, Jia L, Barski A, Pregizer S, et al. (2007) Identification of novel androgen receptor target genes in prostate cancer. Mol Cancer 6: 39.
9. Ngan S, Stronach EA, Photiou A, Waxman J, Ali S, et al. (2009) Microarray coupled to quantitative RT-PCR analysis of androgen-regulated genes in human LNCaP prostate cancer cells. Oncogene 28: 2051–2063.

10. Liu AY, Corey E, Vessella RL, Lange PH, True LD, et al. (1997) Identification of differentially expressed prostate genes: increased expression of transcription factor ETS-2 in prostate cancer. Prostate 30: 145–153.
11. Petrovics G, Liu A, Shaheduzzaman S, Furusato B, Sun C, et al. (2005) Frequent overexpression of ETS-related gene-1 (ERG1) in prostate cancer transcriptome. Oncogene 24: 3847–3852.
12. Rostad K, Mannelqvist M, Halvorsen OJ, Oyan AM, Bo TH, et al. (2007) ERG upregulation and related ETS transcription factors in prostate cancer. Int J Oncol 30: 19–32.
13. Hu P, Greenwood CM, Beyene J (2007) Integrative analysis of gene expression data including an assessment of pathway enrichment for predicting prostate cancer. Cancer Inform 2: 289–300.
14. Gorlov IP, Byun J, Gorlova OY, Aparicio AM, Efstathiou E, et al. (2009) Candidate pathways and genes for prostate cancer: a meta-analysis of gene expression data. BMC Med Genomics 2: 48.
15. Gleave M, Hsieh JT, Gao CA, von Eschenbach AC, Chung LW (1991) Acceleration of human prostate cancer growth in vivo by factors produced by prostate and bone fibroblasts. Cancer Res 51: 3753–3761.
16. Cunha GR, Hayward SW, Wang YZ (2002) Role of stroma in carcinogenesis of the prostate. Differentiation 70: 473–485.
17. Cunha GR, Hayward SW, Wang YZ, Ricke WA (2003) Role of the stromal microenvironment in carcinogenesis of the prostate. Int J Cancer 107: 1–10.
18. Cunha GR, Ricke W, Thomson A, Marker PC, Risbridger G, et al. (2004) Hormonal, cellular, and molecular regulation of normal and neoplastic prostatic development. J Steroid Biochem Mol Biol 92: 221–236.
19. Chung LW, Baseman A, Assikis V, Zhau HE (2005) Molecular insights into prostate cancer progression: the missing link of tumor microenvironment. J Urol 173: 10–20.
20. Webber MM, Trakul N, Thraves PS, Bello-DeOcampo D, Chu WW, et al. (1999) A human prostatic stromal myofibroblast cell line WPMY-1: a model for stromal-epithelial interactions in prostatic neoplasia. Carcinogenesis 20: 1185–1192.
21. Draghici S, Khatri P, Tarca AL, Amin K, Done A, et al. (2007) A systems biology approach for pathway level analysis. Genome Res 17: 1537–1545.
22. Sar M, Lubahn DB, French FS, Wilson EM (1990) Immunohistochemical localization of the androgen receptor in rat and human tissues. Endocrinol 127: 3180–3186.
23. Iwamura M, Abrahamsson PA, Benning CM, Cockett AT, di Sant'Agnese PA (1994) Androgen receptor immunostaining and its tissue distribution in formalin-fixed, paraffin-embedded sections after microwave treatment. J Histochem Cytochem 42: 783–788.
24. Mohler JL, Chen Y, Hamil K, Hall SH, Cidlowski JA, et al. (1996) Androgen and glucocorticoid receptors in the stroma and epithelium of prostatic hyperplasia and carcinoma. Clin Cancer Res 2: 889–895.
25. Price DT, Rudner X, Michelotti GA, Schwinn DA (2000) Immortalization of a human prostate stromal cell line using a recombinant retroviral approach. J Urol 164: 2145–2150.
26. Snoek R, Cheng H, Margiotti K, Wafa LA, Wong CA, et al. (2009) In vivo knockdown of the androgen receptor results in growth inhibition and regression of well-established, castration-resistant prostate tumors. Clin Cancer Res 15: 39–47.
27. Heisler LE, Evangelou A, Lew AM, Trachtenberg J, Elsholtz HP, et al. (1997) Androgen-dependent cell cycle arrest and apoptotic death in PC-3 prostatic cell cultures expressing a full-length human androgen receptor. Mol Cell Endocrinol 126: 59–73.
28. Jiang M, Ma Y, Chen C, Fu X, Yang S, et al. (2009) Androgen-responsive gene database: integrated knowledge on androgen-responsive genes. Mol Endocrinol 23: 1927–1933.
29. Shigemura K, Isotani S, Wang R, Fujisawa M, Gotoh A, et al. (2009) Soluble factors derived from stroma activated androgen receptor phosphorylation in human prostate LNCaP cells: roles of ERK/MAP kinase. Prostate 69: 949–955.
30. Basanta D, Strand DW, Lukner RB, Franco OE, Cliffel DE, et al. (2009) The role of transforming growth factor-beta-mediated tumor-stroma interactions in prostate cancer progression: an integrative approach. Cancer Res 69: 7111–7120.
31. Li X, Placencio V, Iturregui JM, Uwamariya C, Sharif-Afshar AR, et al. (2008) Prostate tumor progression is mediated by a paracrine TGF-beta/Wnt3a signaling axis. Oncogene 27: 7118–7130.
32. Unni E, Sun S, Nan B, McPhaul MJ, Cheskis B, et al. (2004) Changes in androgen receptor nongenotropic signaling correlate with transition of LNCaP cells to androgen independence. Cancer Res 64: 7156–7168.
33. Cano P, Godoy A, Escamilla R, Dhir R, Onate SA (2007) Stromal-epithelial cell interactions and androgen receptor-coregulator recruitment is altered in the tissue microenvironment of prostate cancer. Cancer Res 67: 511–519.
34. Mechlin CW, Tanner MJ, Chen M, Buttyan R, Levin RM, et al. (2010) Gli2 expression and human bladder transitional carcinoma cell invasiveness. J Urol 184: 344–351.
35. Chen M, Tanner M, Levine AC, Levina E, Ohouo P, et al. (2009) Androgenic regulation of hedgehog signaling pathway components in prostate cancer cells. Cell Cycle 8: 149–157.

Published in final edited form as:
Expert Rev Endocrinol Metab. 2011 ; 6(3): 453–467. doi:10.1586/EEM.11.2.

The hedgehog/Gli signaling paradigm in prostate cancer

Mengqian Chen[1], **Richard Carkner**[1], and **Ralph Buttyan**[1,2,†]

[1] Ordway Research Institute, 150 New Scotland Avenue, Albany, NY 12208, USA

[2] Division of Urology, Albany Medical College, New York, NY, USA

Abstract

Hedgehog is a ligand-activated signaling pathway that regulates Gli-mediated transcription. Although most noted for its role as an embryonic morphogen, hyperactive hedgehog also causes human skin and brain malignancies. The hedgehog-related gene anomalies found in these tumors are rarely found in prostate cancer. Yet surveys of human prostate tumors show concordance of high expression of hedgehog ligands and Gli2 that correlate with the potential for metastasis and therapy-resistant behavior. Likewise, prostate cancer cell lines express hedgehog target genes, and their growth and survival is affected by hedgehog/Gli inhibitors. To date, the preponderance of data supports the idea that prostate tumors benefit from a paracrine hedgehog microenvironment similar to the developing prostate. Uncertainty remains as to whether hedgehog's influence in prostate cancer also includes aspects of tumor cell autocrine-like signaling. The recent findings that Gli proteins interact with the androgen receptor and affect its transcriptional output have helped to identify a novel pathway through which hedgehog/Gli might affect prostate tumor behavior and raises questions as to whether hedgehog signaling in prostate cancer cells is suitably measured by the expression of Gli target genes alone.

Keywords

androgen signaling; cyclopamine; Gli; hedgehog signaling; prostate cancer; Smoothened

Hedgehog is a cell signaling pathway that is most noted for its involvement in embryogenesis. Increasingly, however, inappropriate hedgehog signaling activity is viewed as a factor in the development of human malignancy or as a factor involved in the acquisition of aggressive behaviors of already established tumors. Here, we review the putative role(s) of hedgehog signaling in prostate cancer. Prostate cancer is a challenging disease. Aside from the fact that it is the most common malignancy in males [201], it poses a considerable dilemma for public health policy with regards to screening and treatment issues. For example, even though prostate tumors are highly invasive, the majority of afflicted men experience prostate cancer as an indolent disease with a relatively slow growth rate [1]. Since it is usually diagnosed in men older than 60 years of age, the predominance of

[†]Author for correspondence: Tel.: +1 518 641 6980, Fax: +1 518 641 6305, rbuttyan@gmail.com.

Financial & competing interests disclosure

Mengqian Chen is supported by a training grant from the United States Department of Defense Prostate Cancer Research Program (W81XH-10-1-0125). Ralph Buttyan is supported from grants from the NIH (RO1-CA11618) and from the United States Department of Defense Prostate Cancer Research Program (W81XH-10-1-0493 and W81XH-06-0061). The authors have no other relevant affiliations or financial involvements with any organization or entity with a financial interest in or financial conflict with the subject matter or materials discussed in the manuscript apart from those disclosed.

No writing assistance was utilized in the production of this manuscript.

indolent prostate cancers raises questions regarding the effectiveness of prostate cancer screening efforts that are thought to identify large numbers of patients for whom the treatment may be more problematic than the tumor itself [2–4]. These facts highlight the need to understand the etiology that underlies the widespread occurrence of this disease and to develop a means of selectively diagnosing those individuals with aggressive form(s).

Second, despite the abundance of indolent disease, owing to its overall high incidence, prostate cancer remains a leading cause of deaths from cancer in males [201]. This fact underscores the urgent need for better treatments for aggressive disease to reduce mortality. Finally, prostate cancer, in contrast to other human tumors, is distinguished by a remarkable dependency on androgenic steroids. Prostate cancer only arises in androgenically intact males, and, when it has spread beyond the confines of the prostate, is commonly treated by hormone therapies that deplete the patient's circulating androgenic steroid levels [5,6]. Acutely, androgen-deprivation therapies can be very effective and can shrink both primary and metastatic tumors while slowing the growth of residual tumor cells. With chronic use, however, hormone therapies usually prove to be only palliative; patients often recur with more aggressive, therapy-resistant disease referred to as castration-recurrent prostate cancer (CRPC). Here the tumor cells are able to grow in a seemingly androgen-independent (AI) fashion, and this is the form of disease that is overwhelmingly associated with mortality from prostate cancer. Despite the behavior of CRPC tumor cells, whose ability to grow in castrated patients mimics that of tumor cells that are completely independent of androgens, there is extensive evidence that CRPC cells continue to utilize their endogenous androgen signaling system to drive their growth. Enigmatically, CRPC cells are believed to have acquired the means to maintain androgen signaling even though the systemic milieu of androgens in hormone-treated patients remains at castrate levels [7–10]. Since CRPC cells remain dependent on androgen signaling to grow, this dilemma creates the need to understand the molecular process(es) that enables androgen receptors (ARs) in the CRPC cell to continue to function in the castrate state. With this understanding, one might be able to conceive novel therapies to block the aberrant androgen signaling in CRPC cells and extend the effectiveness of hormone therapies in prostate cancer patients.

The focus here on hedgehog signaling in prostate cancer is driven by a growing body of literature that addresses various aspects of the signaling pathway in prostate tumors or in prostate cancer cells. This literature is plagued by contradictions and controversies, yet, despite these problems, many investigators continue to view the outcomes of their studies as evidence for involvement of hedgehog signaling in prostate cancer development or in progression of prostate tumors to aggressive or therapy-resistant states. In addition, the outcomes of some preclinical studies that showed some striking effects of hedgehog-blocking drugs in animal-based prostate cancer models give strong reason to consider whether these types of therapies might have value for prostate cancer patients, especially those with advanced or therapy-resistant disease.

Abnormal (hyperactive) hedgehog signaling is already established as being a causative factor for the development of certain types of human skin, brain or cartilage-derived tumors (discussed later). Likewise, published literature supports the potential for the involvement of particular aspects of the hedgehog/Gli signaling pathway in other types of solid human tumors [11–16]. Here we will first address the nature of hedgehog signaling in normal and malignant cells and then describe the literature that suggests that hedgehog contributes to human prostate cancer. We will address the controversy as to whether hedgehog acts in prostate cancer exclusively through a paracrine response pathway that mimics hedgehog's involvement in normal prostate development or whether there is any evidence to support a role for a tumor cell-autonomous hedgehog signaling process similar to that found in basal cell carcinoma and medulloblastoma. We will also propose that hedgehog may have an

especially important role in promoting progression of prostate cancer to CRPC, at least partly through Gli support of abnormal androgen signaling in tumors of patients subsequent to hormone therapy. While the validation of any potential relationship between prostate cancer and hedgehog signaling or between the aggressive behavior of the CRPC cell and hedgehog/Gli might provide insights leading to improved diagnosis or prognostication of disease behavior, the availability of several small-molecule inhibitors that target hedgehog/Gli at different parts of the signaling pathway suggests that the most useful benefit in exploring this relationship lies in the possibility of using hedgehog-/Gli-blocking drugs to treat patients with advanced or hormone therapy-resistant disease who currently have a very poor prognosis.

Overview of the hedgehog signaling pathway

Hedgehog is considered to be one of the primal cell signaling pathways that regulates cell fate during embryonic development (along with Wnt and Notch) [17–19]. Originally discovered in *Drosophila*, this signaling pathway acquired its name from the distinctive morphology of certain mutant larvae that were characteristically short and stubby with clustered, spine-like denticles that occurred as a consequence of disruption of the normal anterior–posterior segmental pattern formation during embryogenesis [20]. This developmental anomaly was then attributed to a mutation in a drosophila gene termed ‘hedgehog’ that encodes a secreted polypeptide (ligand) that can initiate hedgehog signaling in receptive drosophila cells [21]. We now know that some form of hedgehog signaling is evolutionarily conserved throughout metazoans and that hedgehog is an important tissue morphogen that participates in the establishment of embryonic polarity and the early patterning of tissues that sets the stage for acquisition of adult tissue structure and function.

Canonical hedgehog signaling is initiated by peptide ligands that are still referred to as hedgehogs, and it serves, at the end point, to activate transcription from the Gli family of transcription factors in responsive cells. Humans have three gene homologs that encode hedgehog ligands (Sonic [Shh], Indian [Ihh] or Desert [Dhh] hedgehog) [22,23]. Shh is the most well studied and is predominant with regards to its more widespread expression throughout different tissues of the body, although all can similarly engage with receptor to initiate the signaling process. Shh is synthesized as a propolypeptide that is processed by a unique autocatalytic reaction in which the C-terminal domain catalyzes a cholesterol-dependent internal cleavage of the pro-form that simultaneously attaches a cholesterol moiety to the cleaved N-terminal domain [24]. The autocatalysis is not sufficient for secretion of the mature ligand; this requires the action of an independent membrane protein referred to as Dispatched [25]. Cholesterol-modified mature Shh is inherently highly hydrophobic and this can limit its diffusion away from the cells that secrete it. The short-acting nature of the hedgehog signaling process in early development helps to promote the formation of patterns in tissues that are based upon ligand diffusion gradients that restrict ligand access to target cells more distal from the hedgehog-secreting cells.

The signaling process proceeds when the mature ligand engages a receptor on a target cell and, for hedgehog, proteins of the Patched (Ptch) family serve this purpose. Ptch proteins are large, 12-pass membrane proteins, and humans encode two homologs [26], Ptch1 and Ptch2, with differing affinities for hedgehog ligands and differential expression in various tissues of the body. A diagram of the general intracellular process that accompanies hedgehog signaling is shown in Figure 1. It should be noted that the brief schema described here is specific for vertebrate-derived cells as evolution from invertebrates was accompanied by modifications that tether the proximal stage of hedgehog signal processing to the subcellular organelle referred to as the primary cilia [27,28]. The integration of hedgehog signaling into the primary cilia provides vertebrate cells with unique opportunities to regulate the signaling

process, but the linkage also has some important implications for our understanding of hedgehog action in human tumors, as will be discussed later. Likewise, vertebrates have a more complex end-response to hedgehog signaling through evolutionary divergence of the function of the invertebrate Ci transcription factor that is activated by hedgehog onto three different Gli proteins (Gli1, 2 and 3) in vertebrates [29,30]. Since the topic of this treatise is human prostate cancer, hereafter our discussion will focus on the signaling pathway as it is known to function in higher vertebrates (mouse through humans).

Ligand engagement of Ptch relieves repression of the Smoothened (Smo) protein that is required for further signaling. Smo, a seven-pass transmembrane protein of the extended G-protein-coupled receptor family, has an active and an inactivate state that appears to be defined both by its location within the cell (inside or outside of the primary cilia) [31] and by other modifications that may include its ability to capture oxysterols at an active site [32,33]. Smo activation requires two steps that were operationally defined by certain low-molecular-weight compounds that disrupt the activation process [34]. The first step involves the movement of Smo proteins from the plasma membrane and endoplasmic vesicles into primary cilium and here unliganded Ptch acts as a gatekeeper that restricts access of Smo to the primary cilium. Ptch action in this regard is mimicked by the drug, SANT-1, which similarly suppresses ciliary accumulation of Smo, even in the presence of ligand [35,36]. Once in the primary cilia, however, Smo activation requires a secondary step that is also regulated by Ptch, and this activation step is operationally defined by inhibition with cyclopamine or derivatives that allow Smo ciliary accumulation but prevent any further downstream signaling activities. The nature of the secondary Smo activation event remains enigmatic, although it probably involves a conformational shift and/or a change in Smo interaction with other ciliary proteins that are involved in hedgehog signal processing. Regardless of our understanding of this particular event, the presence of active Smo within primary cilia induces a functional change in the organelle that fundamentally alters the manner in which the two dominant Gli proteins, Gli2 and Gli3, are post-translationally processed.

As transcription factors with shared function, all Gli proteins have a homologous internal DNA-binding domain that recognizes and binds a *cis*-regulatory consensus motif on DNA: G–A–C–C–A–C–C–A [37]. The lack of this consensus sequence within or near any given gene does not preclude regulation by Gli since functional nonconsensus binding sites are also described [38]. Given their nature as transcription factors, all Gli proteins also possess activation domains within their C-terminal region that interact with other transcriptional accessory proteins needed for the chromatin remodeling involved in active transcription. Outside of this organizational similarity, however, there are distinct differences between the three homologs that provide the basis for separation of functions in the Gli-mediated transcription process. For one, the proteins encoded by Gli2 and 3 also possess repressor domains within their N-terminus that can preferentially attract corepressor protein complexes to the DNA-binding sites when the activation domain is proteolytically removed [39,40]. It is the relative efficiency with which these two Gli forms are specifically proteolyzed that distinguishes the inactive versus the active hedgehog signaling state. In the absence of activated Smo, Gli2 and 3 proteins traffic into primary cilium where they are modified into repressor forms [41]. This process is initiated by a series of sequential phosphorylations, initiated by protein kinase A and then followed by glycogen synthase kinase-3-β and casein kinase 1. Following phosphorylation, the Gli2/3 repressor forms are generated by proteolysis that may be guided by site-directed ubiquitylation under the control of SCF-β^{TRCP} [42]. The Gli2/3 modification and proteolytic process also requires the presence of certain ciliary kinesin motor proteins to shepherd Glis through the primary cilium and to scaffold the modification complex during the process [27]. The Gli2/3 proteins are also distinguished by their differing contributions to the repressive or activated Gli state

of a cell. Whereas native Gli2 is a more avid transcriptional activator than native Gli3, cleaved Gli3 is a stronger transcriptional repressor when compared with cleaved Gli2, so the intensity of the response to hedgehog signaling in a target cell also depends upon the relative expression levels of the two different proteins in that cell. Gli proteins are also targeted for ubiquitylation by the SPOP ubiquitin ligase [43] but it is unclear whether proteasomal degradation under this element is involved in the specific generation of repressor forms rather than their generalized degradation along with Gli1 [44]. In summary, the presence of activated Smo within the primary cilium suppresses the generation of the Gli2/3 repressor forms so they accumulate within the primary cilium in this state. They are also much more likely to exit the cilium with an intact C-terminal domain that is able to enter the nucleus, bind to Gli response elements and capture the chromatin accessory proteins required for an active transcription complex.

Given the importance of hedgehog/Gli signaling for vertebrate development and cancers, there is considerable interest in the targets of active Gli-mediated transcription. Here, it is somewhat ironic that the most well-recognized targets of active Gli transcription include Gli1 and the *Ptch* genes that are mechanistically involved in the signaling process [45]. The nature of the Gli1 protein, which lacks a repressor form, and its short-lived character suggests that it functions mainly as a means for amplifying the output of the hedgehog signaling process once it is initiated. Indeed, this function is consistent with lack of an overt phenotype in Gli1-knockout mice, whereas Gli2- or Gli3-knockouts are more severely affected [46,47]. By contrast, Ptch upregulation by active hedgehog provides a means to eventually diminish the activity of the signaling process once initiated, so this action appears to be part of a negative-feedback loop controlling hedgehog activity in any given target cell. Other genes reported to be hedgehog targets include hedgehog-interacting protein (*HIP*), whose gene product also feeds back to diminish local signaling activity; cell cycle regulators, including N-myc, cyclin D1 and D2, which may partially explain hedgehog effects on cell growth; effectors of other developmental signaling pathways including Wnt and Notch ligands and other gene products (bcl-2, FOX transcription factors, bone morphogenetic proteins and follistatin) (Table 1) that are probably associated with differentiated states. In summary, the spectrum of known hedgehog target genes reveals the autoregulating nature of the signaling pathway and explains its obvious involvement in developmental organization of tissues, cell growth and differentiation.

The complex and unique characteristics of the basic hedgehog signaling process, described in the previous section, allows for its regulation at many alternative steps. These include interference with hedgehog ligand processing, release or receptor binding by effectors of sterol biosynthesis [32] or direct interference with mature ligand function by the presence of the HIP protein that binds to ligands and prevents their interaction with receptors [48]. For the target cell, hedgehog signaling can be facilitated by the presence of heparin proteoglycans and lower affinity hedgehog coreceptor proteins that include CDON and BOC [49]. Further downstream, integration of vertebrate hedgehog signaling into the primary cilium means that signal processing requires the activities of numerous ciliar transport proteins to shuttle Gli proteins into and out of the cilium [41,50,51]. Genetic ablation of individual ciliar transport proteins in mice confers phenotypes that are reiterative of mutations in the primary hedgehog regulatory genes. End-stage Gli transcriptional activity is also affected by acetylation or sumoylation of the Gli proteins [52,53]. Finally, Gli transcriptional function is tempered by the presence of the multifunctional SuFu protein that can bind and sequester Gli active forms in the cytoplasm or attract transcriptional corepressors to activator Gli complexes already bound to chromatin [54,55]. The multiplicity of alternative regulatory sites along the hedgehog signaling cascade provides copious opportunities for signal facilitation or interference and it complicates attempts to

understand the reason why hedgehog signaling abnormalities strongly underlie certain types of developmental defects or malignancies but not others.

Another notable aspect of hedgehog signaling is its remarkably sensitivity to small-molecule manipulation. This is mainly attributable to the unique nature of the Smo molecule, whose activity is strongly influenced by its association with sterols or other low-molecular-weight compounds. Sterol-like compounds, such as Smo agonist [35] or purmorphomine [56], promote the activated Smo state and these molecules provide an alternative means of antagonizing hedgehog for experimental purposes. By contrast, sterols modeled after the phyto-derived jerveratrum alkaloid, cyclopamine, strongly inhibit Smo activation and these drugs are frequently used experimentally to antagonize hedgehog signaling [57]. The evidence that hyperactive hedgehog signaling plays a role in human cancers has been a tremendous impetus for the discovery of novel compounds that might be used for the purpose of therapeutics and these efforts have resulted in the identification of numerous other low-molecular-weight compounds that can antagonize hedgehog or block Gli action. Since many of these newer compounds are being considered for clinical utilization in oncology, we will assess the spectrum of potential hedgehog/Gli-targeting agents in a later section of this article.

Hedgehog in prostate development

Hedgehog's importance as a developmental morphogen for vertebrates is established by the striking developmental anomalies that are associated with abrogation of pathway activity. Loss of Shh, Gli2 or Gli3 function in mutant or knockout mice can be embryonically lethal or result in the death of the neonate shortly after birth associated with developmental defects that include holoproencephaly/cyclopism [58], spinal cord anomalies and other neuronal deficits [59], defects in the formation of the axial skeleton and limbs [60], underdeveloped lungs, and anorectal malformations that include persistent cloaca [61], depending on the severity of the pathway ablation. For males, sexual accessory tissue development is also affected by hedgehog deficiencies and this effect includes hypodevelopment of the prostate gland.

The prostate gland is derived from the embryonic urogenital sinus (UGS) and Shh is expressed in rodent and human UGS and in the buds and ducts that outgrow from it during the process of prostate organogenesis and maturation [62]. Embryonic male mice that lack functional Shh as a consequence of homozygous mutation fail to show the early inductive budding from the UGS that initiates prostate formation [63,64]. However, it is remarkable that inductive budding can be restored simply by supplementing testosterone to the female mouse (*in vivo*) or to isolated mutant male UGS tissues (*in vitro*) [63]. These observations are highly consistent with a requirement of hedgehog for embryonic testicular steroidogenesis and fetal androgenization that guides the inductive phase of male sexual accessory tissue development [65] and they are inconsistent with the idea that any prostate-autonomous hedgehog activity is required for initial organogenesis. Despite the evidence that prostate-autonomous Shh is unnecessary for UGS inductive budding, later embryonic ductal branching and neonatal maturation of the rodent prostate gland is markedly hampered by the lack of Shh, even when supplemental testosterone is provided. Thus, the secondary budding and ductal extension associated with late embryonic and neonatal prostate development is dependent upon prostate-autonomous hedgehog signaling. This developmental situation may be analogous to the regrowth of the regressed prostate in chronically castrated adult rodents that occurs subsequent to testosterone replenishment. Here, cyclopamine treatment was shown to block the androgen-stimulated regrowth of the regressed adult mouse prostate associated with testosterone replacement and this outcome

suggests that testosterone replacement induces hedgehog expression needed for prostate ductal expansion in adults [66].

With regards to the nature of the hedgehog signaling process in the developing prostate, *in situ* hybridization and immunohistochemical analyses of embryonic or neonatal mouse and rat tissues tends to localize expression of Shh to the epithelium of the rodent UGS and to the growing tips of the prostate epithelial buds as they invade into the surrounding mesodermally derived mesenchyme [67–70]. By contrast, Ptch and Gli1 (the surrogate Gli target gene) were found to be mainly expressed by UGS mesenchyme or stromal cells adjacent to buds of the developing prostate gland that also stain positive for smooth muscle actin. The striking juxtaposition of ligand expression restricted to the developing prostate epithelium with receptor and target gene expression that is mainly found in the adjacent mesenchyme shows that hedgehog encompasses a typical paracrine signaling process in the developing prostate that is characteristic of the hedgehog signaling paradigm in other types of developing tissues. There are, however, some reports that also find reduced expression of Ptch1 and Gli1 in the epithelium at bud tips [67] and these findings raise questions that extend to human prostate cancer tissue studies as to whether there may be some autocrine-like hedgehog activity in prostate epithelial cells that manifests exclusively under conditions of rapid growth.

Hedgehog & human cancers

Genetically manipulated mouse models have established an oncogenic role for hedgehog signaling in certain tissues that is remarkably predictive of the occurrence of proven hedgehog-driven tumors in humans. Mice with haploinsufficieny of Ptch1 [71,72], or those with haploinsufficiency of SuFu when combined with p53 haploinsufficiency [73], develop a common spectrum of cutaneous, brain and cartilaginous tumors that corresponds to the specific types of gene anomalies found in basal cell (skin) carcinoma (BCC), medulloblastomas or rhabdomyosarcomas in humans [74]. These types of tumors often have reduced Ptch1 expression associated with loss of heterozygosity at 9q22 (the *Ptch1* locus), which may or may not be associated with a mutation in the remaining *Ptch* allele [75]. Likewise, inactivating mutations in Ptch or SuFu underlie the Gorlin syndrome that predisposes to the development of BCC and/or medulloblastoma [76,77]. Conversely, mutations in the *Smo* gene that confer gain-of-function to the encoded protein are also found in human BCCs and, rarely, in medulloblastomas [78], but exogenous targeted expression of a mutant human *Smo* gene from BCC in transgenic mice similarly induces cutaneous carcinomas, medulloblastomas and rhabdomyosarcomas. Collectively, the reiteration of tumor development in mice by the same genetic aberrations that are found in human tumors of the same class validates the oncogenic nature of unrestricted hedgehog/Gli signaling in this limited subset of tissues. Although these types of genetic lesions confer the appearance of ‘autocrine-like’ autonomous hedgehog signaling activity in the tumor cell, the abnormal activity is independent of the presence of hedgehog ligands in the tumor microenvironment.

Despite the lack of prevailing evidence for the occurrence of genetic lesions of the type previously described in most other types of solid human tumors, considerable interest remains in the potential roles of hedgehog or Gli, especially for lung, breast, pancreas, colon and prostate carcinoma [12,13,66,79,80]. As will be discussed for prostate cancer, the evidence for association usually encompasses findings of high expression of ligand and/or hedgehog target genes in tumor cells or findings that hedgehog/Gli inhibition, usually by cyclopamine or via Gli expression knockdown, suppresses cell growth *in vitro* or *in vivo* as tumor xenografts in mice. The outcomes of these experiments are often used to support the idea that some form of autocrine-like hedgehog signaling is constitutively active in these other types of solid tumor cells. Unfortunately, much less effort is made to establish

whether, indeed, any or all of these tumors demonstrate any actual autonomous hedgehog signaling activity, and experimental evidence more strongly implicates that these tumor systems are more influenced through paracrine hedgehog [81], much like in the tissues from which these tumors develop. The situation for tumors other than BCC, medulloblastoma or rhabdomyosarcoma is especially complicated by observations that Gli expression can be regulated independently of hedgehog signaling. TGF-β-, β-catenin- and hyperactive RAS/RAF/MEK/ERK-mediated signaling upregulates Gli expression/activity in tumor cells independent of the presence of hedgehog ligand [70,82,83] and hyperactivity of these alternate cell signaling pathways is known to occur in many different types of cancer. Given the existence of alternative pathways to Gli expression, one should certainly consider whether simple overexpression of Gli, when combined with post-translational processing deficits that fail to generate Gli repressor forms, would be sufficient to explain Gli involvement in them without invoking further upstream hedgehog activities. This is a paradox that we will explore in our focus on prostate cancer.

Finally, the requirement for the primary cilium to process canonical hedgehog signaling in normal cells raises other questions regarding the existence of active hedgehog signaling in cancers that may lack hedgehog-activating mutations since primary cilia are mainly formed on growth-arrested cells whereas cancer cells, especially in culture, usually lack these organelles [84]. The apparent absence of primary cilium in dividing cancer cells then raises critical questions as to how Smo might transition to the active form in cancer cells without activating mutations or evidence of other hedgehog signaling anomalies, and this is an area of research in which we hope to have advances in the coming years.

For those tumor systems that are commonly associated with hyperactive Smo function (due to loss of Ptch function or Smo mutations), there is good reason to consider the testing and use of Smo-targeting agents as anticancer therapeutics. Whereas there was some initial interest in the use of cyclopamine in clinical practice, this agent has critical attributes that make it unfavorable for this purpose and these include its poor availability through nonvenous routes, as well as concerns that it has off-target effects, especially at higher doses [85]. Nonetheless, the remarkable sensitivity of Smo to small-molecule inhibition has encouraged discovery efforts to identify agents that act in a similar way to cyclopamine (by inhibiting Smo activation) with more favorable clinical profiles. Two contemporary Smo-targeting agents, GDC-0449 and IPI-926, are already subject to clinical testing in human patients [86–88]. Use of GDC-0449 alone in Phase I testing has already demonstrated evidence of objective responses for some cancers [88] and investigators are already considering the possible benefit of combining Smo-targeting drugs with other targeted therapeutics for cancers [89] to improve the response. Considering the evidence that many solid tumors benefit from a paracrine hedgehog signaling environment, Smo-targeting drugs could provide an adjuvant therapy to suppress the hedgehog signaling microenvironment of the tumor and open clinical trials for GDC-0049 are actively accruing patients with these alternate solid tumors. Similar effects might be afforded by agents that target hedgehog ligand processing and interaction with receptors. Robotnikinin, a drug that blocks the interaction of Shh with receptors [90], is of this class. Further down the pathway, the knowledge that Gli activity may be an important factor in tumor biology, independent of hedgehog signaling, has also driven discovery efforts to identify drugs that can block this activity, and the Gli antagonists (GANTs; -58 and -61) [91], and, more recently, the HPI class of drugs [92] that interfere with Gli trafficking and transcription, may have clinical applicability. Finally, the actions of arsenic trioxide, which is being tested as a solid tumor therapeutic [93], may also include the inactivation of Gli function in cancer cells [94,95] so this drug may provide an alternative option for hedgehog targeting in cancers.

Overview of hedgehog/Gli in prostate cancer

The involvement of hedgehog signaling in prostate development forms a foundation for considering whether hedgehog/Gli might have some role in prostate malignancy. This concept received substantial impetus from two early reports of cyclopamine- or Shh antibody-mediated suppression of prostate cancer cell growth *in vitro* and *in vivo* [66,96], and the outcomes of these experimental studies were viewed as evidence for an active autocrine-like hedgehog signaling process in these cell lines. This conclusion should now be reconsidered, especially in light of the concerns discussed previously. A review of relevant literature on this topic with these new perspectives shows remarkable weaknesses in the argument that autocrine hedgehog has an important role in the development of prostate cancer. For one, the genetically altered mouse models that were so useful for establishing a relationship between abnormally hyperactive hedgehog signaling and the development of skin and brain malignancies have not shown any evidence that such aberrations lead to the development of prostate neoplasia or malignancy. It is especially notable that even mice with a prostate (epithelial cell)-specific knock-in of gain-of-function mutated *Smo* gene that is oncogenic when expressed in skin, brain or cartilage, demonstrated no evidence for any type of prostatic pathology [97]. In fact, at this time, the only report of an animal (mouse) model that develops prostate cancer from a hedgehog manipulation involves the direct introduction of a constitutive Shh expression vector into mouse prostate by tissue electroporation [98]. These adult mice uniformly developed prostate intraepithelial neoplasia that rapidly progressed to metastatic prostate adenocarcinoma over time. While this outcome is remarkable and does support the potential for unrestricted hedgehog in prostate cancer development, the electroporation technique lacks the cell-targeting specificity to show that overexpression of Shh in the tissue was acting through any autonomous effect on the prostate epithelium and the outcome could easily be a consequence of an unrestricted hedgehog stimulation of the prostate stroma that destabilizes the tissue, leading to cancer.

With regards to actual human prostate tumors or prostate cancer cell lines, there are no studies identifying abnormalities in *Ptch* or *Smo* genes similar to those found in BCC or medulloblastoma. Allelic loss of 9q22 and/or *Ptch* mutations are not described for this disease, and reports of *Smo* mutations are similarly lacking, although there is no reason to believe that a screening effort to identify the presence of *Smo* gene lesions was ever suitably undertaken for prostate cancers. Perhaps the only description of hedgehog-related gene aberrations in prostate cancer involves the finding of two prostate tumors with loss-of-function mutations in the *SuFu* gene [99]. These mutations were found in a small cohort of tumors in which SuFu immunostaining was also notably reduced. Of further note, the human *SuFu* gene lies in a chromosomal region (10q24.32) that encompasses an area of frequent allelic loss in prostate cancer. While these coincidences are insufficient to establish a more widespread pattern involving loss of SuFu in prostate cancer development or progression, they do at least establish precedence to seek further evidence that changes in the *SuFu* gene or in reduced expression of the encoded protein may be a factor in the disease.

Given the paucity of evidence for disruption of genes encoding intermediate hedgehog signaling elements in prostate tumors, what can be learned regarding hedgehog involvement in prostate cancer from gene-expression studies of human prostate tumor specimens? Unfortunately, varied outcomes from the numerous published efforts that describe and quantify expression of hedgehog-related genes in prostate tumors challenge efforts to provide consensus on this issue. There are general concerns that the so-called ‘normal’ regions of human prostate specimens that are available for study might be affected by the common prostate benign disease states that might also invoke abnormal hedgehog responses [100] and this raises questions regarding the establishment of normal prostate basal expression levels for any of these genes. Approaches that assess RNA levels by *in situ*

hybridization are complicated by the uneven cellular architecture of a prostate tumor (in which the cellularity of the stroma can appear sparse compared with the adjacent epithelium) and this might account for the conflicting findings of Gli1 RNAs localized to benign and malignant prostate epithelium in one study [96] versus selective expression in the stroma around tumors in another [100]. Likewise, quantitative reverse-transcriptase PCR approaches that involve bulk extraction from tumor tissues are complicated by the comixtures of tumor and benign stromal cells in the specimens that complicate analysis, so it is difficult to comment on observations based on this approach. *In situ* immunohistochemical approaches using antibodies against hedgehog-related proteins offer the potential for higher detection specificity, with appropriately validated antibodies, but this approach suffers from a diminished ability to quantify outcomes.

With these considerations, the observations of Azoulay *et al.*, who evaluated hedgehog ligand expressions in a cohort of 231 different prostate tumors, some of which were obtained from patients treated with hormone therapies, were remarkable [101]. They described a significant correlation between high(er) expression of Shh in malignant epithelium with tumor grade or metastasis to lymph nodes. Sheng *et al.* evaluated 55 different tumors for multiple parameters, including Shh, Ptch1 and HIP expression (the latter being surrogate Gli targets) [99]. Here, the investigators described elevated immunostaining for Shh in malignant epithelium compared with benign epithelium, with increased Ptch1 and HIP expression in tumor cells that correlated with tumor grade. Narita *et al.* characterized Gli2 expression in 21 localized prostate tumors from androgenically intact patients compared with 14 benign prostatic hyperplasia specimens and described a significant increase in Gli2 immunostaining in the malignant compared with the benign epithelium [102]. Overall, the most validated studies appear to support that expression of Shh in prostate tumor cells tends to increase as a function of tumor grade (and potential for metastasis), that prostate tumor cells tend to show higher Gli2 expression and productive Gli transcriptional activity compared with their benign counterparts, and that Gli2 expression rises further in therapy-resistant tumor cells. These outcomes then suggest that a more active hedgehog signaling microenvironment around a prostate tumor in conjunction with increased tumor cell Gli activity is associated with aggressive cancer cell behaviors that include potential for metastasis and therapy resistance. The outcomes do not, however, sufficiently establish that there is any direct association between the overexpression of hedgehogs in more aggressive prostate tumor cells and the enhanced Gli expression/activity that is also reported to be found in prostate tumor cells.

What can be learned from study of human prostate cancer cell lines? Use of some of the lines as xenografts in mice has revealed additional features of hedgehog effects that provide insight into the *in vivo* situation. For one, overexpression of the ligand (Shh) in LNCaP cells significantly increased the *in vivo* tumor growth rate of tumor xenografts compared with control xenografted LNCaP cells [100]. This indicates that the higher expression of Shh found in prostate tumors of higher grade has the potential to impact on prostate tumor growth rates. The fact that similar tumor growth acceleration can also be achieved by co-mixing unmodified LNCaP cells with UGS mesenchymal cells lacking Gli3 repressor ($Gli3^{-/-}$) [103] certainly shows that signaling action through the paracrine pathway, at least has the potential to significantly contribute to the hedgehog-mediated tumor growth acceleration effect. Finally, observations that the treatment of mice with Shh-targeting antibodies, cyclopamine, Gli2-targeting antisense oligotides [102] or Gli-blocking drugs of the GANT class significantly inhibits the growth of prostate tumor cell xenografts (CWR22rv1 or PC3 cells) identify the potential for use of hedgehog-/Gli-suppressive therapeutics for prostate cancer treatment, although, to date, no actual clinical trials using hedgehog-blocking approaches for prostate cancer patients have been reported.

Evaluation of prostate cancer cell lines in a culture setting provides a means of testing for the presence of any autocrine-like hedgehog signaling activities in the cells and whether activation or interference at various sites of the signaling pathway affects hedgehog target genes or cell growth outside the influence of a paracrine signaling environment. For the most commonly utilized human prostate cancer cell lines (LNCaP and derivatives, DU145, PC3 or CWR22rv1) grown in culture, Shh, Gli1/2 and other key hedgehog target genes (*Ptch1*, *Gli1* and *HIP*) are, in general, reported to be expressed, although there is wide variability in individual levels among the different lines. The most comprehensive survey for basal expression of hedgehog effector genes (mRNAs) in the common prostate cancer cell lines was published by Zhang *et al.* [104] and this survey showed no overt concordance between the expression of hedgehog ligands (Shh or Ihh) and the basal expression of hedgehog surrogate targets (Gli1 and Ptch1), except for HIP; no concordance in the expression of the different hedgehog target genes in any of the lines; and, finally, no concordance between the expression of any of the Gli RNAs with Ptch or HIP expression. Likewise, the common prostate cancer cell lines were shown to be refractory to treatment with recombinant Shh protein or to adenoviral transduction of a mutated *Smo* gene [104]. Collectively, these findings do not lend support to the presence of a basally active or even an accessible endogenous hedgehog signaling process in any of the cell lines evaluated based upon the idea that the activity of the pathway is solely indicated by expression levels of known Gli target genes. Conceptually, the lack of evidence for intermediate hedgehog signaling activity in prostate cancer cell lines based upon these considerations then challenges the idea that cyclopamine treatment, which invariably affects the growth of these cells *in vitro*, is functionally targeting an active hedgehog signaling process guided by Smo activation. Here again, the failure of cyclopamine to suppress expression of hedgehog target genes (*Ptch1*, *Gli1* or hedgehog reporter) in the cultured prostate cancer cell lines [104,105] provides additional support for the lack of intermediate signaling pathway activity in the cancer cell lines, as long as one can be reassured that pathway activity is exclusively reflected by the relative expression levels of Gli target genes. As we will discuss later, this may not always be the case, at least in prostate cancer cells that express the AR protein. Regardless of these concerns, there are prominent indications that Gli proteins, at least, play some role in the growth potential of prostate cancer cells. Suppression of Gli1 or Gli2 expression using gene-specific si-/shRNAs or antisense oligonucleotides significantly reduced their *in vitro* growth rate and invasiveness [102,106,107] and increased the propensity for apoptosis. The mechanism supporting the presence of active Gli in these cells remains uncertain.

Hedgehog/Gli & androgen cross-talk in prostate cancer

The androgen signaling pathway that is so central to prostate cancer is remarkably interactive with other cell-signaling pathways. These interactions often occur at the level of the AR protein where AR activity can be increased under stimulation of signal-activated protein kinases [108] or by interaction with other pathway-regulated transcription factors, as is exemplified by β-catenin in the Wnt signaling pathway [109]. These signaling interactions are especially notable when they support promiscuous androgen signaling under low androgen conditions, as this allows for the possibility that the secondary signaling pathway is a druggable target for suppression of CRPC. Recently, we learned of a unique bidirectional interaction between androgen and hedgehog signaling in prostate cancer cells. The nature of this interaction is defined by the androgenic milieu of the prostate cancer cell and it appears to have the potential to produce a more active paracrine hedgehog microenvironment of a tumor in hormone-treated patients and, at the same time, promote promiscuous activity of the tumor cell AR that enables androgen-independent growth.

The nature of this interaction is first defined by evidence that hedgehog ligands are androgen-repressed genes in prostate cancer cells. Using the example of cultured prostate cancer cell lines that express AR and are growth-responsive to the presence of androgens in their medium, expression of mRNA encoding hedgehogs was found to be markedly increased by a switch to an androgen-depleted medium [101,110]. For LNCaP cells, androgen depletion upregulated Shh by 30,000-fold, and the expression of Ihh and Dhh was also upregulated, although not to this extent. This response was not unique to LNCaP; other androgen-responsive prostate cancer cells demonstrated similar changes in hedgehog expression when treated in this manner. Moreover, the changes in Shh mRNA were accompanied by similar increases in the expression and release of the mature Shh polypeptide with intact paracrine function, shown by the finding that the conditioned growth medium from androgen-deprived, but not androgen-supplemented, LNCaP cells was able to elicit a hedgehog response from mouse fibroblasts [110]. The clinical relevance of these *in vitro* findings is supported by the previously mentioned survey of hedgehog expression in human prostate tumors [101], which included a group of tumors obtained from patients who had been adjuvantly treated with hormone therapy prior to surgery. Here, hormone treatment essentially doubled the percentage of tumors found to express Shh or Dhh in malignant epithelium compared with untreated tumors.

In addition to its effect on hedgehog expression, androgen deprivation was also shown to significantly increase the expression of Gli2 mRNA in LNCaP and other prostate cancer cell lines [110]. Considering the fact that this action was also accompanied by upregulated Ptch1 expression, one might reasonably suppose that the coincidental increases in Shh, Gli2 and Ptch expression represent the activities of an autocrine hedgehog cascade initiated by androgen deprivation. Indeed, since cyclopamine treatment conferred a small but significant decrease in Ptch expression under this condition [110], the outcome further supports the idea that androgen deprivation is associated with a reawakening of some autocrine-like activity in prostate cancer cells. Arguing against this is the fact that Gli1 mRNA expression was significantly decreased by this same condition and it is difficult to explain the striking discordance in the response of these two foremost Gli target genes (*Gli1* and *Ptch1*), unless one invokes different regulatory mechanisms for each gene operating in the confines of the androgen-deprived cell. This remains an unresolved issue, which is further complicated by the evidence that active hedgehog/Gli affects androgen signaling in prostate cancer cells.

The notion that hedgehog/Gli also affects androgen signaling originated from observations of a dose-dependent effect of cyclopamine on the expression of androgen-regulated genes [111] in LNCaP and other prostate cancer cells. Here, cyclopamine treatment was shown to specifically suppress expression of kallikrein-related peptidase (KLK)2, KLK3 and PGC in androgen-deprived, but not androgen-supplemented, LNCaP cells, whereas it further induced expression of Shh, which represents an androgen-repressed gene. Cyclopamine had similar effects on expression of luciferase reporters from androgen-dependent promoter elements in these cells. These effects were most pronounced in androgen-deprived cells in which Gli2 levels were elevated. Whereas questions remain regarding cyclopamine's specificity and its mechanism of action in prostate cancer cell lines, a similar outcome was observed after knockdown of Smo expression using siRNA. The fact that this effect also involves elements of hedgehog (Gli activity) downstream of Smo is indicated by the ability to suppress androgen-dependent gene expression by specific reduction of Gli2 expression or by treatments with the Gli inhibitor drugs, GANT-58 and -61 (Figure 2). Here, it is notable that the GANT drugs did not significantly affect expression of Ptch1. Finally, in the reverse paradigm, exogenous expression of Gli1 or Gli2 in androgen-deprived prostate cancer cells not only increased the expression of androgen-dependent genes but also enabled these cells to grow in an androgen-deficient medium [111]. Collectively, the outcomes of these studies support the presence of a Smo-dependent signaling process, at least in androgen-deprived

prostate cancer cells, which cross-talks with the androgen signaling pathway through Gli to affect androgen-regulated gene expression. The involvement of Gli in the regulation of androgen-dependent genes suggests that the effect might be mediated by some form of Gli/AR interaction. Indeed, coimmunoprecipitation or two-hybrid analysis shows that Gli1 or Gli2 can directly bind to the AR protein [111,112]. Based on these reports, the Gli proteins may have AR coactivation functions that contribute to androgen signaling, especially in the androgen-deprived state.

Expert commentary

Since its discovery in 1980, we have learned a great deal regarding the mechanistic aspects of hedgehog signaling and its role in vertebrate development. In addition, we have come to accept its causative role in some forms of human cancer. The association of hedgehog signaling abnormalities with human tumors has spurred the development and testing of clinically useful drugs that target hedgehog/Gli, some of which are already demonstrating efficacy as cancer therapeutics. However, our current knowledge regarding the role of hedgehog/Gli signaling in prostate cancer remains relatively limited to the notion that the disease, once acquired, benefits from a paracrine hedgehog signaling influence that is driven by the production of hedgehog ligands by prostate tumor cells that act on adjacent benign (stromal) cells and feeds back to the tumor, stimulating tumor cell growth and metastasis. With regards to prostate tumor cells themselves, there is little evidence for the types of mutations or defects in hedgehog signaling genes that are found in human skin and brain tumors, but this does not rule out the possibility that genetic anomalies in other hedgehog-regulating genes might be a factor in the disease. Furthermore, the indications that tumor Gli activity has a role in advanced/aggressive disease are relatively convincing, but there are many reasons to be skeptical as to whether the hyperactive Gli is a consequence of tumor cell-autonomous hedgehog signaling through an active autocrine-like signaling process. Recent findings that the hormone therapies used to treat advanced prostate cancers have the potential to augment the paracrine hedgehog signaling microenvironment of a prostate tumor, in conjunction with the findings that Gli proteins can interact with AR and confer androgen-independent growth behavior on human prostate cancer cells, support the consideration of hedgehog-blocking drug therapy used in conjunction with hormone therapy for patients with advanced/therapy-resistant disease. While drugs that target Smo are now clinically available and should be effective for suppression of hedgehog paracrine effects, the questions regarding the source of Gli activity in prostate cancers suggest that drugs that specifically target Gli may be more useful than Smo blockers alone as they might act on the paracrine hedgehog tumor microenvironment, as well as on tumor-autonomous Gli, allowing effective disease control when used as an adjunct to hormone therapy.

Five-year view

The availability of clinically tested drugs that target hedgehog/Gli suggests that clinical trials of hedgehog therapeutics for prostate cancer are likely to advance faster than the resolution of critical research issues that might guide the most effective application of these therapies. With this perspective, the field requires research advances in three focus areas to help resolve the hedgehog/Gli contribution to prostate cancer. The first involves further exploration of the hedgehog paracrine effect in prostate cancer. Here, the knowledge that hedgehog expression is induced by inflammation, as is common in the prostate, suggests that hyperactive paracrine hedgehog could explain the link between prostate inflammation and prostate carcinogenesis and identify a role for hedgehog in prostate cancer etiology. Development of this concept should encompass surveys of human prostate tissues to correlate the presence of prostate inflammation with hedgehog expression in adjacent epithelium and involve attempts to create a mouse model of prostate cancer by conditional

targeted over-expression of Shh in the adult prostate epithelium. Further work is needed to identify the paracrine hedgehog-induced substances that are produced by hedgehog-stimulated tumor support cells that induce prostate tumor growth. The second area of focus involves addressing the source of Gli hyperactivity in prostate cancer cells and defining the extent to which increased tumor-autonomous Gli activity is associated with progression to aggressive (metastatic) disease. We have described the considerations leading many to questions about whether intermediary hedgehog signaling is even possible in prostate cancer cells and the evidence that Gli expression is not solely dependent upon an active hedgehog signaling process in prostate or other solid tumors. Can we then attribute Gli overexpression in prostate cancer to some specific alternate signaling process that increases with disease progression? The third area of research involves expanding our understanding of the cross-talk between hedgehog/Gli and its consequences for androgen signaling in prostate cancer cells. Research in this area should attempt to dissect the interaction sites of Gli with AR and define the extent to which the alternate Gli forms can coactivate or corepress AR transcription. More work is needed to resolve the question of the extent to which Gli is hijacked by the AR in prostate cancer cells and whether Gli activity is best measured in these cells by expression of androgen-regulated, rather than Gli-regulated, genes. Finally, the evidence that a reduction in Smo expression in prostate cancer cells affects the expression of androgen-regulated genes also suggests the need to better understand Smo function in the context of the prostate cancer cell.

References

Papers of special note have been highlighted as:

• of interest

•• of considerable interest

1. Kessler B, Albertsen P. The natural history of prostate cancer. Urol Clin North Am. 2003; 30(2): 219–226. [PubMed: 12735499]
2. Brawley OW, Ankerst DP, Thompson IM. Screening for prostate cancer. CA Cancer J Clin. 2009; 59(4):264–273. [PubMed: 19564245]
3. Shteynshlyuger A, Andriole GL. Prostate cancer: to screen or not to screen? Urol Clin North Am. 2010; 37(1):1–9. [PubMed: 20152514]
4. Wolf AM, Wender RC, Etzioni RB, et al. American Cancer Society guideline for the early detection of prostate cancer: update 2010. CA Cancer J Clin. 2010; 60(2):70–98. [PubMed: 20200110]
5. McConnell JD. Physiologic basis of endocrine therapy for prostatic cancer. Urol Clin North Am. 1991; 18(1):1–13. [PubMed: 1899494]
6. Culig Z, Bartsch G. Androgen axis in prostate cancer. J Cell Biochem. 2006; 99(2):373–381. [PubMed: 16598769]
7. Mohler JL. Castration-recurrent prostate cancer is not androgen-independent. Adv Exp Med Biol. 2008; 617:223–234. [PubMed: 18497046]
8. Yuan X, Balk SP. Mechanisms mediating androgen receptor reactivation after castration. Urol Oncol. 2009; 27(1):36–41. [PubMed: 19111796]
9. Attar RM, Takimoto CH, Gottardis MM. Castration-resistant prostate cancer: locking up the molecular escape routes. Clin Cancer Res. 2009; 15(10):3251–3255. [PubMed: 19447877]
10. Knudsen KE, Scher HI. Starving the addiction: new opportunities for durable suppression of AR signaling in prostate cancer. Clin Cancer Res. 2009; 15(15):4792–4798. [PubMed: 19638458]
11. Clement V, Sanchez P, de Tribolet N, Radovanovic I, Ruiz i Altaba A. HEDGEHOG-GLI1 signaling regulates human glioma growth, cancer stem cell self-renewal, and tumorigenicity. Curr Biol. 2007; 17(2):165–172. [PubMed: 17196391]

12. Morton JP, Mongeau ME, Klimstra DS, et al. Sonic hedgehog acts at multiple stages during pancreatic tumorigenesis. Proc Natl Acad Sci USA. 2007; 104(12):5103–5108. [PubMed: 17372229]

13. Varnat F, Duquet A, Malerba M, et al. Human colon cancer epithelial cells harbour active HEDGEHOG-GLI signalling that is essential for tumour growth, recurrence, metastasis and stem cell survival and expansion. EMBO Mol Med. 2009; 1(6–7):338–351. [PubMed: 20049737]

14. Bar EE, Chaudhry A, Lin A, et al. Cyclopamine-mediated hedgehog pathway inhibition depletes stem-like cancer cells in glioblastoma. Stem Cells. 2007; 25(10):2524–2533. [PubMed: 17628016]

15. Stecca B, Mas C, Clement V, et al. Melanomas require HEDGEHOG-GLI signaling regulated by interactions between GLI1 and the RAS-MEK/AKT pathways. Proc Natl Acad Sci USA. 2007; 104(14):5895–5900. [PubMed: 17392427]

16. Kasper M, Jaks V, Fiaschi M, Toftgard R. Hedgehog signalling in breast cancer. Carcinogenesis. 2009; 30(6):903–911. [PubMed: 19237605]

17••. Ingham PW, McMahon AP. Hedgehog signaling in animal development: paradigms and principles. Genes Dev. 2001; 15(23):3059–3087. Outstanding early review of the hedgehog signaling process invertebrates. [PubMed: 11731473]

18••. Jiang J, Hui CC. Hedgehog signaling in development and cancer. Dev Cell. 2008; 15(6):801–812. Updated review of the hedgehog signaling process that includes a focus on hedgehog in cancer. [PubMed: 19081070]

19. Wilson CW, Chuang PT. Mechanism and evolution of cytosolic Hedgehog signal transduction. Development. 2010; 137(13):2079–2094. [PubMed: 20530542]

20. Nusslein-Volhard C, Wieschaus E. Mutations affecting segment number and polarity in Drosophila. Nature. 1980; 287(5785):795–801. [PubMed: 6776413]

21. Lee JJ, von Kessler DP, Parks S, Beachy PA. Secretion and localized transcription suggest a role in positional signaling for products of the segmentation gene hedgehog. Cell. 1992; 71(1):33–50. [PubMed: 1394430]

22. Marigo V, Roberts DJ, Lee SM, et al. Cloning, expression, and chromosomal location of SHH and IHH: two human homologues of the Drosophila segment polarity gene hedgehog. Genomics. 1995; 28(1):44–51. [PubMed: 7590746]

23. Bitgood MJ, Shen L, McMahon AP. Sertoli cell signaling by Desert hedgehog regulates the male germline. Curr Biol. 1996; 6(3):298–304. [PubMed: 8805249]

24. Breitling R. Greased hedgehogs: new links between hedgehog signaling and cholesterol metabolism. Bioessays. 2007; 29(11):1085–1094. [PubMed: 17935218]

25. Burke R, Nellen D, Bellotto M, et al. Dispatched, a novel sterol-sensing domain protein dedicated to the release of cholesterol-modified hedgehog from signaling cells. Cell. 1999; 99(7):803–815. [PubMed: 10619433]

26. Carpenter D, Stone DM, Brush J, et al. Characterization of two patched receptors for the vertebrate hedgehog protein family. Proc Natl Acad Sci USA. 1998; 95(23):13630–13634. [PubMed: 9811851]

27•. Wong SY, Reiter JF. The primary cilium at the crossroads of mammalian hedgehog signaling. Curr Top Dev Biol. 2008; 85:225–260. An excellent review of primary cilium that focuses on its role in regulating hedgehog action. [PubMed: 19147008]

28. Goetz SC, Anderson KV. The primary cilium: a signalling centre during vertebrate development. Nat Rev Genet. 2010; 11(5):331–344. [PubMed: 20395968]

29. Ruiz i Altaba A, Sanchez P, Dahmane N. Gli and hedgehog in cancer: tumours, embryos and stem cells. Nat Rev Cancer. 2002; 2(5):361–372. [PubMed: 12044012]

30. Varjosalo M, Taipale J. Hedgehog: functions and mechanisms. Genes Dev. 2008; 22(18):2454–2472. [PubMed: 18794343]

31. Corbit KC, Aanstad P, Singla V, Norman AR, Stainier DY, Reiter JF. Vertebrate Smoothened functions at the primary cilium. Nature. 2005; 437(7061):1018–1021. [PubMed: 16136078]

32. Corcoran RB, Scott MP. Oxysterols stimulate Sonic hedgehog signal transduction and proliferation of medulloblastoma cells. Proc Natl Acad Sci USA. 2006; 103(22):8408–8413. [PubMed: 16707575]

33. Dwyer JR, Sever N, Carlson M, Nelson SF, Beachy PA, Parhami F. Oxysterols are novel activators of the hedgehog signaling pathway in pluripotent mesenchymal cells. J Biol Chem. 2007; 282(12): 8959–8968. [PubMed: 17200122]
34. Rohatgi R, Milenkovic L, Corcoran RB, Scott MP. Hedgehog signal transduction by Smoothened: pharmacologic evidence for a 2-step activation process. Proc Natl Acad Sci USA. 2009; 106(9): 3196–3201. [PubMed: 19218434]
35. Chen JK, Taipale J, Young KE, Maiti T, Beachy PA. Small molecule modulation of Smoothened activity. Proc Natl Acad Sci USA. 2002; 99(22):14071–14076. [PubMed: 12391318]
36. Wilson CW, Chen MH, Chuang PT. Smoothened adopts multiple active and inactive conformations capable of trafficking to the primary cilium. PLoS ONE. 2009; 4(4):e5182. [PubMed: 19365551]
37. Hallikas O, Palin K, Sinjushina N, et al. Genome-wide prediction of mammalian enhancers based on analysis of transcription-factor binding affinity. Cell. 2006; 124(1):47–59. [PubMed: 16413481]
38. Winklmayr M, Schmid C, Laner-Plamberger S, et al. Non-consensus GLI binding sites in Hedgehog target gene regulation. BMC Mol Biol. 2010; 11:2. [PubMed: 20070907]
39. Koebernick K, Pieler T. Gli-type zinc finger proteins as bipotential transducers of Hedgehog signaling. Differentiation. 2002; 70(2–3):69–76. [PubMed: 12076333]
40. Pan Y, Wang C, Wang B. Phosphorylation of Gli2 by protein kinase A is required for Gli2 processing and degradation and the Sonic Hedgehog-regulated mouse development. Dev Biol. 2009; 326(1):177–189. [PubMed: 19056373]
41. Wen X, Lai CK, Evangelista M, Hongo JA, de Sauvage FJ, Scales SJ. Kinetics of hedgehog-dependent full-length Gli3 accumulation in primary cilia and subsequent degradation. Mol Cell Biol. 2010; 30(8):1910–1922. [PubMed: 20154143]
42. Smelkinson MG, Zhou Q, Kalderon D. Regulation of Ci-SCFSlimb binding, Ci proteolysis, and hedgehog pathway activity by Ci phosphorylation. Dev Cell. 2007; 13(4):481–495. [PubMed: 17925225]
43. Zhang Q, Shi Q, Chen Y, et al. Multiple Ser/Thr-rich degrons mediate the degradation of Ci/Gli by the Cul3-HIB/SPOP E3 ubiquitin ligase. Proc Natl Acad Sci USA. 2009; 106(50):21191–21196. [PubMed: 19955409]
44. Wang C, Pan Y, Wang B. Suppressor of fused and Spop regulate the stability, processing and function of Gli2 and Gli3 full-length activators but not their repressors. Development. 2010; 137(12):2001–2009. [PubMed: 20463034]
45. Kasper M, Regl G, Frischauf AM, Aberger F. GLI transcription factors: mediators of oncogenic Hedgehog signalling. Eur J Cancer. 2006; 42(4):437–445. [PubMed: 16406505]
46. Ding Q, Motoyama J, Gasca S, et al. Diminished Sonic hedgehog signaling and lack of floor plate differentiation in Gli2 mutant mice. Development. 1998; 125(14):2533–2543. [PubMed: 9636069]
47. Park HL, Bai C, Platt KA, et al. Mouse Gli1 mutants are viable but have defects in SHH signaling in combination with a Gli2 mutation. Development. 2000; 127(8):1593–1605. [PubMed: 10725236]
48. Chuang PT, McMahon AP. Vertebrate Hedgehog signalling modulated by induction of a Hedgehog-binding protein. Nature. 1999; 397(6720):617–621. [PubMed: 10050855]
49. McLellan JS, Zheng X, Hauk G, Ghirlando R, Beachy PA, Leahy DJ. The mode of Hedgehog binding to Ihog homologues is not conserved across different phyla. Nature. 2008; 455(7215):979–983. [PubMed: 18794898]
50. Haycraft CJ, Banizs B, Aydin-Son Y, Zhang Q, Michaud EJ, Yoder BK. Gli2 and Gli3 localize to cilia and require the intraflagellar transport protein polaris for processing and function. PLoS Genet. 2005; 1(4):e53. [PubMed: 16254602]
51. Kim J, Kato M, Beachy PA. Gli2 trafficking links Hedgehog-dependent activation of Smoothened in the primary cilium to transcriptional activation in the nucleus. Proc Natl Acad Sci USA. 2009; 106(51):21666–21671. [PubMed: 19996169]
52. Canettieri G, Di Marcotullio L, Greco A, et al. Histone deacetylase and Cullin3-REN(KCTD11) ubiquitin ligase interplay regulates Hedgehog signalling through Gli acetylation. Nat Cell Biol. 2010; 12(2):132–142. [PubMed: 20081843]

53. Cox B, Briscoe J, Ulloa F. SUMOylation by Pias1 regulates the activity of the Hedgehog dependent Gli transcription factors. PLoS ONE. 2010; 5(8):e11996. [PubMed: 20711444]
54. Chen MH, Wilson CW, Li YJ, et al. Cilium-independent regulation of Gli protein function by Sufu in Hedgehog signaling is evolutionarily conserved. Genes Dev. 2009; 23(16):1910–1928. [PubMed: 19684112]
55. Jia J, Kolterud A, Zeng H, et al. Suppressor of Fused inhibits mammalian Hedgehog signaling in the absence of cilia. Dev Biol. 2009; 330(2):452–460. [PubMed: 19371734]
56. Sinha S, Chen JK. Purmorphamine activates the Hedgehog pathway by targeting Smoothened. Nat Chem Biol. 2006; 2(1):29–30. [PubMed: 16408088]
57. Incardona JP, Gaffield W, Kapur RP, Roelink H. The teratogenic Veratrum alkaloid cyclopamine inhibits sonic hedgehog signal transduction. Development. 1998; 125(18):3553–3562. [PubMed: 9716521]
58. Roessler E, Du YZ, Mullor JL, et al. Loss-of-function mutations in the human *GLI2* gene are associated with pituitary anomalies and holoprosencephaly-like features. Proc Natl Acad Sci USA. 2003; 100(23):13424–13429. [PubMed: 14581620]
59. Machold R, Hayashi S, Rutlin M, et al. Sonic hedgehog is required for progenitor cell maintenance in telencephalic stem cell niches. Neuron. 2003; 39(6):937–950. [PubMed: 12971894]
60. Mo R, Freer AM, Zinyk DL, et al. Specific and redundant functions of Gli2 and Gli3 zinc finger genes in skeletal patterning and development. Development. 1997; 124(1):113–123. [PubMed: 9006072]
61. Motoyama J, Liu J, Mo R, Ding Q, Post M, Hui CC. Essential function of Gli2 and Gli3 in the formation of lung, trachea and oesophagus. Nat Genet. 1998; 20(1):54–57. [PubMed: 9731531]
62•. Podlasek CA, Barnett DH, Clemens JQ, Bak PM, Bushman W. Prostate development requires Sonic hedgehog expressed by the urogenital sinus epithelium. Dev Biol. 1999; 209(1):28–39. First and thorough description of an association between hedgehog signaling and prostate development. [PubMed: 10208740]
63. Berman DM, Desai N, Wang X, et al. Roles for Hedgehog signaling in androgen production and prostate ductal morphogenesis. Dev Biol. 2004; 267(2):387–398. [PubMed: 15013801]
64. Freestone SH, Marker P, Grace OC, et al. Sonic hedgehog regulates prostatic growth and epithelial differentiation. Dev Biol. 2003; 264(2):352–362. [PubMed: 14651923]
65. Barsoum IB, Yao HH. Fetal Leydig cells: progenitor cell maintenance and differentiation. J Androl. 2010; 31(1):11–15. [PubMed: 19875489]
66•. Karhadkar SS, Bova GS, Abdallah N, et al. Hedgehog signalling in prostate regeneration, neoplasia and metastasis. Nature. 2004; 431(7009):707–712. Highly publicized article citing evidence for hedgehog involvement in prostate cancer. [PubMed: 15361885]
67. Pu Y, Huang L, Prins GS. Sonic hedgehog-patched Gli signaling in the developing rat prostate gland: lobe-specific suppression by neonatal estrogens reduces ductal growth and branching. Dev Biol. 2004; 273(2):257–275. [PubMed: 15328011]
68. Lamm ML, Catbagan WS, Laciak RJ, et al. Sonic hedgehog activates mesenchymal Gli1 expression during prostate ductal bud formation. Dev Biol. 2002; 249(2):349–366. [PubMed: 12221011]
69. Haraguchi R, Motoyama J, Sasaki H, et al. Molecular analysis of coordinated bladder and urogenital organ formation by Hedgehog signaling. Development. 2007; 134(3):525–533. [PubMed: 17202190]
70. Jenkins D. Hedgehog signalling: emerging evidence for non-canonical pathways. Cell Signal. 2009; 21(7):1023–1034. [PubMed: 19399989]
71. Hahn H, Wojnowski L, Miller G, Zimmer A. The patched signaling pathway in tumorigenesis and development: lessons from animal models. J Mol Med. 1999; 77(6):459–468. [PubMed: 10475061]
72. Zurawel RH, Allen C, Wechsler-Reya R, Scott MP, Raffel C. Evidence that haploinsufficiency of Ptch leads to medulloblastoma in mice. Genes Chromosomes Cancer. 2000; 28(1):77–81. [PubMed: 10738305]
73. Lee Y, Kawagoe R, Sasai K, et al. Loss of suppressor-of-fused function promotes tumorigenesis. Oncogene. 2007; 26(44):6442–6447. [PubMed: 17452975]

74. Taylor MD, Liu L, Raffel C, et al. Mutations in SUFU predispose to medulloblastoma. Nat Genet. 2002; 31(3):306–310. [PubMed: 12068298]

75. Reifenberger J, Wolter M, Knobbe CB, et al. Somatic mutations in the *PTCH*, *SMOH*, *SUFUH* and *TP53* genes in sporadic basal cell carcinomas. Br J Dermatol. 2005; 152(1):43–51. [PubMed: 15656799]

76. Pan S, Dong Q, Sun LS, Li TJ. Mechanisms of inactivation of *PTCH1* gene in nevoid basal cell carcinoma syndrome: modification of the two-hit hypothesis. Clin Cancer Res. 2010; 16(2):442–450. [PubMed: 20068110]

77. Pastorino L, Ghiorzo P, Nasti S, et al. Identification of a *SUFU* germline mutation in a family with Gorlin syndrome. Am J Med Genet A. 2009; 149A(7):1539–1543. [PubMed: 19533801]

78. Lam CW, Xie J, To KF, et al. A frequent activated smoothened mutation in sporadic basal cell carcinomas. Oncogene. 1999; 18(3):833–836. [PubMed: 9989836]

79. Watkins DN, Berman DM, Burkholder SG, Wang B, Beachy PA, Baylin SB. Hedgehog signalling within airway epithelial progenitors and in small-cell lung cancer. Nature. 2003; 422(6929):313–317. [PubMed: 12629553]

80. Kubo M, Nakamura M, Tasaki A, et al. Hedgehog signaling pathway is a new therapeutic target for patients with breast cancer. Cancer Res. 2004; 64(17):6071–6074. [PubMed: 15342389]

81••. Yauch RL, Gould SE, Scales SJ, et al. A paracrine requirement for hedgehog signalling in cancer. Nature. 2008; 455(7211):406–410. Succinct experimental platform that demonstrates primal relevance for paracrine hedgehog in several solid tumor systems as opposed to autocrine hedgehog. [PubMed: 18754008]

82•. Lauth M, Toftgard R. Non-canonical activation of GLI transcription factors: implications for targeted anti-cancer therapy. Cell Cycle. 2007; 6(20):2458–2463. Establishes the involvement of non-hedgehog signaling pathways in Gli activities that forms the basis for understanding Gli involvement in solid tumor systems that may not have autocrine hedgehog activities. [PubMed: 17726373]

83. Dennler S, Andre J, Verrecchia F, Mauviel A. Cloning of the human *GLI2* promoter: transcriptional activation by transforming growth factor-β via SMAD3/β-catenin cooperation. J Biol Chem. 2009; 284(46):31523–31531. [PubMed: 19797115]

84. Zhang J, Lipinski RJ, Gipp JJ, Shaw AK, Bushman W. Hedgehog pathway responsiveness correlates with the presence of primary cilia on prostate stromal cells. BMC Dev Biol. 2009; 9:50. [PubMed: 19811645]

85. Zhang X, Harrington N, Moraes RC, Wu MF, Hilsenbeck SG, Lewis MT. Cyclopamine inhibition of human breast cancer cell growth independent of Smoothened (Smo). Breast Cancer Res Treat. 2009; 115(3):505–521. [PubMed: 18563554]

86. Tremblay MR, Lescarbeau A, Grogan MJ, et al. Discovery of a potent and orally active hedgehog pathway antagonist (IPI-926). J Med Chem. 2009; 52(14):4400–4418. [PubMed: 19522463]

87. Von Hoff DD, LoRusso PM, Rudin CM, et al. Inhibition of the hedgehog pathway in advanced basal-cell carcinoma. N Engl J Med. 2009; 361(12):1164–1172. [PubMed: 19726763]

88. Lorusso PM, Rudin CM, Reddy JC, et al. Phase I trial of hedgehog pathway inhibitor GDC-0449 in patients with refractory, locally-advanced or metastatic solid tumors. Clin Cancer Res. 2011; 17:2502–2511. [PubMed: 21300762]

89. Mimeault M, Johansson SL, Vankatraman G, et al. Combined targeting of epidermal growth factor receptor and hedgehog signaling by gefitinib and cyclopamine cooperatively improves the cytotoxic effects of docetaxel on metastatic prostate cancer cells. Mol Cancer Ther. 2007; 6(3): 967–978. [PubMed: 17363490]

90. Stanton BZ, Peng LF, Maloof N, et al. A small molecule that binds Hedgehog and blocks its signaling in human cells. Nat Chem Biol. 2009; 5(3):154–156. [PubMed: 19151731]

91. Lauth M, Bergstrom A, Shimokawa T, Toftgard R. Inhibition of GLI-mediated transcription and tumor cell growth by small-molecule antagonists. Proc Natl Acad Sci USA. 2007; 104(20):8455–8460. [PubMed: 17494766]

92. Hyman JM, Firestone AJ, Heine VM, et al. Small-molecule inhibitors reveal multiple strategies for Hedgehog pathway blockade. Proc Natl Acad Sci USA. 2009; 106(33):14132–14137. [PubMed: 19666565]

93. Murgo AJ. Clinical trials of arsenic trioxide in hematologic and solid tumors: overview of the National Cancer Institute Cooperative Research and Development Studies. Oncologist. 2001; 6(Suppl 2):22–28. [PubMed: 11331437]

94. Kim J, Lee JJ, Gardner D, Beachy PA. Arsenic antagonizes the Hedgehog pathway by preventing ciliary accumulation and reducing stability of the Gli2 transcriptional effector. Proc Natl Acad Sci USA. 2010; 107(30):13432–13437. [PubMed: 20624968]

95. Beauchamp EM, Ringer L, Bulut G, et al. Arsenic trioxide inhibits human cancer cell growth and tumor development in mice by blocking Hedgehog/GLI pathway. J Clin Invest. 2011; 121(1):148–160. [PubMed: 21183792]

96•. Sanchez P, Hernandez AM, Stecca B, et al. Inhibition of prostate cancer proliferation by interference with SONIC HEDGEHOG–GLI1 signaling. Proc Natl Acad Sci USA. 2004; 101(34):12561–12566. Seminal paper that first described evidence for hedgehog involvement in prostate cancer cells. [PubMed: 15314219]

97. Mao J, Ligon KL, Rakhlin EY, et al. A novel somatic mouse model to survey tumorigenic potential applied to the Hedgehog pathway. Cancer Res. 2006; 66(20):10171–10178. [PubMed: 17047082]

98. Chen BY, Lin DP, Liu JY, et al. A mouse prostate cancer model induced by Hedgehog overexpression. J Biomed Sci. 2006; 13(3):373–384. [PubMed: 16374524]

99. Sheng T, Li C, Zhang X, et al. Activation of the hedgehog pathway in advanced prostate cancer. Mol Cancer. 2004; 3:29. [PubMed: 15482598]

100. Fan L, Pepicelli CV, Dibble CC, et al. Hedgehog signaling promotes prostate xenograft tumor growth. Endocrinology. 2004; 145(8):3961–3970. [PubMed: 15132968]

101. Azoulay S, Terry S, Chimingqi M, et al. Comparative expression of Hedgehog ligands at different stages of prostate carcinoma progression. J Pathol. 2008; 216(4):460–470. [PubMed: 18825689]

102•. Narita S, So A, Ettinger S, et al. GLI2 knockdown using an antisense oligonucleotide induces apoptosis and chemosensitizes cells to paclitaxel in androgen-independent prostate cancer. Clin Cancer Res. 2008; 14(18):5769–5777. Finds clinical relevance for Gli2 expression in human prostate cancer progression. [PubMed: 18794086]

103•. Shaw A, Gipp J, Bushman W. The Sonic Hedgehog pathway stimulates prostate tumor growth by paracrine signaling and recapitulates embryonic gene expression in tumor myofibroblasts. Oncogene. 2009; 28(50):4480–4490. First paper to challenge the idea of autocrine hedgehog in prostate cancer cells that express hedgehog target genes. [PubMed: 19784071]

104. Zhang J, Lipinski R, Shaw A, Gipp J, Bushman W. Lack of demonstrable autocrine hedgehog signaling in human prostate cancer cell lines. J Urol. 2007; 177(3):1179–1185. [PubMed: 17296441]

105. McCarthy FR, Brown AJ. Autonomous Hedgehog signalling is undetectable in PC-3 prostate cancer cells. Biochem Biophys Res Commun. 2008; 373(1):109–112. [PubMed: 18544338]

106. Thiyagarajan S, Bhatia N, Reagan-Shaw S, et al. Role of GLI2 transcription factor in growth and tumorigenicity of prostate cells. Cancer Res. 2007; 67(22):10642–10646. [PubMed: 18006803]

107. Stecca B, Mas C, Ruiz i Altaba A. Interference with HH-GLI signaling inhibits prostate cancer. Trends Mol Med. 2005; 11(5):199–203. [PubMed: 15882606]

108. Reddy GP, Barrack ER, Dou QP, et al. Regulatory processes affecting androgen receptor expression, stability, and function: potential targets to treat hormone-refractory prostate cancer. J Cell Biochem. 2006; 98(6):1408–1423. [PubMed: 16619263]

109. Terry S, Yang X, Chen MW, Vacherot F, Buttyan R. Multifaceted interaction between the androgen and Wnt signaling pathways and the implication for prostate cancer. J Cell Biochem. 2006; 99(2):402–410. [PubMed: 16741972]

110. Chen M, Tanner M, Levine AC, Levina E, Ohouo P, Buttyan R. Androgenic regulation of hedgehog signaling pathway components in prostate cancer cells. Cell Cycle. 2009; 8(1):149–157. [PubMed: 19158486]

111•. Chen M, Feuerstein MA, Levina E, et al. Hedgehog/Gli supports androgen signaling in androgen deprived and androgen independent prostate cancer cells. Mol Cancer. 2010; 9:89. First evidence for hedgehog/Gli interaction with androgen signaling pathway in prostate cancer cells. [PubMed: 20420697]

112. Chen G, Goto Y, Sakamoto R, et al. GLI1, a crucial mediator of sonic hedgehog signaling in prostate cancer, functions as a negative modulator for androgen receptor. Biochem Biophys Res Commun. 2011; 404(3):809–815. [PubMed: 21172305]

113. Keys DN, Lewis DL, Selegue JE, et al. Recruitment of a hedgehog regulatory circuit in butterfly eyespot evolution. Science. 1999; 283(5401):532–534. [PubMed: 9915699]

114. Agren M, Kogerman P, Kleman MI, Wessling M, Toftgard R. Expression of the *PTCH1* tumor suppressor gene is regulated by alternative promoters and a single functional Gli-binding site. Gene. 2004; 330:101–114. [PubMed: 15087129]

115. Bonifas JM, Pennypacker S, Chuang PT, et al. Activation of expression of hedgehog target genes in basal cell carcinomas. J Invest Dermatol. 2001; 116(5):739–742. [PubMed: 11348463]

116. Bishop CL, Bergin AM, Fessart D, et al. Primary cilium-dependent and -independent Hedgehog signaling inhibits p16(INK4A). Mol Cell. 2010; 40(4):533–547. [PubMed: 21095584]

117. Yoon JW, Kita Y, Frank DJ, et al. Gene expression profiling leads to identification of GLI1-binding elements in target genes and a role for multiple downstream pathways in GLI1-induced cell transformation. J Biol Chem. 2002; 277(7):5548–5555. [PubMed: 11719506]

118. Mill P, Mo R, Hu MC, Dagnino L, Rosenblum ND, Hui CC. Shh controls epithelial proliferation via independent pathways that converge on N-Myc. Dev Cell. 2005; 9(2):293–303. [PubMed: 16054035]

119. Rizvi S, Demars CJ, Comba A, et al. Combinatorial chemoprevention reveals a novel smoothened-independent role of GLI1 in esophageal carcinogenesis. Cancer Res. 2010; 70(17): 6787–6796. [PubMed: 20647328]

120. Sasaki H, Hui C, Nakafuku M, Kondoh H. A binding site for Gli proteins is essential for HNF-3β floor plate enhancer activity in transgenics and can respond to Shh *in vitro*. Development. 1997; 124(7):1313–1322. [PubMed: 9118802]

121. Teh MT, Wong ST, Neill GW, Ghali LR, Philpott MP, Quinn AG. FOXM1 is a downstream target of Gli1 in basal cell carcinomas. Cancer Res. 2002; 62(16):4773–4780. [PubMed: 12183437]

122. Eichberger T, Regl G, Ikram MS, et al. FOXE1, a new transcriptional target of GLI2 is expressed in human epidermis and basal cell carcinoma. J Invest Dermatol. 2004; 122(5):1180–1187. [PubMed: 15140221]

123. Laner-Plamberger S, Kaser A, Paulischta M, Hauser-Kronberger C, Eichberger T, Frischauf AM. Cooperation between GLI and JUN enhances transcription of JUN and selected GLI target genes. Oncogene. 2009; 28(13):1639–1651. [PubMed: 19219074]

124. Vokes SA, Ji H, McCuine S, et al. Genomic characterization of Gli-activator targets in sonic hedgehog-mediated neural patterning. Development. 2007; 134(10):1977–1989. [PubMed: 17442700]

125. Yoon JW, Gilbertson R, Iannaccone S, Iannaccone P, Walterhouse D. Defining a role for Sonic hedgehog pathway activation in desmoplastic medulloblastoma by identifying GLI1 target genes. Int J Cancer. 2009; 124(1):109–119. [PubMed: 18924150]

126. Vokes SA, Ji H, Wong WH, McMahon AP. A genome-scale analysis of the cis-regulatory circuitry underlying sonic hedgehog-mediated patterning of the mammalian limb. Genes Dev. 2008; 22(19):2651–2663. [PubMed: 18832070]

127. Yu M, Gipp J, Yoon JW, Iannaccone P, Walterhouse D, Bushman W. Sonic hedgehog-responsive genes in the fetal prostate. J Biol Chem. 2009; 284(9):5620–5629. [PubMed: 19095649]

128. Katoh Y, Katoh M. WNT antagonist, SFRP1, is Hedgehog signaling target. Int J Mol Med. 2006; 17(1):171–175. [PubMed: 16328026]

129. Eichberger T, Kaser A, Pixner C, et al. GLI2-specific transcriptional activation of the bone morphogenetic protein/activin antagonist follistatin in human epidermal cells. J Biol Chem. 2008; 283(18):12426–12437. [PubMed: 18319260]

130. Regl G, Kasper M, Schnidar H, et al. Activation of the BCL2 promoter in response to Hedgehog/GLI signal transduction is predominantly mediated by GLI2. Cancer Res. 2004; 64(21):7724–7731. [PubMed: 15520176]

131. Tanese K, Fukuma M, Ishiko A, Sakamoto M. Endothelin-2 is upregulated in basal cell carcinoma under control of Hedgehog signaling pathway. Biochem Biophys Res Commun. 2010; 391(1):486–491. [PubMed: 19914214]

Website

201. American Cancer Society. Cancer facts and figures 2010. www.cancer.org/acs/groups/content/@nho/documents/document/acspc-024113.pdf

Key issues

- Hedgehog signaling regulates the activities of Gli transcription factors.
- Paracrine hedgehog signaling guides developmental growth of the prostate gland.
- Gene anomalies that dysregulate hedgehog signaling are causative of some forms of human cancers.
- These gene anomalies are rarely found in prostate tumor cells.
- Aggressive prostate tumor behaviors correlate with high expression of hedgehog ligands and Gli2.
- Overexpression of Sonic hedgehog increases the growth of human prostate cancer xenografts in mice, and treatment hedgehog/Gli inhibitors strongly inhibits tumor xenograft growth.
- Knockdown of Gli1 or Gli2 expression reduces prostate cancer cell growth *in vitro.*
- Gli proteins (1 and 2) bind to the androgen receptor and affect androgen signaling in prostate cancer cells.
- Overexpression of Gli2 allows androgen-independent growth of prostate cancer cells *in vitro* and may be a factor in the development of castration-recurrent prostate cancers.

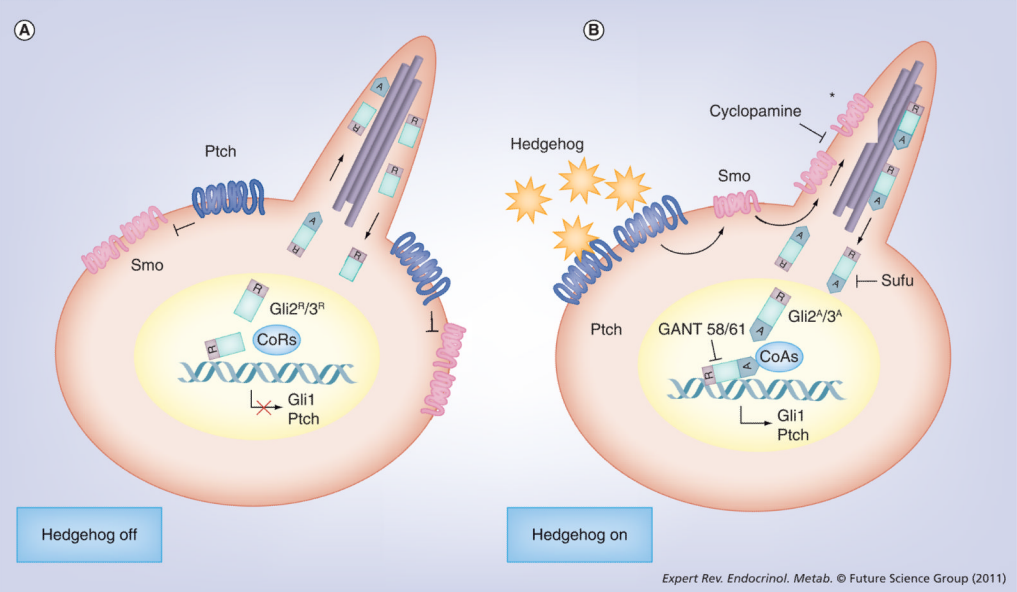

Figure 1. Schematic of the hedgehog signaling process in a target cell

(A) Hedgehog-off. In the absence of hedgehog ligand, Ptch gates the movement of Smo into the primary cilia and prevents its activation. Without activated Smo, Gli2/3 cilia where they are processed to remove the C-terminal activation domain. Lacking this domain, the truncated Gli proteins exit the cilia and migrate into the nucleus where they bind to Gli-response elements on DNA and attract a transcription corepressor protein complex that blocks transcription of Gli target genes. **(B)** Hedgehog-on. Hedgehog ligand binds to Ptch and enable Smo to traffic into cilia where it becomes activated (*). With activated Smo in the primary cilia, Gli protein processing to the repressor Gli2/3 proteins exit the primary cilia with an activation domain intact and they can enter the nucleus, bind to Gli-response elements on DNA and attract a transcription coactivator protein complex that enables transcription of Gli target genes.

CoA: Coactivator; CoR: Corepressor; GANT: Gli antagonist; Gli^A: Activated Gli; Gli^R: Repressed Gli; Ptch: Patched; Smo: Smoothened; Sufu: Suppressor of fused.

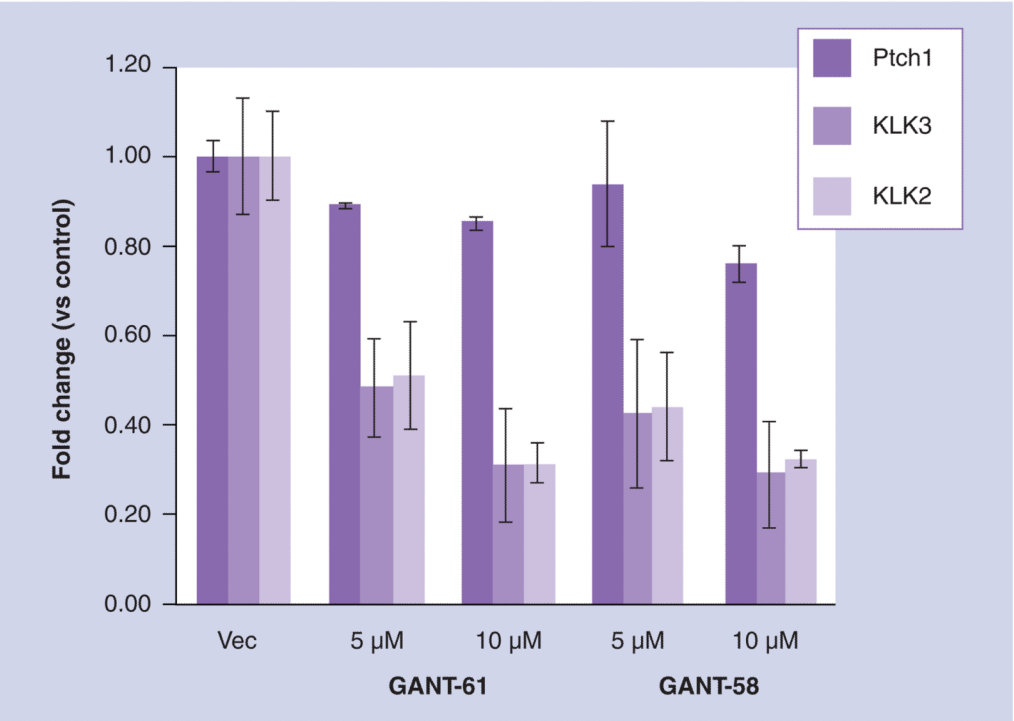

Figure 2. Suppression of androgen-dependent gene expression in androgen-deprived prostate cancer cells by the Gli-suppressing drugs GANT-58 and -61

LNCaP cells were seeded onto plates overnight in RPMI-1640 medium containing 10% fetal bovine serum, then switched to an androgen-depleted medium as was previously described [110] containing Vec or GANT-58 or GANT-61 dissolved in dimethyl sulfoxide at the indicated concentrations and was incubated for an additional 72 h. RNAs were then extracted from these cells and were assessed by quantitative real-time PCR for the expression of KLK2 or KLK3 (prostate-specific antigen), as described, and the results are normalized to the expression of GAPDH in the same samples. Each point indicates the means ± standard deviation from triplicate cultures.

GANT: Gli antagonist; KLK: Kallikrein-related peptidase; Ptch: Patched; Vec: Dimethyl sulfoxide vehicle only.

Table 1

Genes that are known to be regulated by Gli binding.

Gli-regulated genes	Ref.
GLI1	[113]
PTCH1	[114]
HHIP	[115]
CDKN2A/p16	[116]
CCND2/cyclin D2	[117]
MYCN/N-myc	[118]
CDK2	[119]
FOXA2	[120]
FOXM1	[121]
FOXE1	[122]
JUN	[123]
NKX2–1/Nkx2.1	[124]
NKX2–2/Nkx2.2	[124]
EGR2/Krox20	[125]
PRDM1/Blimp1	[126]
IGFBP3	[127]
IGFBP6	[117]
SFRP1	[128]
FST	[129]
SPP1/OPN	[117]
RAB34	[124]
RGS4	[127]
BCL2	[130]
EDN2/ET-2	[131]
JUP/PKGB	[117]
FBN2	[127]

The Prostate 72:817–824 (2012)

Paracrine Hedgehog Increases the Steroidogenic Potential of Prostate Stromal Cells in a Gli-Dependent Manner

Elina Levina,[1] Mengqian Chen,[1] Richard Carkner,[2] Michael Shtutman,[1] and Ralph Buttyan[3]*

[1]South Carolina College of Pharmacy, Department of Biomedical and Pharmaceutical Sciences, Columbia, South Carolina
[2]The Ordway Research Institute, Albany, New York
[3]The Vancouver Prostate Centre, Vancouver, BC, Canada

Acquired intratumoral steroidogenesis is involved in progression of prostate cancer to castration resistant disease (CRPC) and a target for improved therapeutics. Recent work has shown that prostate cancer cells can acquire steroidogenic activity as they progress to a therapeutic-resistant state. However, benign prostate stromal cells (PrSCs) also have steroidogenic potential though they are often overlooked as a source of intratumoral androgens. Here, we present preliminary studies showing that the steroidogenic activity of primary human PrSCs is significantly increased by exposure to a Hedgehog agonist (SAG) or by transduction of PrSCs with lentiviruses that expresses active Gli2 (Gli2ΔN), a transcription factor that is triggered by Hh signaling. Comparative gene expression profiling on Chips, that was confirmed by quantitative real-time PCR, revealed that hedgehog agonist treatment induced in these cells expressions of hedgehog target genes (Gli1, Ptch1, and SCUBE1) plus a specific cadre of genes involved in cholesterol/steroid biosynthesis, metabolism, and transport. Genes involved downstream in steroid hormone generation, including CYP17A1 and CYP19A1 were also induced. Both the hedgehog agonist and the Gli2-expressing lentivirus significantly increased the output of testosterone (T) from PrSCs that were supplemented with dihydroepiandrosterone (DHEA), an adrenal precursor of T. Finally, knockdown of Gli2 by siRNA suppressed the ability of SAG to induce this response. Collectively, our data indicate that hedgehog/Gli signaling may be a factor in acquired intratumoral steroidogenesis of a prostate tumor through its actions on stromal cells in the tumor microenvironment and an influence for the development of CRPC *Prostate 72:817–824, 2012*.

KEY WORDS: **prostate cancer; intratumoral steroidogenesis; prostate stromal cells; hedgehog; Gli; cholesterol; testosterone**

INTRODUCTION

Androgen deprivation therapies (ADT) used to treat advanced prostate cancer reduce systemic androgen levels in patients, providing palliative relief from symptoms of metastatic disease and often brings about regression of metastatic lesions [1]. For many though, the tumor will recur in a more lethal form now referred to as castrate resistant prostate cancer (CRPC) that underlies the mortality associated with the disease [2]. The contemporary view of the cellular paradigm by which prostate cancer progresses to CRPC

Grant sponsor: DOD; Grant number: W81XWH-10-1-0493; Grant sponsor: Division of Urology of Albany Medical Center, New York.

Disclosure statement: The authors declare no financial interests in the subject matter of this work.

Richard Carkner present address is Regeneron, Inc., 81 Columbia Turnpike, Rensselaer, NY 12144.

*Correspondence to: Ralph Buttyan, The Vancouver Prostate Centre, 2660 Oak Street, Vancouver, BC, Canada V6H 3Z6.
E-mail: rbuttyan@prostatecentre.com

Received 28 August 2011; Accepted 19 September 2011
DOI 10.1002/pros.21500
Published online 24 October 2011 in Wiley Online Library (wileyonlinelibrary.com).

involves the unexpected emergence of intratumoral steroidogenic potential that locally replaces the androgens lost as a consequence of ADT [3–6]. Current evidence strongly supports the idea that prostate cancer cells themselves can be a source of this activity. Prostate cancer cell lines that acquire the ability to grow in androgen-unsupplemented medium express higher levels of critical steroidogenic genes and they can secrete androgens into their medium through de novo as well as derivative biosynthetic pathways (by metabolism of dihydroepiandrosterone [DHEA]) [6,7]. More recently, we have also learned that cultured benign prostate stromal cells (PrSCs) also have steroidogenic capabilities. These cells can, at least, metabolize adrenal-derived DHEA to testosterone (T) and dihydrotestosterone (DHT) [8,9]. Co-culture studies have shown that DHEA-supplemented PrSCs can increase prostate cancer cell growth through their ability to synthesize and release androgens into the common medium and this supports the idea that benign stromal cells in the microenvironment of a prostate tumor can contribute to intratumoral steroidogenesis [8].

Here we present findings showing that activation of Hedgehog (Hh) signaling in PrSCs markedly increases their steroidogenic potential. Hh is a cell signaling pathway that is best known for its role as a morphogen in embryonic development [10]. The canonical Hh pathway is driven by the presence of peptide ligands (hedgehogs) and, at the end-point, activates Gli-mediated transcription [11]. Hyperactive Hh/Gli is thought to be involved in several human tumors including prostate cancer [12–14]. In an effort to identify the effects of Hh signaling on PrSCs, we tested the effects of Hh activation on gene expression in these cells. The outcome shows that Hh can induce expression of a remarkable cadre of genes that are involved in cholesterol and steroid hormone biosynthesis and that it can also significantly boost the ability of PrSCs to produce androgens (T and DHT) when supplemented with DHEA. We believe that these observations have significant implications for understanding mechanisms involved in acquired intratumoral steroidogenesis during prostate tumor progression and for consideration of novel, more effective treatments for CRPC.

MATERIALS AND METHODS

Cells and Culture Conditions

Human primary PrSCs were obtained from Lonza, Inc. (Walkersville, MD) and maintained and passaged according to the supplier's recommendation. For routine culture, cells (passage 4–10) were grown in Stromal Cell Growth Medium (SCGM, Lonza, Inc.) with all supplements provided. For experiments, cells were plated in 6-well plates in SCGM and grown to 70% confluence. The medium was changed to Stromal Cell Basal Medium (SCBM) lacking supplements for 48 hr. Medium was replaced with SCBM containing 100 nM SAG (EMD Chemicals, Gibbstown, NJ) dissolved in ETOH or an equivalent volume of ETOH (vehicle). For T output measurement, the medium was also supplemented with 10 μM DHEA (Sigma Aldrich, St. Louis, MO). 293FT cells were obtained from Invitrogen, Inc. (Carlsbad, CA) and were maintained in DMEM with 10% fetal bovine serum (FBS, HyClone).

Expression Vectors, Lentiviral Transduction, siRNA and Transfection

The pLenti6-Gli2ΔN vector was previously described [15] and lentiviral particles were derived in conditioned medium after transfection of 293FT cells also as described. The conditioned medium from transfected 293FT cells (containing lentivirus) was diluted in SCBM and applied to PrSC cultures overnight before replacing medium with SCBM. Non-targeting and Gli2-targeting siRNA was obtained from Qiagen (Valencia, CA). Plated PrSC cells were transfected with siRNA in SCBM supplemented with 5% FBS, without antibiotics using 20 nM siRNA/per well with SiLentFect Lipid Reagent (BioRad, Hercules, CA) as recommended by the manufacturer. Transfection medium was then replaced with SCBM for 48 hr before treatment with vehicle or SAG, as above.

Testosterone ELISA Assay

PrSC monolayers were grown in SCBM medium for 48 hr then replaced with SCBM (+ vehicle/SAG) supplemented with DHEA and aliquots of conditioned medium were removed and stored at −20°C until assay. T concentrations were measured by Testosterone (Free) ELISA assay (ALPCO Diagnostics, Salem, NH) using unconditioned T-supplemented (positive controls) or T-unsupplemented SCBM with 10 μM DHEA or unsupplemented PrSC conditioned SCBM without added DHEA (negative controls) according to the manufacturer's recommendation. SAG supplementation did not affect the outcome of the positive or negative controls. Readings from unconditioned samples were used for baseline determination. Readings from T-supplemented positive controls were used to generate a T-concentration standard curve and T levels in cell conditioned mediums were compared to this curve to derive a T concentration. Numbers represent the means from biological triplicate samples.

RNA isolation, Microarray Gene Profiling and qPCR Analysis

RNAs were isolated using the RNeasy PLUS Mini Kit (Qiagen, for microarray analysis) or the RNeasy Mini Kit (Qiagen, for qPCR). RNAs used for gene profiling were pre-assessed for integrity on the Agilent 2100 Bioanalyzer (Agilent Tech., Santa Clara, CA) and only RNAs with a RIN > 9.0 were used. RNAs were converted to cDNA, labeled and hybridized to Affymetrix Human Gene Chips 1.0ST in a microarray core facility (Ordway Research Institute, Albany, NY). The scanned hybridization data was processed through GeneSpring GX 10.0 analysis software (Agilent Tech.). Briefly, after normalization using the RMA algorithm, a *T*-test statistical analysis was carried out to select genes whose expression levels significantly change in SAG-treated specimens compared to vehicle-treated controls (*P*-value <0.05). The fold-change for each gene was calculated relative to control. For qPCR, cDNAs were synthesized and quantified as previously described [15]. Each measurement was based on biological triplicate specimens and each specimen was analyzed in duplicate. Primers used for qPCR including the following: *AGT* Forward- (F-) CGGGGGAAGAAGCTGCCGTT, Reverse- (R-) CCAGGCCAGGAGGCAGAGGA; *DHCR24* F-TGTTGCCAAAGGGGATAATG, R-CTGAAGACAAACCGAGAGGG; *DHCR7* F-CTTGAGATGCGGTTCTGTCA, R-TATTTGGCAAGAGGCTGGAG; *FABP3* F-GTGGTAGGCTTGGTCATGCT, R-GCACCTGGAAGCTAGTGGAC; *FDPS* F-TCCATGATGTCATCTGCCAC, R-AGCCAAGGAAACAGGATGC; *HMGCR* F-TGTCCCCACTATGACTTCCC, R-TCGGTGGCCTCTAGTGAGAT; *HMGCS1* F-CTTCAGGTTCTGCTGCTGTG, R-TCCCACTCCAAATGATGACA; *HSD11B1* F-TGATGGAGGAGAAGAACCCA, R-AAGCAGAGCAATGGAAGCAT; *HSD17B7* F-CCTAATGTGCTTTTCCAGTTCC, R-ACCACTGGCTTTGGAAGAAA; *IDI1* F-AACCTGTTGCTTGTCGAGGT; R-GACCGGCGGTTGTCTGT; *INSIG1* F-TCACTATGGGGCTTTTCAGG; R-TCGTTCTTGGCTCCCTTGTA; *LDLR* F-CCGACACCTGCAGCCAGCTC, R-CGCTCCGGTCCAGCGTCATC; *LSS* F-CAGAACTCTAAGCCCTGCGT; R-GTGGAGTGCACCTCAGCC; *MVD* F-TTAACTGGTCCTGGTGCAGA, R-AACATCGCGGTCATCAAGTA; *PLAU* F-CCAGCTCACAATTCCAGTCA, R-TGACCCACAGTGGAAAACAG; *SC4MOL* F-TGCCATTTTTCAAATCTCTGC, R-TTGGAACACCTGGCGAGT; *SCD* F-GCAGCCGAGCTTTGTAAGAG, R-GTTCTACACCTGGCTTTGGG; *SCUBE1* F-GCAGCCACCATTATTGTCCT, R-AACATCCCGGGGAACTACAG; *SREBF1* F-CAGCATAGGGTGGGTCAAAT, R-GAGCCGTGCGATCTGGA; *SREBF2* F-TGCCAGGAAAGGAGCTACAC, R-GAGACCATGGAGACCCTCAC; *PTCH1* F-TCTCCAATCTTCTGGCGAGT, R-TGGGATTAAAAGCAGCGAAC; *GLI1* F-GGCTCGCCATAGCTACTGAT, R-CCAGCGCCCAGACAGAG.

Western Blotting

Mouse monoclonal antibodies to SREBP1 (Abcam, Cambridge, MA) and mouse anti-α-tubulin (Sigma Aldrich) were used for Western blot analysis. Blots were processed as previously described [16].

RESULTS AND DISCUSSION

Effects of Hedgehog Agonist (SAG) on Gene Expression in Prostate Stromal Cells

Our interest in Hh as an effector of CRPC arose as a consequence of observations of striking increases in the expression of mature hedgehogs in prostate cancer cells when they were deprived of androgen and their release into conditioned medium in a paracrine-active state [16]. Whereas there remains some controversy as to whether a Hh signaling microenvironment might directly affect the malignant cells of a prostate tumor [17], there is general acceptance that Hh can affect solid tumor growth through a reciprocal paracrine process in which the malignant cells in the tumor secrete active hedgehogs to act on the benign stromal cells within the tumor microenvironment [17–21]. In turn, the stromal cells are believed to produce diffusible substance(s) that effect malignant cell growth and motility/invasion. In order to better understand the consequences of paracrine Hh on PrSCs, we performed comparative gene expression profiling between vehicle-treated (ETOH) or SAG-treated primary human PrSCs. SAG is a chemical agonist of Hh signaling [22] and a preliminary study had shown that SAG, at 100 nM, was superior to recombinant sonic hedgehog (Shh) protein or purmorphamine, another known chemical agonist of Hh [23], as an inducer of Hh target genes, Gli1 and Ptch1, from PrSCs (not shown). Here we used comparative gene expression profiling on gene Chips to identify PrSC genes whose expressions are induced by Hh signaling with the consideration that these genes might provide insight into the cryptic product produced by stromal cells that can affect malignant prostate cell growth. For this experiment we used cultured primary human PrSCs from a single donor. The cells were grown to near-confluence in serum-supplemented SC medium then pre-starved of serum for 48 hr to enhance formation of primary cilia on the cells that are necessary for Hh signaling. Subsequently, the medium was replaced with serum-free medium supplemented with vehicle or SAG for an additional 48 hr and thereafter, RNAs were extracted from each arm (two biological

replicates each) were then profiled on Affymetrix human ST1.0 gene Chips. Expression levels between the arms were compared using GeneSpring v10 software and the outcome showed that 37 annotated protein-coding genes were induced by 1.4-fold or greater (all $P < 0.005$) (shown in Table I). Three of the upregulated genes (Gli1, Ptch1, and SCUBE2) are known targets of Hh/Gli and this confirms that the Hh signaling was activated by the agonist. Of the other genes, 24 were classified in the Gene Ontogeny functional group ''lipid metabolic process and steroid biosynthetic process.'' Indeed, many of the genes in this group are directly required for cholesterol biosynthesis and/or metabolism of cholesterol to other steroids. A selected subset of these genes (15) were then validated for SAG-induced changes, using fresh RNAs from a second set of PrSCs treated in an equivalent manner, by a quantitative (real-time) RT-PCR procedure (qPCR). Each of the 15 genes were significantly upregulated by SAG treatment (Fig. 1), all to a greater extent than was shown by comparative gene profiling on Chips.

To ensure that this effect was not restricted to the particular donor cells used for the initial work, we obtained a second batch of primary human PrSCs from a different human donor and subjected them to the same treatment plan. Again, a qPCR assay was performed for 20 different genes from our list, using either the original donor sets of cDNAs or the cDNA sets prepared from second donor's cells. Each of the genes analyzed, from both donor sets of cells, showed significant upregulation by SAG-treatment ($P < 0.05$) (Table I). Thus, we believe that this response is characteristic of cultured primary human PrSCs in general and not a finding restricted to cells from a particular donor.

Hedgehog Agonist Treatment and Gli2 Increases Testosterone Output From PrSCs Supplemented With DHEA

Primary human PrSCs were previously shown to have the ability to convert DHEA to T in vitro [8]. Based upon our finding of significant steroid biosynthetic gene upregulation after SAG treatment, we tested whether SAG might also increase the ability of PrSCs to convert DHEA to T. Near-confluent PrSCs were again starved for serum for 48 hr then duplicate sets were treated with vehicle or SAG in the presence of 10 mM DHEA. The use of this high concentration of DHEA enables the detection of T in conditioned medium using an ELISA method for T quantification [8]. Aliquots of medium were obtained from each plate at 24, 48, and 72 hr after treatment. T output increased over time in the vehicle-treated cells and this supports the idea that PrSCs have inherent steroidogenic potential (Fig. 2A). Although T levels in medium from SAG-treated PrSCs were already slightly elevated at 24 hr compared to vehicle treated cells, this did not reach statistical significance until 48 hr and, by 72 hr, T levels were more than doubled (2.19-fold, $P < 0.001$) in the medium of the SAG-treated cells compared to vehicle-treated cells. These data show that the increase in steroidogenic gene expressions associated with Hh agonist treatment were functional in that they enabled increased conversion of DHEA to T compared to control cells.

To confirm that the effects of SAG on DHEA conversion to T were dependent on canonical Hh signaling through Gli, the experiment was repeated, but the 48 hr pre-starvation of serum phase was modified by including transfection with control (non-targeting) or Gli2-targeting siRNA (in serum-free medium) during this time. As is shown in Figure 2B, pre-transfection with Gli2 siRNA blocked the ability of subsequent SAG treatment to upregulate T output from DHEA-fed PrSCs. Thus the effects of SAG on androgen biogenesis in PrSCs appear to be Gli2-dependent. Remarkably, the Gli2 siRNA also significantly suppressed the basal production of T from DHEA in PrSCs, suggesting that Gli function might have some role in basal steroidogenesis by these cells. Finally, we tested whether we could effect increased T production following transduction of DHEA-supplemented PrSCs with a defective lentivirus that expresses the Gli2ΔN protein. Gli2ΔN is an N-terminal truncated variant of Gli2 that lacks the potential for repressive activity and mimics an active Hh response [24]. As with SAG treatment, the introduction of the active Gli2 protein into PrSCs was associated with significantly higher output of T from DHEA (Fig. 2C). This finding also supports the Gli-dependent nature of androgen biogenesis from DHEA in PrSCs.

The question remains as to whether all of the steroidogenic genes induced by SAG in PrSCs are directly regulated by Gli or whether only certain of them are direct Gli targets, but once induced, effect the expression of other steroidogenic genes. With regards to this question, it is notable that SREBF1 was one of the SAG-upregulated genes and several other genes on our upregulated list are known to be targets of active SREBF1-mediated transcription (identified in Table I). We were, at least, able to confirm the effects of SAG treatment on SREBF1 protein expression using a Western blot procedure (Fig. 3). Previously it was noted that SREBF1 gene has a Gli response element within its 5′-transcription upstream regulatory region [25] and our finding further substantiates the idea that SREBF1 is a direct target of Hh/Gli action in PrSCs. Regardless, the fact that many genes involved

TABLE I. Annotated Protein-Coding Genes Upregulated in SAG-Treated Primary Human Prostate Stromal Cells

Gene	Gene description	MA[a]	qPCR D1[b]	qPCR D2[c]
SCD*	Sterol-CoA desaturase	1.90	3.22	7.80
INSIG1*	Insulin-induced gene 1	1.87	3.18	7.06
GLI1	Gli family 1	1.82	23.98	26.97
PTCH1	Patched 1	1.81	3.70	3.16
DHCR7*	7-Dehydrocholesterol reductase	1.77	2.63	6.30
FABP3	Fatty acid binding protein 3	1.75	1.88	3.36
HMGCS1*	3-Hydroxy-3-methylglutaryl-Co A synthase 1	1.73	2.66	5.93
ATP1A2	ATPase, Na + /K+ transporting, Alpha2 peptide	1.71		
AGT	Angiotensinogen	1.61	6.77	7.16
DHCR24	24-Dehydrocholesterol reductase	1.61	2.93	5.20
ACAT2	Actyl-CoA acetyltransferase 2	1.59		
FADS1	Fatty acid desaturase 1	1.58		
CYGB	Cytoglobin B	1.57		
FASN*	Fatty acid synthase	1.57		
LDLR*	Low density lipoprotein receptor	1.55	3.05	6.12
ST3GAL5	ST3 beta-galactoside Alpha2-,3-sialyltransferase 5	1.53		
SCUBE1	Signal peptide, cub domain, EGF-like 1	1.52	2.17	1.61
MVD*	Mevalonate decarboxylase	1.51	3.38	3.87
HSD11B1	Hydroxysteroid (17-beta) dehydrogenase	1.48	2.36	1.20
GGT5	Gamma-glutamyl transferase-5	1.48		
PSG2	Pregnancy specific beta-1-glycoprotein 2	1.46		
SREBF1	Sterol regulatory element binding transcription factor 1	1.46	2.09	2.66
IDI1*	Isopentenyl-diphosphate delta isomerase	1.45	1.54	2.72
HMGCR*	3-Hydroxy-3-methylglutaryl-Co A reductase	1.45	2.20	3.42
PLAU	Plasminogen activator, urokinase	1.45	1.90	2.07
VWA5A	Von Willebrand factor A domain containing 5A	1.45		
SLC14A1	Solute carrier family 14 A1	1.44		
WFDC11	WAP four-disulfide core domain 11	1.43		
FDPS	Farnysl diphosphate synthase	1.43		
PREB	Prolacin regulatory element binding	1.43		
GPR63	G-coupled receptor-63	1.43		
GLDN	Gliomedin	1.43		
PCYT2	Phosphate cytidylyltransferase 2	1.43		
SGK493	Protein kinase-like protein SgK493	1.43		
HSD17B7*	Hydroxysteroid (17-beta) dehydrogenase	1.42	1.51	2.90
SC4MOL*	Sterol-C4-methyl oxidase-like	1.41	2.24	5.13
LSS*	Lanosterol synthase	1.41	3.00	2.49
CYP17A1*	Cytochrome P450, family 17, subfamily A-1			4.28
CYP19A1	Cytochrome P450, family 19, subfamily A-1			1.88

List of protein-coding genes upregulated by 1.4-fold or greater by treatment with 100 nM SAG compared to vehicle treatment.
[a]Fold-upregulation from microarray gene profiling ($P < 0.01$).
[b]Fold-upregulation from qPCR assay ($P < 0.05$) done on PrSCs obtained from Donor 1 (D1).
[c]Fold-upregulation from qPCR assay ($P < 0.05$) done on PrSCs obtained from Donor 2 (D2). Genes belonging to the GO functional group ''Lipid Metabolic Process and Steroid Biosynthetic Process'' are highlighted. Genes reported to be transcriptionally upregulated by SREBP1 transcription factor are marked with *.

in cholesterol/steroid biosynthesis were collectively induced by the Hh agonist also suggests the possibility that Hh signaling enables de novo (through cholesterol) as well as derivative T biosynthesis. However, it will require a more sensitive analytical method (HPLC/mass spectrophotometry) to test this and that work is ongoing. Likewise, although our gene expression studies identified only few genes involved in the downstream pathway involved in T biosynthesis, we subsequently designed specific primers to test whether SAG action might include other known genes, specifically CYP17A1 and CYP19A1, that are involved in T generation and metabolism. Both were found to be upregulated by SAG using a qPCR assay (Table I) though the SAG effect appears to be stronger for CYP17A1. Here it is notable that CYP17A1 is the

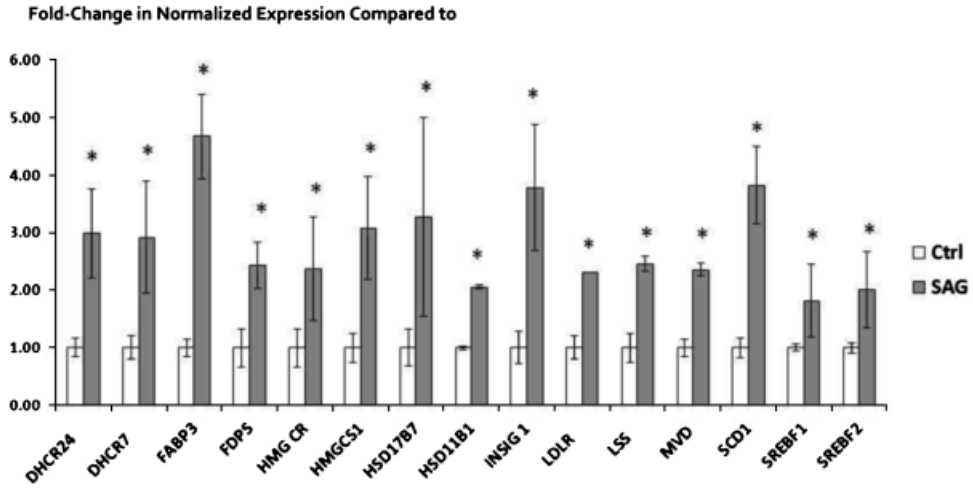

Fig. 1. Quantitative real-time RT-PCR assay confirms that the expressions of 15 genes involved in lipid metabolism and steroid biosynthesis are significantly ($P < 0.05$) upregulated (compared to vehicle-controls) by treatment with SAG.

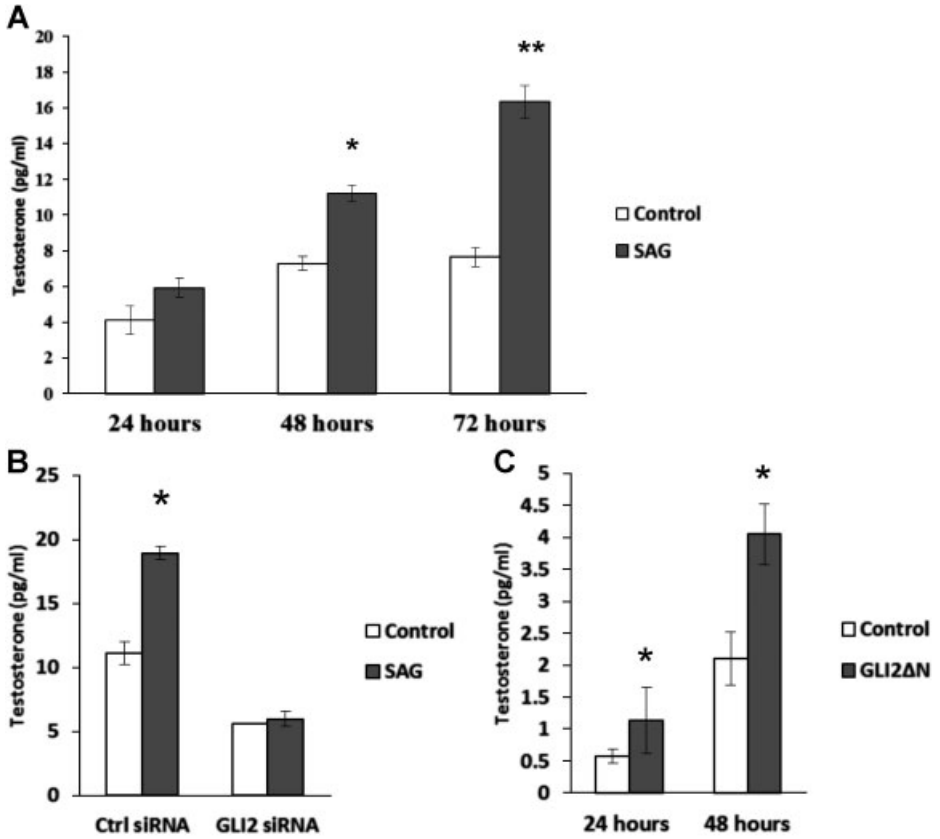

Fig. 2. Testosterone (T) output from dihydroepiandrosterone (DHEA) supplemented PrSCs is increased by Hedgehog agonist (SAG) in a Gli2-dependent manner. **A**: T concentrations in conditioned mediums from vehicle- (control) or SAG-treated cells increased over 72 hr ($^{*}P < 0.05$; $^{**}P < 0.01$ compared to control at same time). **B**: Transfection with Gli2 siRNA reduces basal output of T from DHEA in vehicle-treated PrSCs and blocks SAG-induced increase in T output from DHEA ($P < 0.05$); SAG-treated compared to vehicle-treated transfected with control (Ctrl) (non-targeting) siRNA. **C**: Transduction of PrSCs with Gli2ΔN lentivirus significantly ($^{*}P < 0.05$) increases T output from DHEA compared to empty lentivirus transduction (control).

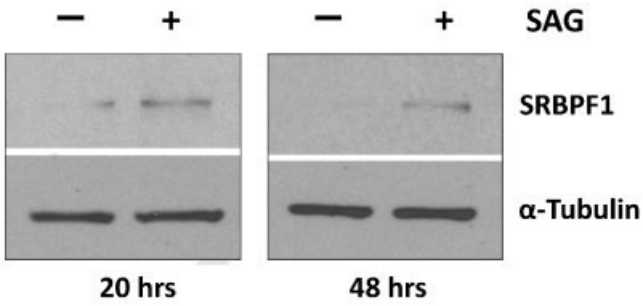

Fig. 3. Expression of SREBFI protein is increased by treatment of PrSCs with SAG. **Top panels**: Western blots of vehicle- (−) or SAG- (+) treated PrSCs at two different times using anti-SREBFI antibody shows upregulation of SREBFI protein by SAG treatment. **Bottom panels**: Blots were cleaned then re-probed with anti-α tubulin antibody to control for protein loading.

target of a new anti-steroidogenic drug for CRPC, abiraterone, that is drawing considerable interest following reports of clinical efficacy [26]. Abiraterone targets CYP17A1 and the fact that Hh upregulates this same gene in PrSCs suggests that Hh/Gli signaling could also be involved in the development of abiraterone resistance in CRPC that can occur as a consequence of upregulation of CYP17A1 expression [27].

Though our interest in the effects of Hh on steroidogenesis in PrSCs was fostered only as a consequence of unbiased exploratory gene profiling work, published literature already identifies a relationship between Hh and testosterone biosynthesis. For one, paracrine Hh signaling is required for differentiation of Leydig cells within the testicular stroma. Leydig cells are the main source for T in the normal male [28]. This likely explains the T deficiency found in embryonic male mice null for Sonic hedgehog (Shh−/−) [29]. Likewise, exogenous expression of Shh in the ovaries of transgenic female mice is associated with a phenotype of severe androgenization wherein the ovary resembles the testis with regards to the amount of T produced [30].

Recently, Shigemura et al. [31] published data showing that human prostate fibroblasts cultured from normal regions of prostate were responsive to stimulation with recombinant Shh but fibroblasts cultured from cancerous regions of the prostate were unresponsive. We presume that all of our studies involved human PrSCs from non-malignant regions though we cannot confirm this. While the outcome of their study implies that fibroblasts around a PCa are not susceptible to paracrine Hh action or its effects, our intent will be to test this using cancer-associated PrSCs generated in our own lab to determine whether it is a general principle or the outcome of a limited analysis. Regardless, the results shown here indicate a need to focus more effort on the potential contribution of the tumor stroma to the generation of androgens found within the microenvironment of a CRPC tumor.

CONCLUSIONS

Exposure to a hedgehog agonist or overexpression of active Gli2 significantly induces the expression of steroidogenic genes in primary human PrSCs and increases their ability to convert DHEA to T. These findings are potentially relevant to CRPC where intratumoral steroidogenesis is believed to support the androgen independent-like phenotype of the tumor. Additionally, these findings support consideration of the use of Hh inhibitors for preventing or treating CRPC. The Hh signaling pathway is a druggable target and several Hh inhibitors are already well into the clinical testing pipeline of major pharmaceuticals.

ACKNOWLEDGMENTS

This work was funded through a grant from the DOD (W81XWH-10-1-0493) (to R.B.) and through the generosity of the Division of Urology of Albany Medical Center, New York. The authors also acknowledge the expert assistance of Gennadi Glinsky, Director of the Microarray Core Facility and Associate, Anna Glinskii, for their expert advice concerning the microarray gene profiling study.

REFERENCES

1. Sharifi N, Gulley JL, Dahut WL. An update on androgen deprivation therapy for prostate cancer. Endocr Relat Cancer 2010; 17(4):R305–R315.
2. Attar RM, Takimoto CH, Gottardis MM. Castration-resistant prostate cancer: Locking up the molecular escape routes. Clin Cancer Res 2009;15(10):3251–3255.
3. Vis AN, Schroder FH. Key targets of hormonal treatment of prostate cancer. Part 1: The androgen receptor and steroidogenic pathways. BJU Int 2009;104(4):438–448.
4. Locke JA, Guns ES, Lubik AA, Adomat HH, Hendy SC, Wood CA, Ettinger SL, Gleave ME, Nelson CC. Androgen levels increase by intratumoral de novo steroidogenesis during progression of castration-resistant prostate cancer. Cancer Res 2008;68(15):6407–6415.
5. Cai C, Balk S. Intratumoral androgen biosynthesis in prostate cancer pathogenesis and response to therapy. Endocr Relat Cancer 2011.
6. Mohler JL, Titus MA, Bai S, Kennerley BJ, Lih FB, Tomer KB, Wilson EM. Activation of the androgen receptor by intratumoral bioconversion of androstanediol to dihydrotestosterone in prostate cancer. Cancer Res 2011;71(4):1486–1496.
7. Mostaghel EA, Montgomery B, Nelson PS. Castration-resistant prostate cancer: Targeting androgen metabolic pathways in recurrent disease. Urol Oncol 2009;27(3):251–257.
8. Mizokami A, Koh E, Izumi K, Narimoto K, Takeda M, Honma S, Dai J, Keller ET, Namiki M. Prostate cancer stromal cells and

LNCaP cells coordinately activate the androgen receptor through synthesis of testosterone and dihydrotestosterone from dehydroepiandrosterone. Endocr Relat Cancer 2009;16(4): 1139–1155.

9. Arnold JT, Gray NE, Jacobowitz K, Viswanathan L, Cheung PW, McFann KK, Le H, Blackman MR. Human prostate stromal cells stimulate increased PSA production in DHEA-treated prostate cancer epithelial cells. J Steroid Biochem Mol Biol 2008;111(3–5):240–246.
10. Ingham PW, McMahon AP. Hedgehog signaling in animal development: Paradigms and principles. Genes Dev 2001;15(23): 3059–3087.
11. Ingham PW, Nakano Y, Seger C. Mechanisms and functions of Hedgehog signalling across the metazoa. Nat Rev Genet 2011; 12(6):393–406.
12. Yang L, Xie G, Fan Q, Xie J. Activation of the hedgehog-signaling pathway in human cancer and the clinical implications. Oncogene 2010;29(4):469–481.
13. Evangelista M, Tian H, de Sauvage FJ. The hedgehog signaling pathway in cancer. Clin Cancer Res 2006;12(20 Pt 1):5924–5928.
14. Barakat MT, Humke EW, Scott MP. Learning from Jekyll to control Hyde: Hedgehog signaling in development and cancer. Trends Mol Med 2010;16(8):337–348.
15. Chen M, Feuerstein MA, Levina E, Baghel PS, Carkner RD, Tanner MJ, Shtutman M, Vacherot F, Terry S, de la Taille A, Buttyan R. Hedgehog/Gli supports androgen signaling in androgen deprived and androgen independent prostate cancer cells. Mol Cancer 2010;9:89.
16. Chen M, Tanner M, Levine AC, Levina E, Ohouo P, Buttyan R. Androgenic regulation of hedgehog signaling pathway components in prostate cancer cells. Cell Cycle 2009;8(1):149–157.
17. Chen M, Carkner R, Buttyan R. The hedgehog/Gli signaling paradigm in prostate cancer. Expert Rev Endocrinol Metab 2011;6(3):453–467.
18. Fan L, Pepicelli CV, Dibble CC, Catbagan W, Zarycki JL, Laciak R, Gipp J, Shaw A, Lamm ML, Munoz A, Lipinski R, Thrasher JB, Bushman W. Hedgehog signaling promotes prostate xenograft tumor growth. Endocrinology 2004;145(8):3961–3970.
19. Scales SJ, de Sauvage FJ. Mechanisms of Hedgehog pathway activation in cancer and implications for therapy. Trends Pharmacol Sci 2009;30(6):303–312.
20. Yauch RL, Gould SE, Scales SJ, Tang T, Tian H, Ahn CP, Marshall D, Fu L, Januario T, Kallop D, Nannini-Pepe M, Kotkow K, Marsters JC, Rubin LL, de Sauvage FJ. A paracrine requirement for hedgehog signalling in cancer. Nature 2008; 455(7211):406–410.
21. Shaw A, Gipp J, Bushman W. The Sonic Hedgehog pathway stimulates prostate tumor growth by paracrine signaling and recapitulates embryonic gene expression in tumor myofibroblasts. Oncogene 2009;28(50):4480–4490.
22. Chen JK, Taipale J, Young KE, Maiti T, Beachy PA. Small molecule modulation of Smoothened activity. Proc Natl Acad Sci USA 2002;99(22):14071–14076.
23. Sinha S, Chen JK. Purmorphamine activates the Hedgehog pathway by targeting Smoothened. Nat Chem Biol 2006;2(1): 29–30.
24. Roessler E, Ermilov AN, Grange DK, Wang A, Grachtchouk M, Dlugosz AA, Muenke M. A previously unidentified amino-terminal domain regulates transcriptional activity of wild-type and disease-associated human GLI2. Hum Mol Genet 2005; 14(15):2181–2188.
25. Lee EY, Ji H, Ouyang Z, Zhou B, Ma W, Vokes SA, McMahon AP, Wong WH, Scott MP. Hedgehog pathway-regulated gene networks in cerebellum development and tumorigenesis. Proc Natl Acad Sci USA 2010;107(21):9736–9741.
26. de Bono JS, Logothetis CJ, Molina A, Fizazi K, North S, Chu L, Chi KN, Jones RJ, Goodman OB Jr, Saad F, Staffurth JN, Mainwaring P, Harland S, Flaig TW, Hutson TE, Cheng T, Patterson H, Hainsworth JD, Ryan CJ, Sternberg CN, Ellard SL, Flechon A, Saleh M, Scholz M, Efstathiou E, Zivi A, Bianchini D, Loriot Y, Chieffo N, Kheoh T, Haqq CM, Scher HI. Abiraterone and increased survival in metastatic prostate cancer. N Engl J Med 2011;364(21):1995–2005.
27. Mostaghel EA, Marck B, Plymate S, Vessella RL, Balk SP, Matsumoto AM, Nelson PS, Montgomery B. Resistance to CYP17A1 inhibition with abiraterone in castration resistant prostate cancer: Induction of steroidogenesis and androgen receptor splice variants. Clin Cancer Res 2011.
28. Yao HH, Whoriskey W, Capel B. Desert Hedgehog/Patched 1 signaling specifies fetal Leydig cell fate in testis organogenesis. Genes Dev 2002;16(11):1433–1440.
29. Berman DM, Desai N, Wang X, Karhadkar SS, Reynon M, Abate-Shen C, Beachy PA, Shen MM. Roles for Hedgehog signaling in androgen production and prostate ductal morphogenesis. Dev Biol 2004;267(2):387–398.
30. Barsoum IB, Bingham NC, Parker KL, Jorgensen JS, Yao HH. Activation of the Hedgehog pathway in the mouse fetal ovary leads to ectopic appearance of fetal Leydig cells and female pseudohermaphroditism. Dev Biol 2009;329(1):96–103.
31. Shigemura K, Huang WC, Li X, Zhau HE, Zhu G, Gotoh A, Fujisawa M, Xie J, Marshall FF, Chung LW. Active sonic hedgehog signaling between androgen independent human prostate cancer cells and normal/benign but not cancer-associated prostate stromal cells. Prostate 2011. April 25 (Epub ahead of print).

MCB
Journals.ASM.org

The Stress Response Mediator ATF3 Represses Androgen Signaling by Binding the Androgen Receptor

Hongbo Wang,[a] Ming Jiang,[b] Hongmei Cui,[a] Mengqian Chen,[c] Ralph Buttyan,[d] Simon W. Hayward,[b] Tsonwin Hai,[e] Zhengxin Wang,[f] and Chunhong Yan[a]

Center for Cell Biology and Cancer Research, Albany Medical College, Albany, New York, USA[a]; Department of Urologic Surgery, Vanderbilt University, Nashville, Tennessee, USA[b]; South Carolina College of Pharmacy, Columbia, South Carolina, USA[c]; Vancouver Prostate Centre, Vancouver, British Columbia, Canada[d]; Department of Molecular and Cellular Biochemistry, Ohio State University, Columbus, Ohio, USA[e]; and Department of Cancer Biology, University of Texas M. D. Anderson Cancer Center, Houston, Texas, USA[f]

Activating transcription factor 3 (ATF3) is a common mediator of cellular stress response signaling and is often aberrantly expressed in prostate cancer. We report here that ATF3 can directly bind the androgen receptor (AR) and consequently repress AR-mediated gene expression. The ATF3-AR interaction requires the leucine zipper domain of ATF3 that independently binds the DNA-binding and ligand-binding domains of AR, and the interaction prevents AR from binding to *cis*-acting elements required for expression of androgen-dependent genes while inhibiting the AR N- and C-terminal interaction. The functional consequences of the loss of ATF3 expression include increased transcription of androgen-dependent genes in prostate cancer cells that correlates with increased ability to grow in low-androgen-containing medium and increased proliferative activity of the prostate epithelium in ATF3 knockout mice that is associated with prostatic hyperplasia. Our results thus demonstrate that ATF3 is a novel repressor of androgen signaling that can inhibit AR functions, allowing prostate cells to restore homeostasis and maintain integrity in the face of a broad spectrum of intrinsic and environmental insults.

The androgen receptor (AR) mediates androgen signaling essential for male sex differentiation and the male reproductive function (48). It is generally believed that defective androgen signaling contributes to various human male urogenital disorders including androgen-insensitivity syndrome and hypospadias (5, 24). Of particular interest, abnormal androgen signaling due to aberrant expression, mutations, or dysregulation of the *AR* gene has been linked to prostate tumorigenesis and progression of prostate cancer into advanced, castration-resistant disease (50, 51).

Following activation by androgen binding to its C-terminal ligand-binding domain (LBD), AR is translocated to the nucleus. There, the central DNA-binding domain (DBD) of the receptor binds to androgen responsive elements (ARE) and subsequently regulates expression of a plethora of genes that drive cell differentiation and proliferation (28). The transcriptional activity of AR is mainly carried by its N-terminal domain (NTD) and is regulated by various proteins that interact with AR through distinct mechanisms (21, 60). These AR regulators include components of chromatin remodeling/modifying complexes (e.g., ARIP4 and p300/CBP) that predispose permissive chromatin environments for AR binding and molecular adapters (e.g., SRC/p160 family members) that function to recruit basal transcriptional machinery or other transcriptional regulators to AR target promoters (21). Transcriptional factors (e.g., Foxa1) can also interact with AR and bind to DNA sequences in close proximity to ARE, thereby cooperating with AR to regulate gene expression (11). Since the transcriptional activity of AR is also regulated by an intermolecular interaction between its N terminus and C terminus (N-C interaction) (18, 19), AR-associated proteins like SMRT and caspase-8 repress AR-mediated gene expression by disrupting the N-C interaction (33, 47). Given the importance of AR-binding proteins in regulating AR activity, it is not surprising that aberrant expression or malfunction of AR regulators has often been causally related to androgen insensitivity syndrome, prostate cancer, and other urogenital disorders (1, 20). However, only a few of these AR regulators have been validated for their effects on androgen signaling using genetically engineered mouse models.

Activating transcription factor 3 (ATF3) is a member of the ATF/CREB family of transcription factors and can regulate gene expression by binding to the consensus ATF/CREB *cis*-regulatory element via a basic-region leucine zipper domain (bZIP) (14). A unique feature distinguishing ATF3 from other ATF/CREB members is that ATF3 is a common stress response mediator and can be rapidly induced by a broad spectrum of cellular stresses, including DNA damage, cell injury, oxidative stress, and endoplasmic reticulum stress (13). Due to its frequent induction by cellular stresses, ATF3 has been considered to play a crucial role in the maintenance of cell integrity and homeostasis under stressful conditions (14, 15). Indeed, whereas ATF3 has been found to play pivotal roles in regulating important cellular signaling pathways mediated by p53, transforming growth factor β (TGF-β), Toll-like receptor 4, or eukaryotic factor 2 kinase (12, 22, 25, 64), aberrant expression of the *ATF3* gene is frequently associated with various human diseases including hypospadias and prostate cancer (3, 31, 56). However, details of the function of this common stress response mediator remain largely unknown. Although ATF3 can

Received 2 February 2012 **Returned for modification** 26 February 2012
Accepted 22 May 2012
Published ahead of print 4 June 2012
Address correspondence to Chunhong Yan, YanC@mail.amc.edu.
Supplemental material for this article may be found at http://mcb.asm.org/.

doi:10.1128/MCB.00159-12

bind to promoters and repress expression of some genes while activating expression of other genes (14), the findings that ATF3 can interact with other proteins (e.g., p53, Smad3, and E6) via its bZIP domain suggest that ATF3 may regulate cellular functions independent of its transcriptional activity (25, 59, 64). Indeed, the binding of ATF3 to the tumor suppressor p53 can activate the latter protein by protecting it from ubiquitin-mediated degradation (64). Since the bZIP structural motif is a major scaffold for protein-protein interaction (29, 46), exploration of the ATF3 interactome might provide a key to a better understanding of its diverse and context-dependent functions in human diseases. In support of this notion, a recent report showed that ATF3 induces expression of the metastasis suppressor *KAI1* gene when it interacts with JunB, whereas the binding of ATF3 to the NF-κB p50 subunit represses expression of the same gene in prostate cancer cells (37).

Here, we sought to explore the potential role of ATF3 in regulating AR-mediated signaling. We report that ATF3 is a novel AR-binding protein. The ATF3-AR interaction not only prevented AR from binding to ARE but also disrupted the N-C interaction of AR, leading to repression of androgen signaling in cultured cells as well as in animals. These findings thus link a common stress response mediator to androgen signaling, suggesting that the ATF3-mediated cellular stress response could serve as a mechanism defending against prostate cancer.

MATERIALS AND METHODS

Cell culture and transfections. LNCaP, VCaP, and PC3 cells were cultured in RPMI 1640 medium supplemented with 10% fetal bovine serum. For androgen treatments, cells were cultured in medium containing 10% charcoal-stripped fetal bovine serum for 2 days, followed by addition of R1881 (methyltrienolone; Perkin Elmer) into the medium. Total cellular lipid levels were measured by AdipoRed assays (Lonza) as described by the manufacturer. Transfections were carried out using Lipofectamine 2000 (Invitrogen).

GST pulldown and co-IP assays. Glutathione *S*-transferase (GST) pulldown assays were carried out as described previously (64). Essentially, GST or GST fusion proteins were immobilized on glutathione-agarose (Sigma) and then incubated with *in vitro*-translated proteins or recombinant proteins at 4°C overnight. After extensive washes, bound proteins were eluted and detected by fluorography or Western blotting. For coimmunoprecipitation (co-IP) assays, cell lysates (1 mg) were incubated with the AR (H280; Santa Cruz Biotechnology), ATF3 (C-19; Santa Cruz), or FLAG antibody (Sigma) at 4°C overnight. Thirty microliters of protein A- or protein G-agarose was added, followed by extensive washes of the agarose. Precipitated proteins were then detected by Western blotting (64).

shRNA knockdown and retroviral infections. Knockdown of ATF3 expression was carried out using a lentivector-based short hairpin RNA (shRNA) system (pSIH-H1 shRNA cloning and lentivector expression system; System Biosciences) following the manufacturer's protocol. The ATF3-targeted sequence was 5′-GCA AAG TGC CGA AAC AAG A-3′ or 5′-GAG AAA CCT CTT TAT CCA A-3′, based on our earlier reports (59). For negative controls, a luciferase-targeted sequence (5′-CTT ACG CTG AGT ACT TCG A-3′) was cloned into the lentivector. For retroviral infections, the ATF3 cDNA was cloned into pBabe-puro and packaged into retroviral particles as previously described (59).

Quantitative reverse transcription-PCR (qRT-PCR). Total RNA was extracted from cells using TRIzol reagent (Invitrogen) and then reverse transcribed and subjected to real-time PCR assays as previously described (63). The sequences of primers used for amplifying AR and AR target genes are available on request. To determine expression of ATF3 and AR target genes in human prostate cancer, we purchased a TissueScan Prostate Cancer qPCR array from Origene (HPRT102) and subjected the cDNA samples to real-time PCR assays. Only cDNA samples derived from tissues consisting of at least 90% prostate cancer cells were used for analysis. All prostate cancer samples were collected by the manufacturer under protocols approved by the Institutional Review Board (Origene, Rockville, MD).

Gel shift assays. Recombinant ATF3 and AR protein containing the DBD region (amino acids [aa] 537 to 644 [AR-DBD]) were purified using nitrilotriacetic acid (NTA)-Ni^{+}-agarose as described previously (36, 64). An oligonucleotide containing the ARE in the *PSA* enhancer (5′-TGGAG GAACATATTGTATTGATTGT-3′) or a mutated oligonucleotide (5′-TG GAGGAATATATTATATTGATTGT-3′; mutations are underlined) (58) was labeled with [α-^{32}P]ATP and incubated with 500 ng of AR-DBD protein in a buffer containing 25 mM HEPES, pH 7.5, 0.5 mM EDTA, 0.5 mM dithiothreitol (DTT), 2.5% glycerol, 50 mM NaCl, and 1 μg of poly(dI-dC) in the absence or presence of recombinant ATF3 (500, 1,000, or 2,000 ng) or bovine serum albumin (BSA) at room temperature for 20 min and then resolved by nondenatured polyacrylamide electrophoresis followed by autography. Nuclear extracts were prepared from LNCaP cells, and 20 μg of nuclear extract was used for binding assays as described previously (65).

Androgen binding assays. The ligand-binding affinity of AR was determined using a whole-cell binding assay as described previously (30, 42). Briefly, PC3 cells (5×10^4) cultured in charcoal-stripped medium (CSM) were transfected with 0.1 μg of pcDNA3-FLAG-AR with or without 0.1 μg of pCG-ATF3 in 48-well plates for 2 days, followed by incubation with various concentrations of [^{3}H]R1881 (Perkin Elmer) for 2 h. Cells were then extensively washed with phosphate-buffered saline (PBS). The total bound [^{3}H]R1881 was extracted with 100 μl of cold ethanol for 20 min and measured using a scintillation counter. Nonspecific binding at each concentration was measured by adding 1 μM unlabeled R1881 and then subtracted from the total binding to generate values for specific binding. The maximal binding (B_{max}) and binding affinity (K_d) values were calculated using SigmaPlot according to the following equation: specific binding $= B_{max}\,[L]/(K_d + [L])$, where $[L]$ is the concentration of [^{3}H]R1881.

ChIP. Chromatin immunoprecipitation (ChIP) assays were carried out as descried previously with modifications (63). Essentially, cells cultured in 150-mm dishes were cross-linked with 1% formaldehyde and then lysed for sonication. Cell lysates were incubated with an AR antibody (H-280; Santa Cruz) at 4°C overnight, followed by addition of 30 μl of single-stranded DNA (ssDNA)-saturated protein A-agarose (Upstate). The protein-DNA complexes were eluted, and cross-link was reversed at 65°C overnight. DNA fragments were then purified using a QIAquick PCR purification kit (Qiagen) for real-time PCR assays using primers described previously (2).

Animal experiments and immunohistochemistry. Animal experiments were carried out according to a protocol approved by the Institutional Committee of Animal Care and Use of the Albany Medical College. For castration, testes of 8-week-old of ATF3 wild-type (WT) and knockout (KO) mice were surgically removed. These mice were housed for 21 days and then injected subcutaneously with 40 mg/kg of testosterone (Sigma) dissolved in corn oil every day for a total of 14 days. Mice in groups of three or four were sacrificed on days 3, 7, 14, and 21 postcastration or on days 3, 7, and 14 after testosterone replenishment, respectively. Prostate lobes were separated from these mice by microdissection and embedded in paraffin for sectioning and histological examination. For immunohistochemistry (IHC), antigens were retrieved in hot citrate buffer. Sections were then blocked in 5% normal horse serum and 1% normal goat serum, incubated with primary antibodies, and stained using an ABC Elite Kit and a DAB (3,3′-diaminobenzidine) Kit (Vector) according to the manufacturer's recommendations. The Ki-67 antibody (1:400) and AR antibody (1:200) were purchased from Abcam (ab15580) and Santa Cruz (N-20), respectively.

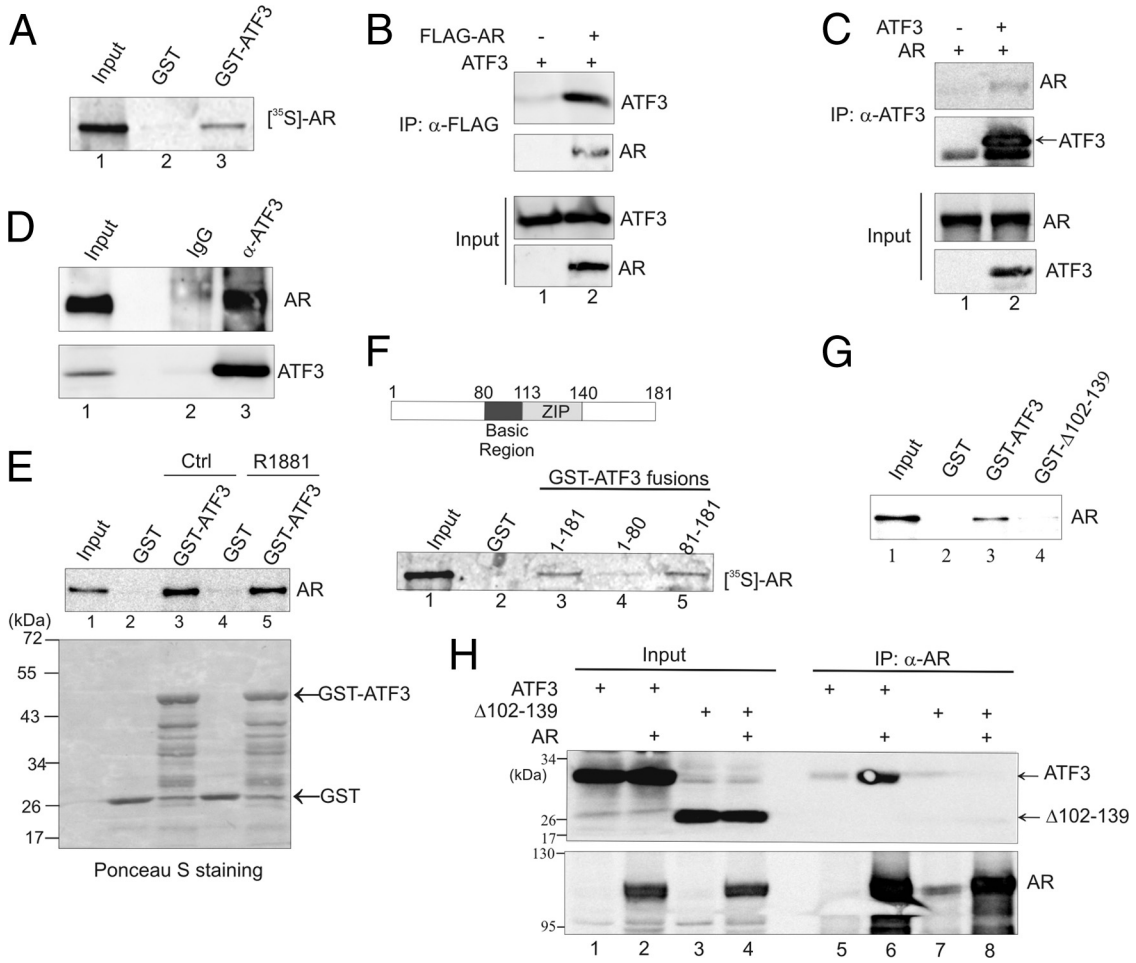

FIG 1 ATF3 interacts with AR via its ZIP domain. (A) GST-ATF3 or GST was immobilized onto glutathione-agarose and incubated with AR labeled with [^{35}S]methionine by *in vitro* translation. After extensive washes, bound proteins were eluted and visualized by electrophoresis followed by fluorography. (B) PC3 cells were transfected with the indicated plasmids and then subjected to co-IP using anti-FLAG antibody. Precipitated proteins were detected by Western blotting. (C) AR was coexpressed with or without ATF3 in PC3 cells by transfections. Cell lysates were subjected to co-IP using anti-ATF3 antibody followed by Western blotting. (D) LNCaP cell lysates were incubated with anti-ATF3 antibody or rabbit IgG at 4°C overnight and then precipitated with protein A-agarose. Bound proteins were eluted and subjected to Western blotting. (E) *In vitro*-translated AR was preincubated with or without 100 nM R1881 for 1 h and then subjected to GST pulldown assays to examine the ATF3-AR interaction. (F) The indicated GST-ATF3 fusions were incubated with ^{35}S-labeled AR and subjected to GST pulldown assays. (G) The full-length ATF3 and a mutant lacking the ZIP domain (Δ102–139) were fused to GST and incubated with *in vitro*-translated AR for GST pulldown assays. Bound proteins were detected by Western blotting with the anti-AR antibody. (H) ATF3 or ATF3 Δ102–139 was coexpressed with or without AR in PC3 cells and then subjected to co-IP assays with anti-AR antibody, followed by Western blotting. α, anti.

RESULTS

ATF3 interacts with AR via its ZIP domain. We carried out GST pulldown assays to determine whether ATF3 interacts with AR. Immobilized GST-ATF3, but not GST, pulled down *in vitro*-translated AR protein (Fig. 1A, lane 3), supporting a direct interaction between ATF3 and AR. To corroborate this finding, we coexpressed ATF3 and AR (tagged with FLAG) in PC3 cells, which are null for AR and express a low level of ATF3 (see Fig. S1, lane 2, in the supplemental material), and performed reciprocal coimmunoprecipitation (co-IP) assays using anti-FLAG (Fig. 1B) and anti-ATF3 antibody (Fig. 1C), respectively. Indeed, the FLAG antibody precipitated ATF3 only in the presence of AR but failed to do so in the absence of AR (Fig. 1B, lane 2 versus lane 1). Similarly, the ATF3 antibody precipitated AR only in the presence of ATF3 (Fig. 1C, lane 2). We also examined the interaction between endogenous ATF3 and AR proteins using LNCaP cells, which express high levels of both proteins (see Fig. S1, lane 1). In line with the notion that ATF3 interacts with AR, the ATF3 antibody, but not IgG, precipitated both ATF3 and AR from the cell lysates (Fig. 1D, lane 3 versus lane 2). It is unlikely that the ATF3-AR interaction is affected by the binding of androgen to AR since GST-ATF3 pulled down AR in the presence of R1881 as efficiently as it did without androgen treatments (Fig. 1E, lane 5 versus lane 3). Further GST-pulldown experiments using truncated ATF3 proteins indicated that the ATF3-AR interaction was mediated by the ATF3 C terminus (amino acids [aa] 81 to 181) (Fig. 1F, lane 5). Moreover, an ATF3 mutant lacking the ZIP region (a deletion of residues 102 to 139 [Δ102-139]) failed to pull down AR in GST pulldown assays (Fig. 1G, lane 4 versus lane 3) and was not coprecipitated with AR by an AR-specific antibody (Fig. 1H, lane 8 versus lane 6). It is unlikely that the inability of ATF3 Δ102-139 to bind AR was caused by inappropriate folding of

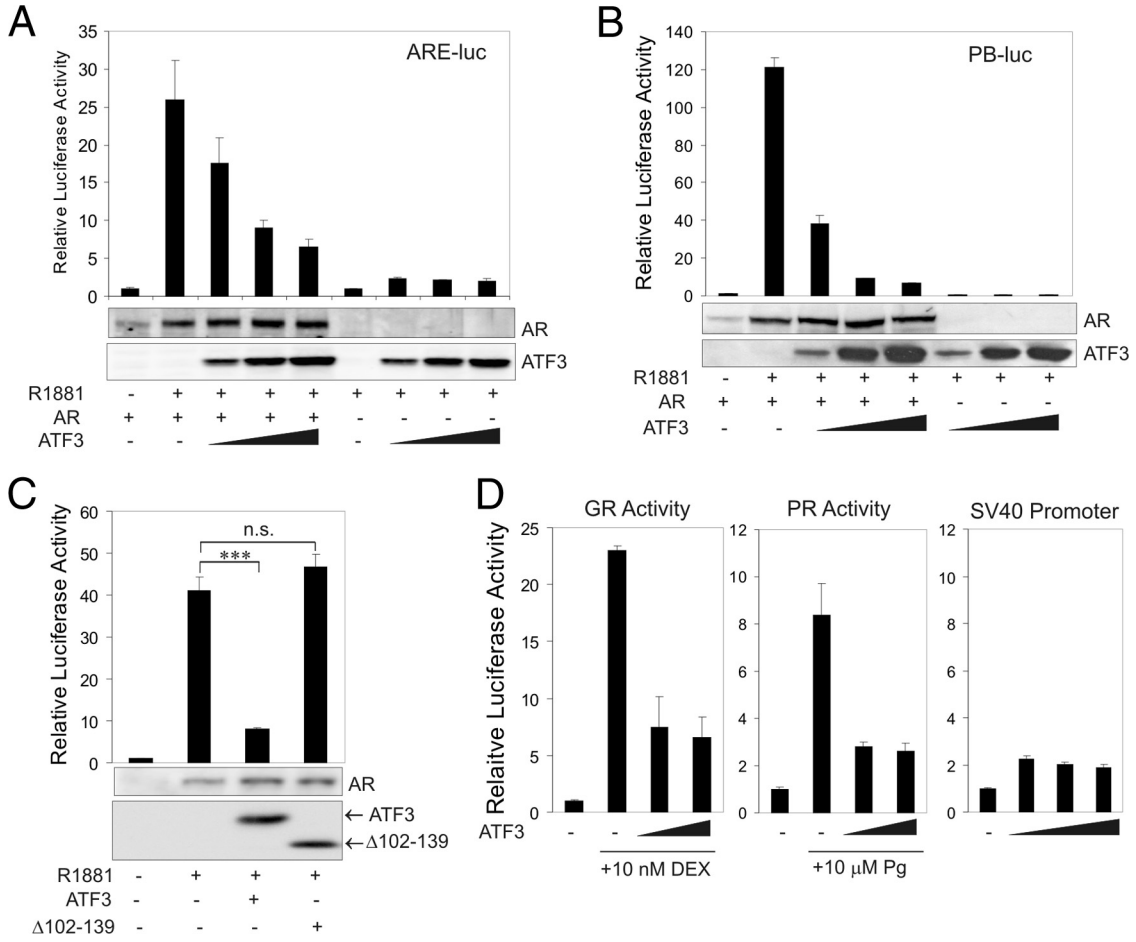

FIG 2 ATF3 represses the transactivation activity of AR. (A) PC3 cells were cotransfected with ARE-Luc, pRL-CMV (where CMV is cytomegalovirus), AR, and/or increasing amounts of ATF3 in charcoal-stripped medium for 1 day and then treated with 1 nM R1881 for dual luciferase activity assays. AR and ATF3 expression levels were determined by Western blotting after normalization using the *Renilla* luciferase activity. Data are depicted as averages ± standard deviations of three determinations. (B) PC3 cells were cotransfected with PB-Luc, pRL-CMV, AR, and/or increasing amounts of ATF3 for dual luciferase activity assays. Immunoblots show expression levels of AR and ATF3. Data are depicted as averages ± standard deviations of three determinations. (C) PC3 cells were cotransfected with PB-Luc, pRL-CMV, ATF3, or ATF3 Δ102–139 for dual luciferase activity assays. Data are depicted as averages ± standard deviations of three determinations. ns, not significant. (D) In the experiments shown in the left and middle graphs, PC3 cells were cotransfected with ARE-Luc, pRL-CMV, GR, or PR and/or increasing amounts of ATF3 in charcoal-stripped medium for 1 day and then treated with 10 nM dexamethasone (DEX) or 10 μM progesterone (Pg) for 1 day for dual luciferase activity assays. In the experiment shown in the right graph, PC3 cells were cotransfected with pGL3-promoter (containing the SV40 promoter), pRL-CMV, and/or increasing amounts of ATF3 for dual-luciferase activity assays. Data are depicted as averages ± standard deviations of three determinations.

the mutant protein as we previously showed that ATF3 Δ102-139 retained the ability to dimerize with wild-type ATF3 through the N terminus (64). These results thus demonstrate that ATF3 binds AR and that this interaction requires the ZIP domain of ATF3.

ATF3 represses the transactivation activity of AR. Since the transactivation activity of AR is often regulated by its associated proteins (21), we carried out luciferase reporter assays to test whether ATF3 affects the ability of AR to regulate gene expression. As expected, AR promoted transcription of a luciferase reporter driven by a synthetic promoter (ARE-luc) containing four tandem repeats of ARE (5′-AGAACAGCAAGTGCT-3′) (36) (Fig. 2A). Intriguingly, expression of ATF3 repressed AR-mediated transactivation of the reporter in a dose-dependent manner (Fig. 2A). Such repression was not due to a decrease in the AR expression level nor caused by direct repression of the promoter by ATF3 (Fig. 2A). Similar results were obtained using a reporter driven by a native AR target promoter, the probasin (*PB*) promoter (67) (Fig. 2B). Of note, the synthetic ARE promoter and the *PB* promoter do not contain any ATF/CREB sequence (5′-TGACGTCA-3′), and thus the repression of AR-mediated transcription was likely independent of the transcriptional activity of ATF3. The repression of the AR transcriptional activity by ATF3 was rather a consequence of binding of ATF3 to AR, as the ATF3 mutant (Δ102–139) deficient in AR binding (Fig. 1G and H) failed to repress AR-mediated activation of the *PB* promoter (Fig. 2C). These results indicate that the ATF3-AR interaction repressed the transactivation activity of AR. ATF3 also repressed transcription mediated by glucocorticoid receptor (GR) or progesterone receptor (PR) (Fig. 2D), two steroid receptors that are highly homologous to AR in the DNA binding domain (7). However, ATF3 did not decrease the activity of a constitutively active simian virus 40

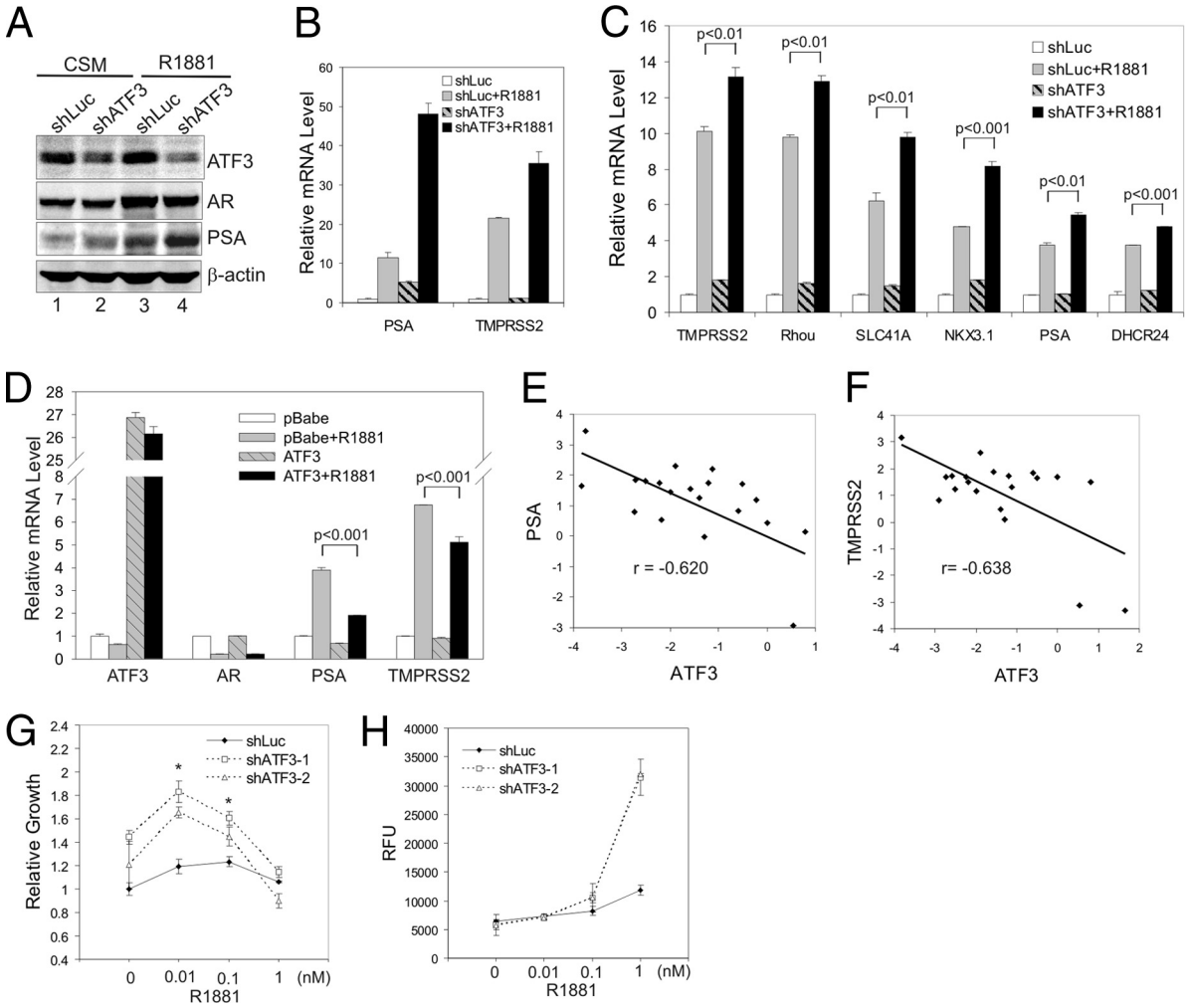

FIG 3 ATF3 represses androgen signaling in prostate cancer cells. (A and B) LNCaP cells were infected with lentiviruses expressing shATF3 or shLuc and selected with puromycin for 4 weeks. A clone stably expressing shATF3 was cultured in CSM for 2 days, treated with 1 nM R1881 for 24 h, and then lysed for Western blotting (A) or qRT-PCR assays (B). Data are depicted as averages ± standard deviations of three determinations. (C) LNCaP cells were infected with shATF3-expressing lentiviruses for 2 days, followed by being cultured in CSM for 2 days and then treated with 1 nM R1881 for 24 h. Cells were lysed for qRT-PCR assays to measure mRNA levels of indicated androgen-dependent genes. Data are depicted as averages ± standard deviations of three determinations. (D) VCaP cells infected with retroviruses expressing ATF3 or empty vector (pBabe) were cultured in CSM for 2 days, followed by treatments with 1 nM R1881 for 1 day. Levels of the indicated mRNAs were measured by qRT-PCR. Data are depicted as averages ± standard deviations of three determinations. (E and F) A qRT-PCR tissue array was used to measure *ATF3*, *PSA*, and *TMPRSS2* mRNA levels in human prostate cancer samples ($n = 20$). Relative mRNA levels were converted to logarithms ($\log_2$) and plotted for each sample. A linear regression line and Pearson's correlation (r) are shown for each graph. (G) LNCaP cells infected with lentiviruses expressing ATF3-specific shRNA (shATF3-1 and shATF3-2) or shLuc were cultured in CSM for 2 days. Various amounts of R1881 were added on days 0, 3, 6, and 9, and numbers of viable cells were measured on day 10 by MTT [3-(4,5-dimethylthiazol-2-yl)2 2,5-diphenyl tetrazolium bromide] assays. Data are depicted as averages ± standard deviations of three determinations. (H) LNCaP cells expressing shATF3 or shLuc were cultured in CSM for 2 days, followed by treatments with R1881. Levels of cellular lipids were measured by AdipoRed assays. Data are depicted as averages ± standard deviations of three determinations. RFU, relative fluorescence units.

(SV40) promoter (Fig. 2D), arguing against the possibility that ATF3 repressed gene transcription in general.

ATF3 represses androgen signaling in prostate cancer cells. AR-mediated androgen signaling regulates gene expression, leading to multiple outcomes that include increased cell proliferation and *de novo* synthesis of intracellular lipids (43). To test whether ATF3 can affect androgen signaling in prostate cancer cells, we stably knocked down ATF3 expression with a shRNA (shATF3) (59) in LNCaP cells and determined expression of AR target genes using qRT-PCR. Consistent with the notion that ATF3 represses AR transactivation, downregulation of ATF3 expression increased androgen-induced *PSA* expression at both the protein (Fig. 3A, lane 4 versus lane 3) and the mRNA level (Fig. 3B). The R1881-mediated induction of *TMPRSS2*, another well-characterized AR target gene, was also significantly enhanced in shATF3-expressing cells (Fig. 3B). The shATF3 cells appeared to express a higher level of PSA than the control cells expressing shRNA targeting luciferase (shLuc) in the absence of R1881 (Fig. 3A, lane 2 versus lane 1, and B), probably due to the fact that the charcoal-stripped medium (CSM) contained trace amounts of androgens sufficient to promote AR to bind to target genes. Indeed, AR bound to the *PSA* enhancer at a low level under similar conditions (see Fig. 7E). To

confirm these results and ensure that the observation was not a consequence of clonal variation, we transiently knocked down ATF3 expression in LNCaP cells using lentiviral infection (see Fig. S2 in the supplemental material) and then determined mRNA levels of various androgen-dependent genes including *PSA*, *TMPRSS2*, *Rhou*, *SLC41A*, *NKX3.1*, and *DHCR24* by qRT-PCR. Consistent with the results shown in Fig. 3A and B, transient knockdown of ATF3 expression significantly increased R1881-induced *PSA* and *TMPRSS2* expression (Fig. 3C). Moreover, the androgen-induced expression of other AR target genes was also increased by downregulation of ATF3 expression (Fig. 3C). These results indicate that ATF3 can indeed repress AR-mediated gene expression. To further test this notion, we overexpressed ATF3 in VCaP cells, which normally express low levels of the protein (see Fig. S1, lane 4), using a retroviral vector (pBabe) and determined effects of ATF3 expression on androgen-dependent gene expression. As expected, androgen-induced expression of AR target genes (i.e., *PSA* and *TMPRSS2*) was significantly repressed in VCaP cells expressing ectopic ATF3 (Fig. 3D). The androgen-induced decrease in the *AR* mRNA level in VCaP cells (Fig. 3D) was likely due to self-repression (6). ATF3 expression did not appear to have an effect on this regulation (Fig. 3D). Taken together, our results demonstrate that ATF3 can repress AR-mediated gene expression in prostate cancer cells. In line with this notion, expression levels of *PSA* and *TMPRSS2* in human prostate cancer samples were inversely correlated to the *ATF3* expression level (Pearson's correlation r of -0.620 and -0.638, respectively; $P < 0.01$) (Fig. 3E and F).

AR-mediated gene expression promotes prostate cancer cell growth and intracellular lipid synthesis (43). We therefore tested whether ATF3 expression affects these androgen signaling events in prostate cancer cells. Consistent with the increased expression of AR target genes, knockdown of ATF3 expression with two independent shRNAs (59) sensitized LNCaP cells to respond to androgen stimulation (Fig. 3G and H). Both cell growth in response to low concentrations of R1881 (Fig. 3G) and androgen-stimulated total lipid accumulation (Fig. 3H) were significantly increased in the shATF3 cells compared to levels in control shLuc cells. Our results thus indicate that ATF3 is a novel repressor of androgen signaling in prostate cancer cells.

ATF3 deficiency promotes prostate epithelial proliferation in mice. Transgenic *AR* gene expression in mice results in increased cell proliferation in the prostate (53), in line with the notion that androgen signaling functions to sustain epithelial proliferation in adult prostates. To determine whether ATF3 represses androgen signaling under physiological conditions, we examined proliferation of prostate epithelial cells in adult ATF3 knockout (KO) mice by immunohistochemical (IHC) staining for Ki-67 expression. The ATF3 KO mice were developed and characterized previously (16). As expected, proliferating (Ki-67-positive) cells were rare in the wild-type (WT) prostates (53). Interestingly, although the AR expression levels were similar between the WT and KO cells (Fig. 4A), we found that numbers of Ki-67-positive cells in ATF3-deficient prostates were significantly increased (Fig. 4A and B). Consistent with the increased cell proliferation, benign epithelial hyperplasia was frequently found in prostates of the ATF3 KO mice starting at the age of 2 months (Fig. 4C). The anterior (AP), ventral (VP), and dorsal-lateral (DLP) prostates of KO mice (8 weeks of age) exhibited increased numbers of epithelial cells, enhanced epithelial infolding and focal tufting, decreased secretion, and a thickened smooth-muscle layer in stroma around epithelial hyperplasia (Fig. 4C). In comparison, the WT glands showed a secretory duct-acinus system composed of cuboidal luminal epithelial cells with no apparent infolding or tufting morphology (Fig. 4C). We did not detect any overt malignant lesions in the prostates of these young ATF3 KO mice, an observation which is not unexpected as *AR*-transgenic mice developed prostatic lesions only after a long latency (>1 year) (53). These results thus suggest that the AR activity was likely increased in the ATF3 KO mice.

Histopathological changes of prostate glands caused by castration and androgen replacement are often used to evaluate androgen signaling in rodents. To confirm that ATF3 deficiency promotes androgen signaling in mouse prostates, we castrated the WT and KO mice for 21 days and then replenished these mice with testosterone for 14 days. ATF3 expression in prostate epithelial cells of wild-type mice was increased by castration (see Fig. S3A in the supplemental material), similar to the response of LNCaP cells upon androgen deprivation (see Fig. S3B). This result is consistent with the notion that prostate tissues are subjected to acute cellular stresses (e.g., oxidative stress) during the dramatic remodeling that occurs subsequent to castration (54). As expected, androgen deprivation by castration resulted in almost complete loss of proliferation (Fig. 4D and E; see also Fig. S4A and B in the supplemental material) and epithelial atrophy in anterior prostates of the WT mice (see Fig. S3C). In contrast, significant numbers of Ki-67-positive cells were detected in the prostates of the ATF3 KO mice even 21 days after castration (Fig. 4D and E; see also Fig. S4A and B), suggesting that ATF3 deficiency could sensitize AR signaling to respond to the postcastration androgen level. However, the ATF3-deficient prostates still underwent atrophy after castration (see Fig. S4C). Testosterone replenishment subsequent to castration dramatically stimulated proliferation of prostate epithelial cells (Fig. 4D and E), resulting in luminal epithelial repopulation in the WT mice (Fig. 4F). In contrast, the epithelium of prostates of ATF3 KO mice was hyperplastic by 7 days after androgen replenishment (Fig. 4F), consistent with a significant increase in the numbers of Ki-67-positive luminal cells in the KO animals (Fig. 4D and E; see also Fig. S4A and B). Most importantly, testosterone-induced expression of AR target genes (i.e., *Pbsn* and *Msmb*) was significantly increased in ATF3-deficient prostates compared to levels in WT prostates (Fig. 4G). These results thus support the notion that ATF3 deficiency enhances androgen signaling in regrowing mouse prostates. Of note, ATF3 deficiency had negligible effects on AR expression under these experimental conditions (see Fig. S4D).

ATF3 does not block AR nuclear translocation. Having shown that ATF3 represses androgen signaling in both cultured cells and a genetically engineered animal model, we sought to explore the underlying mechanism. Upon androgen stimulation, AR translocates from the cytoplasm to the nucleus and binds to ARE to transactivate gene expression. AR-interacting proteins may interfere with AR nuclear translocation and consequently repress AR signaling (60). To test whether ATF3 affected AR nuclear translocation, we coexpressed ATF3 (fused to mCherry) and AR (fused to green fluorescent protein [GFP]) in PC3 cells and examined cells under a fluorescence microscope. As expected (41, 64), ATF3 was predominantly localized in the nucleus, and this subcellular localization pattern was not altered in the presence of androgen (Fig. 5A). Conversely, AR was mainly localized in the

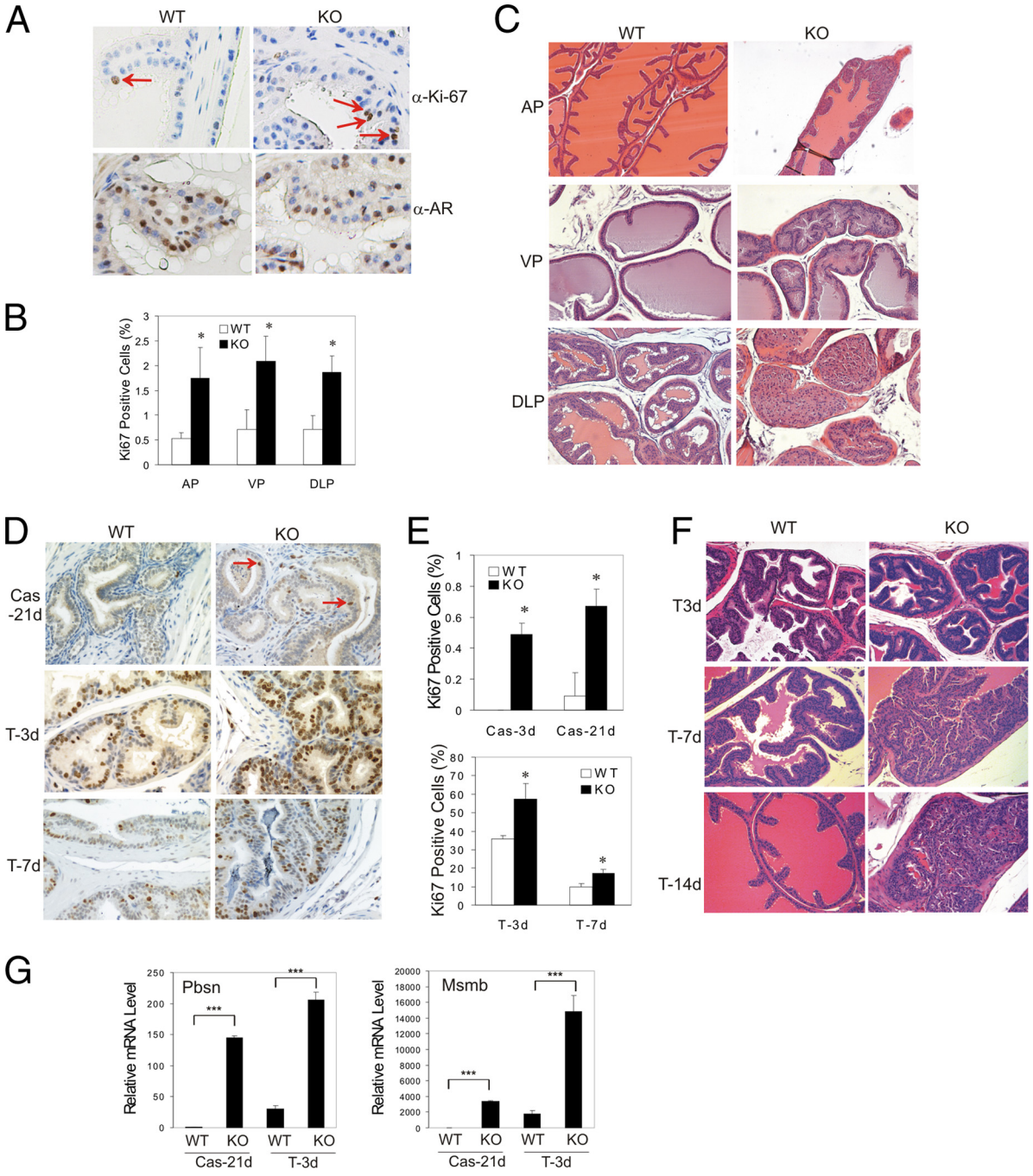

FIG 4 ATF3 deficiency promotes prostate epithelial proliferation in mice. (A) Anterior prostates of ATF3 wild-type (WT) and knockout (KO) mice (8 weeks of age) were embedded in paraffin, sectioned, and stained for Ki-67 or AR expression. Arrows indicate Ki-67-positive cells. (B) At least 1,000 luminal cells of anterior prostates (AP), ventral prostates (VP), or dorso-lateral prostates (DLP) of ATF3 WT and KO mice were counted for Ki-67 positivity under a microscope (random ×20 fields). Data are depicted as averages ± standard deviations of three determinations. *, $P < 0.05$, Student t test ($n = 3$). (C) Prostates of WT and ATF3 KO mice were subjected to hematoxylin and eosin staining. (D, E, and F) ATF3 WT and KO mice were castrated for 21 days, followed by subcutaneous injections of 40 mg/kg testosterone for 14 days. Prostates were sectioned and stained for Ki-67 expression (D). Ki-67-positive epithelial cells in anterior prostates were counted, and the results are shown in panel E. Hematoxylin and eosin staining of representative AP sections is shown in panel F. Data are depicted as averages ± standard deviations of three determinations. *, $P < 0.05$, Student t test ($n = 3$). (G) Ventral prostates were dissected for RNA preparation and used for qRT-PCR assays for AR target gene expression. Data are depicted as averages ± standard deviations of three determinations. ***, $P < 0.001$, Student t test.

cytoplasm in the absence of the androgen but rapidly translocated to the nucleus after androgen stimulation (Fig. 5A). Coexpression of ATF3 with AR did not change the percentage of cells with nuclear AR following androgen supplementation (Fig. 5A and B), indicating that ATF3 did not block AR nuclear translocation.

ATF3 binds AR at its DBD and LBD regions. To gain an insight into the mechanism by which ATF3 represses AR signaling, we carried out GST pulldown assays to identify the AR region(s) responsible for ATF3 binding using various truncated AR proteins. The results indicate that ATF3 bound two AR regions: (ii) aa

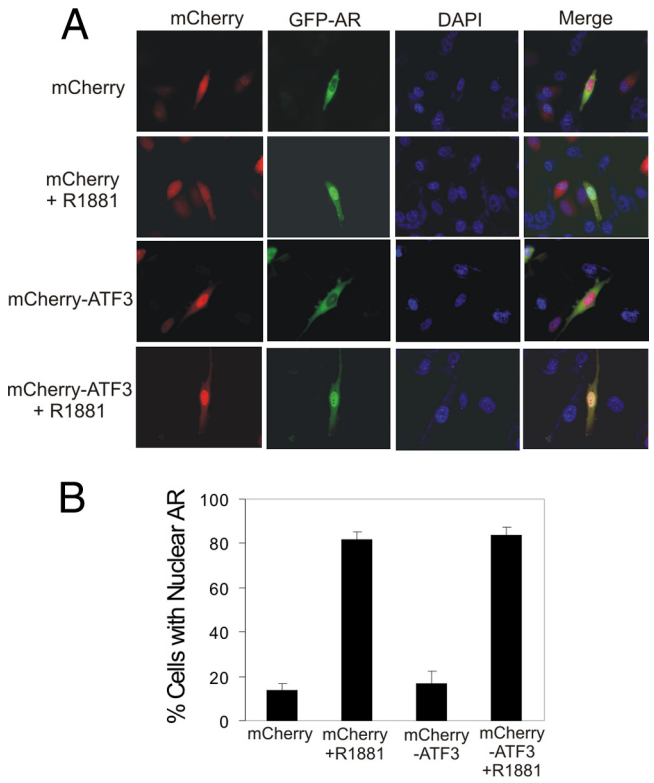

FIG 5 ATF3 does not affect nuclear translocation of AR. PC3 cells were cotransfected with GFP-AR with mCherry-ATF3 or mCherry and then cultured in CSM for 2 days followed by treatments with 1 nM R1881 for 1 h. Cells were then fixed with paraformaldehyde, stained with DAPI (4′,6′-diamidino-2-phenylindole), and observed under a fluorescence microscope (A). At least 300 GFP/mCherry-positive cells were counted for nuclear AR localization (B). Data are depicted as averages ± standard deviations of three determinations.

537 to 662 (Fig. 6A, lane 3), which contains the DBD and hinge regions, and (ii) aa 663 to 919 (Fig. 6A, lane 4), which coincides with the LBD region. The interaction between ATF3 and aa 537 to 662 was stronger than the interaction with the LBD. Further experiments showed that ATF3 did not bind the hinge region (aa 624 to 662) or the neighboring region within the LBD (aa 624 to 804) (Fig. 6A, lanes 7 and 8), indicating that ATF3 binds AR at the DBD and the C terminus of LBD. To corroborate these results, we incubated a purified, histidine-tagged, recombinant AR protein that contains the DBD region (aa 537 to 644) (AR-DBD) (36) with GST-ATF3 for GST pulldown experiments. Indeed, the immobilized GST-ATF3, but not GST, could pull down the recombinant AR-DBD protein (Fig. 6B, lane 3 versus lane 2). Since the recombinant LBD C-terminal peptide (aa 804 to 919 of AR [$AR_{804–919}$]) was insoluble in our bacterial lysates, we constructed a vector expressing a FLAG-tagged C-terminal fragment (FLAG-$AR_{804–919}$) and carried out co-IP assays to confirm the ATF3-LBD interaction. ATF3 was efficiently immunoprecipitated by the FLAG antibody in the presence of the AR C-terminal fragment (Fig. 6C, lane 2), confirming that ATF3 indeed bound the C terminus of the LBD.

ATF3 blocks AR binding to its target promoters/enhancers. The finding that ATF3 directly bound the AR DBD region suggests a possibility that ATF3 represses AR-mediated gene expression by preventing AR from binding to ARE. To explore this possibility, we carried out gel shift assays using a recombinant ATF3 protein (59) and the recombinant AR-DBD protein to determine whether ATF3 can affect the DNA binding activity of AR. The recombinant ATF3 protein retained the capability to bind the AR DBD region (see Fig. S5, lane 3, in the supplemental material). As expected, the AR-DBD protein bound and reduced the electrophoretic motility of an oligonucleotide containing an ARE derived from the *PSA* enhancer region (58) (Fig. 7A, lane 2) but failed to bind an oligonucleotide containing the mutated ARE (Fig. 7A, lane 6). The specificity of the AR DNA binding was further evidenced by re-

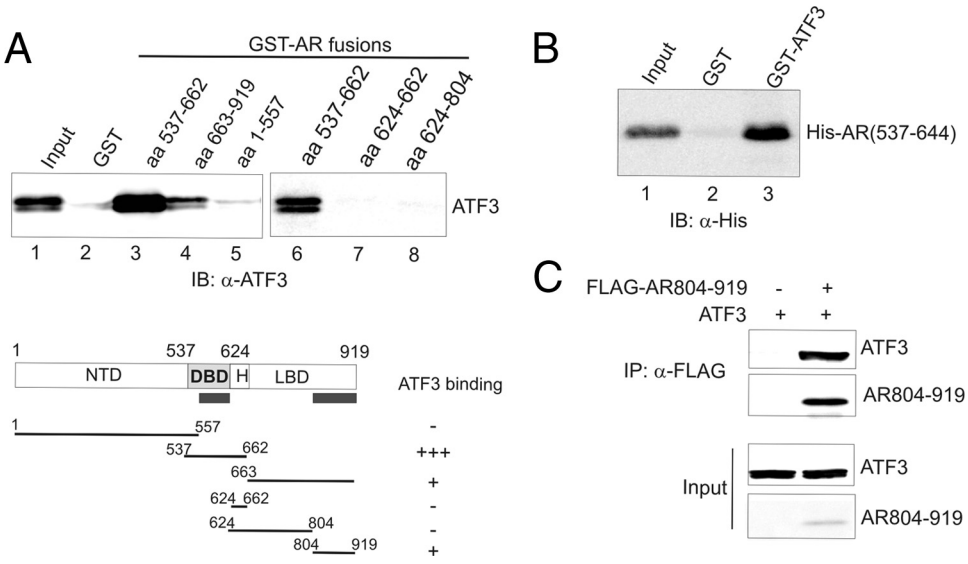

FIG 6 ATF3 binds AR at the DBD and LBD regions. (A) Indicated GST-AR fusion proteins were incubated with *in vitro*-translated ATF3 and subjected to GST pulldown assays. (B) A histidine-tagged AR fragment (aa 537 to 644) containing the DBD was purified by NTA-Ni^+-agarose and incubated with immobilized GST-ATF3 or GST for GST pulldown assays. (C) ATF3 was coexpressed with or without FLAG-$AR_{804–919}$ in PC3 cells by transfections. Cell lysates were subjected to co-IP assays with anti-FLAG antibody.

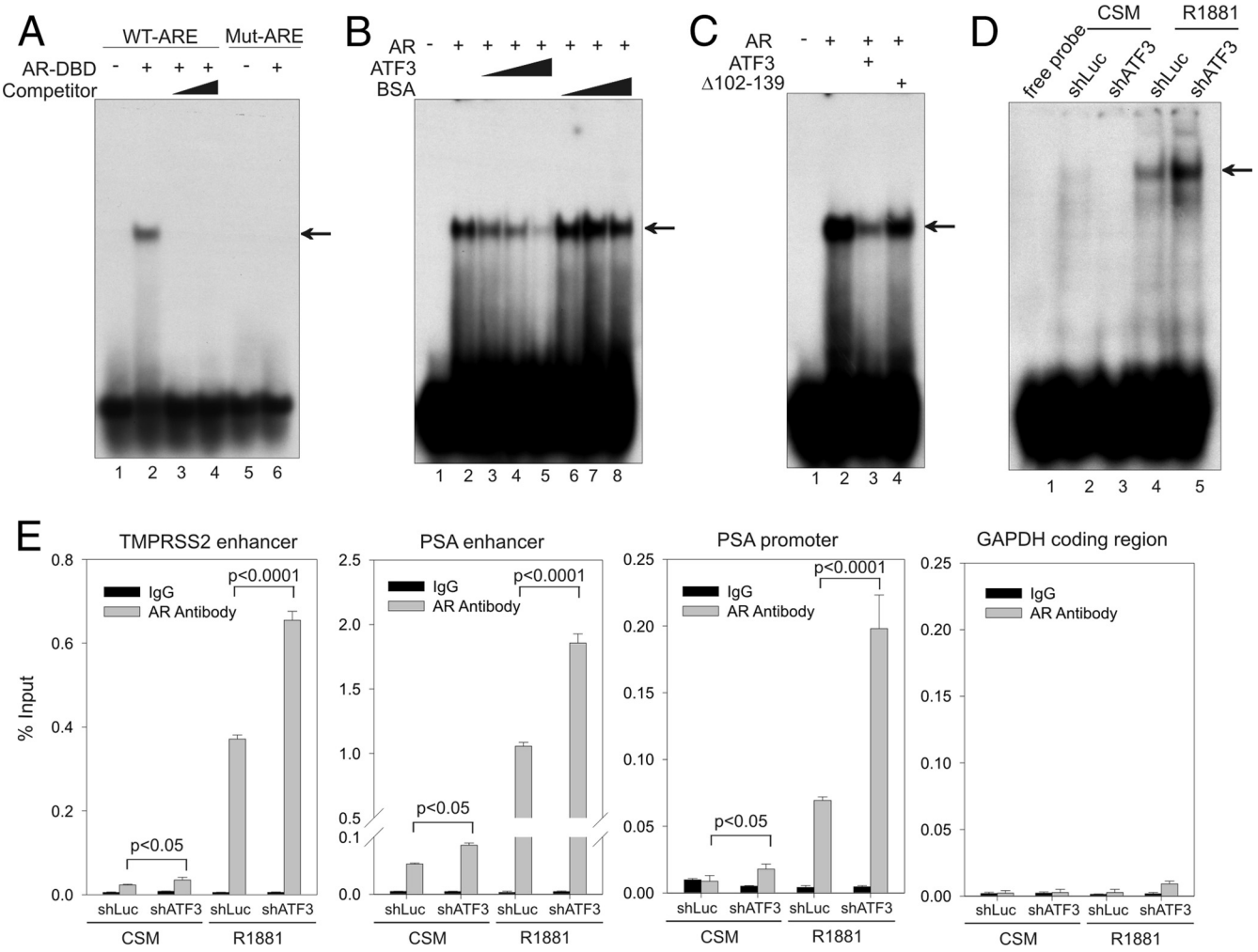

FIG 7 ATF3 prevents AR from binding to ARE both *in vitro* and *in vivo*. (A) The purified AR-DBD protein (aa 537 to 644; 500 ng) was incubated with ^{32}P-labeled oligonucleotide containing ARE derived from the *PSA* enhancer (lanes 1 to 4) or a mutated oligonucleotide (lanes 5 and 6) and subjected to gel shift assays. For competition assays (lanes 3 and 4), 50-fold and 100-fold amounts of unlabeled oligonucleotide were mixed with labeled oligonucleotide and AR-DBD protein. The arrow indicates the AR-ARE binding complex. (B) Increasing amounts of purified ATF3 proteins (100, 200, and 500 ng) or BSA were preincubated with AR-DBD protein at 4°C for 30 min and then subjected to gel shift assays. The arrow indicates the AR-DNA complex. (C) An equal amount (500 ng) of ATF3 or the ATF3 Δ102–139 mutant was preincubated with the AR-DBD protein for gel shift assays. The arrow indicates the AR-DNA complex. (D) LNCaP cells stably expressing shATF3 or shLuc were cultured in CSM for 2 days and then treated with 1 nM R1881 for 24 h. Nuclear extracts were prepared and incubated with ^{32}P-labeled oligonucleotide as described for panel A. The main AR-DNA binding band is indicated by the arrow. (E) LNCaP cells expressing shATF3 or shLuc were treated as described for panel D and then fixed with formaldehyde for ChIP assays using anti-AR antibody or control IgG. Real-time PCR was used to quantify amounts of DNA fragments spanning the ARE in the *TMPRSS2* enhancer, the *PSA* enhancer, or the *PSA* proximal promoter, as indicated. For specificity control, a random fragment in the GAPDH coding region was also amplified and quantified by real-time PCR. Data are depicted as averages ± standard deviations of three determinations. The *P* values were calculated using the Student *t* test.

sults demonstrating that the shifted band was diminished in the presence of the unlabeled oligonucleotide (competitor) (Fig. 7A, lanes 3 to 4). Interestingly, addition of ATF3, but not an AR-unrelated protein (BSA), to the assays significantly decreased AR binding to the oligonucleotide in a dose-dependent manner (Fig. 7B, lanes 3 to 5 versus lane 2). The largest amount of ATF3 almost completely blocked AR from binding to the ARE (Fig. 7B, lane 5). These results were probably not due to competitive binding of the ARE by ATF3 since no additional protein-DNA complex was noted in the assays. Rather, the ATF3-induced loss of DNA binding was due to direct interaction of ATF3 with the DBD region of AR as the recombinant ATF3 Δ102-139 protein deficient in binding to the AR DBD region (see Fig. S5, lane 8, in the supplemental material) failed to inhibit the DNA binding activity of AR (Fig. 7C, lane 4 versus lane 3). These results thus indicate that the ATF3-AR interaction could indeed prevent AR from binding to ARE. To corroborate these results, we carried out gel shift assays using nuclear extracts prepared from LNCaP cells where ATF3 expression was knocked down by shRNA (shATF3) (Fig. 3A). Knockdown of ATF3 expression, which had little effect on AR expression (Fig. 3A), significantly increased the amount of AR bound by the labeled oligonucleotide (Fig. 7D, lane 5 versus lane 4). The observed DNA-binding band(s) was likely specific to AR as the binding was negligible when the cells were cultured in the androgen-deprived medium (CSM) but was strongly induced when the cells were treated with R1881 (Fig. 7D). Thus, our results indicated that

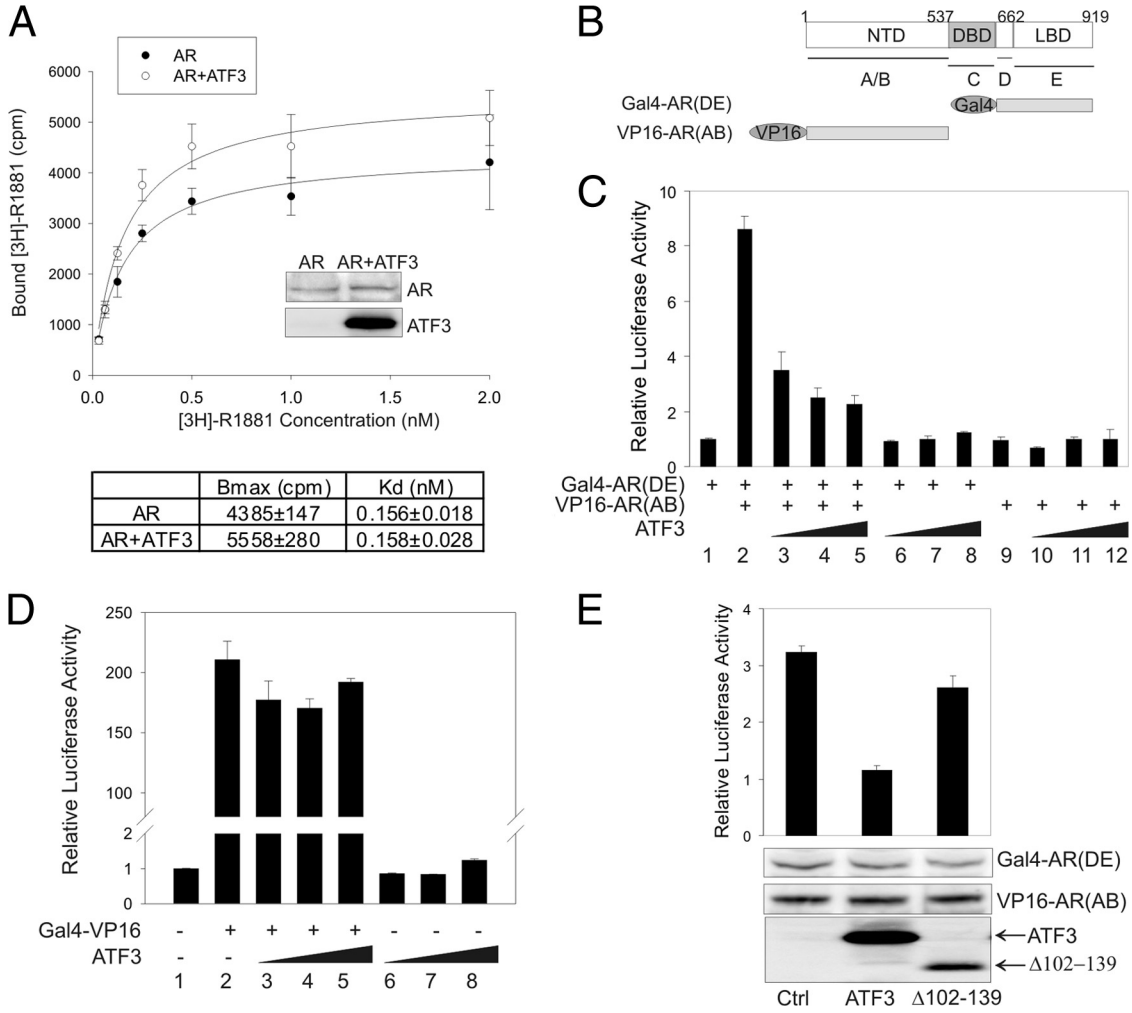

	Bmax (cpm)	Kd (nM)
AR	4385±147	0.156±0.018
AR+ATF3	5558±280	0.158±0.028

FIG 8 ATF3 does not affect the AR-androgen interaction but inhibits the AR N-C interaction. (A) PC3 cells cotransfected with AR and/or ATF3 were cultured in charcoal-stripped medium for 2 days and then incubated with the indicated amounts of [^{3}H]R1881 for 2 h. After extensive washing, bound [^{3}H]R1881 was extracted with methanol, and extract solutions were subjected to scintillation counting. Nonlinear regression was used to calculate B_{max} and K_d. Inserted blots show AR expression levels. (B) Diagram representing the AR fragments used in the mammalian two-hybrid assay. (C) PC3 cells were transfected with Gal4-Luc, pRL-TK, Gal4-AR(DE), VP16-AR(AB), and/or increasing amounts of ATF3 in charcoal-stripped medium and then treated with 1 nM R1881 for 1 day for dual luciferase activity assays. Data are depicted as averages ± standard deviations of three determinations. (D) PC3 cell were transfected with Gal4-Luc, Gal4-VP16 (in pBIND), and/or increasing amounts of ATF3 as indicated for dual luciferase activity assays. Data are depicted as averages ± standard deviations of three determinations. (E) PC3 cells were transfected with Gal4-Luc, pRL-TK, Gal4-AR(DE), VP16-AR(AB), ATF3, or Δ102–139 for dual luciferase activity assays. Expression of the AR fragments and ATF3 and Δ102–139 was determined by Western blotting. Data are depicted as averages ± standard deviations of three determinations.

ATF3 could affect AR binding to its target genes. To further explore this possibility, we carried out chromatin immunoprecipitation (ChIP) assays to determine enrichment of AR on the genomic regions spanning the functional ARE in the *TMPRSS2* enhancer and the *PSA* enhancer, as well as the *PSA* proximal promoter, using LNCaP cells expressing a high (shLuc) or decreased (shATF3) ATF3 level. As expected, while very little AR was associated with these ARE-containing regions in the absence of R1881, the androgen strongly promoted AR binding to these promoter/enhancers but not an unrelated genomic region (glyceraldehyde-3-phosphate dehydrogenase [GADPH] coding region) (Fig. 7E). Intriguingly, the amounts of AR bound to these AR target genes were significantly increased in the shATF3 cells (Fig. 7E). Of note, trace amounts of androgens existing in CSM appeared sufficient to mediate a low level of AR binding to the promoters/enhancers (Fig. 7E). Taken together, our results demonstrate that ATF3 binds AR and prevents the latter protein from binding to target genes.

ATF3 does not affect androgen binding but disrupts the AR N-C interaction. Although it bound to the AR C-terminal ligand-binding domain, ATF3 did not appear to interfere with the AR-androgen interaction since R1881 bound to AR in the presence of ATF3 with the same affinity (K_d of 0.158 ± 0.028) as it did without ATF3 expression (K_d of 0.156 ± 0.018) (Fig. 8A). The slight increase (~27%) in the maximal binding capability (B_{max}) of the ATF3-expressing cells was probably because AR was expressed at a slightly high level in these cells (Fig. 8A, inset blots). Since the intermolecular N-C interaction is required for AR binding to ARE and can promote AR transactivation activity (18, 19), we explored, using a mammalian two-hybrid assay (52), whether the binding of

ATF3 to the AR C terminus could affect the AR N-C interaction. The binding of the AR N-terminal fragment [VP16-AR(AB)] to the AR C-terminal fragment [Gal4-AR(DE)] (Fig. 8B) recruited the VP16 transactivation domain to a promoter containing Gal4-binding sites (Gal4-Luc) in the presence of androgen, resulting in increased luciferase expression, as expected (Fig. 8C, bar 2 versus bar 1). Expression of ATF3 dramatically decreased the VP16-induced reporter activity in the presence of Gal4-AR(DE) (Fig. 8C, bars 3 to 5) but had little effect on the reporter activity when only one of the AR fragments was present (Fig. 8C, bars 6 to 12), indicating that ATF3 inhibited the AR N-C interaction. Of note, ATF3 had little effect on the transactivation activity of VP16 as measured using a Gal4-VP16 fusion protein (Fig. 8D, bars 3 to 5). The inhibitory effect on the N-C interaction likely required the ATF3-AR interaction, since loss of the AR-binding region (Δ102-139) significantly impaired the effect (Fig. 8E). Therefore, ATF3 bound the AR DBD and LBD regions and likely repressed androgen signaling through two distinct mechanisms: by preventing AR from binding to target promoters/enhancers and by disrupting the AR N-C interaction.

DISCUSSION

The cellular stress response is a common mechanism safeguarding cell integrity under various intrinsic and extrinsic insults. The fact that ATF3 expression is rapidly induced by diverse cellular stresses including DNA damage and oxidative stress suggests that ATF3 plays a general role in regulating the cellular stress response (14). Here, we have identified ATF3 as a novel repressor of AR-mediated cell signaling in normal and cancerous prostate epithelial cells. To our knowledge, ATF3 is the only AR regulator known to directly interact with AR and respond to such a broad range of intracellular and environmental cues. Our finding thus has revealed a missing link between androgen signaling and the cellular stress response. In this regard, the repression of AR-mediated gene expression by ATF3 may function as a common mechanism for the cell to repress AR functions (e.g., to inhibit cell proliferation) in order to restore homeostasis under various adverse and stressed conditions. Indeed, whereas AR can drive chromosomal translocations and subsequent expression of fusion genes to promote cellular transformation (34, 38), androgen signaling is repressed by cellular stresses such as DNA damage and oxidative stress (26, 39). Given that a failure to mount an appropriate stress response is often associated with human diseases including cancer (27), our finding suggests that ATF3-mediated repression of AR functions may serve as a general mechanism which can serve to defend against prostate cancer. This contention is supported by the observations that ATF3 expression is often downregulated in prostate cancers (31, 56).

As a DNA-binding protein, ATF3 is generally thought to regulate cellular functions through direct regulation of gene expression. However, our results argue for a mechanism by which ATF3 represses androgen signaling independent of ATF3 transcriptional activity. Indeed, we found no evidence indicating that ATF3 binds ARE and directly represses androgen-induced expression of AR target genes. Rather, ATF3 repressed androgen signaling through direct interaction with AR, as the ATF3 Δ102–139 protein deficient in AR binding failed to counteract AR-mediated gene expression (Fig. 2C) and failed to block the binding of AR to ARE (Fig. 7C). This mechanism is reminiscent of mechanisms utilized by many other AR repressors (60) and is in line with our previous findings that ATF3 can regulate cellular functions independent of its transcriptional activity (59, 64). Whereas both the basic region and the ZIP domain of ATF3 can mediate protein-protein interactions (25, 41, 59, 64), we found that ATF3 directly bound AR through the ZIP domain. c-Jun, a bZIP protein capable of promoting prostate cancer cell growth (10), was previously shown to interact with AR (49), suggesting that the characteristic leucine residues in the ZIP domain might be responsible for AR binding. However, these hydrophobic residues and the coiled-coil ZIP structure (29) are probably insufficient for ATF3 binding to AR as CREB, another bZIP-containing protein, does not interact with AR (23). Moreover, JDP-2, the closest family member whose ZIP domain has 90% homology with ATF3, only weakly bound AR (see Fig. S6 in the supplemental material). Therefore, the ability to bind AR and repress androgen signaling might set ATF3 apart from other bZIP proteins. Although ATF3 can form a heterodimer with c-Jun (14), it is important that ATF3 does not seem to bind AR through c-Jun as recombinant ATF3 and AR proteins could interact (see Fig. S5 in the supplemental material).

The AR transactivation activity is tightly controlled by multiple mechanisms, including regulation of ligand binding, nuclear translocation, and DNA-binding activity (21). Our results suggest that neither androgen-induced AR nuclear translocation nor the binding of androgens to AR was affected by ATF3. Rather, our results indicate that ATF3 bound the DBD region of AR, thereby preventing AR from binding to its target genes, a mechanism similar to that for Daxx and HOXB13 (35, 43). Such an inhibitory effect argues against a possibility that AR recruits ATF3 to DNA, thereby allowing ATF3 to directly regulate expression of androgen-dependent genes. However, given that a large portion of AR-binding sites revealed by genome-wide ChIP-microarray (ChIP-chip) or ChIP with high-throughput sequencing (ChIP-seq) approaches do not seem to contain ARE (40, 61), it would be interesting to explore whether AR could be recruited to these genomic sites through binding to ATF3. Since the AR DBD region has a high degree of similarity with other steroid receptors (62), ATF3 may exert a similar effect on these receptors. Indeed, we found that ATF3 additionally repressed PR- and GR-mediated gene expression (Fig. 2D).

In addition to DBD, ATF3 also bound AR at the LBD C terminus. This region coincides with the second transactivation domain (AF-2) of AR and can mediate an intermolecular interaction with the N terminus of AR (8). Like SMRT (33), the binding of ATF3 to the AR LBD disrupted the N-C interaction. Whereas this effect could dissociate transcriptional coactivators (e.g., SRC-1) from AR, thereby directly impairing AR transactivation (17), it might also inhibit the AR DNA-binding activity (32). However, interference with the N-C interaction is unlikely to be the only mechanism by which ATF3 prevented AR from binding to target genes as ATF3 could significantly decrease the amount of DNA bound by the recombinant AR protein that lacks the LBD (Fig. 7B). Therefore, the disruption of the N-C interaction might serve as an additional mechanism by which ATF3 prevents AR from binding to androgen-responsive promoters. Although it does not directly bind AR, the tumor suppressor p53 was shown to exert a similar effect as ATF3 on the AR N-C interaction (52). Since ATF3 is a p53-associated protein (64), it might be that p53 indirectly regulates AR transactivation through interaction with ATF3. It is important that PC3 cells used in our experiments are null for p53. Regardless of this likelihood, given that ATF3 can activate p53 in

the DNA damage response (64), ATF3 might protect prostate epithelial cells from transformation through two distinct mechanisms, i.e., transactivating p53 target genes and repressing AR-mediated gene expression.

Like many other transcription factors, ATF3 plays a complicated, context-dependent role in cancer development (15). A recent model suggests that ATF3 may prevent the onset of a cancer but promote distant dissemination of malignant cells (66). Our finding that ATF3 can repress androgen signaling indicates that ATF3 expression might be detrimental to the growth of prostate cancer cells, a notion supported by several unbiased cDNA microarray analyses demonstrating that ATF3 expression is downregulated in prostate cancer (31, 56). However, these results are not consistent with other studies showing elevated ATF3 expression in prostate cancer cells (45, 55). Whereas this discrepancy might be reflective of the context-dependent nature of the role that ATF3 plays in cancer, it is worth noting that the *ATF3* gene can be expressed as distinct splicing variants, many of which lack the ZIP domain (44) and therefore might counteract the activity of the full-length ATF3 through dimerization with the latter (9). Interestingly, whereas ATF3 could bind AR in the absence of androgens (Fig. 6C), this interaction was not altered by R1881 (Fig. 1E), suggesting that ATF3 might inhibit the growth of prostate cancer cells under castration or androgen-deprived conditions. Accordingly, the development of castration resistance in prostate cancer cells might be accompanied by decreased ATF3 expression. Indeed, the ATF3 expression level was lower in castration-resistant C4-2 cells than in the parental LNCaP cells (see Fig. S7A in the supplemental material). Moreover, a recent unbiased study revealed that ATF3 expression was significantly decreased in castration-resistant prostate cancers compared to expression in untreated primary cancers (see Fig. S7B) (4). Our results thus suggest that therapeutic agents such as thapsigargin that can induce ATF3 expression (57) would repress AR signaling and therefore be of benefit to patients with advanced, castration-resistant prostate cancer.

ACKNOWLEDGMENTS

This work was supported by NIH grants (R01CA139107 and R01CA164006) and a Department of Defense award (W81XWH-07-1-0095) to C.Y. and NIH grant (R01DK067049) to S.W.H.

We thank Lirim Shemshedini, Elizabeth Wilson, Marianne Sadar, and Ami Aronheim for providing materials. We are also grateful to Robert Matusik and Xiuping Yu for technical support.

REFERENCES

1. **Adachi M, et al.** 2000. Androgen-insensitivity syndrome as a possible coactivator disease. N. Engl. J. Med. **343**:856–862.
2. **Andersen R, et al.** 2010. Regression of castrate-recurrent prostate cancer by a small-molecule inhibitor of the amino-terminus domain of the androgen receptor. Cancer Cell **17**:535–546.
3. **Beleza-Meireles A, et al.** 2008. Activating transcription 3: a hormone responsive gene in the etiology of hypospadias. Eur. J. Endocrinol. **158**: 729–739.
4. **Best CJM, et al.** 2005. Molecular alterations in primary prostate cancer after androgen ablation therapy. Clin. Cancer Res. **11**:6823–6834.
5. **Brinkmann AO.** 2001. Molecular basis of androgen insensitivity. Mol. Cell Endocrinol. **179**:105–109.
6. **Cai C, et al.** 2011. Androgen receptor gene expression in prostate cancer is directly suppressed by the androgen receptor through recruitment of lysine-specific demethylase 1. Cancer Cell **20**:457–471.
7. **Carson-Jurica MA, Schrader WT, O'Malley BW.** 1990. Steroid receptor family: structure and functions. Endocr. Rev. **11**:201–220.
8. **Centenera MM, Harris JM, Tilley WD, Butler LM.** 2008. The contribution of different androgen receptor domains to receptor dimerization and signaling. Mol. Endocrinol. **22**:2373–2382.
9. **Chen BPC, Liang G, Whelan J, Hai T.** 1994. ATF3 and ATF3ΔZip: transcriptional repression versus activation by alternatively spliced isoforms. J. Biol. Chem. **269**:15819–15826.
10. **Chen SY, et al.** 2006. c-Jun enhancement of androgen receptor transactivation is associated with prostate cancer proliferation. Oncogene **25**: 7212–7223.
11. **Gao N, et al.** 2003. The role of hepatocyte nuclear factor-3 alpha (Forkhead Box A1) and androgen receptor in transcripitonal regulation of prostatic genes. Mol. Endocrinol. **17**:1484–1507.
12. **Gilchrist M, et al.** 2006. Systems biology approaches identify ATF3 as a negative regulator of Toll-like receptor 4. Nature **441**:173–178.
13. **Hai T, Hartman MG.** 2001. The molecular biology and nomenclature of the activating transcription factor/cAMP responsive element binding family of transcription factors: activating transcription factor proteins and homeostasis. Gene **273**:1–11.
14. **Hai T, Wolfgang CD, Marsee DK, Allen AE, Sivaprasad U.** 1999. ATF3 and stress responses. Gene Expr. **7**:321–325.
15. **Hai T, Wolford CC, Chang Y-S.** 2010. ATF3, a hub of the cellular adaptive-response network, in the pathogenesis of diseases: is modulation of inflammation a unifying component? Gene Exp. **15**:1–11.
16. **Hartman MG, et al.** 2004. Role for activating transcription factor 3 in stress-induced β-cell apoptosis. Mol. Cell. Biol. **24**:5721–5732.
17. **He B, Kemppainen JA, Voegel JJ, Gronemeyer H, Wilson EM.** 1999. Activation function 2 in the human androgen receptor ligand binding domain mediates interdomain communication with the NH2-terminal domain. J. Biol. Chem. **274**:37219–37225.
18. **He B, Kemppainen JA, Wilson EM.** 2000. FXXLF and WXXLF sequences mediate the NH2-terminal interaction with the ligand binding domain of the androgen receptor. J. Biol. Chem. **275**:22986–22994.
19. **He B, Lee LW, Minges JT, Wilson EM.** 2002. Dependence of selective gene activation on the androgen receptor NH2- and COOH-terminal interaction. J. Biol. Chem. **277**:25631–25639.
20. **Heemers HV, Tindall DJ.** 2005. Androgen receptor coregulatory proteins as potential therapeutic targets in the treatments of prostate cancer. Curr. Cancer Ther. Rev. **1**:175–186.
21. **Heemers HW, Tindall DJ.** 2008. Androgen receptor (AR) coregulators: a diversity of functions converging on and regulating the AR transcriptional complex. Endocr. Rev. **28**:778–808.
22. **Jiang H-Y, et al.** 2004. Activating transcription factor 3 is integral to the eukaryotic initiation factor 2 kinase stress response. Mol. Cell. Biol. **24**: 1365–1377.
23. **Jorgensen JS, Nilson JH.** 2001. AR suppresses transcription of the α glycoprotein hormone subunit gene through protein-protein interactions with cJun and activating transcription factor 2. Mol. Endocrinol. **15**: 1496–1504.
24. **Kalfa N, Philibert P, Sultan C.** 2008. Is hypospadias a genetic, endocrine or environmental disease, or still an unexplained malformation? Int. J. Androl. **32**:187–197.
25. **Kang Y, Chen C, Massague J.** 2003. A self-enabling TGFß response coupled to stress signaling: Smad engages stress response factor ATF3 for *Id1* repression in epithelial Cells. Mol. Cell **11**:915–926.
26. **Ketola K, Vainio P, Fey V, Kallioniemi O, Iljin K.** 2010. Monensin is a potent inducer of oxidative stress and inhibitor of androgen signaling leading to apoptosis in prostate cancer cells. Mol. Cancer Ther. **9**:3175–3185.
27. **Kourtis N, Tavernarakis N.** 2011. Cellular stress response pathways and ageing: intricate molecular relationships. EMBO J. **30**:2520–2531.
28. **Lamont KR, Tindall DJ.** 2010. Androgen regulation of gene expression. Adv. Cancer Res. **107**:137–162.
29. **Landschulz WH, Johnson PF, McKnight SL.** 1988. The leucine zipper: A hypothetical structure common to a new class of DNA binding proteins. Science **240**:1759–1764.
30. **Langley E, Kemppainen JA, Wilson EM.** 1998. Intermolecular NH2-/carboxyl-terminal interactions in androgen receptor dimerization revealed by mutations that cause androgen insensitivity. J. Biol. Chem. **273**: 92–101.
31. **Lapointe J, et al.** 2004. Gene expression profiling identifies clinically relevant subtypes of prostate cancer. Proc. Natl. Acad. Sci. U. S. A. **101**: 811–816.
32. **Li J, Fu J, Toumazou C, Yoon H-G, Wong J.** 2006. A role of the

amino-terminal (N) and carboxyl-terminal (C) interaction in binding of androgen receptor to chromatin. Mol. Endocrinol. **20**:776–785.
33. **Liao G, et al.** 2003. Regulation of androgen receptor activity by the nuclear receptor corepressor SMRT. J. Biol. Chem. **278**:5052–5061.
34. **Lin C, et al.** 2009. Nuclear receptor-induced chromosomal proximity and DNA breaks underlies specific translocations in cancer. Cell **139**:1069–1083.
35. **Lin D-Y, et al.** 2004. Negative regulation of androgen receptor transcriptional activity by Daxx. Mol. Cell. Biol. **24**:10529–10541.
36. **Liu G-Z, Wang H, Wang Z.** 2003. Identification of a highly conserved domain in the androgen receptor that suppresses the DNA-binding domain-DNA interactions. J. Biol. Chem. **278**:14956–14960.
37. **Liu W, et al.** 2011. KAI1 gene is engaged in NDRG1 gene-mediated metastasis suppression through the ATF3-NFκB complex in human prostate cancer. J. Biol. Chem. **286**:18949–18959.
38. **Mani R-S, et al.** 2009. Induced chromosomal proximity and gene fusions in prostate cancer. Science **326**:1230.
39. **Mantoni TS, Reid G, Garrett MD.** 2006. Androgen receptor activity is inhibited in response to genotoxic agents in a p53-independent manner. Oncogene **25**:3139–3149.
40. **Massie CE, et al.** 2007. New androgen receptor genomic targets show an interaction with the ETS1 transcription factor. EMBO Rep. **8**:871–878.
41. **Mo P, Wang H, Lu H, Boyd DD, Yan C.** 2010. MDM2 mediates ubiquitination and degradation of activating transcription factor 3. J. Biol. Chem. **285**:26908–26915.
42. **Ni L, Yang C-S, Gioeli D, Frierson H, Toft DO, Paschal BM.** 2010. FKBP51 promotes assembly of the Hsp90 chaperone complex and regulates androgen receptor signaling in prostate cancer cells. Mol. Cell. Biol. **30**:1243–1253.
43. **Norris J, et al.** 2009. The homeodomain protein HOXB13 regulates the cellular response to androgens. Mol. Cell **36**:405–416.
44. **Pan Y, Chen H, Siu F, Kilberg MS.** 2003. Amino acid deprivation and endoplasmic reticulum stress induce expression of multiple activating transcription factor-3 mRNA species that, when overexpressed in HepG2 cells, modulate transcription by the human asparagine synthetase promoter. J. Biol. Chem. **278**:38402–38412.
45. **Pelzer AE, et al.** 2006. The expression of transcription factor activating transcription factor 3 in the human prostate and its regulation by androgen in prostate cancer. J. Urol. **175**:1517–1522.
46. **Phizicky E, Fields S.** 1995. Protein-protein interactions: Methods for detection and analysis. Microbiol. Rev. **59**:94–123.
47. **Qi W, Wu H, Yang L, Boyd DD, Wang Z.** 2007. A novel function of caspase-8 in the regulation of androgen-receptor-driven gene expression. EMBO J. **26**:65–75.
48. **Quigley CA, et al.** 1995. Androgen receptor defects: historical, clinical, and molecular perspectives. Endocr. Rev. **16**:271–321.
49. **Sato N, et al.** 1997. Androgenic induction of prostate-specific antigen gene is repressed by protein-protein interaction between the androgen receptor and AP-1/c-Jun in the human prostate cancer cell line LNCaP. J. Biol. Chem. **272**:17485–17494.
50. **Scher HI, Sawyers CL.** 2005. Biology of progressive, castration-resistant prostate cancer: Directed therapies targeting the androgen-receptor signaling axis. J. Clin. Oncol. **23**:8253–8261.
51. **Shen M, Abate-Shen C.** 2010. Molecular genetics of prostate cancer: new prospects for old challenges. Gene Dev. **24**:1967–2000.
52. **Shenk J, et al.** 2001. p53 represses androgen-induced transactivation of prostate-specific antigen by disrupting hAR amino- to carboxyl-terminal interaction. J. Biol. Chem. **276**:38472–38479.
53. **Stanbrough M, Leav I, Kwan PL, Bubley GJ, Balk SP.** 2001. Prostatic intraepithelial neoplasia in mice expressing an androgen receptor transgene in prostate epithelium. Proc. Natl. Acad. Sci. U. S. A. **98**:10823–10828.
54. **Tam NN, Gao Y, Leung YK, Ho SM.** 2003. Androgenic regulation of oxidative stress in the rat prostate: Involvement of NAD(P)H oxidases and antioxidant defense machinery during prostatic involution and regrowth. Am. J. Pathol. **163**:2513–2522.
55. **Taylor B, et al.** 2010. Integrative genomic profiling of human prostate cancer. Cancer Cell **18**:11–22.
56. **Tomlins SA, et al.** 2007. Integrative molecular concept modeling of prostate cancer progression. Nat. Genet. **39**:41–51.
57. **Vander Griend DJ, et al.** 2009. Amino acid containing thapsigargin analogues deplete androgen receptor protein via synthesis inhibition and induce the death of prostate cancer cells. Mol. Cancer Ther. **8**:1340–1349.
58. **Wang C, et al.** 2003. Identification of a novel transcription factor, GAG ATA-binding protein, involved in androgen-mediated expression of prostate-specific antigen. J. Biol. Chem. **278**:32423–32430.
59. **Wang H, Mo P, Ren S, Yan C.** 2010. Activating transcription factor 3 activates p53 by preventing E6-associated protein from binding to E6. J. Biol. Chem. **285**:13201–13210.
60. **Wang L, Hsu C-L, Chang C.** 2005. Androgen receptor corepressors: an overview. Prostate **63**:117–130.
61. **Wang Q, et al.** 2009. Androgen receptor regulates a distinct transcription program in androgen-independent prostate cancer. Cell **138**:245–256.
62. **Weatherman RV, Fletterick RJ, Scanlan TS.** 1999. Nuclear-receptor ligands and ligand-binding domains. Annu. Rev. Biochem. **68**:559–581.
63. **Yan C, Boyd DD.** 2006. Histone H3 acetylation and H3 K4 methylation define distinct chromatin regions permissive for transgene expression. Mol. Cell. Biol. **26**:6357–6371.
64. **Yan C, Lu D, Hai T, Boyd DD.** 2005. Activating transcription factor 3, a stress sensor, activates p53 by blocking its ubiquitination. EMBO J. **24**:2425–2435.
65. **Yan C, Wang H, Boyd DD.** 2001. *KiSS-1* represses 92-kDa type IV collagenase expression by down-regulating NF-κB binding to the promoter as a consequence of IκBα-induced block of p65/p50 nuclear translocation. J. Biol. Chem. **276**:1164–1172.
66. **Yin X, Dewille JW, Hai T.** 2008. A potential dichotomous role of ATF3, an adaptive-response gene, in cancer development. Oncogene **27**:2118–2127.
67. **Zhang J, Thomas TZ, Kasper S, Matusik RJ.** 2000. A small composite probasin promoter confers high levels of prostate-specific gene expression through regulation by androgens and glucocorticoids in vitro and in vivo. Endocrinology **141**:4698–4710.

Supplementary Figures

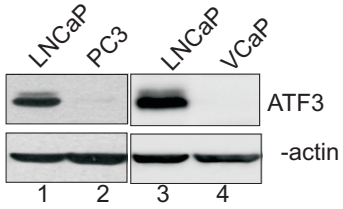

Fig S1. **ATF3 expression in prostate cancer cells.** Indicated cells were lysed for Western blotting assays.

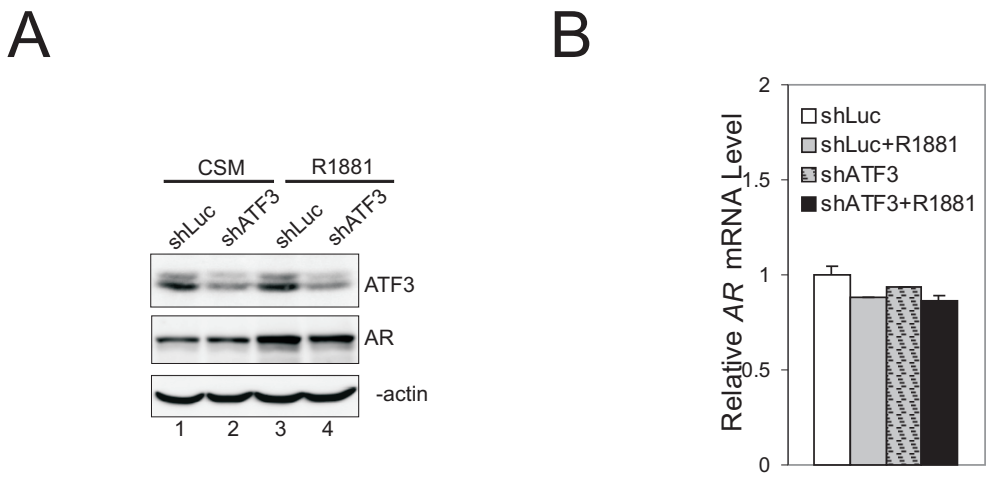

Fig S2. K**nockdown of ATF3 expression in LNCaP cells does not affect AR expression.** LNCaP cells were infected with shATF3 Lentiviruses for 3 days, and then cultured in CSM for 2 days followed by R881 treatments for 24 h. Cells were lysed for Western blotting (A) or qRT-PCR assays (B).

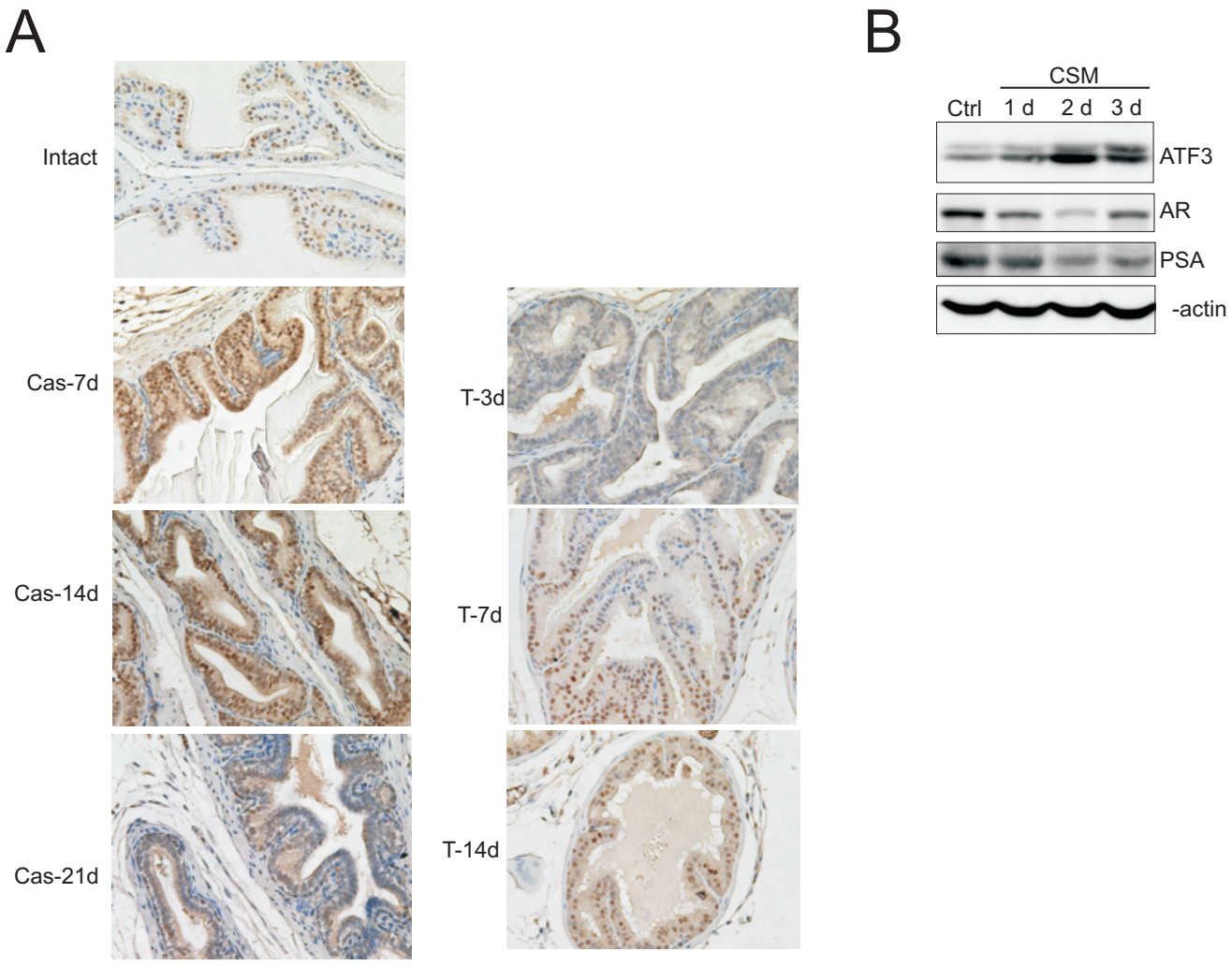

Fig S3. ATF3 expression is induced by androgen deprivation. (**A**) Anterior prostates from wild-type mice castrated (Cas-) for indicated days or injected with testosterone (T-) for indicated days were fixed, paraffin embedded, and subjected to IHC for ATF3 expression. (**B**) LNCaP cells were cultured in charcol-stripped medium (CSM) for indicated days, and then lysed for Western blotting.

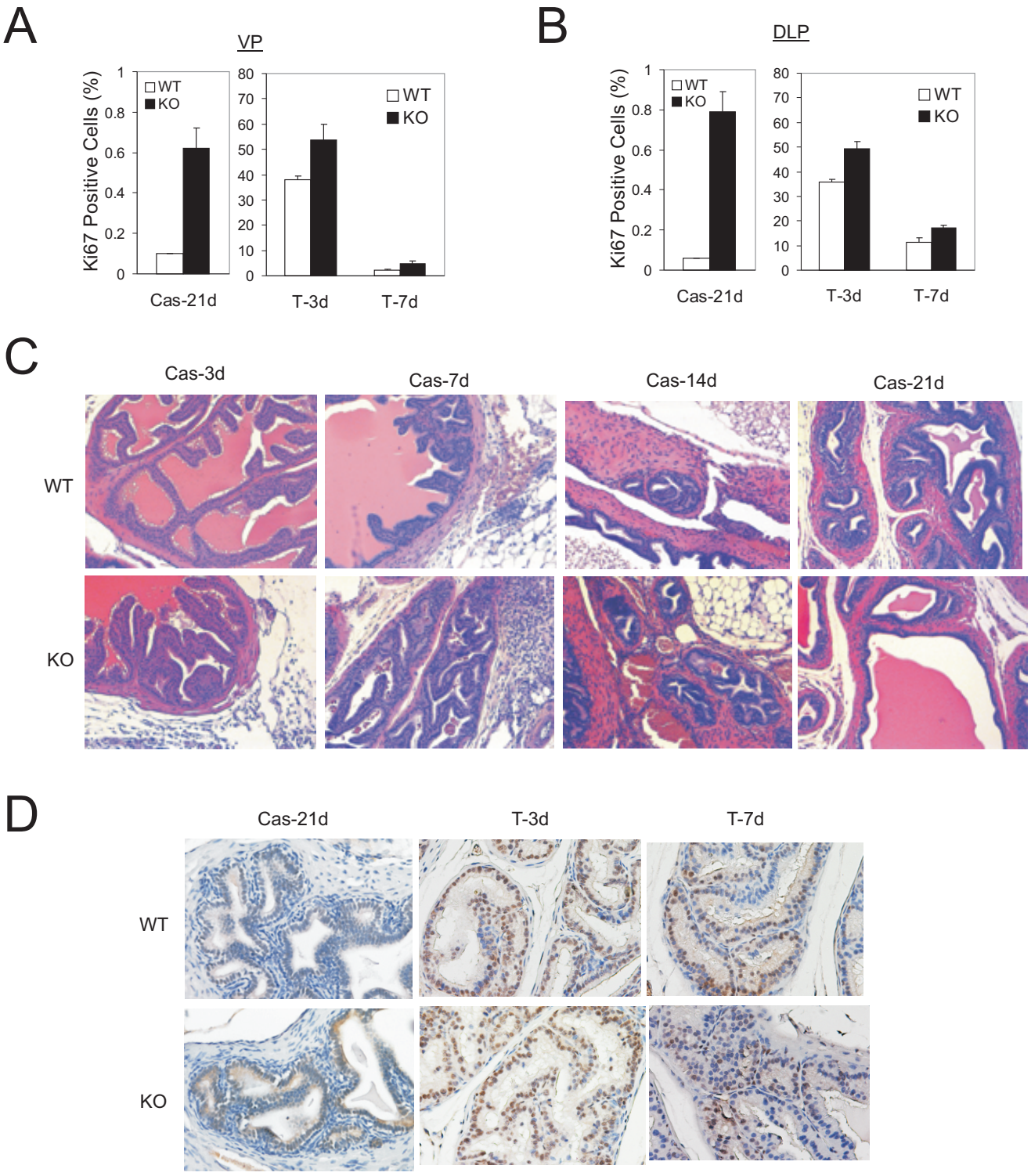

Fig S4. ATF3 deficiency results in prostatic epithelial proliferation.(**A**,**B**) Ki-67 positive epithelial cells in ventral prostates (VP) (A) or dorsolateral prostates (DLP) (B) of the wildtype (WT) and ATF3 knockout (KO) mice were counted. (**C**) Sections of anterior prostates of wildtype (WT) and ATF3 knockout (KO) mice castrated or injected with testosterone for indicated days were stained by H&E. (**D**) ATF3 deficiency does not alter AR expression. AP sections from WT and KO mice were stained for AR expression by IHC.

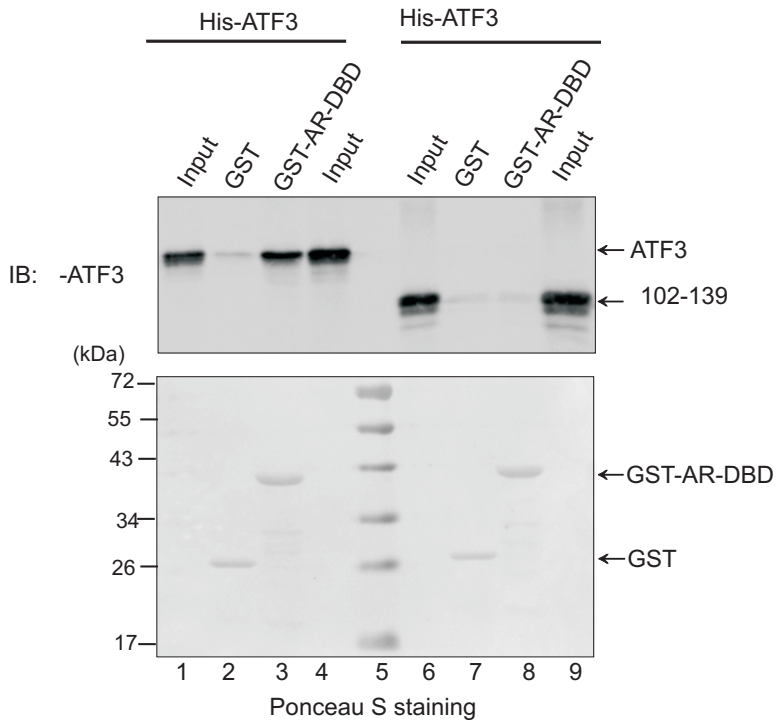

Fig S5. Purified recombinant ATF3 but not zip protein can directly interact with the AR DBD. Histidine-tagged recombinant ATF3 and were produced in *E. coli* and purified with Ni+-NTA agarose. The purified proteins were incubated with immobilized GST-AR-DBD for GST-pulldown assays. Bound proteins were detected by Western blotting using anti- ATF3 antibody. The immunoblot was then stained with Ponceau S stain.

ATF3 ^{100}AAKCRNKKKEKTECLQKESEKLESVNAELKAQ I EELKNEKQHL^{142}

JDP2 ^{86}AARCRNKKKERTEFLQRESERLELMNAELKTQ IEELKQERQQL^{128}

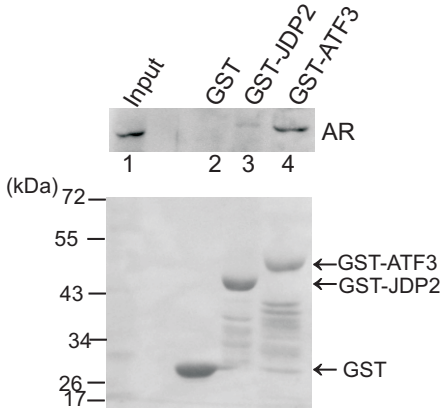

Fig S6.JDP2 weakly binds AR. (A) Alignment of the ZIP sequences of ATF3 and JDP2 shows high similarity. Underlined are residues different between ATF3 and JDP2.(**B**)The AR protein translated *in vitro* was incubated with GST, GST-JDP2, or GST-ATF3 at 4 C overnight, and then subjected to GST-pulldown assays. The binding proteins were resolved in polyacryladmide gel and detected with the anti-AR antibody.

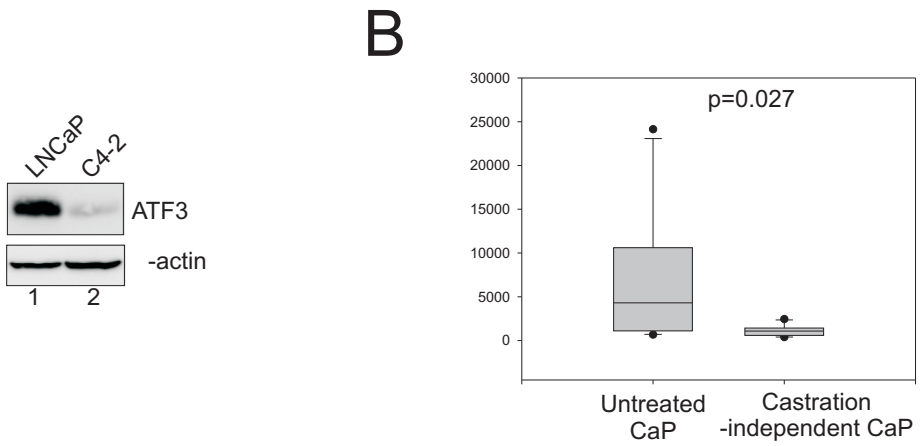

Fig S7.ATF3 expression is down-regulated in castration-resistant prostate cancer. (**A**) LNCaP and C4-2 cells were lysed for Western blotting assays. (**B**) ATF3 expression data were retrieved from the GEO dataset GDS1390 (Best *et al*., 2005) and used to compare ATF3 expression levels between untreated and castration-independent prostate cancer (CaP). Each group contains 10 samples laser-captured from primary prostate tumors. The *p* value was calculated using the Student *t*-test.

Cyclin-dependent kinase 8 mediates chemotherapy-induced tumor-promoting paracrine activities

Donald C. Porter[a,1], Elena Farmaki[b,1], Serena Altilia[a,c], Gary P. Schools[c,d], Deborah K. West[a], Mengqian Chen[d], Bey-Dih Chang[a], Anatoliy T. Puzyrev[a], Chang-uk Lim[c,d], Rebecca Rokow-Kittell[a], Lawrence T. Friedhoff[a], Athanasios G. Papavassiliou[b], Swathi Kalurupalle[c], Gregory Hurteau[c], Jun Shi[e], Phil S. Baran[e], Balazs Gyorffy[f], Mark P. Wentland[g], Eugenia V. Broude[c,d], Hippokratis Kiaris[b], and Igor B. Roninson[c,d,2]

[a]Senex Biotechnology, Inc., Columbia, SC 29208; [d]Department of Pharmaceutical and Biomedical Sciences, South Carolina College of Pharmacy, University of South Carolina, Columbia, SC 29208; [b]Laboratory of Biological Chemistry, University of Athens Medical School, 115 27 Athens, Greece; [c]Cancer Center, Ordway Research Institute, Albany, NY 12208; [e]Department of Chemistry, The Scripps Research Institute, La Jolla, CA 92037; [f]Research Laboratory for Pediatrics and Nephrology, Hungarian Academy of Sciences, Budapest H-1083, Hungary; and [g]Department of Chemistry and Chemical Biology, Rensselaer Polytechnic Institute, Troy, NY 12180

Edited by George R. Stark, Lerner Research Institute, Cleveland, OH, and approved July 16, 2012 (received for review May 8, 2012)

Conventional chemotherapy not only kills tumor cells but also changes gene expression in treatment-damaged tissues, inducing production of multiple tumor-supporting secreted factors. This secretory phenotype was found here to be mediated in part by a damage-inducible cell-cycle inhibitor p21 (CDKN1A). We developed small-molecule compounds that inhibit damage-induced transcription downstream of p21. These compounds were identified as selective inhibitors of a transcription-regulating kinase CDK8 and its isoform CDK19. Remarkably, p21 was found to bind to CDK8 and stimulate its kinase activity. p21 and CDK8 also cooperate in the formation of internucleolar bodies, where both proteins accumulate. A CDK8 inhibitor suppresses damage-induced tumor-promoting paracrine activities of tumor cells and normal fibroblasts and reverses the increase in tumor engraftment and serum mitogenic activity in mice pretreated with a chemotherapeutic drug. The inhibitor also increases the efficacy of chemotherapy against xenografts formed by tumor cell/fibroblast mixtures. Microarray data analysis revealed striking correlations between CDK8 expression and poor survival in breast and ovarian cancers. CDK8 inhibition offers a promising approach to increasing the efficacy of cancer chemotherapy.

transcriptional damage response | senescence | tumor microenvironment | nucleolus | chemical genomics

Chemotherapy and radiation therapy not only kill tumor cells but also induce tumor-promoting paracrine activities in the tumor environment, which may decrease treatment efficacy and contribute to de novo carcinogenesis. These paracrine effects include the promotion of tumor formation (1), stimulation of angiogenesis (2, 3), metastasis (4), tumor resistance to chemotherapy (5), and secretion of multiple tumor-promoting cytokines in vivo (6) and in vitro (7). These damage responses also occur in the stromal components of solid tumors (endothelial cells and fibroblasts), where they are mediated by p53 (8, 9). Tumor-promoting secretory phenotypes have been associated with cell senescence induced by DNA damage or aging (10–15). The DNA damage- and senescence-associated secretory phenotype results at least in part from increased transcription of genes encoding secreted proteins. This transcriptional response is observed in drug-treated cells before the development of the senescent phenotype and is "fixed" at the highest level in cells that become senescent (11).

Transcriptional activation of some tumor-promoting genes in drug-damaged cells was decreased upon the knockout of p21 (CDKN1A), a cell-cycle inhibitor induced, primarily by p53, in response to different types of damage and at the onset of senescence (11). p21 expression from an inducible promoter in HT1080 fibrosarcoma cells activated transcription of multiple damage-responsive tumor-promoting genes and produced mitogenic and antiapoptotic activities in conditioned media (10). p21 expression up-regulates not only cancer-associated genes but also different proteins implicated in age-related diseases (10), and it stimulates viral promoters, including those of HIV and CMV (16, 17). p21 binds several members of the cyclin-dependent kinase (CDK) family. The best-known CDKs (CDK1, CDK2, CDK4/6) mediate cell-cycle progression, but many others function as regulators of transcription or RNA processing but not of the cell cycle (18). p21 usually inhibits CDK activity, although it may stimulate CDK4/6 (19). Aside from the CDKs, p21 interacts with many transcription factors and cofactors (20). p21-induced transcription was shown to be mediated in part through transcription factor NF-κB (16, 17), but the mechanism of NF-κB stimulation by p21 is not yet fully understood.

The ability to reproduce transcriptional damage response and its paracrine effects by inducible p21 expression in HT1080 cells, without DNA damage (10), offers a unique system to identify "druggable" mediators of this pathway downstream of p21. We have now generated a class of noncytotoxic small molecules that inhibit p21-induced transcription and that were identified as selective inhibitors of CDK8 and its isoform CDK19 (21, 22). CDK8 is an oncogenic CDK family member that plays no role in cell-cycle progression but regulates several transcriptional programs involved in carcinogenesis (23) and the stem-cell phenotype (24). We have discovered that p21 interacts with CDK8 and, surprisingly, stimulates its activity, thereby explaining why p21 activates transcription. The CDK8 inhibitor not only suppressed the induction of transcription downstream of p21 but also blocked different chemotherapy-induced tumor-promoting paracrine activities of normal and tumor cells, in vitro and in vivo. In agreement with this tumor-supporting function of CDK8, its expression showed a striking correlation with treatment failure in human cancers. These results suggest that CDK8 inhibitors may become a unique class of anticancer drugs that increase the efficacy of cancer therapy by blocking chemotherapy-induced production of tumor-promoting secreted factors.

Author contributions: D.C.P., P.S.B., M.P.W., E.V.B., H.K., and I.B.R. designed research; D.C.P., E.F., S.A., G.P.S., D.K.W., M.C., B.-D.C., A.T.P., C.-u.L., R.R.-K., S.K., G.H., J.S., H.K., and I.B.R. performed research; D.C.P., S.A., G.P.S., D.K.W., M.C., B.-D.C., L.T.F., A.G.P., B.G., M.P.W., E.V.B., H.K., and I.B.R. analyzed data; and I.B.R. wrote the paper.

Conflict of interest statement: D.C.P., S.A., D.K.W., A.T.P., and R.R.-K. are employees, I.B.R. is the Founder and President, L.T.F. is the Chief Executive Officer, and M.P.W. is a consultant and a member of Scientific Advisory Board of Senex Biotechnology, Inc.

This article is a PNAS Direct Submission.

Data deposition: The data reported in this paper have been deposited in the Gene Expression Omnibus (GEO) database, www.ncbi.nlm.nih.gov/geo (accession no. GSE39464).

[1]D.C.P. and E.F. contributed equally to this work.

[2]To whom correspondence should be addressed. E-mail: roninsoni@sccp.sc.edu.

This article contains supporting information online at www.pnas.org/lookup/suppl/doi:10.1073/pnas.1206906109/-/DCSupplemental.

Results

Development of Small-Molecule Inhibitors of p21-Induced Transcription. High-throughput screening (HTS) for downstream inhibitors of p21-activated transcription used HT1080 p21-9 cells with isopropyl β-D-1-thiogalactopyranoside (IPTG)-inducible p21 (10, 25), carrying a construct that expresses GFP from the CMV promoter. CMV was chosen as the strongest of the p21-stimulated promoters (17), providing sufficient signal intensity for HTS. A total of 62 of >100,000 compounds from diversified small-molecule libraries inhibited CMV-GFP induction by p21. Five of these hits were closely related 4-aminoquinazolines, designated SNX2-class compounds. The introduction of a carbonitrile group at position 6 during subsequent structure optimization greatly increased the efficacy of these compounds (Fig. 1*A*), one of which, designated Senexin A, was used for biological studies. Senexin A inhibited CMV-GFP induction by p21 when GFP expression was normalized either by relative cell number (Fig. 1*B*) or by the protein amount (Fig. 1*C*), an assay that compensates for p21-induced increase in cell size and autofluorescence. p21 was shown to activate NF-κB–dependent transcription (17), and Senexin A inhibited p21-stimulated activity of the consensus NF-κB–dependent promoter (17) (Fig. 1*D*). Senexin A had no effect on p21 induction by IPTG (Fig. 1*E*), on cell growth with or without p21 (Fig. S1*A*), or on p21-induced senescent phenotype [increased cell size, flattening, and senescence-associated β-galactosidase activity (26)] (Fig. S1*B*). Though Senexin A partly decreased the basal CMV promoter activity (Fig. 1 *B* and *C*), it had almost no effect on the basal activity of the NF-κB–dependent promoter (Fig. 1*D*). Together with the lack of growth inhibition (Fig. S1*A*), this result indicates that Senexin A does not affect overall transcription. Microarray analysis of the effects of p21 and Senexin A showed that Senexin A did not affect the inhibition of gene expression by p21 (Fig. 1*F*, *Lower Left*) and did not interfere with p21-mediated inhibition of large sets of genes belonging to Gene Ontology (GO) categories of mitosis and DNA replication (Fig. 1*G*). In contrast, many (but not all) p21-inducible genes were induced less when p21 was expressed in the presence of Senexin A (Fig. 1*F*, *Upper Right* and Fig. S2), including GO categories of proteolysis and extracellular space (Fig. 1*G*). Hence, Senexin A inhibits only p21-induced transcription but not other biological effects of p21.

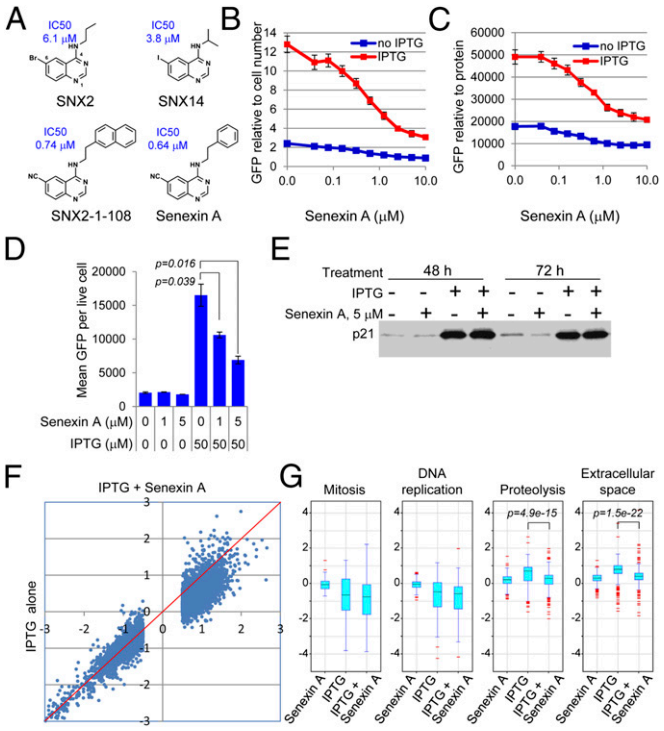

Fig. 1. Effects of Senexin A on the induction of transcription by IPTG-inducible p21. (*A*) Structures of some SNX2-class compounds. SNX2 and SNX14 were isolated through HTS; Senexin A and SNX2-1-108 were generated through chemical optimization. (*B*) Effects of Senexin A on CMV-GFP expression in HT1080-p21-9 cells, untreated or treated for 48 h with 50 μM IPTG (quadruplicate assays). *y* axis: GFP fluorescence normalized by Hoechst 33342 DNA staining (a measure of relative cell number). (*C*) Same as in *A*, except that GFP fluorescence was normalized by sulphorhodamine B staining (a measure of protein amount). (*D*) Effects of Senexin A on GFP expression from NF-κB–dependent consensus promoter in HT1080 p21-9 cells, untreated or treated for 72 h with 50 μM IPTG. *y* axis: Mean GFP fluorescence per live cell (measured by flow cytometry). (*E*) Immunoblotting analysis of p21 protein in HT1080 p21-9 cells, untreated or treated with 50 μM IPTG and 5 μM Senexin A, singly and in combinations. (*F*) Effects of Senexin A on the inhibition and induction of gene expression in HT1080-p21-9 cells treated with 50 μM IPTG alone (*x* axis) or with 50 μM IPTG and 5 μM Senexin A (*y* axis) for 48 h (microarray data). Fold changes in gene expression are plotted as log2; genes showing IPTG-induced fold changes with log2 < 0.5 are excluded. See Fig. S2 for quantitative PCR confirmation of gene expression changes. (*G*) Box-whisker plots of fold changes in the expression of all of the genes in the indicated GO categories in cells treated with Senexin A, IPTG, or IPTG plus Senexin A.

Transcriptional Effect of SNX2-Class Compounds Is Mediated by CDK8 Inhibition. The structure of SNX2-class compounds resembles known protein kinase inhibitors, and therefore we tested their effects on kinome panels. Indeed, SNX14, a compound originally discovered through HTS, inhibited many of 442 kinases screened by an ATP site-dependent competition binding assay (27) (Fig. 2*A*). In contrast, the optimized carbonitrile derivatives showed striking selectivity for only two closely related kinases, CDK8 and CDK19, as shown in Fig. 2*B* and Table S1 for SNX2-1-108. CDK8 and CDK19 inhibition showed excellent correlations with biological activity of SNX2-class compounds (Fig. S3*A*). Senexin A inhibited CDK8 and CDK19 ATP site binding with Kd50 of 0.83 μM and 0.31 μM, respectively (Fig. S3*B*) and CDK8 kinase activity with IC_{50} of 0.28 μM (Fig. 2*C*). To test if Senexin A inhibits cellular CDK8 functions, we have measured its effects on known biological activities of CDK8. CDK8 stimulates Wnt/β-catenin (28, 29), and we have found that Senexin A inhibits β-catenin–dependent transcription in HCT116 colon carcinoma cells (Fig. 2*D*). Another effect of CDK8 is positive regulation of transcriptional serum response (30). The induction of transcription factor EGR1 upon serum starvation, followed by readdition of serum, was strongly inhibited by Senexin A in HT1080 cells (Fig. 2*E*), as expected for a CDK8 inhibitor.

To test if CDK8/19 inhibition is responsible for the effect of Senexin A on p21-induced transcription, we asked if this effect of Senexin A can be reproduced by unrelated CDK8/19 inhibitors. Aside from pan-tropic CDK inhibitors, the only compound reported to inhibit CDK8/19 is a steroidal alkaloid cortistatin A (31). As predicted, an equipotent synthetic version of cortistatin A (32) inhibited CMV-GFP induction by p21 in HT1080 p21-9 cells (Table S2). Cortistatin A inhibits not only CDK8/19 but also ROCK kinases, an activity probably responsible for its antiproliferative effect on endothelial cells (31). In contrast, Senexin A, a selective CDK8/19 inhibitor, did not inhibit ROCK and did not share cortistatin A's strong antiendothelial cell activity (Table S2). We then asked if the effect of Senexin A can be reproduced by shRNA knockdown of CDK8 and CDK19. Lentiviral vectors expressing the corresponding shRNAs decreased CDK8 and CDK19 RNA and protein expression (Fig. S4 *A*–*D*). Fig. 2*F* shows the effects of CDK8 and CDK19 knockdown on mean fluorescence intensity of GFP expressed from the CMV promoter in HT1080 cells. The knockdown of CDK8 alone or of both CDK8 and CDK19 decreased p21-induced CMV-GFP expression. The knockdown of CDK19 alone did not have this effect

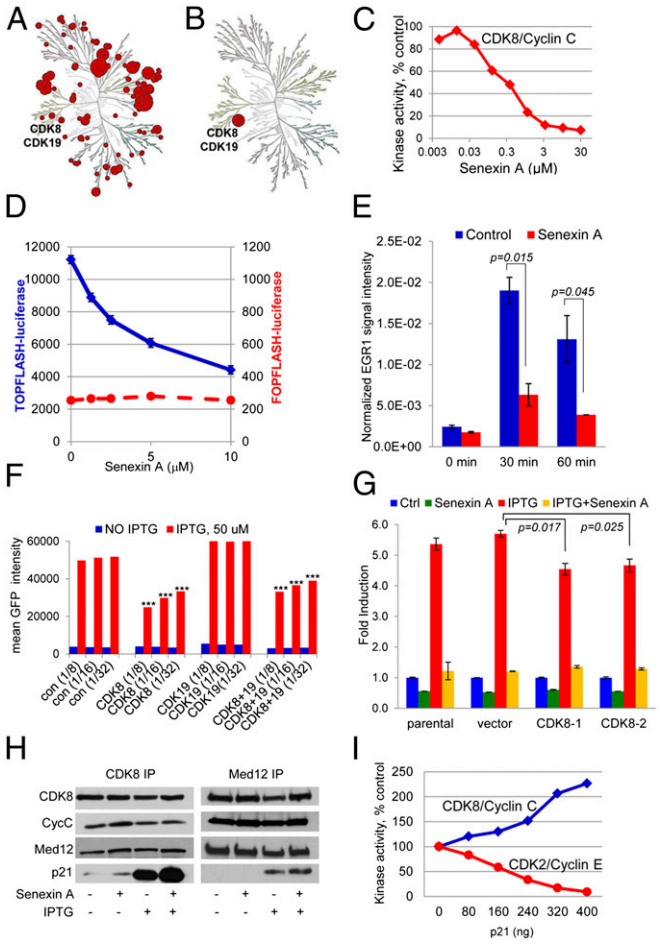

Fig. 2. Identification of CDK8 as a mediator of p21-induced transcription and target of SNX2-class compounds. (*A*) Effects of 10 μM SNX14 on the activity of 442 kinases, measured by ATP binding competition assay. The kinases are displayed in the form of an evolutionary dendrogram; red circles indicate the inhibited kinases. (*B*) Same analysis as in *A* conducted with 2 μM SNX2-1-108. (*C*) Effect of Senexin A on CDK8/cyclin C kinase activity in a cell-free assay. (*D*) Luciferase expression from β-catenin–dependent promoter (TOPflash) or its β-catenin–independent version (FOPflash) in HCT116 cells, after 48 h treatment with Senexin A (quadruplicate assays). (*E*) Quantitative PCR analysis of EGR1 mRNA expression in HT1080 p21-9 cells upon serum starvation for 48 h, followed by readdition of serum for the indicated periods of time, in the presence or absence of 5 μM Senexin A (triplicate assays). Primer sequences are listed in Table S3. (*F*) Mean fluorescence intensity of CMV-GFP expression in live (propidium iodide-negative) cells, infected with the indicated dilutions of pLKO.1 lentiviral vector (control) or with pLKO.1-expressing shRNAs targeting CDK8 or CDK19, singly or in combination, with or without 3-d treatment with 50 μM IPTG. ***Decrease relative to cells infected with control lentivirus, with $P = 0$ (two-tailed t test). (*G*) CMV-GFP expression in cells, untransduced or transduced with a control lentivirus or with lentiviruses expressing two different shRNAs against CDK8, with or without 48-h treatment with 50 μM IPTG or 5 μM Senexin A, alone or in combination. Bars represent fold changes in mean fluorescence intensity of the GFP-expressing live cells in test samples relative to the same untreated cells, in biological triplicates. (*H*) Coimmunoprecipitation analysis of CDK8, Med12, cyclin C, and p21 in HT1080 p21-9 cells, untreated, or treated for 48 h with 10 μM Senexin A and 50 μM IPTG, singly or in combination. (*I*) Dose-dependent effects of recombinant p21 on CDK2/cyclin E and CDK8/cyclin C kinase activities in cell-free assays (a representative from three experiments).

(Fig. 2*F*), but HT1080 cells express hardly any CDK19 protein (Fig. S4*C*). In the experiment in Fig. 2*G*, CDK8 knockdown with two different shRNAs was followed by the analysis of CMV-GFP induction by p21 in the presence or absence of Senexin A. Both shRNAs significantly decreased the induction of CMV-GFP expression by IPTG-induced p21 in the absence of Senexin A but had no effect on CMV-GFP induction in the presence of Senexin A (Fig. 2*G*), verifying that CDK8 is the target of Senexin A responsible for the inhibition of transcription downstream of p21.

p21 Stimulates CDK8 Kinase Activity and Cooperates with CDK8 in the Formation of Internucleolar Bodies. We have used immunoprecipitation to determine if p21 interacts with CDK8, its binding partner cyclin C, and CDK8-binding Mediator protein Med12. Both CDK8 and Med12 antibodies coprecipitated p21 with CDK8, cyclin C, and Med12 from extracts of HT1080 p21-9 cells (Fig. 2*H*). We have also analyzed the effects of p21 on kinase activities of CDK2 (the principal p21-inhibited kinase) and CDK8 in cell-free assays. As expected, recombinant p21 exerted concentration-dependent inhibition of CDK2/cyclin E kinase activity. In contrast, p21 stimulated CDK8/cyclin C kinase (Fig. 2*I*). The surprising CDK8 activation by p21 explains why an effect of p21, a protein conventionally described as a pleiotropic CDK inhibitor, was counteracted by CDK8 inhibition.

We have also used immunofluorescence confocal microscopy to analyze the effects of p21 and Senexin A on subcellular localization of CDK8 and p21 (Fig. S5*A*). Both proteins were found predominantly in the nuclei of HT1080 p21-9 cells. Aside from the nucleoplasm, p21 was highly concentrated within internucleolar bodies (INoBs), where p21 was reported to accumulate upon DNA damage (33). Remarkably, we found that p21 expression led not only to the protein's accumulation in INoBs, but actually caused INoB formation, as demonstrated by time-lapse video microscopy (Fig. S5*B* and Movie S1) and by the drastic increase in the fraction of INoB-containing cells upon p21 expression (Fig. S5*C*). CDK8 also becomes concentrated in the INoBs upon p21 induction, where it colocalizes with p21 (Fig. S5*A*). The addition of the CDK8 inhibitor greatly decreased INoB formation and nucleolar localization of both CDK8 and p21 (Fig. S5*A* and *C*). Hence, p21 and CDK8 cooperate in the formation of INoBs, where these proteins coaccumulate.

Role of p21 and the Effects of a CDK8 Inhibitor on Paracrine Tumor-Promoting Effects of DNA Damage. After identifying CDK8/19 inhibitor Senexin A as an inhibitor of transcription downstream of p21, we tested the effects of p21 and Senexin A on paracrine antiapoptotic activities of HCT116 cells treated with a DNA-damaging drug doxorubicin. This analysis used an assay that measures the ability of these cells to protect apoptosis-sensitive C8 murine-transformed fibroblasts from apoptosis in low-serum media (10). Coculture with HCT116 cells increased C8 cell survival in low serum, and this paracrine activity was strongly increased when HCT116 were pretreated with doxorubicin (Fig. 3*A*). This response to doxorubicin was abolished in HCT116 derivatives with the knockout of either p21 (34) or its positive regulator p53 (35) (Fig. 3*A*), demonstrating that p21 is required for damage-induced antiapoptotic activity. When wild-type HCT116 were treated with doxorubicin or carrier in the presence of Senexin A, their paracrine activity was drastically diminished (Fig. 3 *B* and *C*), but Senexin A had no effect on the antiapoptotic activity of $p21^{-/-}$ cells (Fig. 3*B*). Senexin A also decreased the expression of many secreted tumor-promoting factors in doxorubicin-treated wild-type HCT116 cells, as determined using an antibody array that measures the levels of 55 secreted proteins related to angiogenesis and other aspects of tumor growth. Notably, Senexin A did not inhibit doxorubicin-induced expression of Maspin, a tumor suppressor protein that is upregulated by damage through a p21-independent pathway (11) (Fig. S6). p21 immunoblotting showed that Senexin A moderately decreased p21 induction in HCT116 cells treated with 150 nM doxorubicin (Fig. 3*D*), but the magnitude of this reduction was much less than the effect of Senexin A on the antiapoptotic

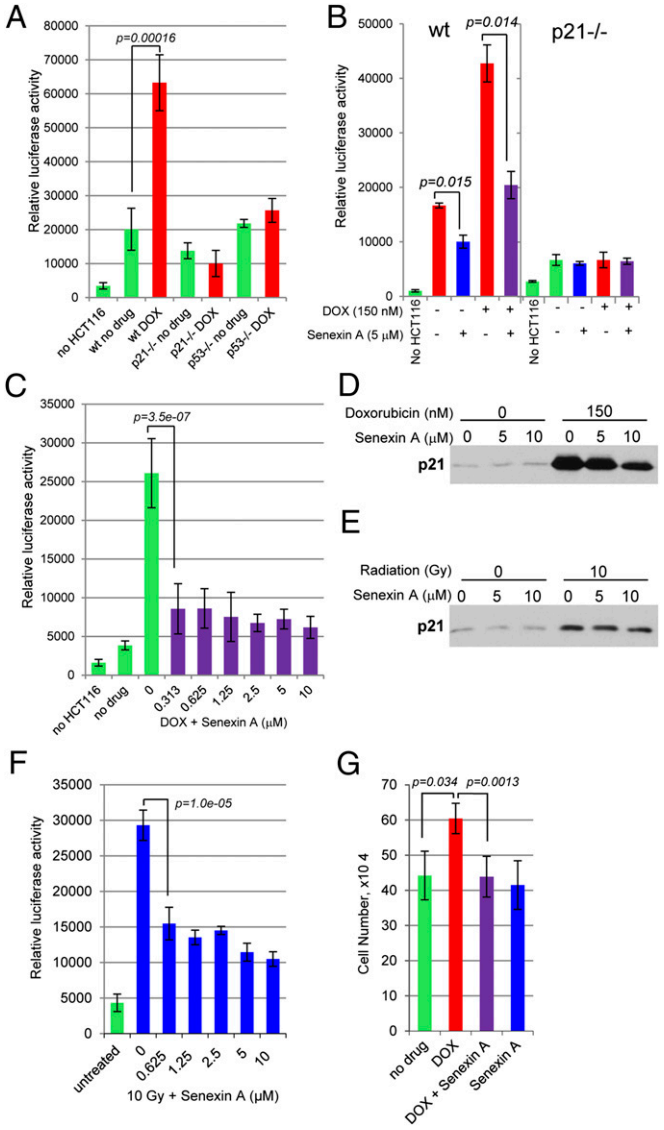

Fig. 3. Effects of p21 and CDK8 inhibitor on paracrine tumor-promoting activities. (*A*) Survival of luciferase-labeled C8 cells in low-serum media without coculture or in coculture with wild-type, p53-null, or p21-null HCT116 cells, untreated or pretreated for 72 h with 150 nM doxorubicin (quadruplicate assays). (*B*) Same assays as in *A* conducted with wild-type and p21-null HCT116 cells in the presence or in the absence of 5 μM Senexin A. (*C*) Same assays as in *A* and *B* conducted with wild-type HCT116 cells, untreated or pretreated for 72 h with 150 nM doxorubicin in the absence or presence of Senexin A (eight replicate assays). (*D*) Effects of Senexin A on p21 expression in HCT116 cells, untreated or treated for 72 h with 150 nM doxorubicin. (*E*) Effects of Senexin A on p21 expression in WI38 fibroblasts, untreated or exposed 3 d earlier to 10 Gy ionizing radiation. (*F*) Same assays as in *A*–*C* conducted with human WI38 fibroblasts, untreated or exposed 3 d earlier to 10 Gy ionizing radiation, in the absence or presence of Senexin A (triplicate assays). (*G*) A549 cell growth in conditioned media from MEF that were either untreated or treated for 24 h with 200 nM doxorubicin, singly or in combination with 5 μM Senexin A (triplicate assays). MEF-conditioned media were collected 48 h after removing the drugs; A549 cells were counted after 48 h.

activity (Fig. 3 *B* and *C*). Senexin A did not affect the senescent phenotype of doxorubicin-treated HCT116 cells (Fig. S7*A*).

We have also tested the effects of Senexin A on damage-induced tumor-promoting activities of normal fibroblasts. In contrast to its effect on damage-induced p21 expression in HCT116 cells, this compound had no effect on radiation-induced p21 expression in human WI38 fibroblasts (Fig. 3*E*), although it appeared to attenuate morphological changes in these cells (Fig. S7*B*). Irradiation of WI38 fibroblasts strongly increased their ability to protect C8 cells from apoptosis in low-serum medium, but this effect was greatly diminished when the fibroblasts were irradiated in the presence of Senexin A (Fig. 3*F*). In a different assay, doxorubicin treatment significantly increased mitogenic activity secreted into conditioned media of mouse embryo fibroblasts (MEF), but Senexin A abolished this damage response (Fig. 3*G*). Hence, the CDK8 inhibitor drastically decreases different damage-induced tumor-promoting paracrine activities of both tumor cells and normal fibroblasts.

CDK8 Inhibitor Reverses Chemotherapy-Induced Paracrine Tumor-Promoting Activities in Vivo. The extensive paracrine effects of DNA damage in cell culture prompted us to test the systemic effect of chemotherapeutic treatment on xenograft tumor growth in mice. Tumor-free C57BL/6-derived SCID mice were injected i.p. with a single dose of doxorubicin or carrier control. Five days later, mice received s.c. injection of 2×10^6 human A549 lung carcinoma cells, and tumor take was measured over 4 wk. As shown in Fig. 4*A*, A549 xenografts showed much better engraftment in mice pretreated with doxorubicin than in the untreated mice. However, this tumor-promoting effect of chemotherapy was fully reversed when doxorubicin treatment was followed by five daily injections of Senexin A (Fig. 4*A*). (Senexin A, administered at the same dose over 5 d, showed no detectable toxicity and no significant effects on body weight, organ weights, or blood cell counts in C57BL/6 mice).

We hypothesized that this systemic tumor-promoting effect of DNA-damaging drugs could manifest itself through the secretion of mitogenic factors into the blood of treated animals. To test this hypothesis, we compared mitogenic activities of sera from C57/BL6 mice that were either untreated or injected i.p. with doxorubicin, with or without Senexin A, by adding mouse sera to serum-free media used to culture A549 cells. Sera from doxorubicin-treated mice significantly increased the growth of lung cancer cells relative to sera from untreated mice. This effect of doxorubicin treatment was completely abolished, however, when doxorubicin injection was followed by in vivo administration of Senexin A (Fig. 4*B*).

We also tested Senexin A for in vivo chemosensitization of xenografts formed by tumor cells admixed with MEF. MEF were previously shown to exert chemoprotective activity, which required functional p53-mediated damage response and was associated with a secretory phenotype (9). SCID mice were injected s.c. with A549 cells mixed with MEF 1:1. Once tumors became palpable, mice were treated by a single i.p. injection of doxorubicin, with five daily injections of either carrier or Senexin A. Senexin A treatment strongly improved the response of A549/MEF tumors to doxorubicin (Fig. 4*C*). Hence, CDK8 inhibition blocks tumor-promoting paracrine activities induced by DNA-damaging chemotherapeutic drugs both in vitro and in vivo.

Clinical Correlations of CDK8 Expression. Our finding that CDK8 mediates paracrine tumor-promoting effects of DNA-damaging chemotherapeutic drugs suggests that CDK8 expression could be associated with chemotherapy failure and poor survival. CDK8 is involved in colon carcinogenesis, and higher CDK8 expression has been correlated with negative prognosis in colorectal and gastric cancers (23). To test the impact of CDK8 expression in cancers where this gene has not been implicated in carcinogenesis, we have used an online survival analysis tool that evaluates the effect of a gene on prognosis using microarray gene expression data from multiple studies on breast cancer (2,897 cases) and ovarian cancer (1,107 cases) (36). High expression of CDK8 showed a striking correlation with poor relapse-free survival in breast cancer patients ($P = 3 \times 10^{-15}$); very strong correlations

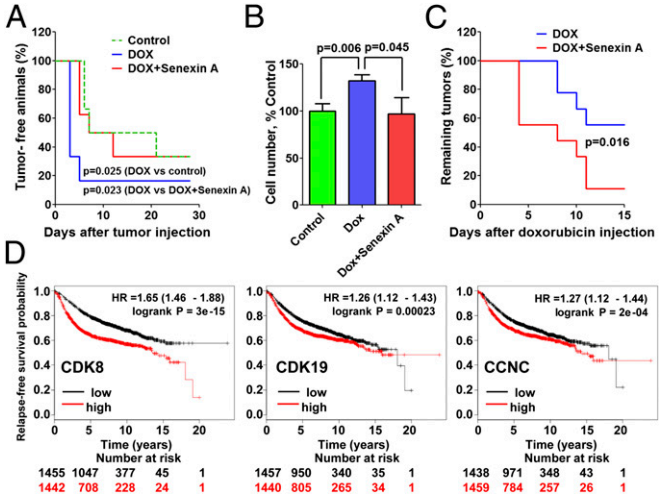

Fig. 4. Effects of CDK8 inhibitor and clinical correlations of CDK8 expression in vivo. (*A*) Effect of pretreatment with doxorubicin, with or without Senexin A, on A549 xenograft tumor engraftment in SCID mice. Mice were either untreated ($n = 6$) or treated with a single i.p. injection of 4 mg/kg doxorubicin, followed by five daily i.p. injections of either carrier ($n = 6$) or 20 mg/kg Senexin A ($n = 8$). A total of 2×10^6 A549 cells were injected s.c. 5 d after doxorubicin injection. The time when tumors became detectable by palpation was recorded. (*B*) Effects of sera from mice that were untreated ($n = 9$) or pretreated i.p. with doxorubicin, with ($n = 8$) or without ($n = 5$) 5-d treatment with Senexin A, on the growth of A549 cells in culture. Serum was isolated 5 d after the initiation of therapy. Cell number was assessed 48 h after the addition of mouse sera (each sample assayed in triplicate). (*C*) Survival of xenograft tumors formed in SCID mice by A549 mixed with MEF (1:1). Once tumors became palpable, mice were treated with a single i.p. injection of 4 mg/kg doxorubicin, followed by five daily i.p. injections of either carrier or 20 mg/kg Senexin A. The time until tumors became undetectable by palpation was recorded. (*D*) Correlations of CDK8, CDK19, and *CCNC* expression with relapse-free patient survival in microarray data from 2,897 breast cancers, determined using an online survival analysis tool. Kaplan–Meier correlations with relapse-free survival are plotted for high (above-median) and low (below-median) expression of each gene.

were also observed for CDK19 and *CCNC* (cyclin C; Fig. 4*D*). This correlation was especially drastic because CDK8, CDK19, and *CCNC*, unlike all of the genes high expression of which showed comparable correlation with bad prognosis in this analysis (36), are not markers of proliferation. CDK8 expression also strongly correlated with poor survival among ovarian cancer patients, and this correlation became even stronger among ovarian cancer patients treated with DNA-damaging platinum compounds (Fig. S8). Remarkably, the correlation of gene expression with poor survival was lost among 529 patients treated with the antimicrotubule drug Taxol (Fig. S8). Similar correlations in platinum-treated ovarian cancers were observed for *CCNC* and CDK19 (Fig. S8). Hence, CDK8/CDK19/cyclin C expression is strongly associated with poor survival and failure of DNA-damaging chemotherapy in clinical cancers.

Discussion

The growing evidence for chemotherapy-induced tumor-promoting paracrine activities is extended by our present findings that pretreatment of tumor-free mice with a DNA-damaging chemotherapeutic drug stimulates tumor engraftment and elevates mitogenic activity in the serum from treated animals. This secretory response, induced by damage in both normal and tumor tissues and perpetuated by the apoptosis-resistant senescent cells that arise upon chemotherapy (11, 14), is expected to decrease treatment efficacy and possibly increase chemotherapy-induced inflammation and fatigue due to the induction of proinflammatory cytokines (6). Several proteins up-regulated in damaged and senescent cells have been implicated in age-related diseases other than cancer (10, 14), and ablation of senescent cells was recently shown to alleviate aging-associated pathologies in mice (37). The results of the present study reveal an essential, druggable mediator of disease-promoting paracrine activities associated with DNA damage and senescence, offering a pharmacological approach to inhibiting these activities in cancer and other aging-associated diseases.

The present finding that p21 is required for damage-induced paracrine antiapoptotic activity (Fig. 3*A*) extends our prior observations that ectopic expression of p21 from an inducible promoter in HT1080 cells mimics transcriptional and paracrine effects of DNA damage (10, 11). We have used the latter cellular system as a tool to develop small-molecule inhibitors of damage-induced transcription downstream of p21 and to identify their druggable targets. Senexin A and related molecules developed in the present study inhibited p21-induced transcription, with no effects on p21 expression, p21-mediated cell-cycle arrest, senescent phenotype, inhibition of genes involved in cell cycle progression, or basal transcription from NF-κB–dependent or FOPflash promoters. These results indicate that p21 induces transcription through a mechanism distinct from its effects on the cell cycle. Senexin A inhibited not only p21-stimulated transcription but also cytokine production by damaged cells and all of the tested paracrine activities of chemotherapy-damaged tumor and normal cells in vitro and in vivo.

SNX2-class compounds were identified as highly selective inhibitors of CDK8 and its isoform CDK19 (Fig. 2*B*), CDK family members that function in the regulation of transcription but not cell-cycle progression (18). The role of CDK8 as a mediator of the induction of transcription by p21 and the target of Senexin A responsible for its transcriptional activity has been demonstrated by shRNA knockdown assays. CDK8 and its binding partner cyclin C form a part of a regulatory module of the Mediator complex that connects transcriptional regulators with RNA polymerase II to initiate transcription of the regulated genes, but CDK8/cyclin C complex also functions outside of the Mediator (23, 24). Senexin A, which inhibits CDK8 kinase activity by binding at the ATP pocket, also inhibits known cellular functions of CDK8, including the potentiation of β-catenin–dependent transcription and induction of gene expression upon serum stimulation. shRNA analysis confirmed the role of CDK8 as a mediator of p21-induced transcription and the target of Senexin A. Surprisingly, we have found that p21 stimulates CDK8 kinase activity. p21 activation of CDK8, leading to transcriptional stimulation, stands in striking contrast to its inhibition of CDK2, the cell-cycle regulator primarily responsible for the ability of p21 to stop cell-cycle progression. p21 also altered the subcellular localization of CDK8, through forming INoBs, where p21 and CDK8 coaccumulated. The CDK8 inhibitor prevented the appearance of INoBs and p21/CDK8 localization to nucleoli, indicating that p21 and CDK8 cooperate in INoB formation. Time-lapse analysis (Movie S1) indicates that the INoBs appear in the first 20 h of p21 induction by IPTG, before the onset of p21-induced transcription in this cellular system (10), suggesting that the INoBs could be mechanistically related to the induction of CDK8-mediated transcription.

CDK8 has been identified as an oncogene amplified in ~50% of colon cancers where it potentiates Wnt/β-catenin (28, 29), and as a melanoma oncogene associated with the loss of a histone variant macroH2A (38). CDK8 has also been implicated in Notch signaling (39) and Smad activation in BMP and TGF-β pathways (40). CDK8 was shown to potentiate transcriptional effects of p53, including p21 induction (41). However, the effects of CDK8 inhibition observed in the present study occurred downstream of p21 and were not due to diminished p21 induction. In fact, Senexin A had no effect on p21 expression from the IPTG-inducible

promoter or in irradiated WI38 fibroblasts. Although the CDK8 inhibitor partially decreased p21 induction by doxorubicin in HCT116 cells, this decrease was minor relative to the overall magnitude of p21 induction and to the effect of Senexin A on the antiapoptotic activity. Importantly, CDK8 inhibitor blocked the stimulating effect of p21 on transcription factor NF-κB (Fig. 1*D*), which plays a major role in damage- and p21-induced transcription (16, 17). The mechanism of the effect of CDK8 on NF-κB is under investigation.

CDK8 is required for embryonic development at the preimplantation stage (42), probably because of its role in the pluripotency of embryonic stem cells (24), and CDK19 haploinsufficiency has been linked to a congenital neurological defect (43). CDK8 knockdown did not, however, affect normal cell growth (28, 42). In the present study, the CDK8/19 inhibitor Senexin A did not inhibit reporter cell growth and showed no detectable toxicity in a mouse study. These observations suggest that pharmacological inhibition of CDK8/19 will likely have an acceptable toxicity profile.

The appeal of CDK8 inhibition in cancer has been suggested by the role of CDK8 in the Wnt/β-catenin pathway (28, 29) and its recently found association with the cancer stem-cell phenotype (24). The present study demonstrates the role of CDK8 in damage-induced tumor-promoting paracrine activities and the striking correlations of CDK8 and cyclin C expression with poor survival in breast cancer and with platinum treatment failure in ovarian cancer. The generation of selective and nontoxic CDK8/19 inhibitors suitable for in vitro and in vivo applications makes it possible now to investigate CDK8 inhibition as a unique approach to improving the treatment of cancer and other aging-associated diseases.

Materials and Methods

SI Materials and Methods provide further details for all of the experiments. CMV-GFP and NF-κB-GFP reporter cell lines were derived from HT1080 p21-9 with IPTG-inducible p21 (25). HTS was conducted on ChemBridge Corp. Microformat 04 and DiverSet collections (50,000 compounds each, screened at 20 μM) and on 2,080 compounds with known activities from the MicroSource SpectrumPlus collection. GFP fluorescence was normalized by Hoechst 33342 staining of cellular DNA. Kinase activity was measured using ProQinase assay kits. Kinase ATP binding-site competition assays (27) were conducted by KinomeScan. Cytokine expression was analyzed using R&D Systems Human Angiogenesis Antibody Array.

ACKNOWLEDGMENTS. We thank Drs. Michael Shtutman, Andrei Gudkov, and Bert Vogelstein for plasmids and cell lines used in this study; George Kampo and Dr. Graham Brock for assistance with high-throughput screening; Drs. Gennadi Glinsky, Jun Ma, and Anna Glinsky for microarray hybridization; and Ming Chen for technical assistance. Funding for this work was provided by National Institutes of Health (NIH) Grants R43AG029023 and R44CA139991 and Department of Defense Breast Cancer Research Grant BC076686 (to D.C.P.); NIH Grant R01 AG028687 (to I.B.R.); and CO-OPERATION-2009 Grant 09SYN11-902 and EXCELLENCE-2011, cofunded by the European Regional Development Fund, the European Social Fund, and National Resources (H.K. and A.G.P.).

1. Barcellos-Hoff MH, Ravani SA (2000) Irradiated mammary gland stroma promotes the expression of tumorigenic potential by unirradiated epithelial cells. *Cancer Res* 60: 1254–1260.
2. Shaked Y, et al. (2006) Therapy-induced acute recruitment of circulating endothelial progenitor cells to tumors. *Science* 313:1785–1787.
3. Shaked Y, et al. (2008) Rapid chemotherapy-induced acute endothelial progenitor cell mobilization: Implications for antiangiogenic drugs as chemosensitizing agents. *Cancer Cell* 14:263–273.
4. Yamauchi K, et al. (2008) Induction of cancer metastasis by cyclophosphamide pretreatment of host mice: An opposite effect of chemotherapy. *Cancer Res* 68:516–520.
5. Gilbert LA, Hemann MT (2010) DNA damage-mediated induction of a chemoresistant niche. *Cell* 143:355–366.
6. Sauter KA, Wood LJ, Wong J, Iordanov M, Magun BE (2011) Doxorubicin and daunorubicin induce processing and release of interleukin-1β through activation of the NLRP3 inflammasome. *Cancer Biol Ther* 11:1008–1016.
7. Levina V, et al. (2008) Chemotherapeutic drugs and human tumor cells cytokine network. *Int J Cancer* 123:2031–2040.
8. Burdelya LG, et al. (2006) Inhibition of p53 response in tumor stroma improves efficacy of anticancer treatment by increasing antiangiogenic effects of chemotherapy and radiotherapy in mice. *Cancer Res* 66:9356–9361.
9. Lafkas D, Trimis G, Papavassiliou AG, Kiaris H (2008) P53 mutations in stromal fibroblasts sensitize tumors against chemotherapy. *Int J Cancer* 123:967–971.
10. Chang BD, et al. (2000) Effects of $p21^{Waf1/Cip1/Sdi1}$ on cellular gene expression: Implications for carcinogenesis, senescence, and age-related diseases. *Proc Natl Acad Sci USA* 97:4291–4296.
11. Chang BD, et al. (2002) Molecular determinants of terminal growth arrest induced in tumor cells by a chemotherapeutic agent. *Proc Natl Acad Sci USA* 99:389–394.
12. Krtolica A, Parrinello S, Lockett S, Desprez PY, Campisi J (2001) Senescent fibroblasts promote epithelial cell growth and tumorigenesis: A link between cancer and aging. *Proc Natl Acad Sci USA* 98:12072–12077.
13. Coppé JP, et al. (2008) Senescence-associated secretory phenotypes reveal cell-nonautonomous functions of oncogenic RAS and the p53 tumor suppressor. *PLoS Biol* 6: 2853–2868.
14. Rodier F, et al. (2009) Persistent DNA damage signalling triggers senescence-associated inflammatory cytokine secretion. *Nat Cell Biol* 11:973–979.
15. Liu D, Hornsby PJ (2007) Senescent human fibroblasts increase the early growth of xenograft tumors via matrix metalloproteinase secretion. *Cancer Res* 67:3117–3126.
16. Perkins ND, et al. (1997) Regulation of NF-kappaB by cyclin-dependent kinases associated with the p300 coactivator. *Science* 275:523–527.
17. Poole JC, Thain A, Perkins ND, Roninson IB (2004) Induction of transcription by p21Waf1/Cip1/Sdi1: Role of NFkappaB and effect of non-steroidal anti-inflammatory drugs. *Cell Cycle* 3:931–940.
18. Malumbres M, et al. (2009) Cyclin-dependent kinases: A family portrait. *Nat Cell Biol* 11:1275–1276.
19. LaBaer J, et al. (1997) New functional activities for the p21 family of CDK inhibitors. *Genes Dev* 11:847–862.
20. Abbas T, Dutta A (2009) p21 in cancer: Intricate networks and multiple activities. *Nat Rev Cancer* 9:400–414.
21. Sato S, et al. (2004) A set of consensus mammalian mediator subunits identified by multidimensional protein identification technology. *Mol Cell* 14:685–691.
22. Tsutsui T, Fukasawa R, Tanaka A, Hirose Y, Ohkuma Y (2011) Identification of target genes for the CDK subunits of the Mediator complex. *Genes Cells* 16:1208–1218.
23. Xu W, Ji JY (2011) Dysregulation of CDK8 and Cyclin C in tumorigenesis. *J Genet Genomics* 38:439–452.
24. Adler AS, et al. (2012) CDK8 maintains tumor dedifferentiation and embryonic stem cell pluripotency. *Cancer Res* 72:2129–2139.
25. Chang BD, et al. (1999) Role of p53 and $p21^{waf1/cip1}$ in senescence-like terminal proliferation arrest induced in human tumor cells by chemotherapeutic drugs. *Oncogene* 18:4808–4818.
26. Dimri GP, et al. (1995) A biomarker that identifies senescent human cells in culture and in aging skin in vivo. *Proc Natl Acad Sci USA* 92:9363–9367.
27. Fabian MA, et al. (2005) A small molecule-kinase interaction map for clinical kinase inhibitors. *Nat Biotechnol* 23:329–336.
28. Firestein R, et al. (2008) CDK8 is a colorectal cancer oncogene that regulates beta-catenin activity. *Nature* 455:547–551.
29. Morris EJ, et al. (2008) E2F1 represses beta-catenin transcription and is antagonized by both pRB and CDK8. *Nature* 455:552–556.
30. Donner AJ, Ebmeier CC, Taatjes DJ, Espinosa JM (2010) CDK8 is a positive regulator of transcriptional elongation within the serum response network. *Nat Struct Mol Biol* 17: 194–201.
31. Cee VJ, Chen DY, Lee MR, Nicolaou KC (2009) Cortistatin A is a high-affinity ligand of protein kinases ROCK, CDK8, and CDK11. *Angew Chem Int Ed Engl* 48:8952–8957.
32. Shi J, et al. (2009) Stereodivergent synthesis of 17-alpha and 17-beta-alpharyl steroids: Application and biological evaluation of D-ring cortistatin analogues. *Angew Chem Int Ed Engl* 48:4328–4331.
33. Abella N, et al. (2010) Nucleolar disruption ensures nuclear accumulation of p21 upon DNA damage. *Traffic* 11:743–755.
34. Waldman T, Lengauer C, Kinzler KW, Vogelstein B (1996) Uncoupling of S phase and mitosis induced by anticancer agents in cells lacking p21. *Nature* 381:713–716.
35. Bunz F, et al. (1998) Requirement for p53 and p21 to sustain G2 arrest after DNA damage. *Science* 282:1497–1501.
36. Győrffy B, et al. (2010) An online survival analysis tool to rapidly assess the effect of 22,277 genes on breast cancer prognosis using microarray data of 1,809 patients. *Breast Cancer Res Treat* 123:725–731.
37. Baker DJ, et al. (2011) Clearance of p16Ink4a-positive senescent cells delays ageing-associated disorders. *Nature* 479:232–236.
38. Kapoor A, et al. (2010) The histone variant macroH2A suppresses melanoma progression through regulation of CDK8. *Nature* 468:1105–1109.
39. Fryer CJ, White JB, Jones KA (2004) Mastermind recruits CycC:CDK8 to phosphorylate the Notch ICD and coordinate activation with turnover. *Mol Cell* 16:509–520.
40. Alarcón C, et al. (2009) Nuclear CDKs drive Smad transcriptional activation and turnover in BMP and TGF-beta pathways. *Cell* 139:757–769.
41. Donner AJ, Szostek S, Hoover JM, Espinosa JM (2007) CDK8 is a stimulus-specific positive coregulator of p53 target genes. *Mol Cell* 27:121–133.
42. Westerling T, Kuuluvainen E, Mäkelä TP (2007) Cdk8 is essential for preimplantation mouse development. *Mol Cell Biol* 27:6177–6182.
43. Mukhopadhyay A, et al. (2010) CDK19 is disrupted in a female patient with bilateral congenital retinal folds, microcephaly and mild mental retardation. *Hum Genet* 128: 281–291.

Supporting Information

Porter et al. 10.1073/pnas.1206906109

SI Materials and Methods

Cell Lines and Genetic Modification. Most of the cell lines were grown in DMEM with 10% HyClone FetalClone II serum (Thermo Scientific). The reporter cell line HT1080 p21-9-CMV-GFP was derived from HT1080 p21-9 cells (1) by transduction with a lentiviral vector expressing EGFP from the CMV promoter of lentiviral vector LentiLoxP (2). The transduced cells were subcloned, and subclones were tested for GFP fluorescence in the presence and absence of 50 μM isopropyl β-D-1-thiogalactopyranoside (IPTG). Cell line showing the highest basal GFP expression and the strongest IPTG inducibility was selected as the reporter for high-throughput screening. NF-κB–dependent reporter cell line HT1080-p21-9-Cignal-NF-κB-GFP was derived by a similar procedure after transducing HT1080 p21-9 cells with Cignal Lenti NF-κB Reporter (GFP) lentivirus (SABiosciences). HT1080 p21-9-CMV-GFP derivatives with the knockdown of CDK8 and CDK19 were generated by transduction with pLKO.1 lentiviral vectors expressing the corresponding shRNAs (Open Biosystems), followed by puromycin selection. The target sequences for CDK8 shRNAs were CCTCTGGCATATAATCAAGTT (Fig. 2*E*; CDK8-2 in Fig. 2*F*) and ATGTCCAGTAGCCAAGTTCCA (CDK8-1 in Fig. 2*F*). The target sequence for CDK19 shRNA was GCTTGTAGAGAGATTGCACTT.

Wild-type HCT116 cells and their p53-null (3) and p21-null (4) derivatives were a gift of Bert Vogelstein (Johns Hopkins University, Baltimore). Wnt/β-catenin reporter cell lines were derived from wild-type HCT116 cells by transduction with lentiviral vectors expressing firefly luciferase from TOPflash or control FOPflash promoters (5) (a gift of Michael Shtutman, University of South Carolina, Columbia, SC), followed by subcloning and identification of cell clones with the highest luciferase expression from each promoter. C8 cells (6) (a gift of Andrei Gudkov, Roswell Park Cancer Institute, Buffalo, NY) were transduced with a lentiviral vector pLenti6/CMVluc expressing firefly luciferase. WI38 fibroblasts and A549 lung carcinoma cells were from ATCC. Mouse embryo fibroblasts (MEFs) were isolated at E11.5 as previously described (7); early passage MEFs (<7 population doublings) were used.

High-Throughput Screening and Promoter Activity Assays. MicroSource SpectrumPlus collection comprising 2,080 synthetic and natural compounds with known biological activities and ChemBridge Corp. Microformat 04 and DiverSet collections, each comprising 50,000 drug-like small molecules, were screened in 96-well plates using the robotic Caliper Staccato Sciclone Cell Station. Follow-up assays were conducted manually, using FluoStar Optima (BMG Labtech) fluorescence reader. The assay involved plating HT1080 p21-9-CMV-GFP cells in the absence (2,000 cells per well) or in the presence (5,000 cells per well) of 50 μM IPTG. Tested compounds were added 3 h after plating (20 μM concentrations for ChemBridge libraries and 10 μM for the MicroSource library). After 3 d, cells were washed with PBS and lysed for 60–90 min with 50 μL of cell lysis buffer (0.22% NaCl, 0.15% Saponin, 1 mM EDTA) containing 0.5 μg/mL Hoechst 33342 that stains cellular DNA. GFP fluorescence was measured at 485 nm (excitation)/520 nm (emission), and Hoechst 33342 fluorescence at 355 nm (excitation)/460 nm (emission). The ratio of GFP/Hoechst 33342 fluorescence was scored as normalized GFP expression, and Hoechst 33342 fluorescence was used as relative cell number. To normalize promoter activity by the protein content, the protein amount was measured by sulforhodamine B staining. In some assays, GFP fluorescence of live (propidium iodide-negative) cells was measured using LSRII flow cytometer (BD Biosciences). Luciferase expression from TOPflash and FOPflash promoters was determined using Promega luciferase assay and FluoStar Optima plate reader.

RNA and Protein Assays. Total cellular RNA was purified with either RNeasy kit (Qiagen) or TRIzol (Invitrogen). Microarray analysis using Affymetrix Exon 1.0ST human oligonucleotide arrays was conducted by Ordway Research Institute's Microarray Facility. Microarray data were analyzed using GeneSpring GX (Agilent). For quantitative PCR (qPCR) analysis, cDNA was prepared using Maxima First Strand cDNA Synthesis (MBI Fermentas). Gene expression was measured by qPCR, with GAPDH or RPL13A as normalization standards (primer sequences in Table S2) using RT^2 SYBR Green qPCR Master Mixes (Qiagen).

Protein extracts were prepared by standard procedures. Immunoblotting was conducted by enhanced chemiluminescence using Western Lightning Plus-ECL (Perkin-Elmer). Immunoprecipitation was carried out essentially as described (8). The assays used monoclonal antibodies against p21 (Calbiochem), rabbit polyclonal antibodies against cyclin C (Santa Cruz) and Med12 (Sigma), and goat polyclonal antibodies against CDK8 and CDK19 (Santa Cruz), with the corresponding secondary antibodies. Growth factor expression in HCT116 colon carcinoma cells was measured using R&D Systems Human Angiogenesis Antibody Array (catalog no. ARY007), using the manufacturer's instructions. Films were scanned on a BioRad FX laser scanner. The spot volumes of the positive control spots on each array were used to normalize the volumes for all conditions.

For immunofluorescence analysis, cells cultured on glass coverslips (Bellco Glass) were fixed with 2% paraformaldehyde in PBS for 30 min at room temperature and stained with the antibodies listed in Table S2. The fixed cells were permeabilized in PBS + 0.1% Triton X-100 (PBS + T) for 5 min, washed with PBS, and blocked with 1.5% normal donkey or goat serum/1% BSA/PBS + T for 1 h at room temperature. Incubation with primary antibody was done in 1% BSA/PBS + T overnight at 4 °C, followed by washing three times with PBS + T and blocking. Incubation with the secondary antibody was done in 1% BSA/PBS + T for 1 h at room temperature, followed by one wash with PBS + T for 5 min and two washes with PBS for 5 min. The coverslips were mounted on glass slides in 50% glycerol in PBS. Stained cells were imaged using a Carl Zeiss LSM 510 META confocal microscope with a 63×/1.4 n.a. objective. Each fluorochrome was imaged individually with the pinhole at 1 airy unit. Single-channel images and merged images were created from the raw data using the Zeiss LSM Image Browser. The differential interference contrast (DIC) images were examined for the presence of internucleolar bodies (INoBs). Only cells with clearly defined nucleoli were scored. A cell with at least one robust (>5 pixels in diameter) INoB was considered positive. Nucleolar expression of p21 and CDK8 was scored by comparing nucleolar signal intensity to that of the surrounding nucleoplasm. Nucleoli were scored positive if they held fluorescent inclusions greater or equal in intensity to that in the nucleoplasm.

For time-lapse microscopy, cells in a 35-mm glass-bottom plate were imaged in the 37 °C chamber of a Leica Microsystems ASMDW microscope, 5% CO_2 in air perfused through the chamber, using a 63×/1.4 n.a. objective with DIC optics. Images were acquired every 6 min for 4 d. The raw image sequences were opened in ImageJ, where brightness and contrast adjustments, time stamps, jpg compression, and movies were made.

CDK8 and CDK2 kinase activity assays used CDK8/cyclin C and CDK2/cyclin E assay kits from ProQinase, with RBER-CHKtide substrate for CDK2 and RBER-IRStide for CDK8 (artificial fusion proteins based on a fragment of Rb protein, amino acids S773–K928), under the manufacturer's protocol. Substrate phosphorylation was measured by gel electrophoresis and scanning the ^{32}P-labeled band. Recombinant p21 was from OriGene Technologies. Kinase ATP binding-site competition assays (9) were conducted by Ambit Biosciences.

Paracrine Activity Assays. In apoptosis protection assays (10) with HCT116 cells, luciferase-labeled C8 cells were plated in 96-well plates at 2,000 cells per well. HCT116 cells, untreated or pretreated for 72 h with 150 nM doxorubicin in the absence or presence of Senexin A, were added at 6,000 cells per well. In assays with WI38 fibroblasts, the fibroblasts were seeded in six-well plates at 125,000 cells (untreated) or 250,000 cells per well (irradiated with 10 Gy); after 72 h, cells were washed with PBS, and 55,000 C8 cells were added per well. After overnight incubation, cells were placed in low (0.5%) serum media and incubated for 3 d. The wells were washed with PBS, cells lysed, and luciferase activity measured.

For conditioned media mitogenic assays, MEF, untreated or treated for 24 h with 200 nM doxorubicin, alone or in combination with 1 μM Senexin A, were washed and cultured for 48 h without drugs to collect conditioned media. The media were added to A549 cells, plated on 12-well plates at 10^4 cells per well; cells were counted after 48 h using the trypan blue exclusion assay. Experiments were performed in triplicate, and cells counted in at least three optical fields per experiment.

Senescence-associated β-galactosidase (SA-β-gal) activity was detected microscopically (10) with a Carl Zeiss Axiovert 200M microscope; brightfield images were overlayed on phase contrast images using ImageJ software.

Animal Studies. Senexin A toxicity study was conducted by Taconic in C57BL/6 mice, using five mice per group treated with 20 mg/kg Senexin A or carrier (80% propylene glycol), with five daily i.p. injections. Mice were weighed on days 3 and 6, and killed on day 6. Organ weights were determined for brain, kidney, thymus, spleen, lung, and liver. Terminal blood samples were analyzed to determine the numbers of total white blood cells, neutrophils, lymphocytes, monocytes, eosinophils, and basophils.

The tumor engraftment study used 6- to 8-wk-old female SCID mice, originally obtained by Jackson Laboratories and subsequently maintained in our laboratory (University of Athens) in mixed C57BL6 X C3H genetic background. Littermates and/or isogenic animals were used in all experiments. Mice were treated with doxorubicin (Sigma) (4 mg/kg), Senexin A (20 mg/kg), a combination of both, or carrier alone. Mice received one i.p. injection of doxorubicin (DOX) or five daily i.p. injections of Senexin A starting on the same day. Five days after the initial treatment, mice were injected s.c. with 2×10^6 A549 cells in 0.1 mL of serum-free DMEM. Animals were observed daily for 28 d for tumor development, and palpable tumors were scored.

For the serum tumor-promoting study, 8- to 10-wk-old female C57 Bl/6 mice were treated with doxorubicin (4 mg/kg), Senexin A (20 mg/kg), or combination of both. Mice received one i.p. injection of DOX or five daily i.p. injections of Senexin A. Sera were isolated 5 d after the initial treatment. A549 cells were cultured for 16 h in serum-free DMEM before the addition of 10% mouse sera. Cell number was assessed 48 h later by the MTT [3-(4, 5-dimethylthiazolyl-2)-2,5-diphenyltetrazolium bromide] assay, in triplicates. Each set of assays included a 10% FBS control (instead of mouse serum), and the results were normalized relative to the FBS control.

For the chemosensitization study, 4.7×10^6 A549 cells admixed with MEF at a 1:1 ratio were resuspended in 0.1 mL of serum-free DMEM and then injected s.c. into SCID mice. As soon as tumors became palpable, usually 4–7 d after inoculation, mice were treated by a single i.p injection of doxorubicin (Sigma) (4 mg/kg), alone or in combination with five daily injections of Senexin A (20 mg/kg) or carrier. Animals were followed for 15 d following doxorubicin treatment or until tumors became undetectable by palpation.

Statistical Analysis. The effects of Senexin A or CDK8 shRNA in different cell culture assays were analyzed using Student's two-tailed *t* test (Microsoft Excel); flow cytometric data were also analyzed using ANOVA and multiple comparison test (Minitab). The data on tumor development and tumor disappearance were analyzed by Wilcoxon statistical test, using Epi Info software package (Centers for Disease Control and Prevention). Correlations between CDK8, CDK19 (CDC2L6), and *CCNC* gene expression and patient survival were analyzed using an online survival analysis tool (11). In the case of CDK19, where the data for three different probe sets were available, probe set 211706_s_at was excluded due to low expression, and the mean values for the other two probe sets were used.

1. Chang BD, et al. (1999) Role of p53 and p21$^{waf1/cip1}$ in senescence-like terminal proliferation arrest induced in human tumor cells by chemotherapeutic drugs. *Oncogene* 18:4808–4818.
2. Rubinson DA, et al. (2003) A lentivirus-based system to functionally silence genes in primary mammalian cells, stem cells and transgenic mice by RNA interference. *Nat Genet* 33:401–406.
3. Bunz F, et al. (1998) Requirement for p53 and p21 to sustain G2 arrest after DNA damage. *Science* 282:1497–1501.
4. Waldman T, Lengauer C, Kinzler KW, Vogelstein B (1996) Uncoupling of S phase and mitosis induced by anticancer agents in cells lacking p21. *Nature* 381:713–716.
5. Korinek V, et al. (1997) Constitutive transcriptional activation by a beta-catenin-Tcf complex in APC$^{-/-}$ colon carcinoma. *Science* 275:1784–1787.
6. Lowe SW, et al. (1994) p53 status and the efficacy of cancer therapy in vivo. *Science* 266:807–810.
7. Lafkas D, Trimis G, Papavassiliou AG, Kiaris H (2008) P53 mutations in stromal fibroblasts sensitize tumors against chemotherapy. *Int J Cancer* 123:967–971.
8. Harwell RM, Mull BB, Porter DC, Keyomarsi K (2004) Activation of cyclin-dependent kinase 2 by full length and low molecular weight forms of cyclin E in breast cancer cells. *J Biol Chem* 279:12695–12705.
9. Fabian MA, et al. (2005) A small molecule-kinase interaction map for clinical kinase inhibitors. *Nat Biotechnol* 23:329–336.
10. Chang BD, et al. (2000) Effects of p21$^{Waf1/Cip1/Sdi1}$ on cellular gene expression: Implications for carcinogenesis, senescence, and age-related diseases. *Proc Natl Acad Sci USA* 97:4291–4296.
11. Győrffy B, et al. (2010) An online survival analysis tool to rapidly assess the effect of 22,277 genes on breast cancer prognosis using microarray data of 1,809 patients. *Breast Cancer Res Treat* 123:725–731.

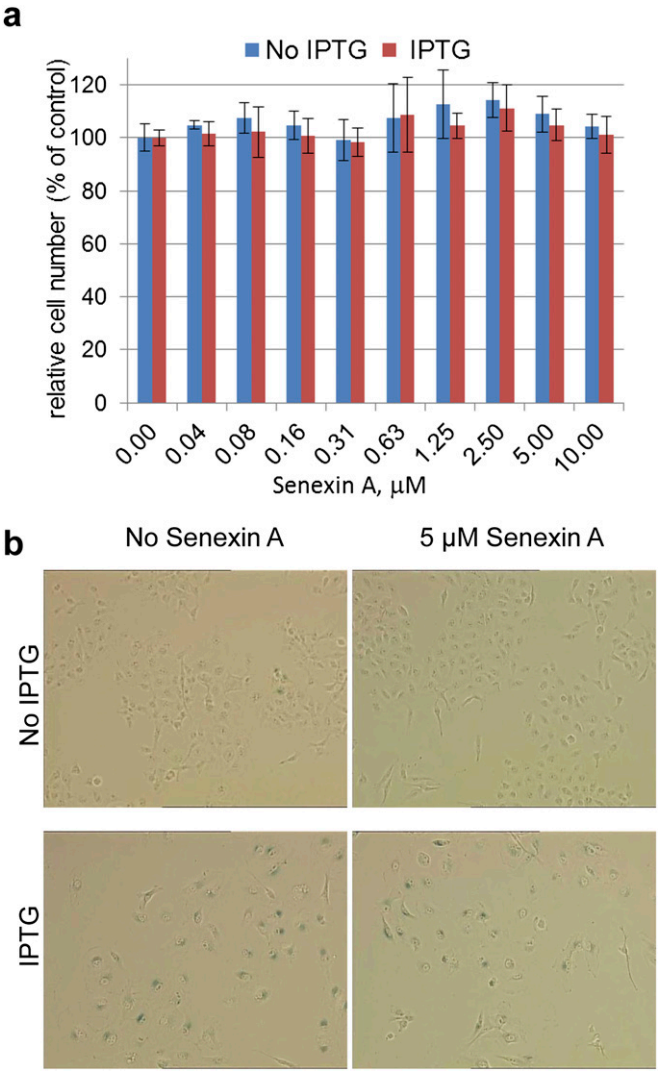

Fig. S1. Effects of Senexin A in HT1080 p21-9 cells, untreated or treated for 48 h with 50 μM p21-inducing IPTG. (*A*) Effects of different concentrations of Senexin A on relative cell number (as measured by Hoechst 33342 fluorescence) after 72 h culture in the presence or absence of IPTG (quadruplicate assays). Because p21 inhibits cell growth, cells were initially plated at 2,000 cells per well in the absence of IPTG or at 5,000 cells per well in the presence of 50 μM IPTG. (*B*) Effects of 5 μM Senexin A on cell morphology and SA-β-gal staining in HT1080 p21-9 cells, untreated or treated for 48 h with 50 μM IPTG. Microscopic images of cells stained for SA-β-gal were generated by merging of brightfield and phase-contrast photographs.

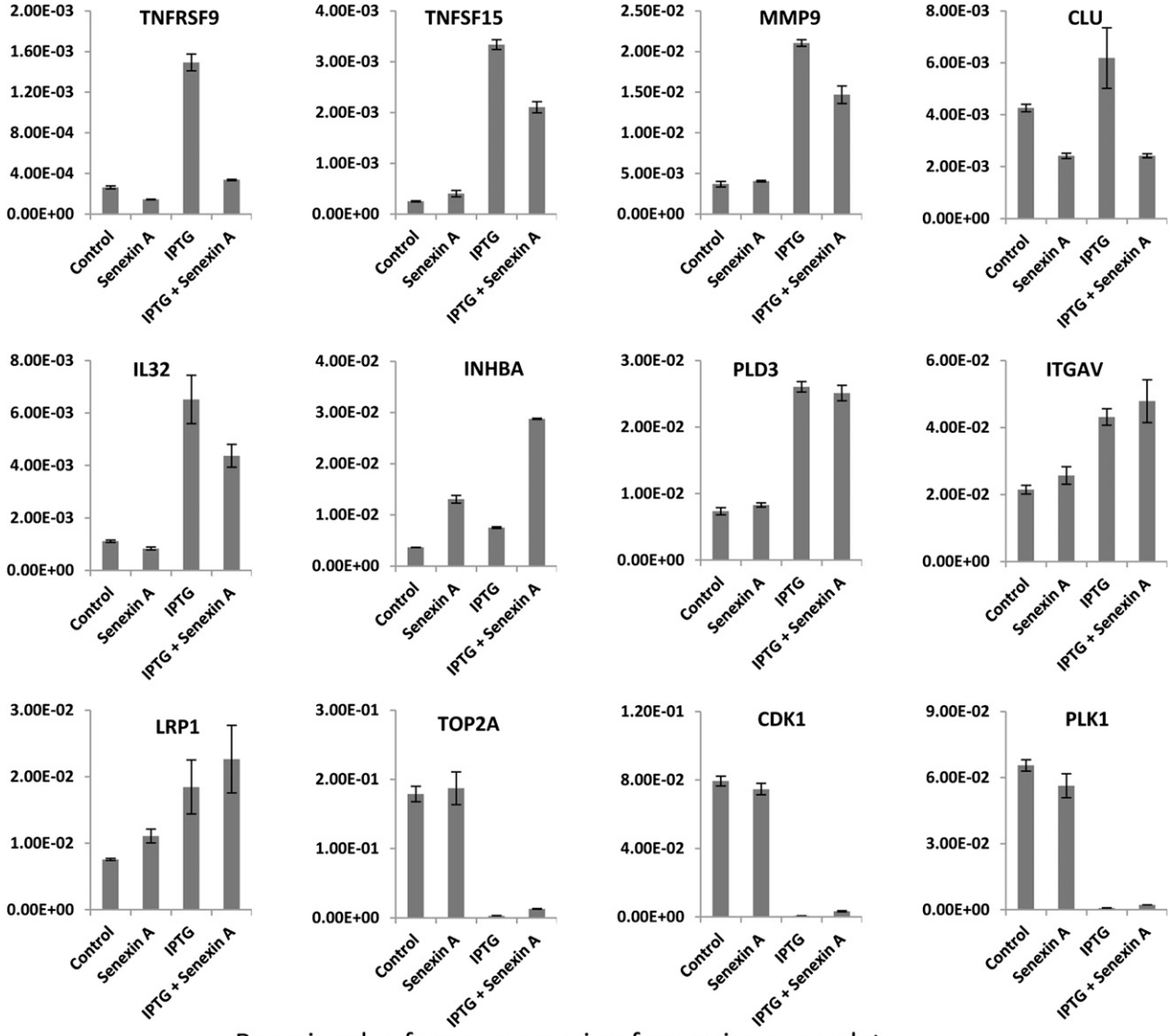

Raw signals of gene expression from microarray data

Gene Symbol	Control	Senexin A	IPTG	IPTG + Senexin A
TNFRSF9	169	147	323	147
TNFSF15	178	177	457	290
MMP9	438	741	2853	1728
CLU	284	208	473	285
IL32	776	829	2379	1913
INHBA	410	958	595	1906
PLD3	577	605	1738	1717
ITGAV	726	779	2050	2142
LRP1	690	870	2099	2188
TOP2A	943	1003	118	186
CDK1	357	365	45	54
PLK1	2639	2659	352	378

Fig. S2. (*Upper*) qPCR validation of microarray data on changes in the expression of indicated genes in HT1080 p21-9 cells treated for 48 h with 50 μM of p21-inducing IPTG and 5 μM Senexin A, alone or in combination (triplicate assays, normalized by RPL13A expression). (*Lower*) Table shows the corresponding raw signal values from microarray analysis.

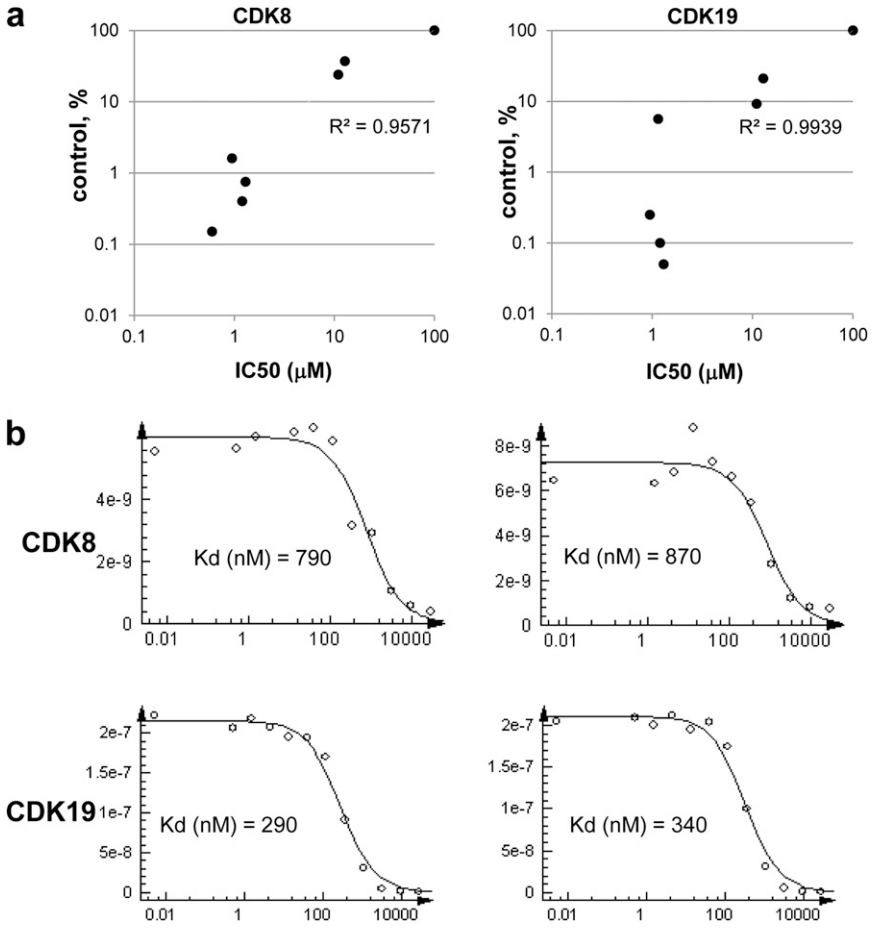

Fig. S3. CDK8 and CDK19 ATP pocket binding by Senexin A and related compounds. (*A*) Correlations of IC_{50} values (as determined by the inhibition of CMV-GFP induction by p21) with the effect on CDK8 and CDK19 (percent of control binding) for nine Senexin A-related compounds. The compounds were tested at 10-μM concentrations. The IC_{50} values for two compounds that showed no activity at the highest tested concentration (40 μM) are plotted as 100 μM. Correlation coefficient determined by standard regression analysis (Microsoft Excel). (*B*) Effects of different concentrations of Senexin A on ATP pocket binding of CDK8 and CDK19. Kinase ATP binding-site competition assays were conducted in duplicates. *y* axis, ATP pocket binding (a.u.).

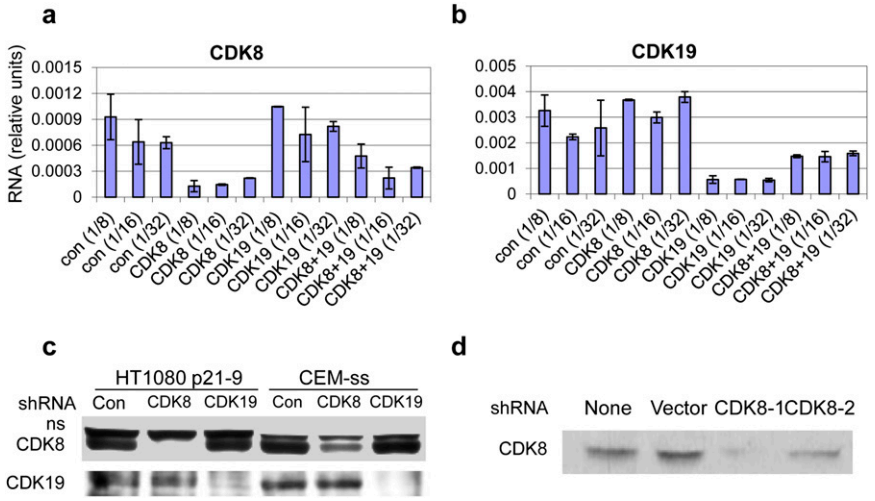

Fig. S4. shRNA knockdown of CDK8 and CDK19 in the experiments in main Fig. 2 *F* and *G*. (*A*) qPCR measurements (triplicates, normalized by GAPDH expression) of CDK8 mRNA levels in HT1080-p21-9-CMV-GFP cells that were infected with pLKO.1 lentiviral vector (control) or with pLKO.1-expressing shRNAs targeting CDK8 or CDK19, alone or in combination. Cells were infected with the indicated dilutions of packaging cell supernatant (1:8, 1:16, or 1:32) and used in Fig. 2*F*. (*B*) CDK19 mRNA levels in the same samples as in *A*. (*C*) Immunoblotting of CDK8 and CDK19 in HT1080 p21-9 and CEM-ss leukemia cells, transduced with a control lentivirus or with lentiviruses expressing shRNAs against CDK8 or CDK19 (Fig. 2*F*). (*D*) Immunoblotting of CDK8 in HT1080 p21-9 cells, untransduced or transduced with a control lentivirus or with lentiviruses expressing two different shRNAs against CDK8 (Fig. 2*G*).

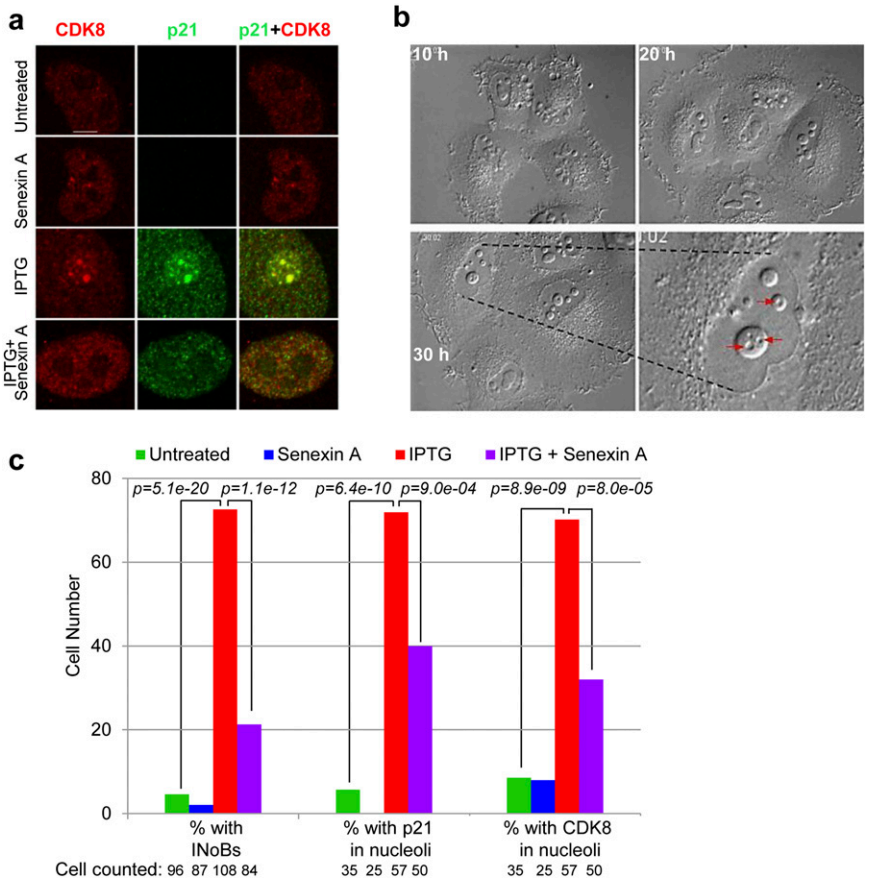

Fig. S5. p21 and CDK8 cooperate in the formation of and coaccumulate in the INoB. (*A*) Example of CDK8 (red) and p21 (green) localization by immunofluorescence confocal microscopy in HT1080 p21-9 cells, untreated or treated for 48 h with 10 μM Senexin A and 50 μM IPTG, alone or in combination. (*B*) Time-lapse DIC microscopy of the formation of INoBs (arrows) in HT1080 p21-9 cells upon p21 induction by 50 μM IPTG. (*C*) Frequencies of INoB formation and nucleolar staining for p21 and CDK8 in HT1080 p21-9 cells, untreated or treated for 48 h with 10 μM Senexin A and 50 μM IPTG, alone or in combination.

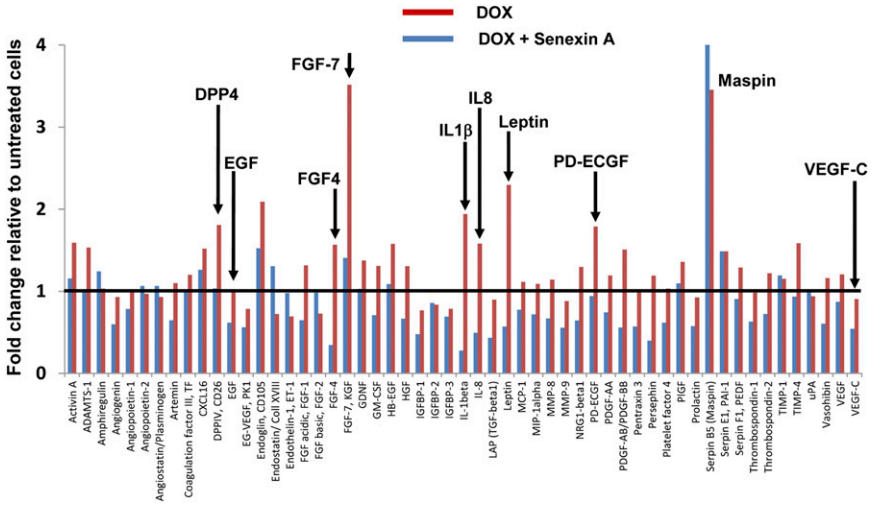

Fig. S6. Effects of Senexin A on cytokine expression in doxorubicin-treated HCT116 colon carcinoma cells. HCT116 cells were untreated or treated with 150 nM doxorubicin alone (red bars), or doxorubicin plus 5 μM Senexin A (blue bars), for 3 d. The expression of the 55 indicated cytokines was measured using R&D Systems Human Angiogenesis Antibody Array, in duplicates. The results for each cytokine are expressed as the ratio of the mean signals from drug-treated cells relative to untreated cells; the raw signal values of the duplicates differed by <17.5% in 98% of the assays. Some of the affected cytokines of biological interest are labeled separately (arrows).

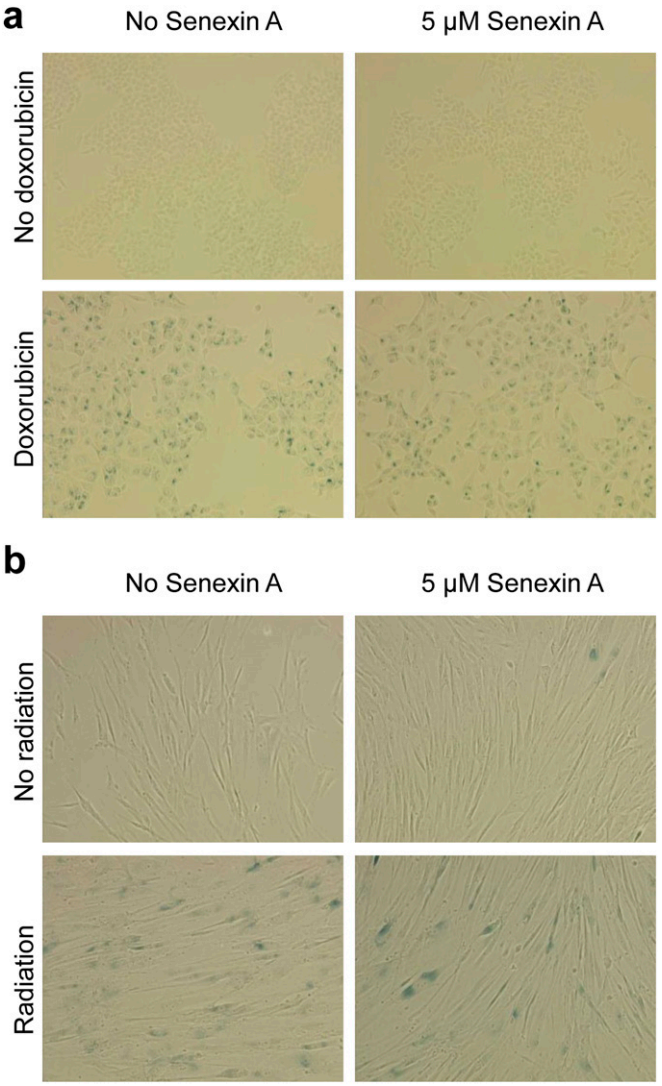

Fig. S7. Effects of Senexin A on cell morphology and SA-β-gal staining in HCT116 cells, untreated or treated for 72 h with 150 nM doxorubicin (*A*), and WI38 fibroblasts, untreated or exposed 3 d earlier to 10 Gy ionizing radiation (*B*).

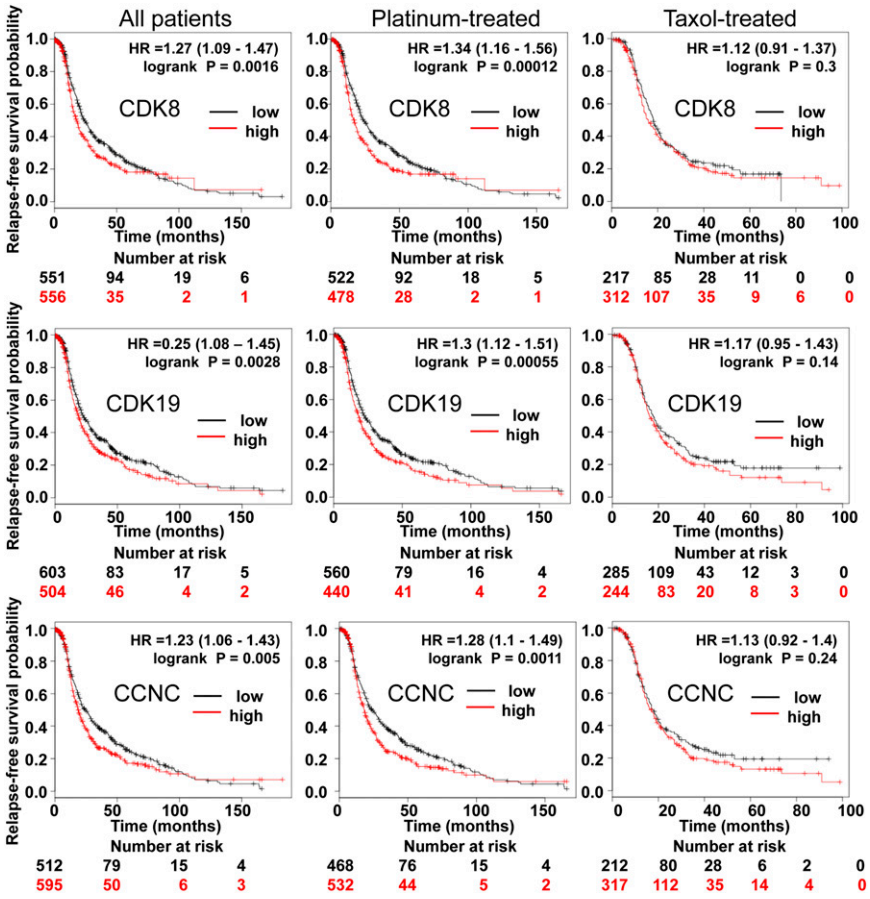

Fig. S8. Correlations of CDK8, *CCNC* (cyclin C), and CDK19 (or CDC2L6) expression with patient survival in microarray data from 1,107 ovarian cancers, determined using an online survival analysis tool. Median values were used as high/low cutoff in the analysis. (*Left*) Correlations for all of the ovarian cancers (1,107 cases). (*Center*) Correlations for the ovarian cancers, treatment of which contained platinum compounds (1,000 cases). (*Right*) Correlations for the ovarian cancers, treatment of which contained Taxol (529 cases).

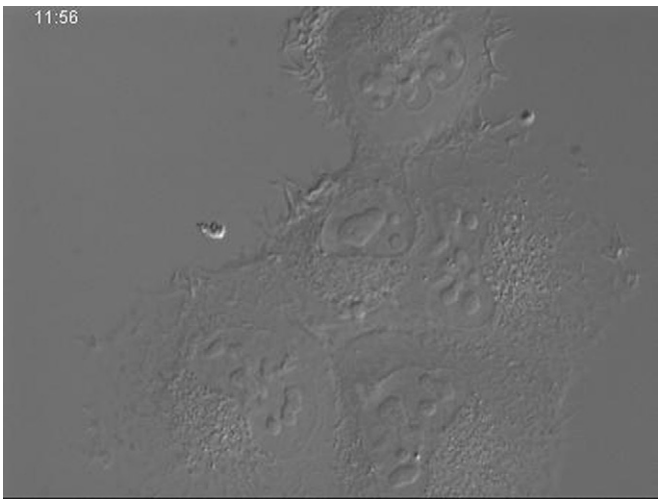

Movie S1. Time-lapse video microscopy of HT1080 p21-9 cells upon p21 induction by IPTG: changes in nucleolar morphology and appearance of internucleolar bodies (marked in still images of Fig. S5*B*).

Movie S1

Other Supporting Information Files

Table S1 (DOCX)
Table S2 (DOCX)
Table S3 (DOCX)